NASA CONTRACTOR REPORT

NASA CR-1468
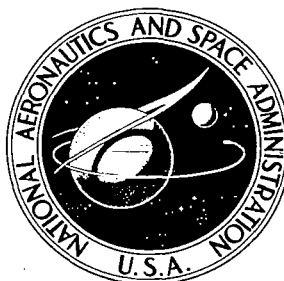
NASA-CR-14

c. 1

CYCLIC AND CONSTANT TEMPERATURE AGING EFFECTS ON MAGNETIC MATERIALS FOR INVERTERS AND CONVERTERS

by A. A. Brown, H. R. Craig, Jr., and W. S. Brink

Prepared by
MAGNETIC METALS COMPANY
Camden, N. J.
for Lewis Research Center

NATIONAL AERONAUTICS AND SPACE ADMINISTRATION • WASHINGTON, D. C. • APRIL 1970

1. Report No. NASA CR-1468	2. Government Accession No.	3. Recipient's Catalog No.
4. Title and Subtitle CYCLIC AND CONSTANT TEMPERATURE AGING EFFECTS ON MAGNETIC MATERIALS FOR INVERTERS AND CONVERTERS		5. Report Date April 1970
		6. Performing Organization Code
7. Author(s) A. A. Brown, H. R. Craig, Jr., and W. S. Brink		8. Performing Organization Report No. L-80001
9. Performing Organization Name and Address Magnetic Metals Company Camden, New Jersey 08101		10. Work Unit No.
		11. Contract or Grant No. NAS 3-9425
12. Sponsoring Agency Name and Address National Aeronautics and Space Administration Washington, D.C. 20546		13. Type of Report and Period Covered Contractor Report
		14. Sponsoring Agency Code

15. Supplementary Notes

16. Abstract

Six different square hysteresis loop ferromagnetic materials in two different types of toroidal core constructions were tested for ambient temperature, temperature cycling, and long term temperature changes. Included was one new material. Changes are tabulated and the applications and design of components utilizing these materials and shapes for inverter/converter systems is discussed.

17. Key Words (Suggested by Author(s)) Magnetic materials Ferromagnetic cores Magnetic aging Magnetic properties Transformer cores	18. Distribution Statement Unclassified - unlimited		
19. Security Classif. (of this report) Unclassified	20. Security Classif. (of this page) Unclassified	21. No. of Pages 152	22. Price* $3.00

FOREWORD

The research described herein, which was conducted at the Magnetic Metals Company under NASA Contract NAS 3-9425, was performed under the project management of Mr. Francis Gourash, Space Power Systems Division, NASA Lewis Research Center. The report was originally issued as Magnetic Metals Co. report L-80001.

TABLE OF CONTENTS

SUMMARY

The object of this program was to determine the extent of aging or change in properties of square hysteresis loop magnetic materials as a result of exposure to temperature cycles to which these materials may be subjected as in orbits having light and dark periods. The aging of these types of materials can affect the performance of the magnetic components used in power conditioning equipment.

Six square hysteresis loop ferromagnetic materials were subjected to 1667 temperature cycles over a 5000 hour period. The cycle, with a period of 3 hours, ranged from -55°C to +200°C. The materials tested were high purity 80% nickel -- 16% iron -- 4% molybdenum alloy; conventional 79% nickel -- 17% iron -- 4% molybdenum alloy; oriented 50% nickel -- 50% iron alloy; 49% cobalt -- 49% iron -- 2% vanadium alloy; doubly oriented 3% silicon steel; singly oriented 3% silicon steel. In addition to cycling tape and stamped ring cores of the above materials, a set of reference cores of the same materials was continuously maintained at 200°C.

The significant changes in magnetic properties were due to mechanical stresses developed within the cores as a result of the dimensional changes of the core with temperature changes. The changes observed were most pronounced for tape cores maintained at 200°C for 5000 hours. Tape cores which were cycled did not experience significant changes, nor did the ring cores whether cycled or maintained at 200°C.

The changes in tape cores maintained at 200°C for 5000 hours were due to mechanical stresses produced when the individual convolutions of the core were restrained from moving. The cycling of the tape cores resulted in a flexing type motion which relieved the induced strain. The significant changes in properties were noticed after 3000 hours of continuous exposure to 200°C. The ring cores were able to expand in an unrestricted manner and did not have stresses develop. This minimized any changes in properties.

The high purity 79% Ni -- 17% Fe -- 4% Mo is a new alloy produced by powdered metallurgy and sintering. This material was tested in toroidal tape core and ring core constructions with D. C. , sine wave and square wave excitations over a temperature range of -55°C to +200°C to determine its magnetic characteristics as applied to static inverters and converters. A. C. tests made at 400, 800, 1600 and 3200 Hertz included Constant Current Flux Reset tests with square wave excitation.

INTRODUCTION

The source of electrical power for aerospace systems is usually in the form of energy conversion devices such as batteries, solar cells and fuel cells. The D. C. power provided by these devices is at relatively low voltages. The demands of the many systems on board, however, may require several D. C. voltage levels and several A. C. voltages at one or more frequencies and of better quality and regulation than is available directly from the energy conversion devices. Static inverters and converters are used in power conditioning to process the raw power of the electrical energy sources into the form and quality levels required. These static circuits generally utilize semiconductor devices operating in switching modes. Because of this, the magnetic components used in these circuits are subjected to square wave, quasi-square wave, stepped and pulse modulated waveforms.

The continually increasing requirements of aerospace electrical systems has caused the power conditioning technology to advance at a rapid rate. This advance has kept pace with the progress in semiconductor technology which has produced high power silicon transistors, capable of switching in one microsecond, and miniature integrated circuits. Sophisticated static inverter and converter circuits utilize these advanced semiconductor devices in power stages and logic and control functions. The technology for magnetic power devices, however, has not progressed as rapidly. New and improved magnetic materials are slow in being developed. The available magnetic design data is rather incomplete and a fair amount of it is somewhat antiquated. A recent survey showed that there is a general lack of design data suitable for use in the design of magnetic components for static inverter and converter circuits. [1] Square wave test data was non-existent, while little or no sine wave data was available for frequencies in excess of 400 hertz. This presents a serious handicap to the solution of the problems of designing aerospace power conditioning systems for optimum weight, efficiency and reliability.

This problem is being alleviated by the investigations aimed at increasing and improving the available data in order to provide the means for achieving better design and performance of magnetic components. These investigations include the testing of magnetic materials with square wave voltages at high frequencies and at temperatures compatible with the capabilities of silicon semiconductor devices. A previous program, Contract NAS-3-2792, obtained such basic data for those magnetic materials commonly used in static inverters and converters. This program, however, is concerned primarily with the long term stability and aging characteristics of the magnetic properties of these same materials and their suitability for use over longer periods of time under conditions where the temperature varies in a periodic manner as may be encountered in extended orbital flights which may expose a space craft to light and dark periods.

To provide this additional and new information, magnetic cores, both in stamped ring and tape wound toroidal constructions were subjected to approximately 1667 temperature cycles between -55° C and +200° C for a 5000 hour test period. The cores were monitored continuously and periodically tested for several properties in order to evaluate the trends of changes. A group of reference cores were maintained at a constant temperature of +200° C throughout the 5000 hour test period for purposes of comparison. Additionally a new high purity, rectangular hysteresis loop material of 80% nickel -- 16% iron -- 4% molybdenum composition, produced by means of powder metallurgy, sintered, reduced and annealed in a magnetic field, was tested not only to the requirements of this program, but was also subjected to the test procedures of the previous program. These results combined with those of the long-term aging study expand the information available and up-date the magnetic design data as well as advance the overall technology.

The materials tested in this program were single and double grain oriented 3% Silicon Steel; conventional square loop 79% Nickel -- 17% Iron -- 4% Molybdenum; high purity 80% Nickel -- 16% Iron -- 4% Molybdenum; oriented 50% Nickel -- 50% Iron; 49% Cobalt -- 49% Iron -- 2% Vanadium. During the temperature cycling tests, periodic measurements were made with 400 Hz square wave excitation to monitor trends and evaluate changes. A. C. and D. C. magnetization curves and major hysteresis loops were obtained as well as A. C. core losses and exciting volt-amperes. The new material was additionally subjected to sine and square wave excitations at 400, 800, 1600 and 3200 Hz, as well as -55° C, +27° C and +200° C tests. Constant Current Flux Reset tests and Resistivity tests were also conducted at these temperatures. These higher frequencies are of interest due to the increased pressure to decrease the size and weight and improve the efficiency of magnetic components. These data and their application to static inverters and converters are presented and discussed.

MATERIALS TESTED

The materials for the tests were insulated with Magnesium Oxide, with the exception of the doubly oriented silicon which was insulated with Alkophos. Each toroidal tape wound core and punched ring lamination core contained 1/2 pound +2% of magnetic material. The core dimensions for both tape wound and punched ring lamination cores were 2.00" x 3.00" x 0.500". The doubly oriented material, was obtained in complete, unboxed, core assemblies measuring 3.225" x 4.00" x 0.750". Each core was encased in an aluminum core box, silicone oil filled, hermetically sealed, and insulated to withstand a breakdown voltage of no less than 1000 volts. The complete boxed core assemblies were capable of withstanding the -55° C and +200° C temperatures with no deterioration of the aluminum box or the insulation.

Cores for New Material Evaluation Tests

Material	Thickness Inches	No. of Samples	Sample Core Configuration
High Purity Square Loop	.002	3	Toroid, Tape Wound
4% Mo-80% Ni-16% Fe	.006	3	Punched Ring Laminations
	.006	1	Strip 12" x 1/4"

3

The number of samples, sample configuration, material composition and material thickness for each configuration are as designated in the following table.

Cores for Temperature Cycling Tests

	Inches	Samples	
Singly Grain Oriented 3%	.002	3	Toroid, Tape Wound
Silicon Iron	.006	3	Punched Ring Laminations
Doubly Grain Oriented 3%	.002	3	Toroid, Tape Wound
Silicon Iron Magnetic Field Annealed	.006	3	Punched Ring Laminations
High Purity	.002	3	Toroid, Tape Wound
49% Co-49% Fe-2% V Magnetic Field Annealed	.006	3	Punched Ring Laminations
Oriented	.002	3	Toroid, Tape Wound
50% Ni-50% Fe	.006	3	Punched Ring Laminations
Square Loop	.002	3	Toroid, Tape Wound
4% Mo-79% Ni-17% Fe	.006	3	Punched Ring Laminations
High Purity-Square Loop	.002	3	Toroid, Tape Wound
4% Mo-80% Ni-16% Fe	.006	3	Punched Ring Laminations

In order to maintain consistancy of properties, the tape wound cores for a given material were obtained from one heat and the punched ring laminations for a given material were obtained from one heat. Due to differences in thickness of tape (.002") and punched ring laminations (.006") the heats in both were not always the same.

All samples were given an incoming inspection prior to acceptance. The finished core samples were pre-evaluated with CCFR measurements and the magnetic properties of $(Bm - Br)$, $(Bm$ at $Hm)$, $(Ho$ at $Bo)$ were matched within a tolerance of $\pm5\%$ and $(H2 - H1$ at $B2 - B1)$ was matched to $\pm10\%$.

The high purity 4% Molybdenum - 80% Nickel - 16% Iron alloy is a relatively new magnetic material. It differs from the more conventional type of similar composition by virtue of being formulated through powdered metallurgy which upon subsequent sintering and eventual reduction produces a material with a much lower impurity content. This material also responds to a magnetic anneal enabling the hysteresis loop to be made squarer than its conventional counterpart.

Core Assembly

All materials were tested in both toroidal tape wound core forms and punched ring forms. The construction of the core case assemblies is indicated in Figure 1.

High Temperature Epoxy

Silicone Rubber Gasket

Glass Phenolic Cover

Core-Tape Wound or Ring

Oil Dampening Agent
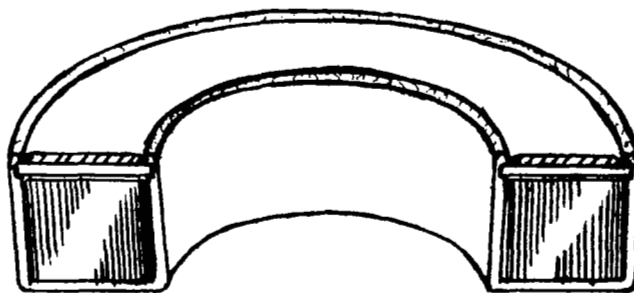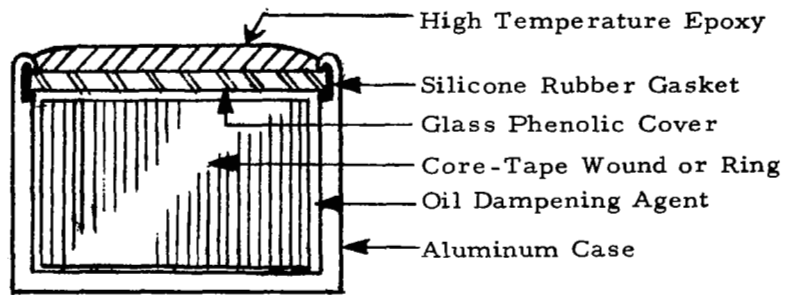
Aluminum Case

Figure L. -- Details of Core Assembly Construction

The assembly consisted of an aluminum case filled with the silicone oil dampening agent, and a glass/phenolic cover for the case which was crimped against a silicone rubber gasket. The crimped edges and the glass/phenolic insert were covered over by a high temperature epoxy sealant. The initial objective of a 250° C maximum temperature was abandoned after initial tests indicated that the seal would not withstand the 5000 hours at this temperature. (This conclusion was also reached in NASA report CR1226, Appendix D, Page 169). It was subsequently determined that 200° C was the maximum temperature that would enable the oil seal to be retained for the period of time required for the tests.

Test Apparatus

The cores were wound with teflon insulated magnet wire. Four windings were placed on each core to provide the necessary turns for the performance of core loss, magnetization curves and hysteresis loop measurements. The leads on the windings were sufficiently long to be run directly out of the test oven chamber without the need for intermediate connections.

The cores were then devided into two groups. One group consisting of one tape core and one ring core of each material tested was placed in a temperature chamber which was maintained at +200° C for the 5000 hour test period. These were referred to as the "reference" cores. The second group consisting of two tape cores and two ring cores of each material tested was placed in a temperature chamber which was programmed to cycle between -55° C and +200.° C. This group was referred to as the "cycled" cores. Both temperature chambers were electrically heated and thermostatically controlled to +1° C. The cycling chamber was cooled by CO_2 gas, also thermostatically controlled. Temperature sensors were placed on the cores to assure that core temperatures were maintained within the specified +3° C. The chamber temperatures were recorded on integral strip chart recorders. The core arrangement in the chambers is shown in Figure 2.

The leads of the individual core windings were wired through selector switches to the external power supplies and test equipment. Two separate square wave power supplies were used for the cycling tests. One supply was a solid state type rated for 1000 watts at 400 Hz and was used to continuously excite the cycled cores to 60% of Bmax while the cores were being cycled. The second supply produced a higher power, better quality square wave, and was used to excite the cores up to Bmax for the evaluation and periodic monitoring tests. This second supply consisted of six excellent quality vacuum tube audio power amplifiers connected in parallel and driven by a variable frequency audio/square wave oscillator. This combination produced a power output of 1200 watts with a 400 Hz square wave voltage rise and fall time of 8 microseconds. Voltages were measured with a vacuum tube voltmeter. Currents were measured with a vacuum tube voltmeter measuring the drop in a precision resistor. Frequency was measured with a standard frequency counter. Core loss was measured with a vacuum tube volt-ampere-wattmeter. D. C. hysteresis loops were recorded on a hysteresograph and X-Y plotter, while the A. C. hysteresis loops were obtained on an oscilloscope and photographed. Elapsed time was recorded by a timer and number of temperature cycles were recorded by a counter.

6
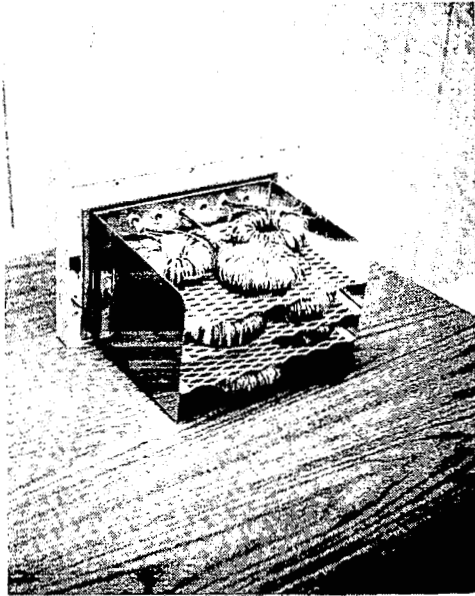
Figure 2 - Arrangement of Cores in Temperature Chamber

Figure 3 - General Layout of Test Equipment

An overall arrangement of the test equipment is shown in Figure 3. Details of the test circuits, equipment ratings, calibration and wave forms are given in Appendix C.

For the new material, ring and tape cores and resistivity strips were placed in a test chamber capable of monitoring -55° C, +27° C and +200° C. This chamber was the same type as used in the cycling and continuous temperature tests. Temperatures were monitored with a mercury thermometer. A. C. and D. C. measurements were made on the same equipment used for the temperature cycling tests. (Constant Current Flux Reset tests were made on a reset tester modified to test with square wave excitation.) Resistivity of the sample strip was measured with a Kelvin double bridge. Details of the test circuits and the Constant Current Flux Reset Tester are described in Appendix C.

Test Procedure

The chamber containing the reference cores and the chamber containing the cycled cores were operated simultaneously. The reference chamber was maintained at +200° C while the cycling chamber cycled between -55° C and +200° C -- the cycle period was approximately 3 hours. All cores whether reference or cycled, were continuously excited with a 400 Hz square wave voltage to a flux level of approximately 60% of Bm. This excitation was maintained throughout all periods when no measurements or data was being obtained. When it was required to make measurements, the cores were excited with the higher quality 400 Hz square wave capable of exciting the cores up to saturation, Bm.

Periodic and monitoring tests were made at scheduled intervals. The data obtained for the periodic tests included:

a) D. C. and 400 Hz square wave magnetization curves at 8 points in order to describe a smooth curve.

b) D. C. and 400 Hz major hysteresis loops.

c) A. C. core loss for 400 Hz square wave at 8 induction levels up to Bm (above knee of curve) to enable a smooth curve to be obtained.

d) Temperatures, elapsed time and number of cycles (for cycled cores) were also recorded.

Room temperature measurements were made on all cores at the start of the testing period, or t = 0 hours. The room temperature tests were repeated at the end of the testing period -- 5000 hours. The measurements were also made at 1000, 3000 and 5000 hours at -55° C and +200° C on all cores -- cycled and reference. These measurements necessitated the interruption of the cycling and continuous high temperatures for a short period of time.

8

Monitoring tests were made to establish trends in the changes of magnetic properties of the cores and to detect possible core failures. The monitoring tests consisted of measuring core losses at low, medium and high induction levels. For the cycled cores the monitoring tests were performed at -55° C and +200° C, while for the reference cores the tests were performed solely at +200° C. The schedule for the monitoring tests was as follows:

a) Once each working day for the first four weeks.

b) Once every second working day for the fifth through the eighth week.

c) Once every third working day for the ninth through the twelfth week.

d) Once every fifth working day for the remainder of the 5000 hour period.

Three tape wound toroidal cores and three punched ring core assemblies were used for the magnetic tests of the high purity 80% nickel -- 16% iron -- 4% molybdenum material. One strip sample was used for resistivity tests. All samples were placed in a single temperature chamber and all tests were conducted at -55° C, +27° C and +200° C after the cores had thermally stabilized. The cores were tested for A. C. magnetic properties, using sine wave and square wave excitations at 400, 800, 1600 and 3200 Hz. D. C. magnetic properties were also obtained. The sine wave and square wave excitations were employed in order to establish a relationship between the properties the material exhibits under these two different, though commonly used, excitations. The square and sine wave power for these tests was obtained from the paralleled electronic amplifier power supply. The wave form analysis for this excitation is indicated in Appendix C. The data obtained for the tape core and ring core samples included:

a) D. C. and A. C. magnetization curves for a minimum of 8 test points from H = 0.1 oersted up to Bm above the curve knee -- in order to provide a smooth and complete curve.

b) A. C. and D. C. major hysteresis loops at an induction level of Bm -- to saturation.

c) Exciting volt-amperes and core loss for a minimum of 8 test points extending from 0.1 oersted to Bm above the curve knee -- in order to provide a smooth and complete curve.

These tests were conducted in accordance with ASTM Test Standards A341, A 346 and A 343. The test circuits, instrumentation accuracy and calibration are described in Appendix C.

The core assemblies were also subjected to Constant Current Flux Reset tests in accordance with AIEE Test Standard No. 432 at the above frequencies, voltages and temperatures. It was necessary, however, to modify the reset tester to accommodate the square wave excitation. These modifications are indicated in Appendix C. The Constant Current Flux Reset data obtained included:

a) Bm at Hm

b) Bm-Br

c) Ho at Bo

d) H1 at B1

e) H2 at B2

f) Gain $= \dfrac{\Delta B}{\Delta H} = \dfrac{B2-B1}{H2-H1}$

Material resistivity was obtained from the strip sample. Tests were made with a Kelvin double bridge in accordance with ASTM Standard A 344 at temperatures of -55° C, +27° C and +200° C. The test circuit and instrumentation are described in Appendix C.

RESULTS AND DISCUSSION

The high purity 80% nickel -- 16% iron -- 4% molybdenum alloy exhibited a Bmax at 27° C, 400 Hz of approximately 7900 gausses -- and ranged from 6400 to 8400 gauss as a function of temperature, frequency and core construction as indicated in Figure 4. The differences in Bmax for square and sine wave excitations were under 200 gauss, or less than 2-1/2%. The Bm-Br of this material was approximately 1100 gauss at 27° C, 400 Hz -- and ranged from 1000 to 19r , gauss depending upon temperature, frequency and core construction. The diff .ences between the square and sine wave excitations, for Bm-Br over the frequen and temperature range, tested were relatively small -- typically under 10%. (Figure 5). The changes in Bm and Bm-Br for increasing frequency were relatively small. Changes with temperature, however, were significantly higher -- especially at -55° C. These changes are sensitive to the materials' lattice structure and degree of ordering, and followed the general pattern for this type material. Differences between the ring cores and the tape wound cores were small.

Ho which is the CCFR equivalent to the more familiar Hc is measured at 1/2 of 2 Bmax, and is indicated in Figure 6. The thinner material tape cores indicate a typical Ho of .04 oersteds, while the thicker rings exhibit an Ho of .05 oersteds, both at 400 Hz, 27° C. Both tape and ring cores exhibit an increase in Ho with increasing frequency which is a result of the increased eddy current losses at these higher frequencies. However, the ring cores exhibit a larger increase in Ho with increasing frequency which is typical for thicker materials due to the more rapid

10

rate the eddy current losses build-up because of the lower resistance of the larger cross section of the thicker material. For increasing frequency the increase in Ho for the .006" thick ring cores is almost threefold, while the increase in Ho for the .002" thick tape cores is approximately twice. With changing temperature, however, the variation in Ho for the ring cores is lower at all frequencies than the tape cores. The change in Ho (or Hc) with temperature is also dependent upon the lattice structure and degree of ordering in the material. Therefore the changes in the ring and tape cores should be more similar than shown in Figure 6. This difference is probably due to the change in the physical strains in the tape core assembly. Ho, (essentially $H1 \pm 1/2 \Delta H$) is quite sensitive to strain. These strains tend to be the result of even a slight degree of sticking between core wraps as well as an out-of-round core and imperfect welding of the last core wrap. The ring core assembly essentially leaves each ring free to move and expand without restraint. Differences between sine and square wave excitation were quite small -- generally under 5%.

The gain of this high purity 80% nickel alloy, expressed in gausses per oersted is indicated in Figure 7. Here the basic difference in gain between the ring and tape cores can be attributed to their difference in thickness. That is, thicker materials subjected to A. C. excitation have higher exciting current requirements, or losses, due to the relatively higher eddy current losses. This requires additional magneto-motive force to change flux a given amount -- hence lower gain. The lower resistance of the thicker material permits eddy currents to increase at a faster rate than for thinner material, for increasing frequency; thus requiring a greater excitation current to establish a flux level in the material. Because of this the decrease in gain with increasing frequency is greater for the thicker .006" ring core than the .002" tape core. The change in gain for temperature changes is also a lattice structure dependent characteristic. However, here again, the variations in gain as a function of temperature change were considerably greater for the tape cores than for the ring cores, which is attributable to tape core assembly problems outlined above. Square wave and sine wave gain differences were under 5%.

The core loss characteristics of this material is indicated in Figures 8 and 9 for sine and square wave excitation for all frequencies and temperatures tested herein. The thicker ring cores exhibited higher losses than the thinner tape core material due to the higher eddy currents which are generated in the lower resistance path. The curves indicate increases in core loss with increased flux level, increased frequency and decreased temperature. Square wave core losses were slightly lower than sine wave losses. The exciting volt amperes (VA) indicated in Figures 10 and 11 follow a similar trend, except here the square wave VA was slightly higher than the sine wave VA -- indicating a lower power factor for square wave excitation.

The D. C. magnetization curves are indicated in Figure 12 and 13. The data obtained from the complete D. C. hysteresis loop, as well as the complete D. C. loop as shown in Figures 14 through 16. The changes with temperature for both the magnetization curves and hysteresis loops are quite similar. The loop of the .006 rings appears somewhat wider than the loop of the .002 tape cores. The D. C. loop is not dependent upon thickness, and since the melting and rolling history of the two materials may have been different, it is possible to have the thicker material exhibit a slightly wider D. C. loop.

11
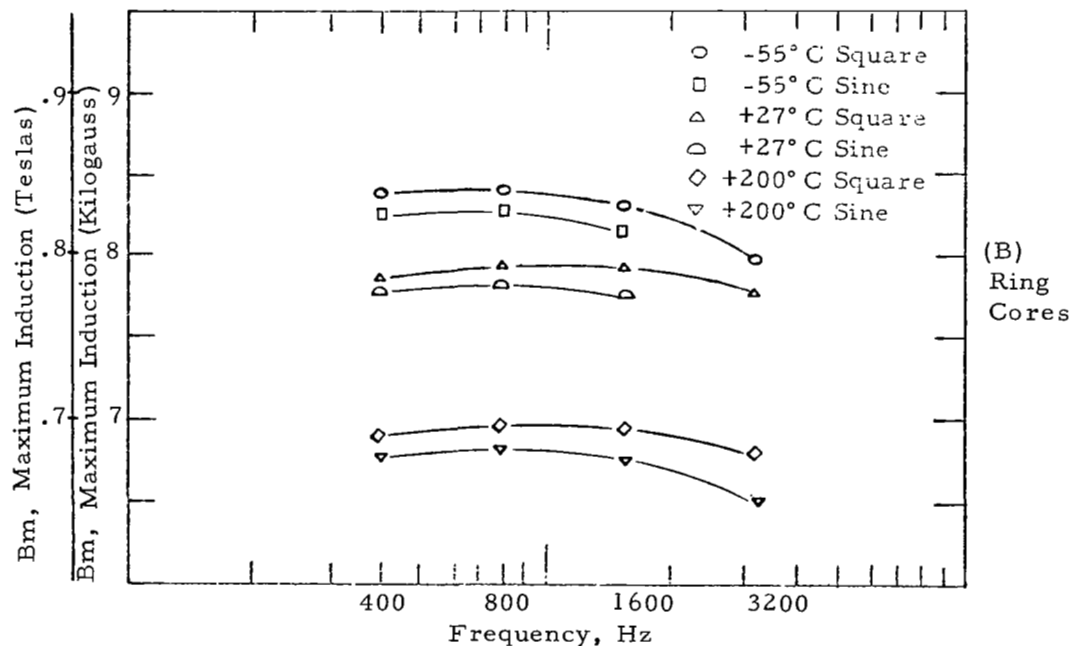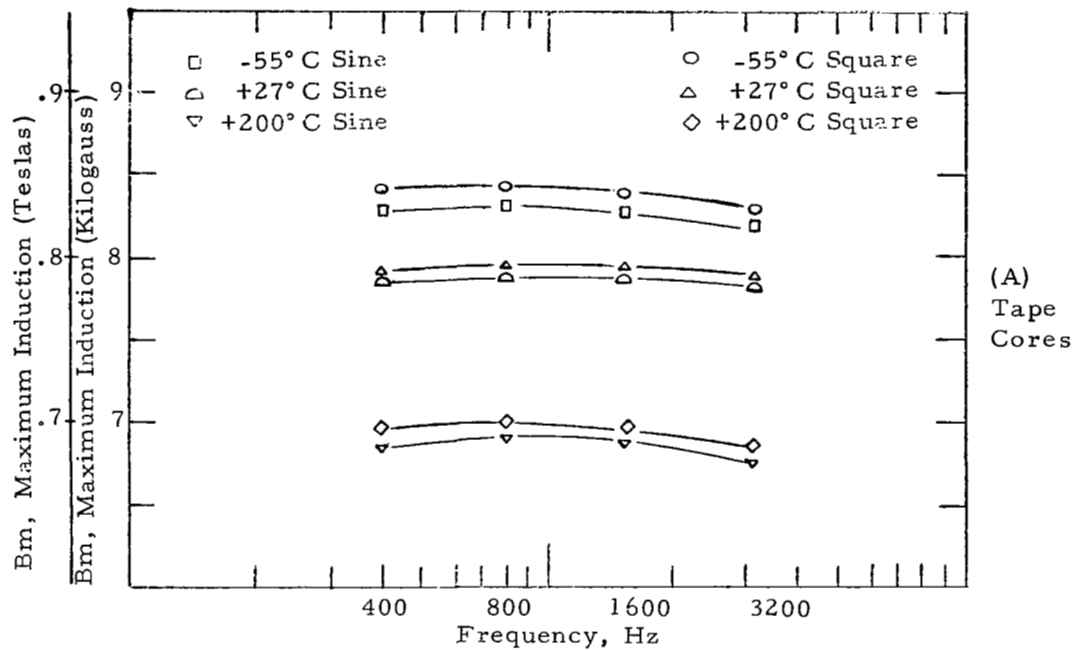
Figure 4 - CCFR Measurements of Bm, Maximum Induction, of High Purity 80% Nickel Alloy
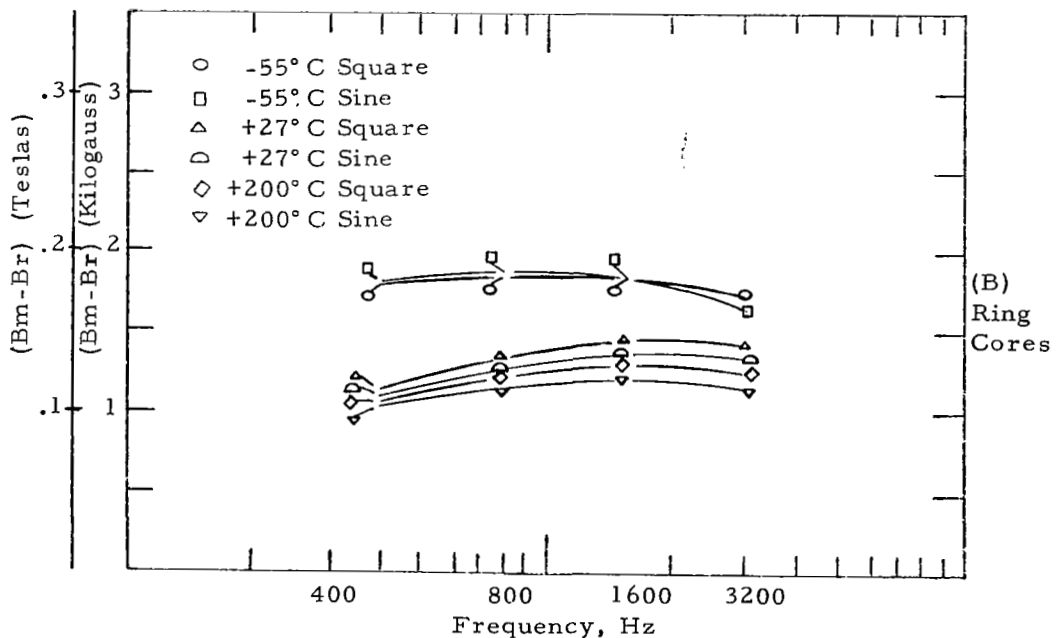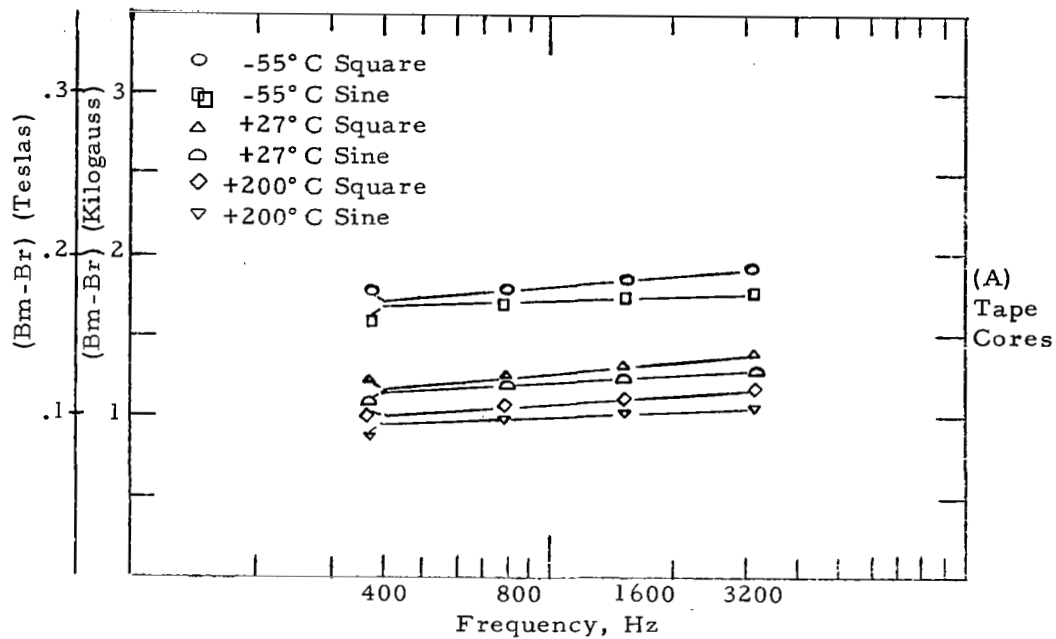
Figure 5 - CCFR Measurement of (Bm-Br) Loop Squareness
of High Purity 80% Nickel Alloy

13
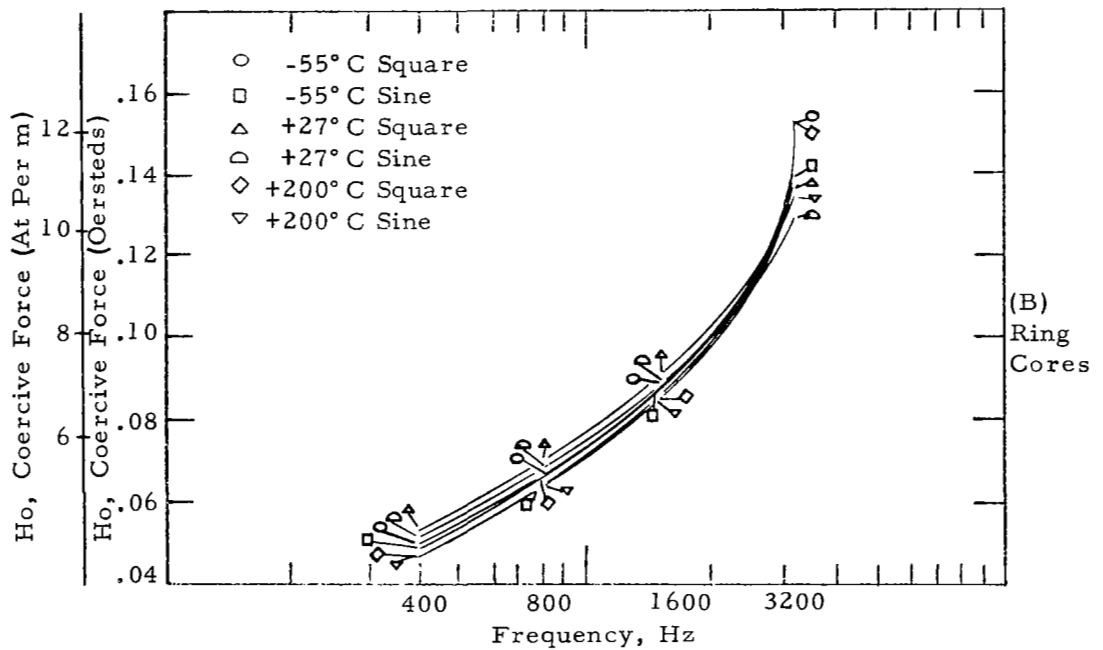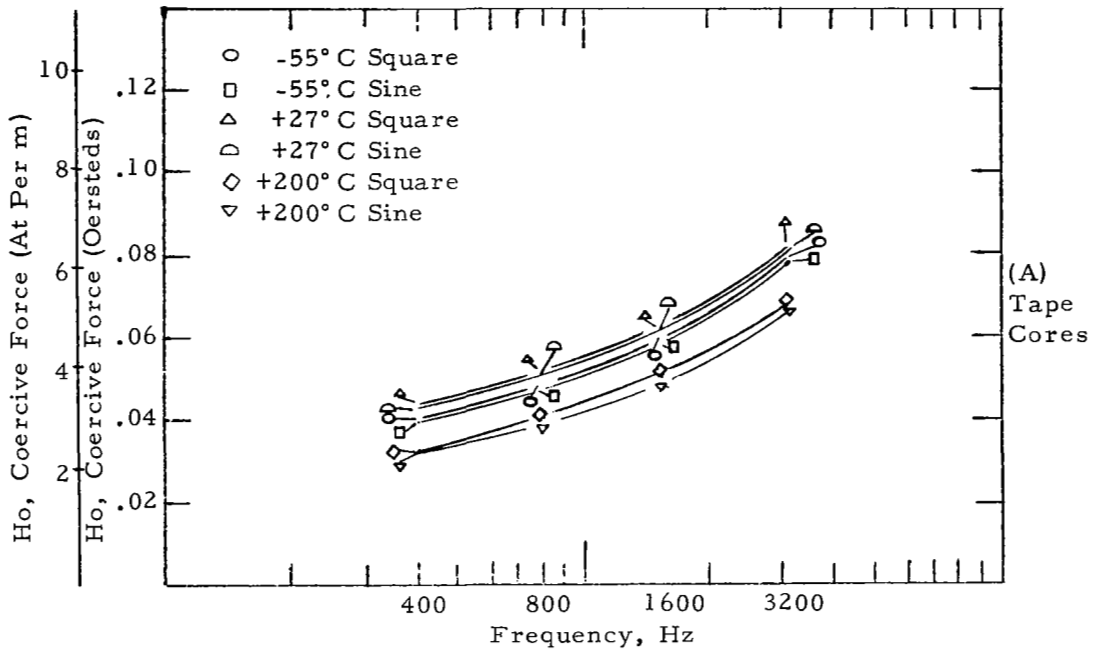
Figure 6 - CCFR Measurements of Ho, Coercive Force, of High Purity 80% Nickel Alloy

14
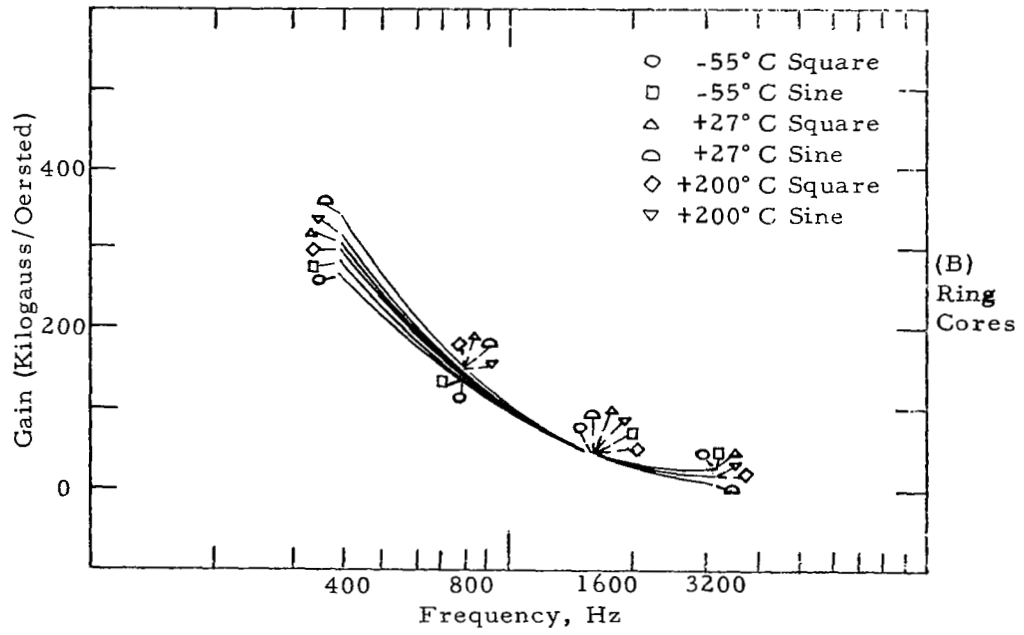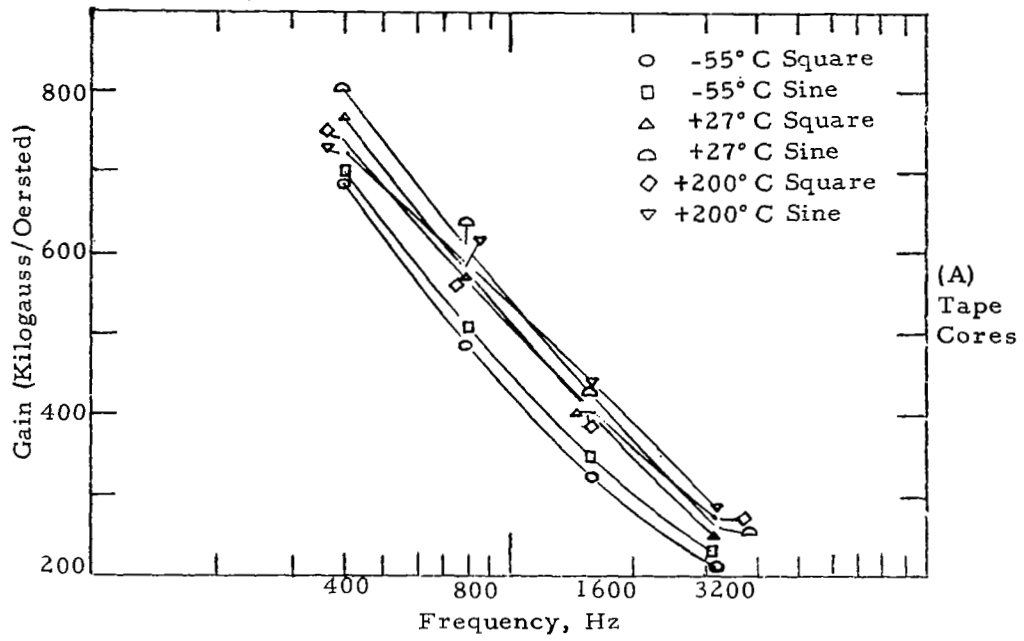
Figure 7 - CCFR Measurements of Gain,
of High Purity 80% Nickel Alloy
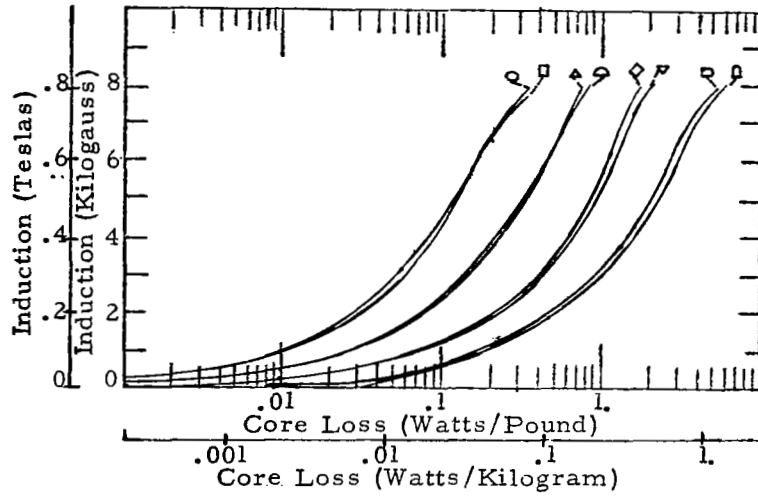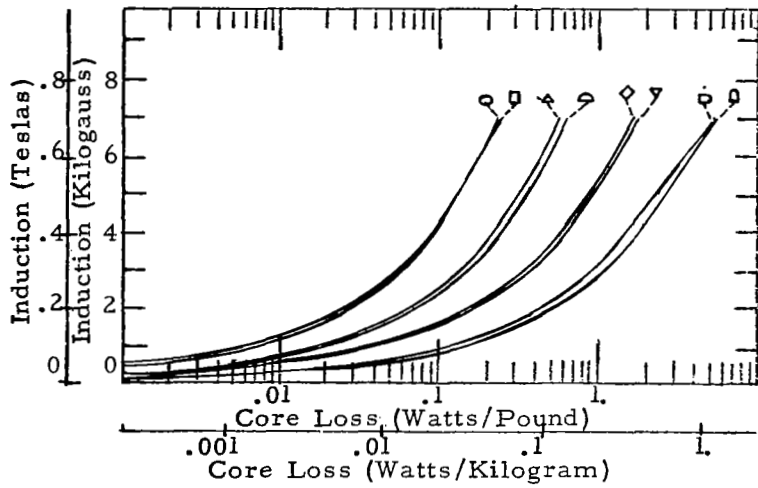
15
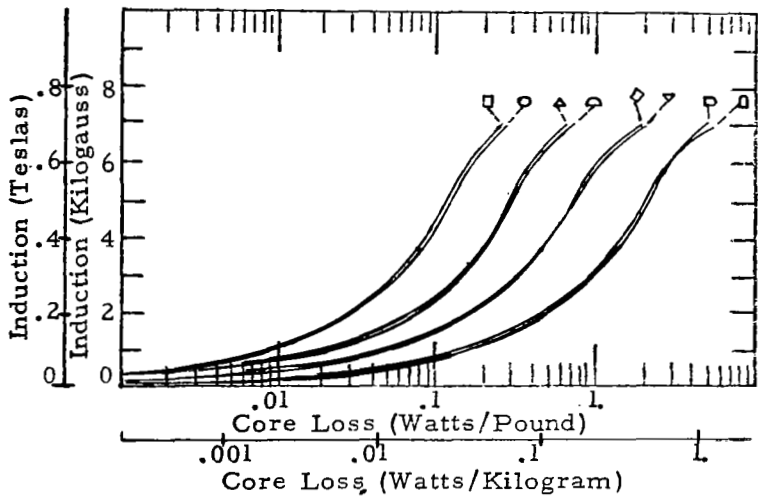
Figure 8 - Total Core Loss Vs Induction and Frequency,
0.002-inch Tape Cores, High Purity 80% Nickel Alloy
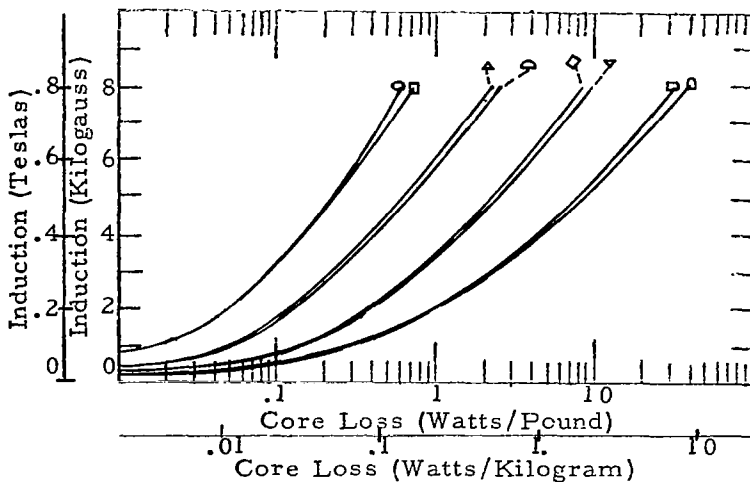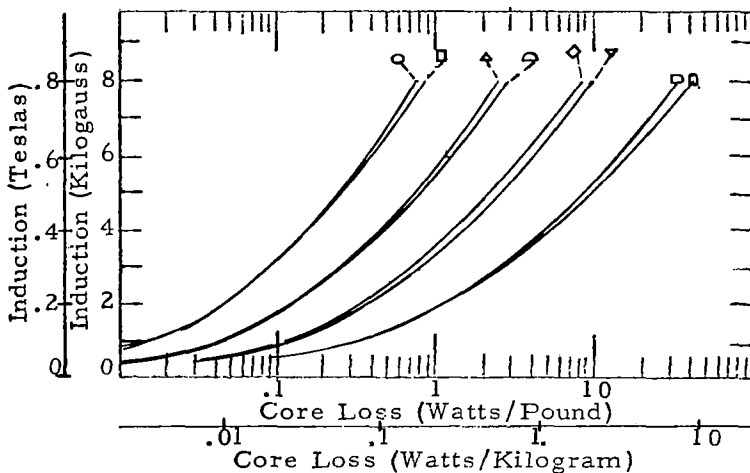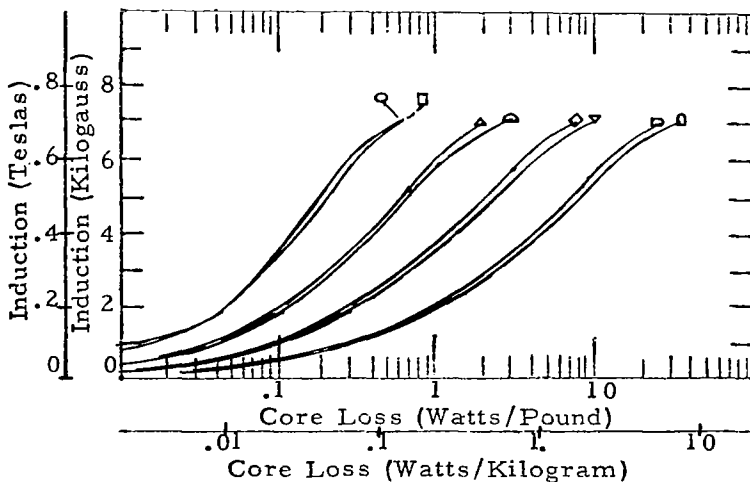
Figure 9 – Total Core Loss Vs Induction and Frequency
0.006 inch Ring Cores, High Purity 80% Nickel Alloy

17
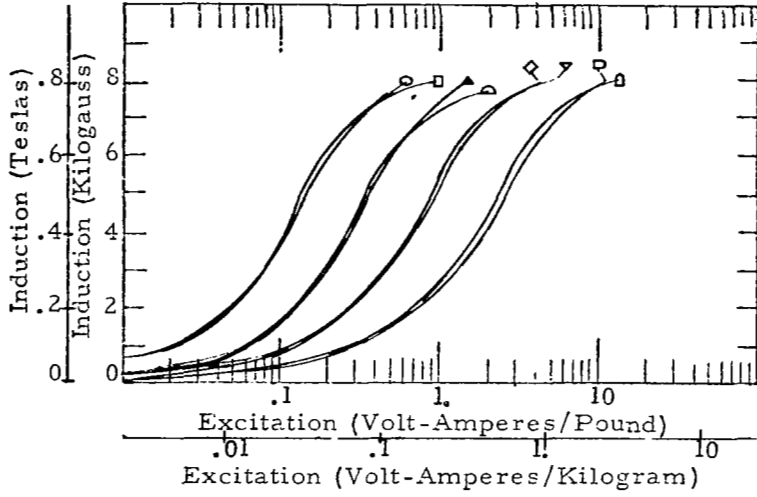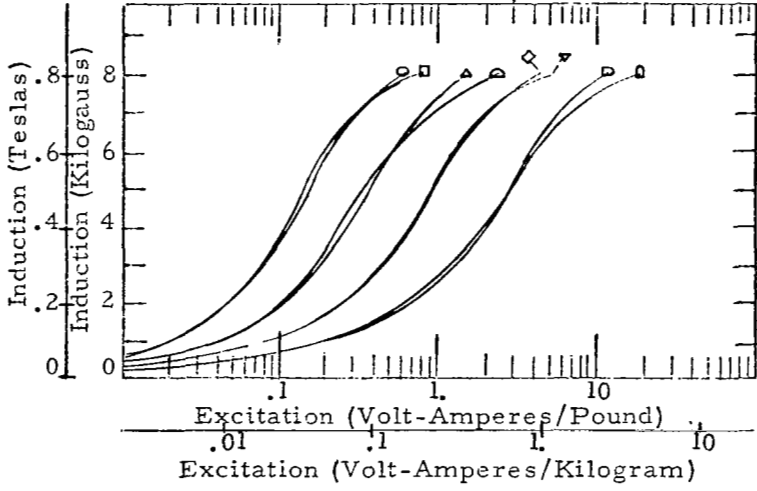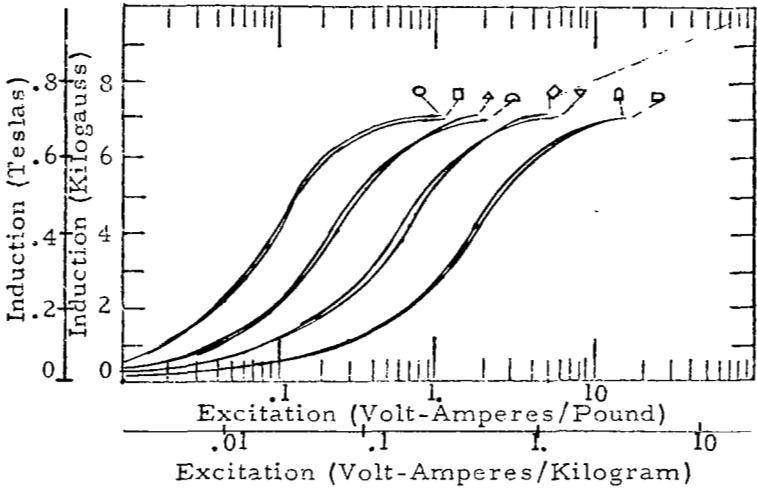
Figure 10 – Excitation Vs Induction and Frequency,
0.002 inch Tape Cores, High Purity 80% Nickel Alloy
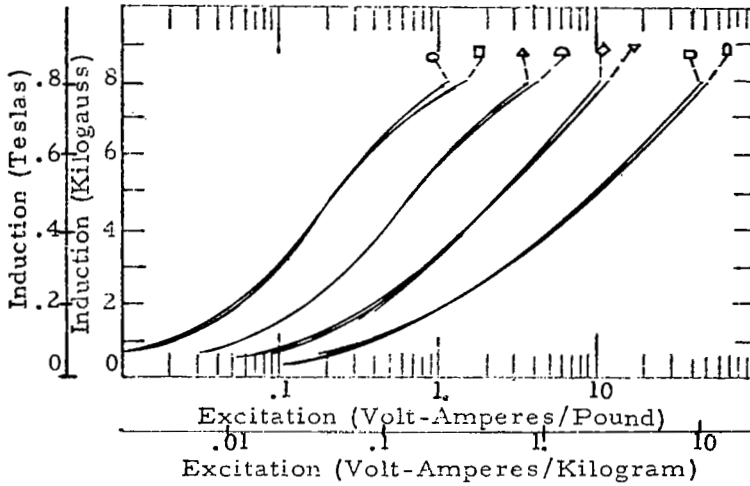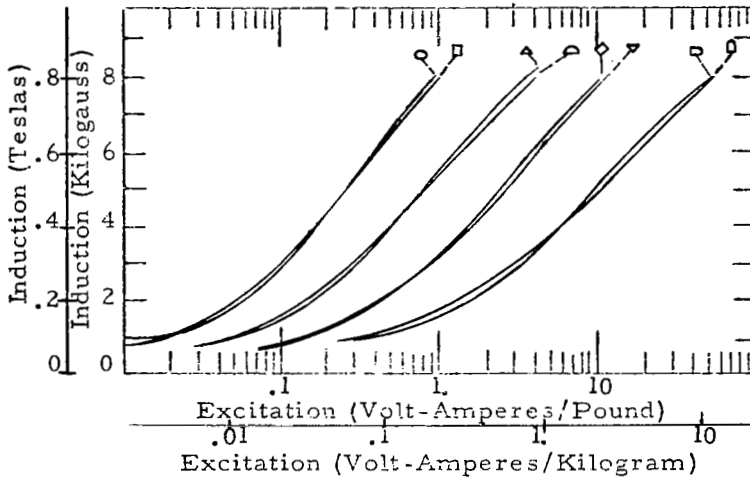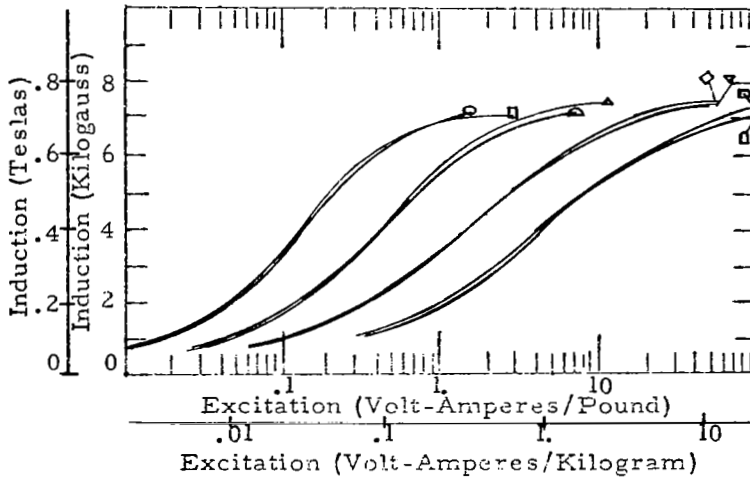
Figure 11 - Excitation Vs Induction and Frequency,
0.006 inch Ring Cores, High Purity 80% Nickel Alloy

19
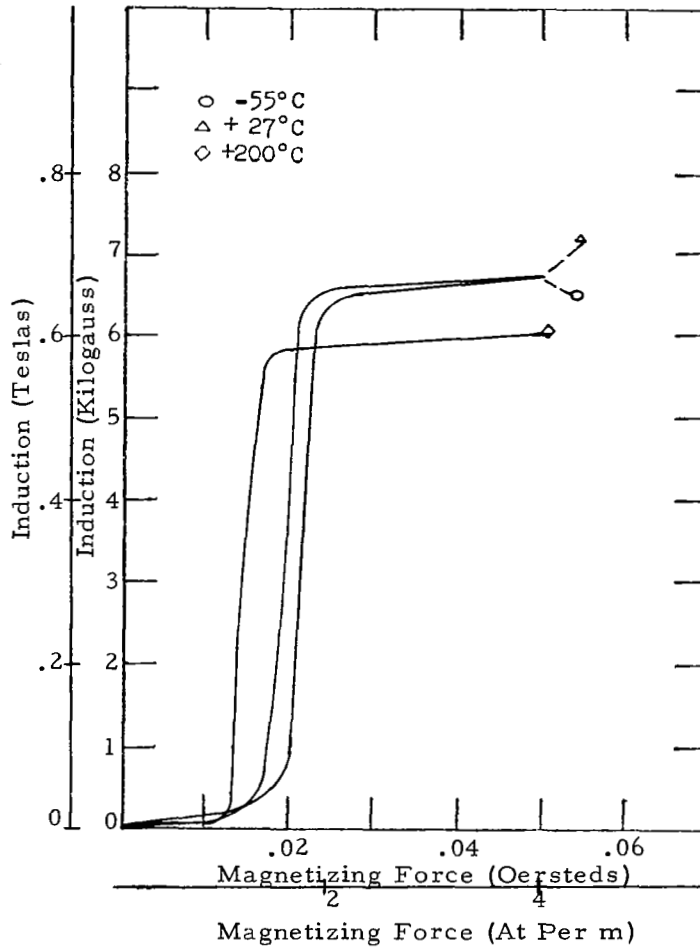
Figure 12 – DC Magnetization, 0.002 inch Tape Cores
High Purity 80% Nickel Alloy

20
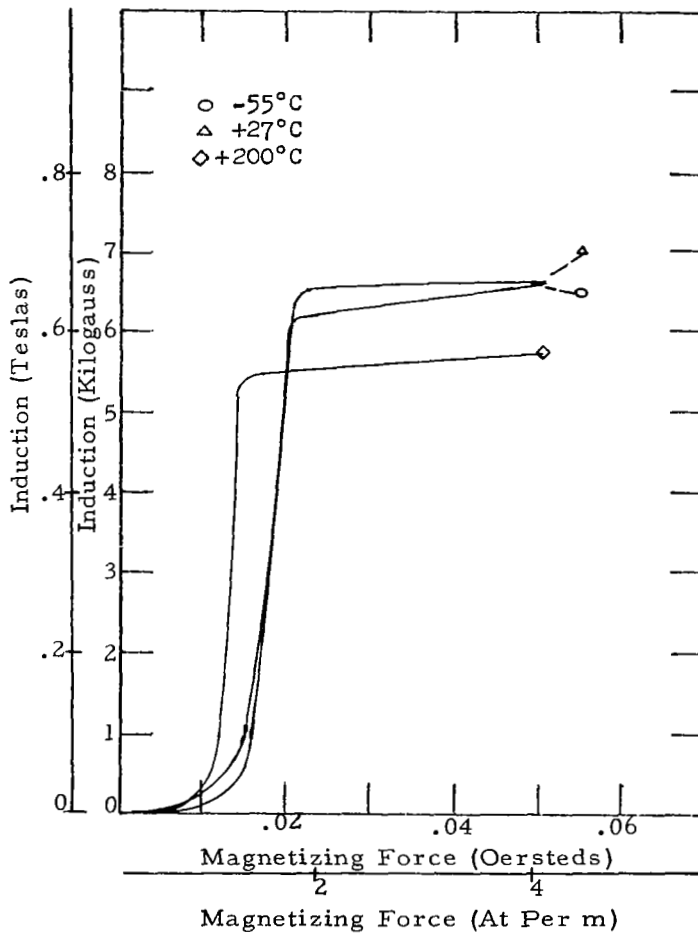
Figure 13 - DC Magnetization, 0.006 inch Ring Cores
High Purity 80% Nickel Alloy

21
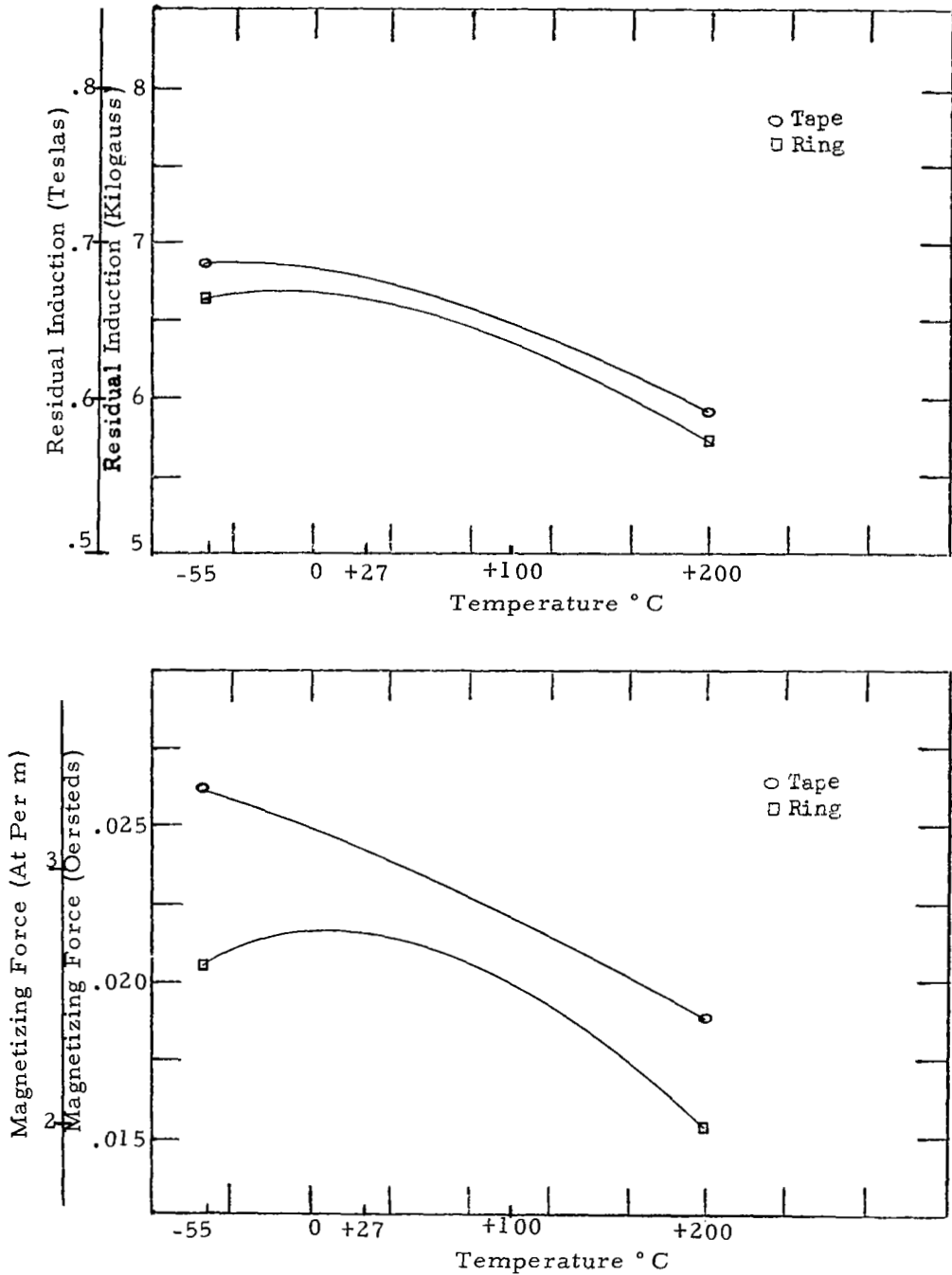
Figure 14 - DC Residual Induction and Coercive Force obtained from
DC Hysteresis data, High Purity 80% Nickel Alloy
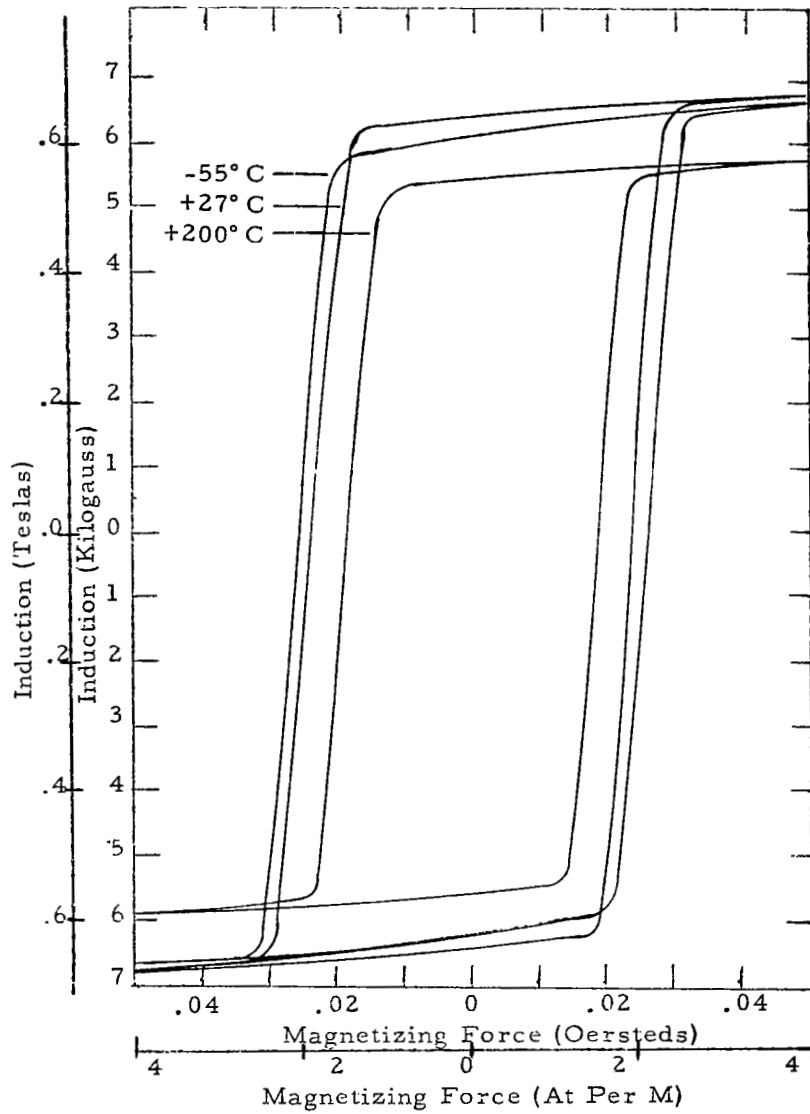
Figure 15 - Major D. C. Hysteresis loops at -55°C, +27°C and +200°C Temperatures.
0.002 inch Tape Cores-High Purity 80% Nickel Alloy.
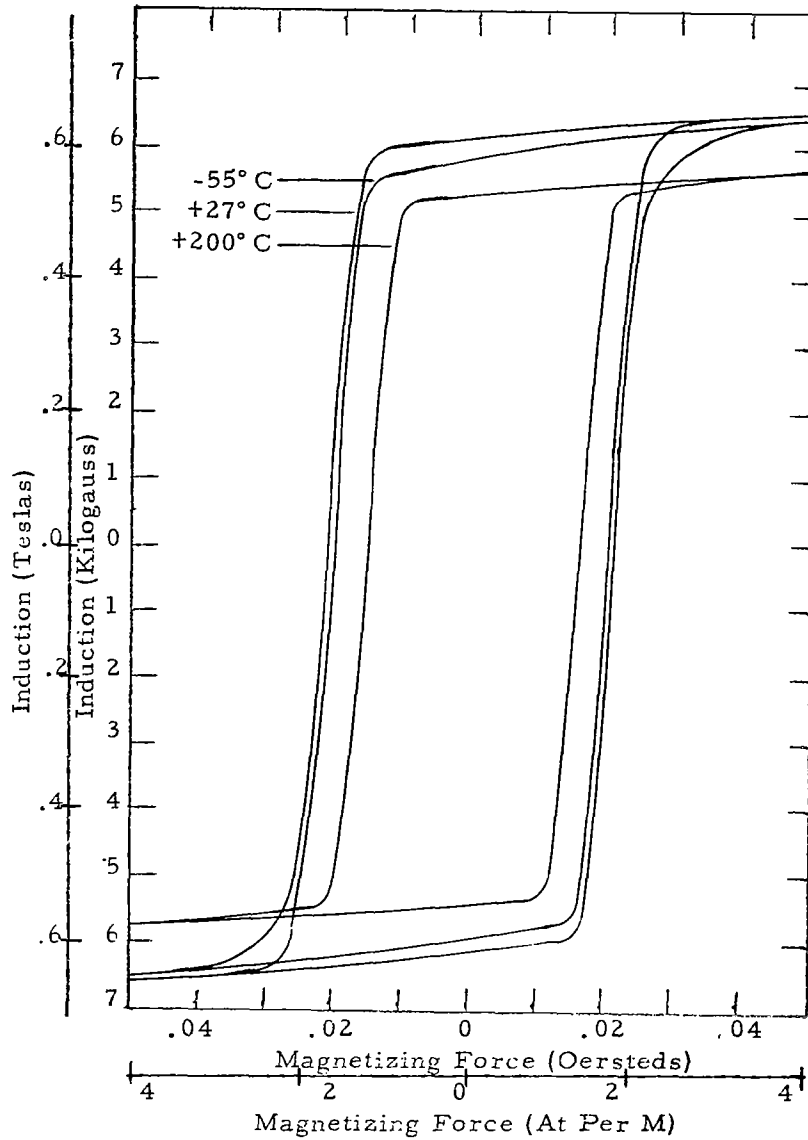
Figure 16 - Major D. C. Hysteresis loops at -55° C, +27° C and +200° C Temperatures.
0.006 inch Ring Cores-High Purity 80% Nickel Alloy.

Hc as obtained from the A. C. hysteresis loops, and as a function of temperature and frequency is indicated in Figure 17. Here is the first area in which there appeared to be a noticeable difference between the results obtained with square wave and sine wave excitations. However, it is to be noted that the excitations were somewhat different due to the criteria set-up for observing the A. C. hysteresis loops, that is, the drive was increased until a flux level, slightly over the knee of the curve was produced. This resulted in less excitation for some cores under square wave drive which would have an affect on the loop width, i. e., Hc. Ho (analogous to Hc) as measured under CCFR conditions for square and sine wave excitations appeared quite similar for the two types of excitation, as did the A. C. magnetization curves and core loss. The A. C. magnetization curves are shown in Figures 18 and 19.

The resistivity of the high purity 80% nickel alloy is 55 microhm-cm at 27° C, which is typical for materials of this type. [2] (Figure 20)

Cyclic and Constant Temperature Core Evaluation

The data obtained from the A. C. hysteresis loops, i. e., Bm, Br and Hc, which essentially describes the gross loop shape, is indicated in Figures 21 through 32. These curves depict the changes in the various properties of all the materials tested as a function of temperature and time. In general, all materials in tape core form exhibited significantly larger changes in Bm and Br for those cores continuously maintained at +200° C for 5000 hours, than for the same material and core construction which were cycled between -55° C and +200° C for the same period of time.

The ring cores in all materials, however, exhibited very similar (almost identical) changes for both continuous aging at 200° C and cycling between -55° C and +200° C. This phenomena of the tape cores exhibiting larger changes than the ring cores can be attributed to the problem of stress previously discussed. That is, in the manufacture of thin gauge tape wound cores, imperfect application of tape insulation, the sticking together of wraps during the high (approximately 2100° F) annealing temperatures, the welding through several wraps when anchoring the last wrap and possible interference with the case due to an out-of-round core condition can cause stresses to be created when the core temperature is changed. To eliminate the possibility that differences in thermal expansion between the core (in all axes) and the case caused stresses, a mathematical analysis was used and is detailed in Appendix D. This analysis shows that the case would not interfere with the normal expansion of the core to create the stresses which resulted in the larger changes. To minimize the effects of sticking between wraps, it is standard practice with most manufacturers to flex the annealed cores prior to casing. This flexing relieves some of the localized strains and generally improves most parameters by up to 10%. When subjected to the cyclic temperature schedule between -55° C and +200° C, the expansion and contraction of the core would cause some degree of movement somewhat similar to flexing, and thus continue this process of stress relieving. Hence the smaller changes in the cycled cores. The cores subjected to the single high (+200° C)

temperature would have stresses set-up due to the expansion of the core for which there would be no relief with the added possibility that this continuously elevated temperature condition caused some degree of creep in the core material, adding further to the stressed condition. This continuous application of the stress would cause continued degradation of core performance. As previously cited, the ring cores, when all rings are essentially insulated and annealed separately, no such problem of sticking or interference occurs. The larger changes noted for the cores continuously elevated to 200° C become noticeable after 1000 hours and very pronounced by 3000 hours.

The changes of greatest significance were typically 20-25% decreases in Bm and Br for all tape wound cores subjected to the continuous +200° C temperature for 5000 hours as shown in Figures 21 through 32. By contrast the changes in these parameters for the cycled cores did not exceed 8% and were typically under 5% for the same 5000 hour period. The start of degradation of core performance for the cores continuously maintained at 200° C commenced almost at the outset of the tests and worsened with time. Some of the original pre-test performance could be recovered by uncasing and flexing the cores -- all could be recovered by rean-nealing.

Hc as determined from the A. C. hysteresis loops exhibited a lesser degree of change for all materials than did Bm and Br. Nickel-iron cores exhibited somewhat larger Hc changes than did the other materials. There was also less difference be-tween the cycled cores and those continuously maintained at +200° C, although the continuously heated cores generally exhibited somewhat larger changes with time than did the cycled cores, as can be seen in Figures 21 through 32. Here again the ring cores, whether cycled or continuously maintained at temper-ature, showed less overall change than did the tape cores of the same materials.

Core loss for all materials at the outset and after 5000 hours for both temper-ature cycled and continuously heated cores is indicated in Figures 33 through 40. . The curves show the core loss characteristics as a function of induction level for the three temperatures of interest (-55° C, +27° C, +200° C) and at the end of 5000 hours, as well as the initial core loss characteristics at 27° C at T = 0 hours. The complete core loss vs. time vs. temperature data is presented in Appendix E . The effect of time, whether cycling or continuously at +200° C appears quite small as can be seen on the above cited curves. The largest change in core losses oc-curred between +27° C and +200° C, whether cycling or not. This may be due to the larger temperature excursion (173° C) in reaching this temperature than in cooling down to -55° (a change of 82° C).

Exciting volt amperes (VA) after 5000 hours is indicated in Figures 41 through 48. These curves present data of VA at T = 0 hours at 27° C and at T = 5000 hours at -55° C, +27° C and +200° C for both cycled and cores continuously maintained at +200° C. Here again the core excitation followed a similar pattern to that of the core losses. However, especially for the continuously heated cores, there were greater differences mainly at the higher inductions, and mainly for the tape cores maintained continuously at +200° C. The previous discussion concerning

tape core problems applies here. If there was sticking which caused stresses, exciting VA would increase, and if there were wrap-to-wrap short circuits this would have the effect of locally increasing material thickness which, as has already been cited, tends to increase losses and excitation requirements. This is supported by the data showing higher VA/lb for the continuously heated tape cores as compared to the cycled tape cores and the fairly consistent VA/lb data for the ring cores whether cycled or not. A convenient set of curves showing core loss and exciting volt-amperes for cycled and continuously heated cores from T = 0 hours to T = 5000 hours at Bm, 2/3 Bm and 1/3 Bm is shown on curves 73 through 84 and appears in Appendix E.

Figures 49 through 52 display the A. C. magnetization curves after 5000 hours for the cycled and continuously heated cores at temperatures of -55° C, +27° C and +200° C; the T = 0 hours at 27° C curve is also indicated. Once again the cycled tape cores and ring cores (whether cycled or not) show a consistency of performance vs. temperature, with the largest (though consistent) change for the 200° C temperature. The tape cores continuously maintained at 200° C, however, exhibit random changes, less predictable and uniform than the cycled cores. Here the large change in Bmax can be noted -- and this verifies that data obtained from the A. C. hysteresis loops (Figures 53 through 64) for the continuously heated tape cores.

The slope of the A. C. magnetization curves between 1/3 Bm and 2/3 Bm for all materials is plotted in Figures 65 through 70. This ratio of $\Delta B/\Delta H$ is related to the gain reading one might obtain through CCFR testing. However, since CCFR testing was not included in this portion of the investigation, the indicated ratios were considered of value. As may be expected from the above discussion of the A. C. magnetization curves, the cycled tape cores generally exhibited less change over the 5000 hour period than those tape cores continuously maintained at +200° C. The ring cores, whether cycled or not, also exhibited lower relative changes than did the tape cores. The general discussion concerning tape core assembly problems -- outlined in preceding sections -- applies here.

During the 5000 hour testing period two cores exhibited changes in some parameters by orders of magnitude larger than similar cores, or that past experience would cause one to expect. These were termed "catastrophic failures". Both of these were tape cores, and both were in the group continuously maintained at +200° C. Both failures occurred between the 3000 hour and 5000 hour tests, and were initially noted by excessively high VA -- in both cases between 2-3 times the VA of the previous reading. The test windings on the cores were tested for failure, but were found satisfactory. Subsequent re-testing of the two cores indicated excessive VA, poor squareness and higher than previous Hc. The external appearance of one core appeared satisfactory (after removal of test windings) with the epoxy seal intact. The other core assembly, however, had its epoxy seal cracked in several places. Disassembly of the core with the cracked epoxy seal revealed that most of the oil dampening had leaked out, and several of the wraps on the inside diameter of the core had stuck together, with the first wrap virtually cemented to the inside wall on the inside diameter of the case. The other core upon disassembly appeared to

have the original volume of oil in the case with no sticking to the case. There was no gross sticking of large sections of the core to itself, but it was not possible to determine if one or two wraps were stuck at random throughout the core assembly. (Past experience with core failures of this type points to a mechanical failure some- place in the core assembly.) Mechanical interference had been eleminated by the previously cited analysis of Appendix D. The mechanical failure was obvious in one of the two cases described above, but could not be substantiated for the second case.

The data obtained and presented for the heats of steel used is quite reliable and may be used with good confidence provided it is realized that the absolute val- ues shown will vary from heat to heat of material. The relative changes, however, will always tend to be similar to that presented herein -- with the possible excep- tion of its application to tape cores exposed continuously to a single temperature.

Results As Applied to Designs

In applying the information discussed herein to an inverter system which might conceivably consist of a static inverter, wave shaping network (filter), mag- netic amplifier regulator and transformer, it is necessary that the limitations of the magnetic materials described be considered in light of the temperatures anti- cipated, length of time of required performance and whether the temperature over the required time will be constant or cyclic.

If the static inverter to be used is a free running type where the Bmax of the inverter transformer core and the applied D. C. excitation determine the frequency of oscillation, then it is important to know whether the temperature is cyclic or con- tinuously elevated (or perhaps even depressed). As previously cited, under constant- ly elevated temperature conditions almost all materials exhibit a 20-25% decrease in Bmax. As far as this specific application is concerned -- this is a permanent change in the core which cannot be altered without disassembly and heat treatment. If the D. C. excitation remains constant the frequency of oscillation will increase by the same ratio as the decrease in Bmax. If this is an A. C. system this would be unsuitable; if it were a D. C. output that was of interest, then the designer would have to consider the higher core losses (which also occur for the A. C. system) which result at the higher frequencies. The compensation here would have to be by varying the D. C. to accommodate the frequency requirement. This would further change the inverter output levels with which the regulator must cope. In a driven inverter system, it is only necessary to limit the Bmax of the transformer to less than the minimum Bmax encountered herein over the time and temperature range anticipated. This would tend to increase the size of the transformer, but this would be compensated for by the increased reliability whereby the transformer would not eventually saturate and draw excessive currents from the energy source and cause large unanticipated changes in the inverter output. These Bmax limitations will also be true for any transformer in the system. Depending upon the type of trans- former, other property changes would have to be considered, such as the change in losses for a current transformer and change in Ho for a saturable transformer.

In the magnetic amplifier, in addition to the Bmax considerations discussed above, the changes in loop squareness (or Bm-Br) and gain as a function of time and temperature must be considered. Higher Bm-Br (or reduced squareness) will result in lower amplifier output for a given firing angle (control signal) since the core's degree of saturation is essentially reduced. Change in gain will produce a change in output firing angle (hence change in output) for a given control signal. These two property changes would then change system performance. Here, however, compensation for change in gain is more readily accomplished through the use of sufficient negative feedback to compensate for the core's change in gain and still meet system requirements. Change in bias point due to a change in Hl is compensated for to some extent by the aforementioned feedback. However, more complete compensation is achieved by a thermistor/resistor network in the bias circuit.

When these square loop materials are included in wave shaping networks, they generally are used to absorb part of a voltage and subsequently saturate at a predetermined point. Here the Bmax is a most important consideration -- with Hc being important in knowing the currents which will be required for the core. In other words, the general shape and expected changes in the A. C. hysteresis loop, for the frequency of interest, are important considerations. Compensation for hysteresis loop changes in this type of application is extremely difficult, with very little information available on the subject.

CONCLUDING REMARKS

Six magnetic materials having rectangular hysteresis loops were tested in tape core form over a temperature range of -55° C to +200° C for 5000 hours, and were found to have a greater deterioration of properties when maintained constantly at +200° C than when continuously cycled between -55° C and +200° C. The changes in the cores maintained at +200° C were random and appeared to be the result of stresses which occurred in the cores as a result of the continuous exposure to this temperature. These stresses are a further result of the techniques presently used in tape core manufacture and assembly.

The same six square loop materials were tested in ring core form under the identical test conditions as above and were found to exhibit the same relative changes in properties whether the temperature was cycled or was maintained continuously at +200° C. These ring cores also exhibited less change with temperature and time than the tape wound cores in the same materials.

A high purity 80% nickel -- 16% iron -- 4% molybdenum alloy was tested. It exhibited properties which make it suitable for application where high gain square hysteresis loop characteristics are required. There was no significant difference between the sine wave and square wave excitation properties obtained for this material.

Of the six magnetic materials tested herein, no one material was significantly more stable, nor was less subject to change than the other materials tested. Therefore

the selection of a material for a component design should be based upon the material best suited to perform the basic functions. The component and/or system design should then be modified to accommodate (or compensate) the anticipated material changes as a function of temperature, time and whether the temperature will be held constant or cycled.

The changes in properties presented herein are typical for the families of materials tested and should repeat for other heats of the same basic materials. The absolute values, however, will vary somewhat from the values shown herein. Bmax and Bm-Br may vary $\pm 10\%$, while Ho, Hc or ΔH may vary up to 20%.
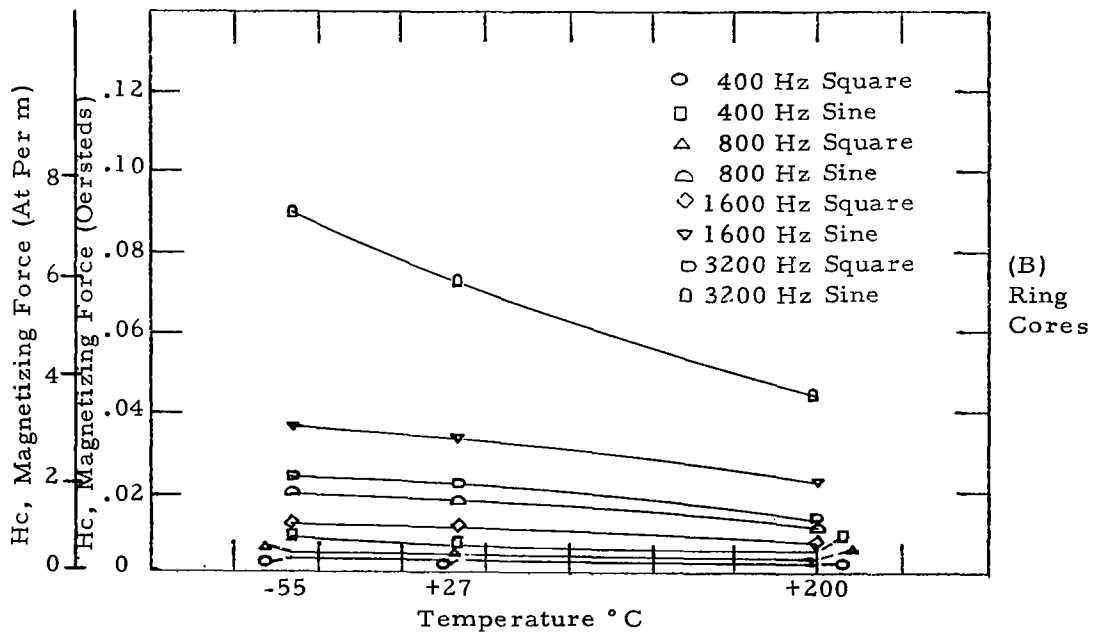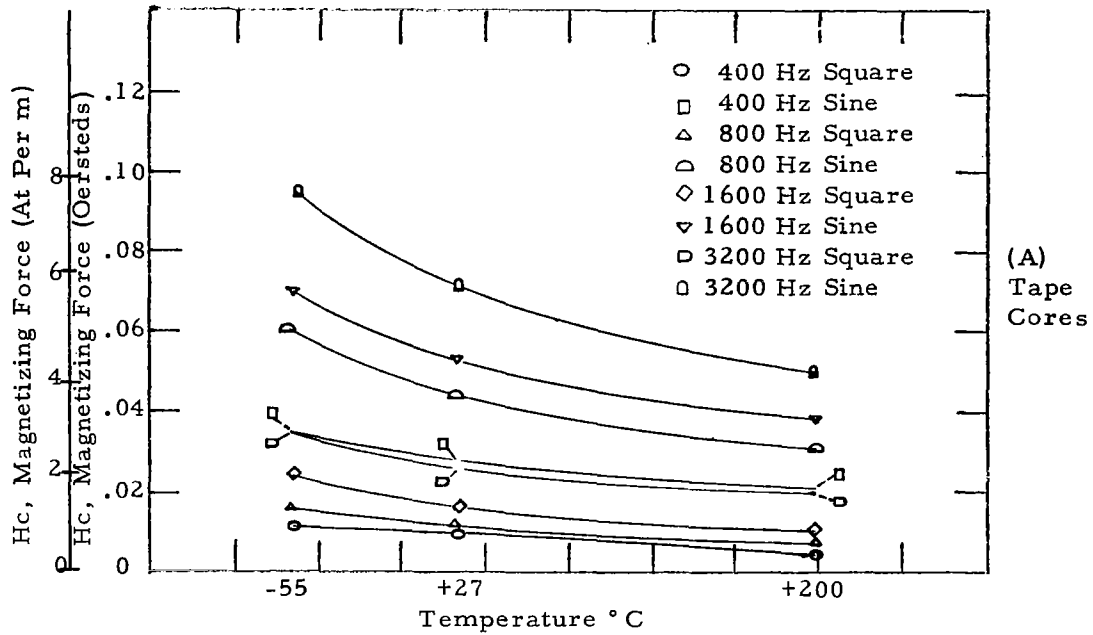
Figure 17 - AC Magnetization obtained from AC Hysteresis
Loop Data, High Purity 80% Nickel Alloy
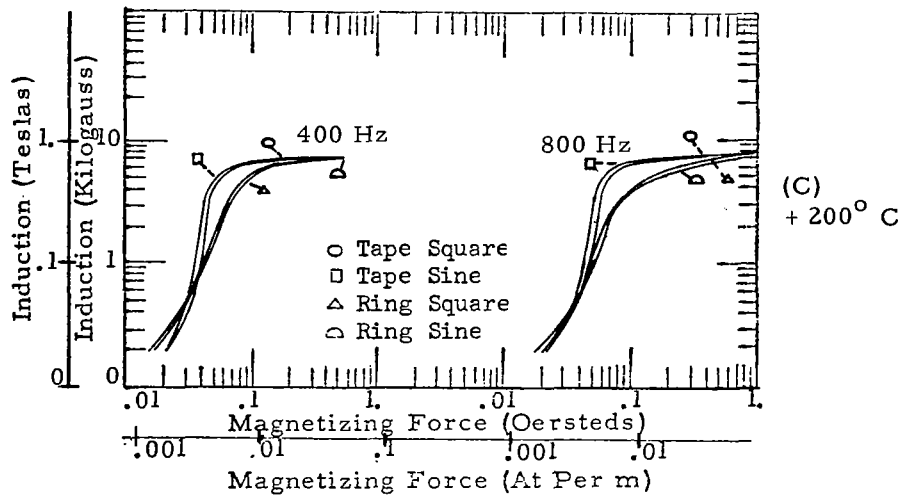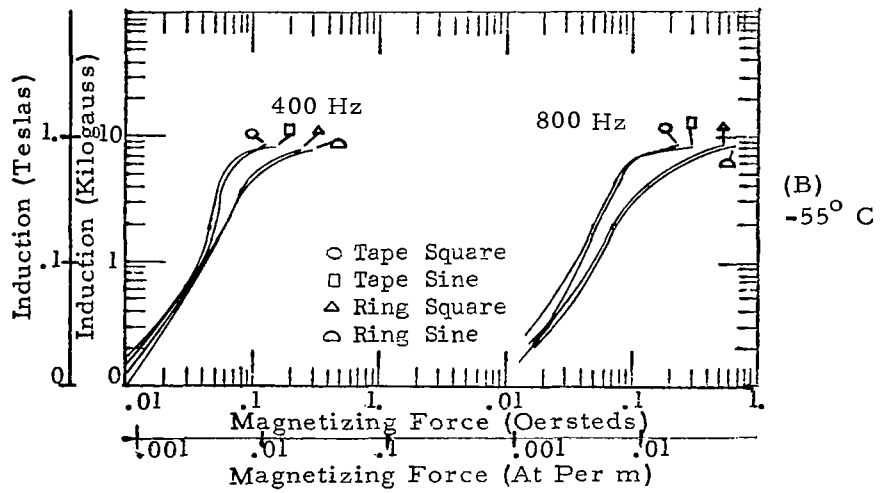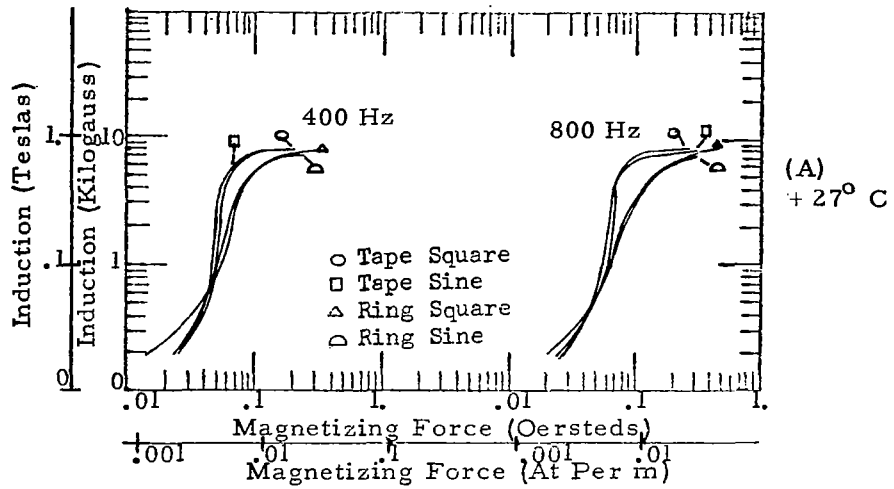
Figure 18 - AC Magnetization, 400 and 800 Hz
High Purity 80% Nickel Alloy
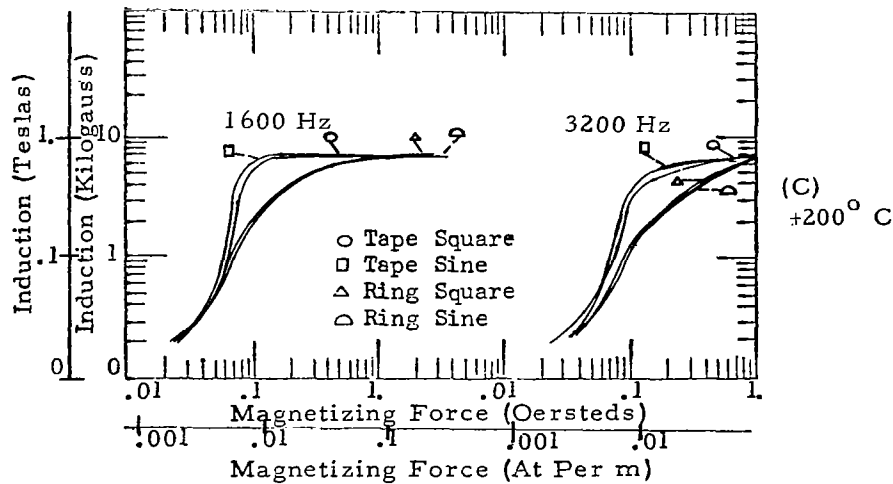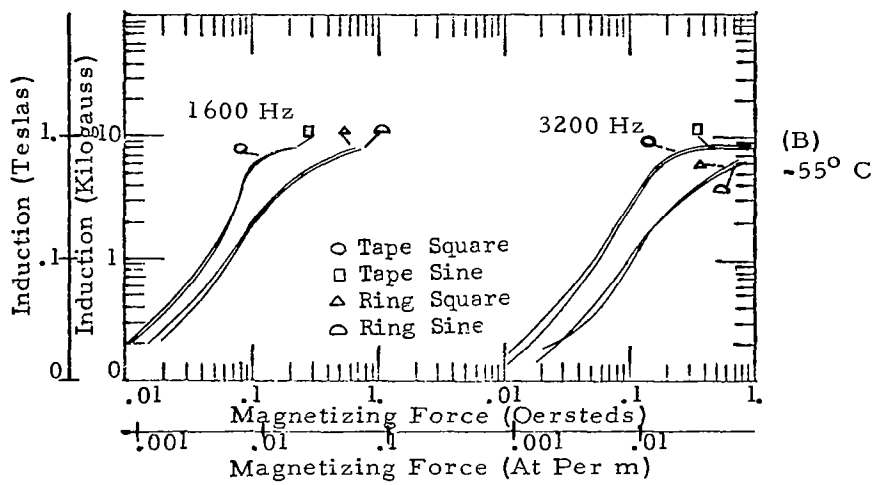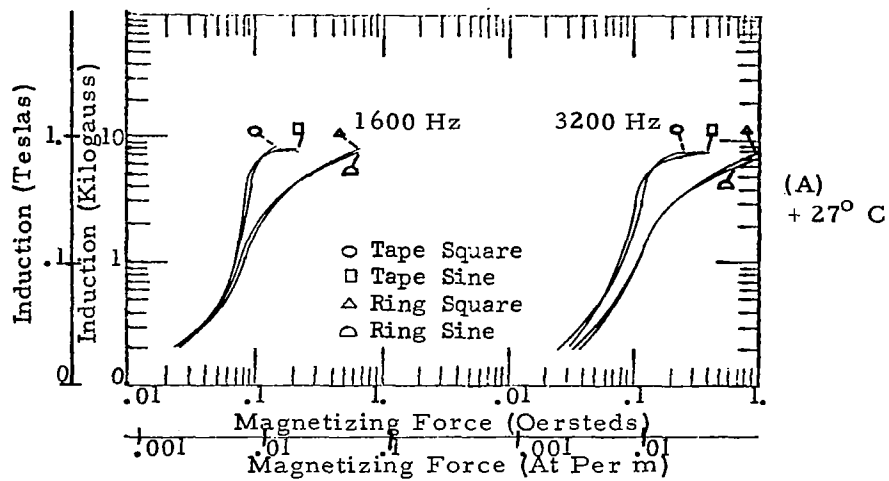
Figure 19 – AC Magnetization, 1600 and 3200 Hz,
High Purity 80% Nickel Alloy
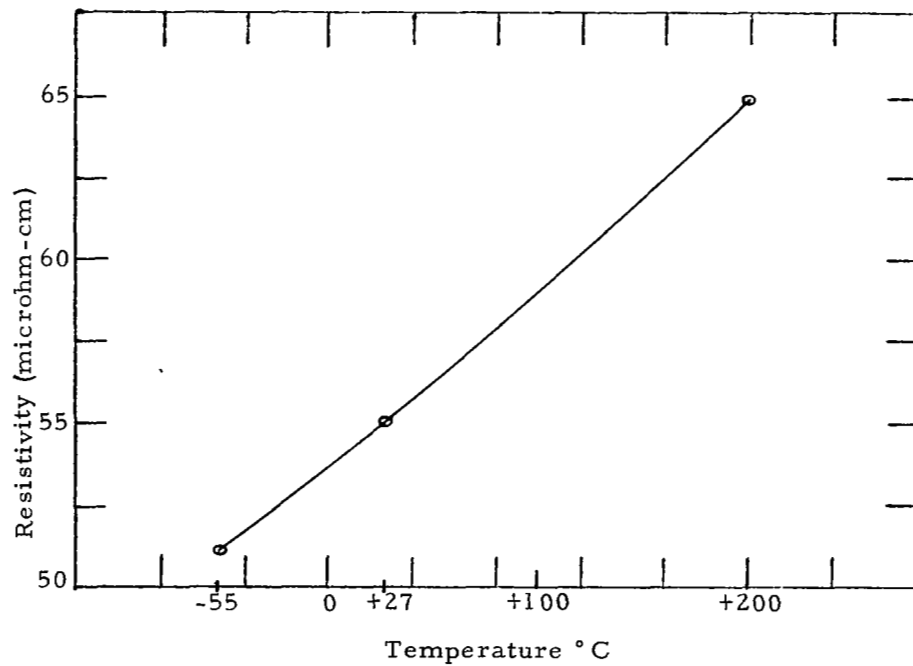
Figure 20 – Change of Resistance with change of Temperature,
High Purity 80% Nickel Alloy.
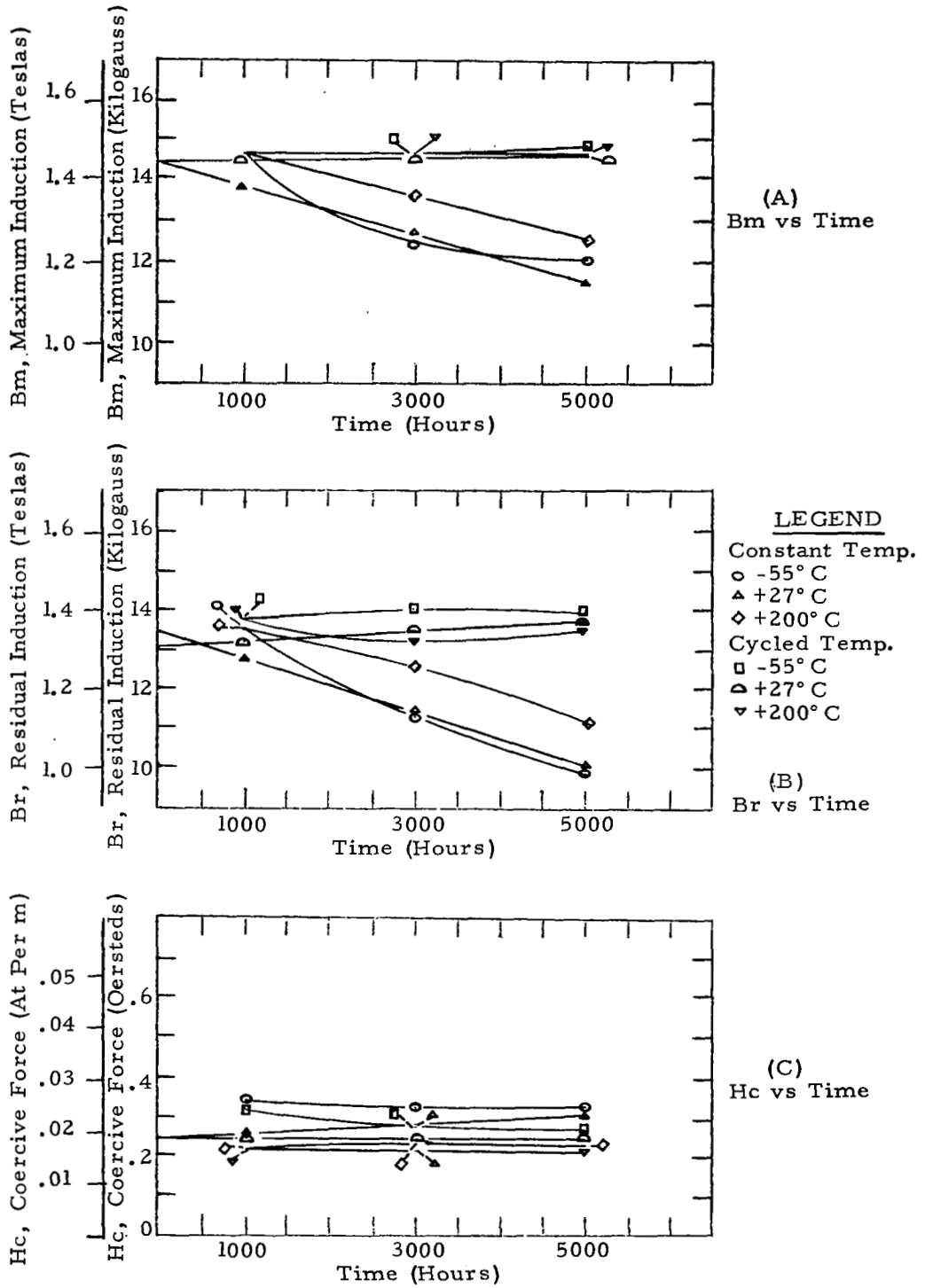
Figure 21 - Maximum and Residual Induction and Coercive Force
obtained from AC Hysteresis Loops, 0. 002 inch Tape Cores,
Single Grain Oriented Silicon Iron

35
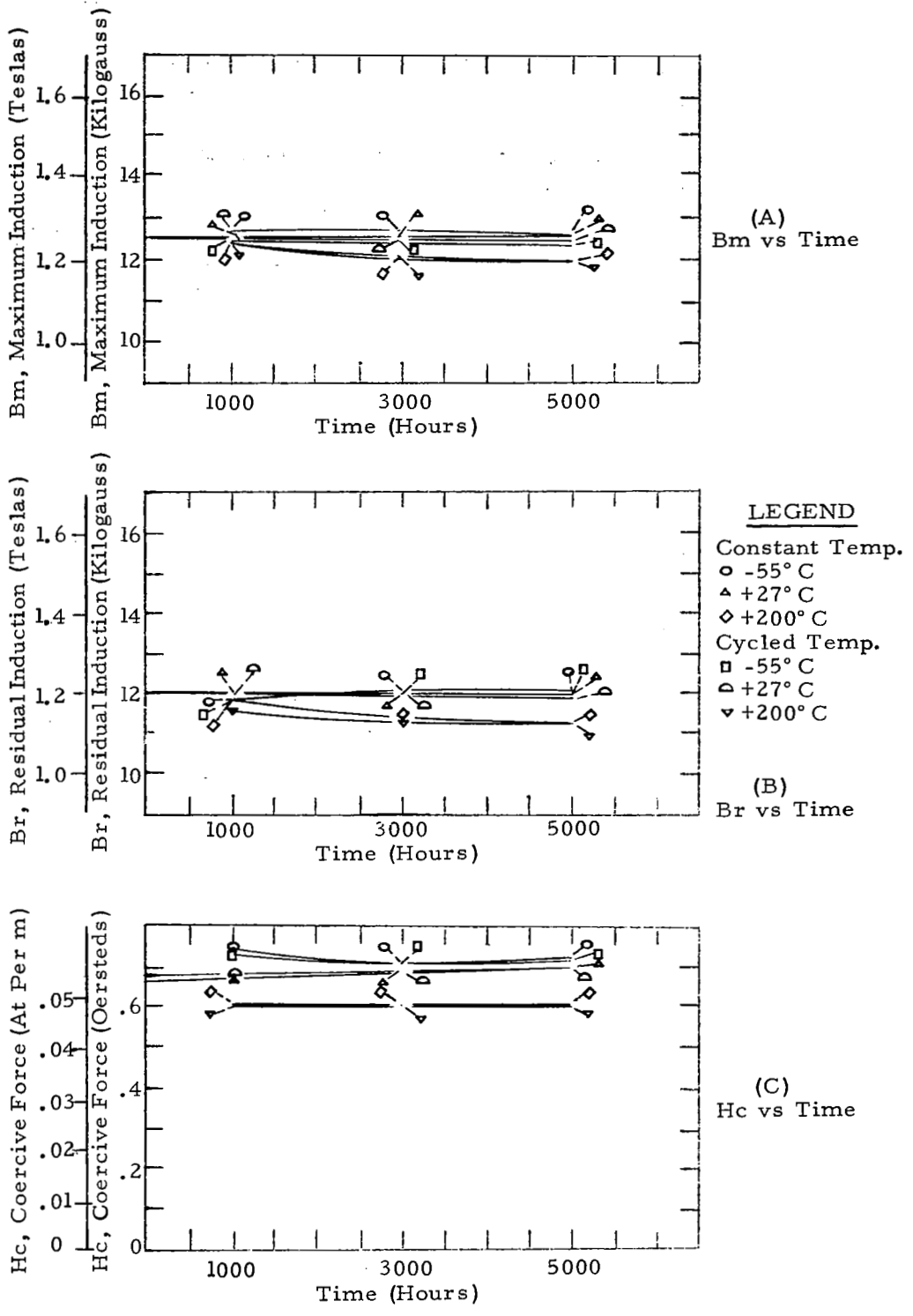
Figure 22 - Maximum and Residual Induction and Coercive Force
obtained from AC Hysteresis Loops, 0.006 inch Ring Cores,
Single Grain Oriented Silicon Iron
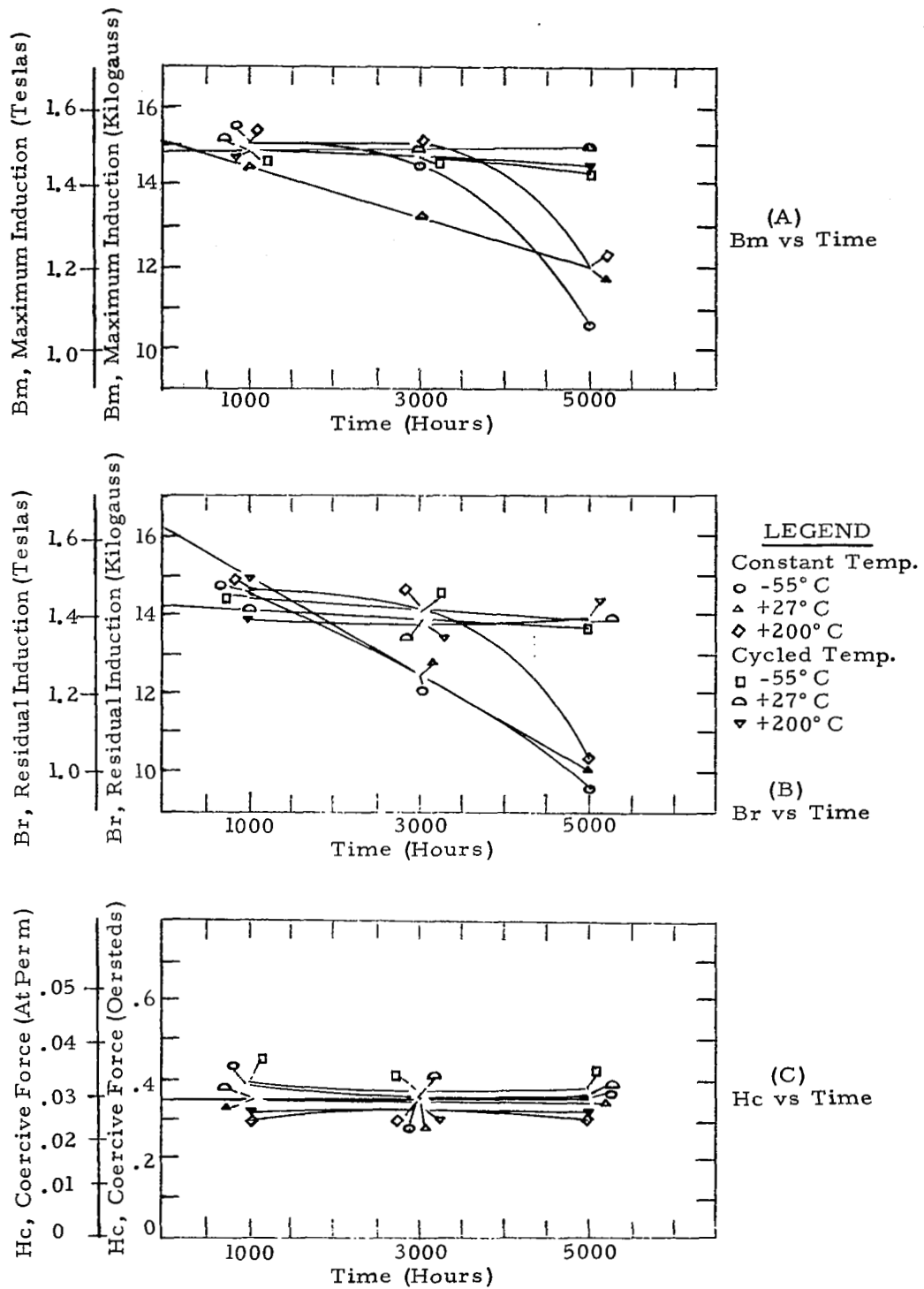
Figure 23 – Maximum and Residual Induction and Coercive Force
obtained from AC Hysteresis Loops, 0.002 inch Tape Cores,
Doubly Grain Oriented Silicon Iron

37
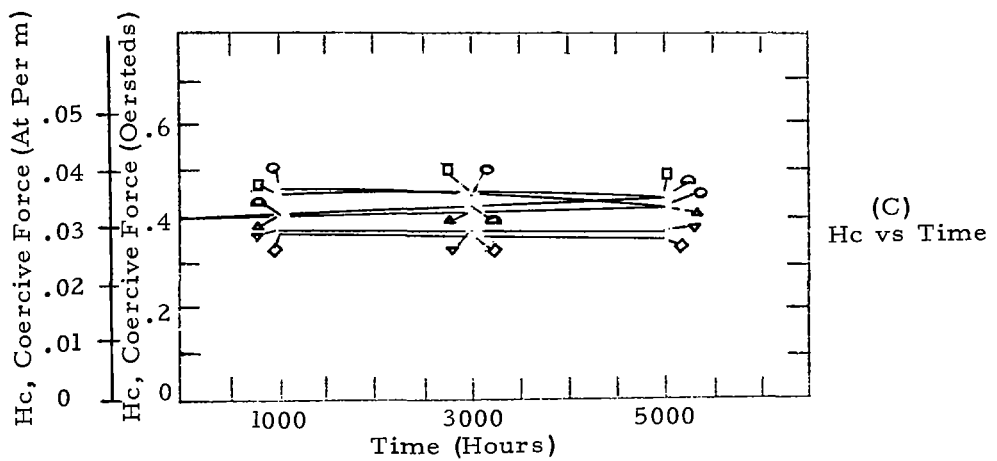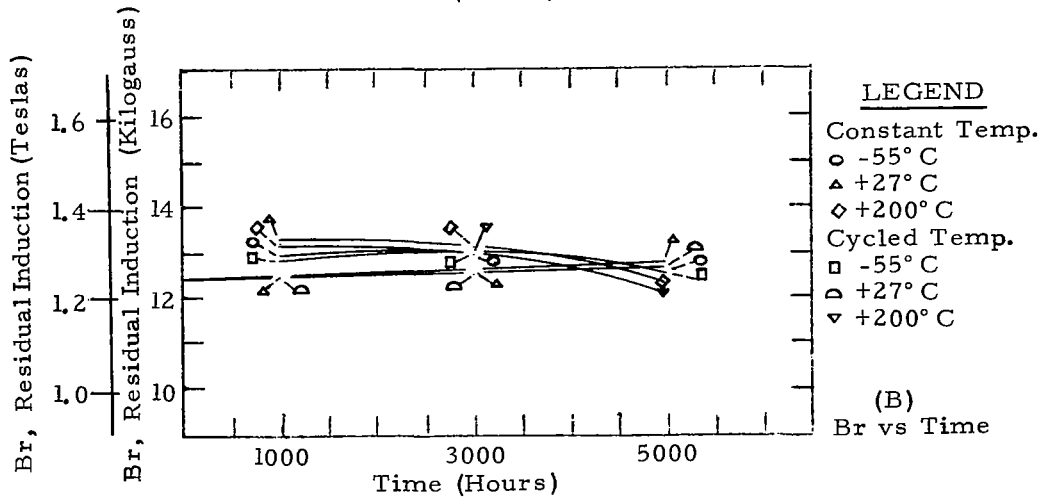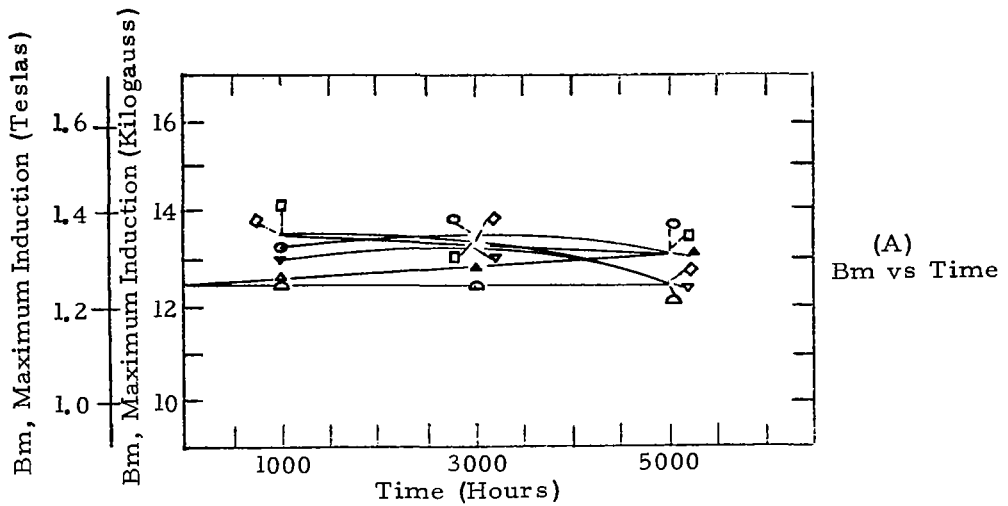
Figure 24 - Maximum and Residual Induction and Coercive Force obtained from AC Hysteresis Loops, 0.006 inch Ring Cores, Doubly Grain Oriented Silicon Iron

38
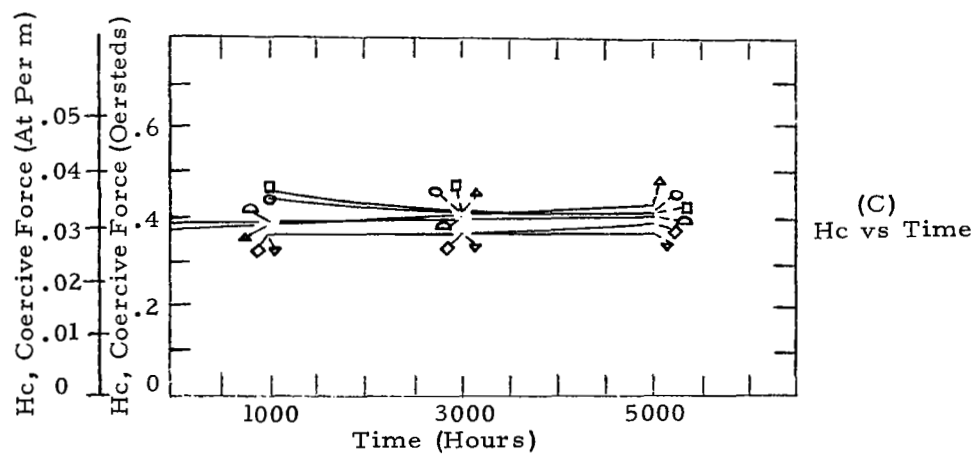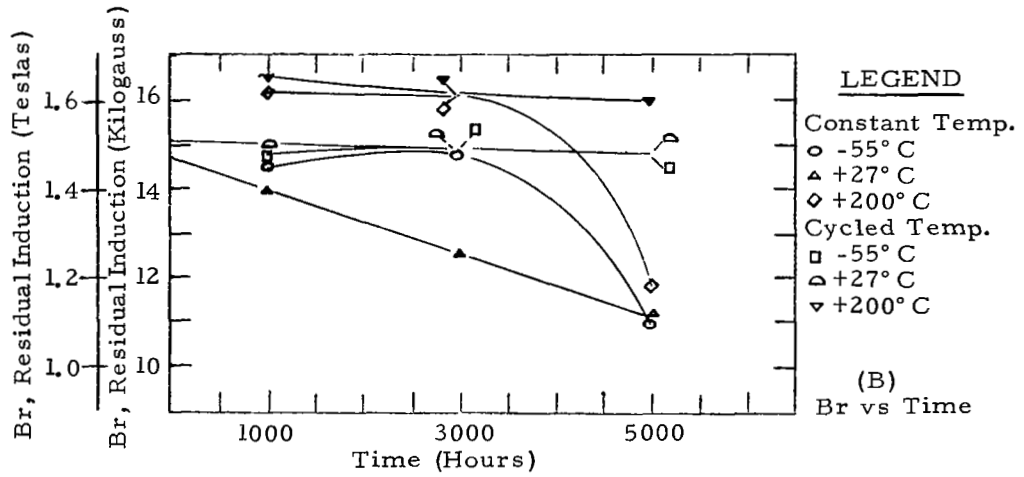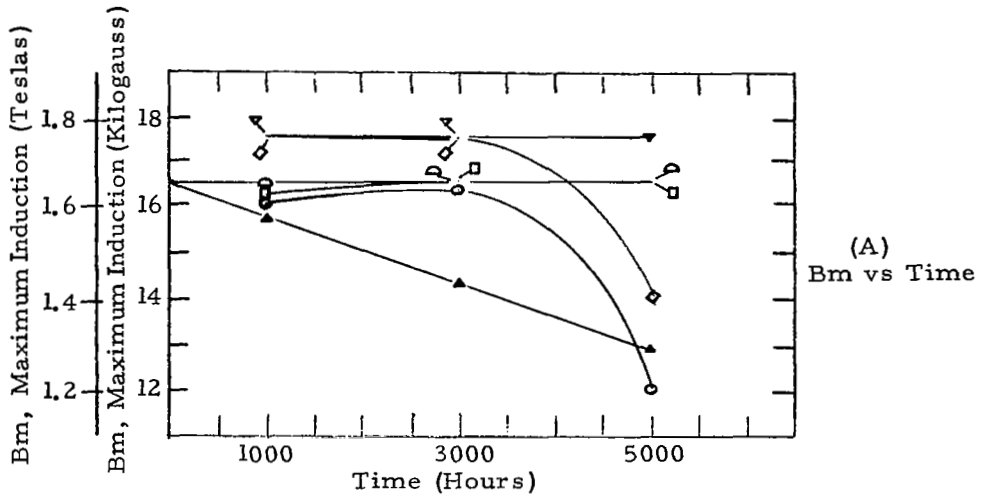
Figure 25 - Maximum and Residual Induction and Coercive Force
obtained from AC Hysteresis Loops, 0.002 inch Tape Cores,
49% Cobalt Alloy
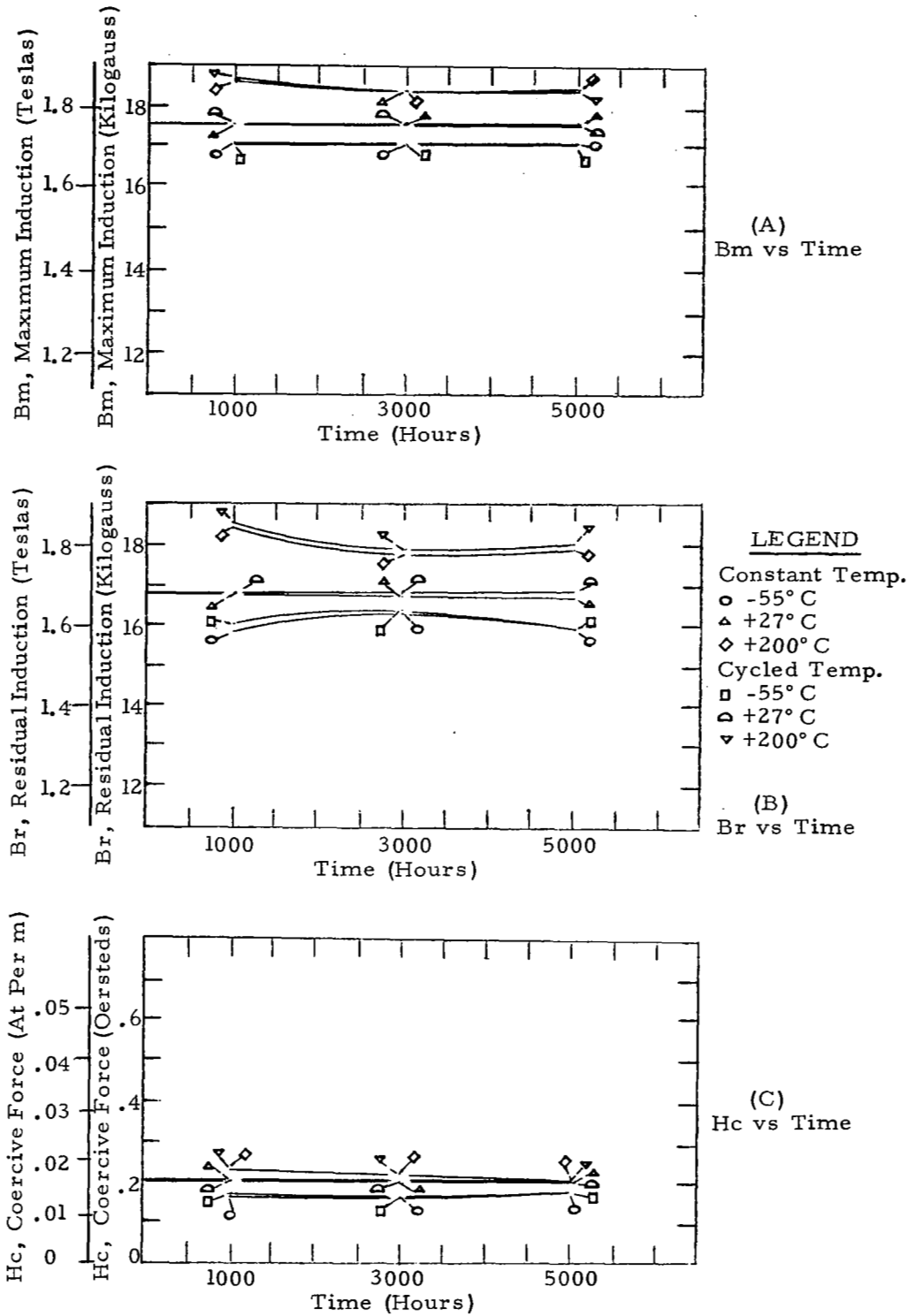
Figure 26 - Maximum and Residual Induction and Coercive Force
obtained from AC Hysteresis Loops, 0.006 inch Ring Cores,
49% Cobalt Alloy
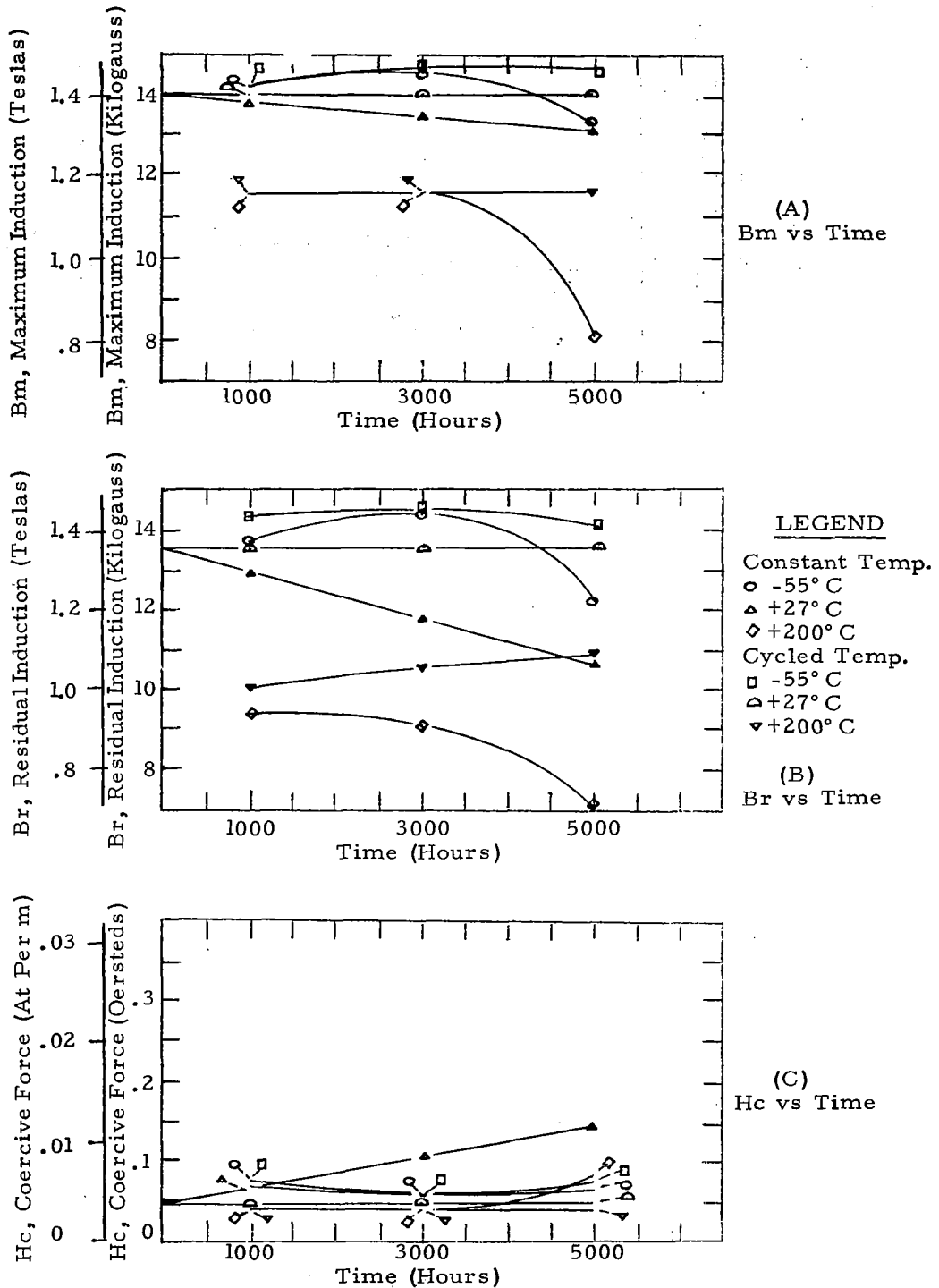
Figure 27 – Maximum and Residual Induction and Coercive Force
obtained from AC Hysteresis Loops, 0.002 inch Tape Cores,
50% Nickel Alloy

41
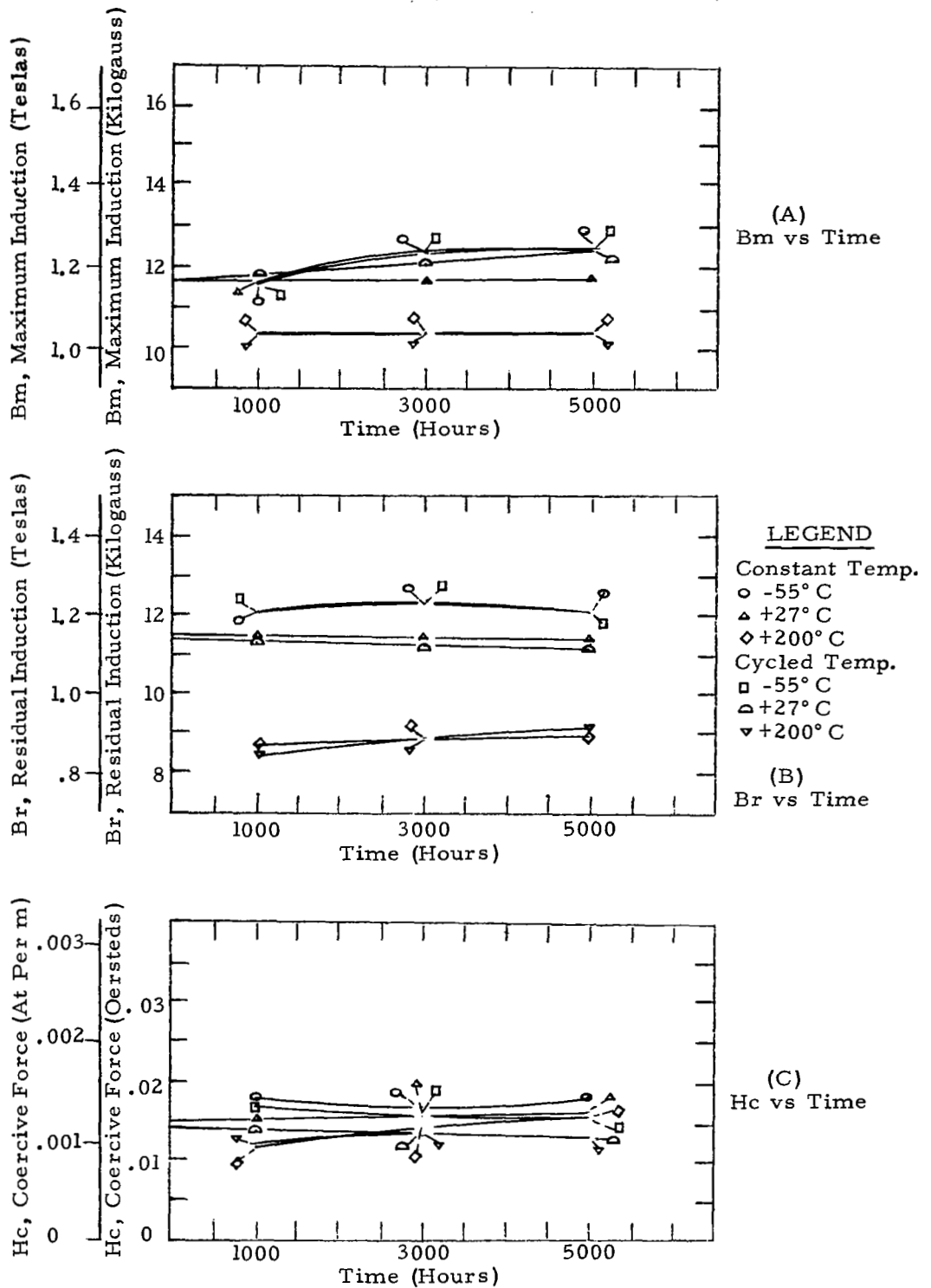
Figure 28 - Maximum and Residual Induction and Coercive Force
obtained from AC Hysteresis Loops, 0.006 inch Ring Cores,
50% Nickel Alloy

42
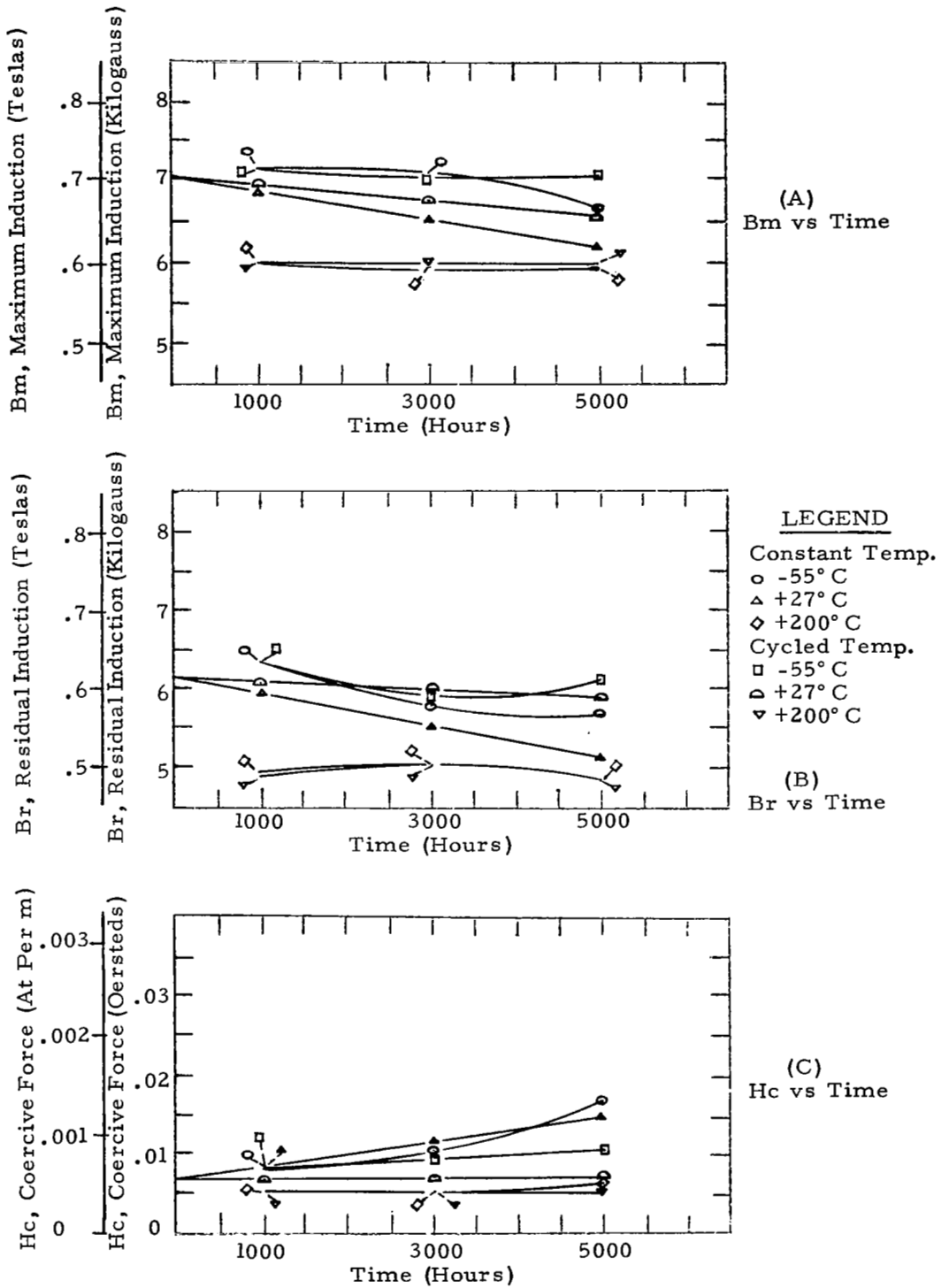
Figure 29 - Maximum and Residual Induction and Coercive Force obtained from AC Hysteresis Loops, 0.002 inch Tape Cores, 79% Nickel Alloy

43
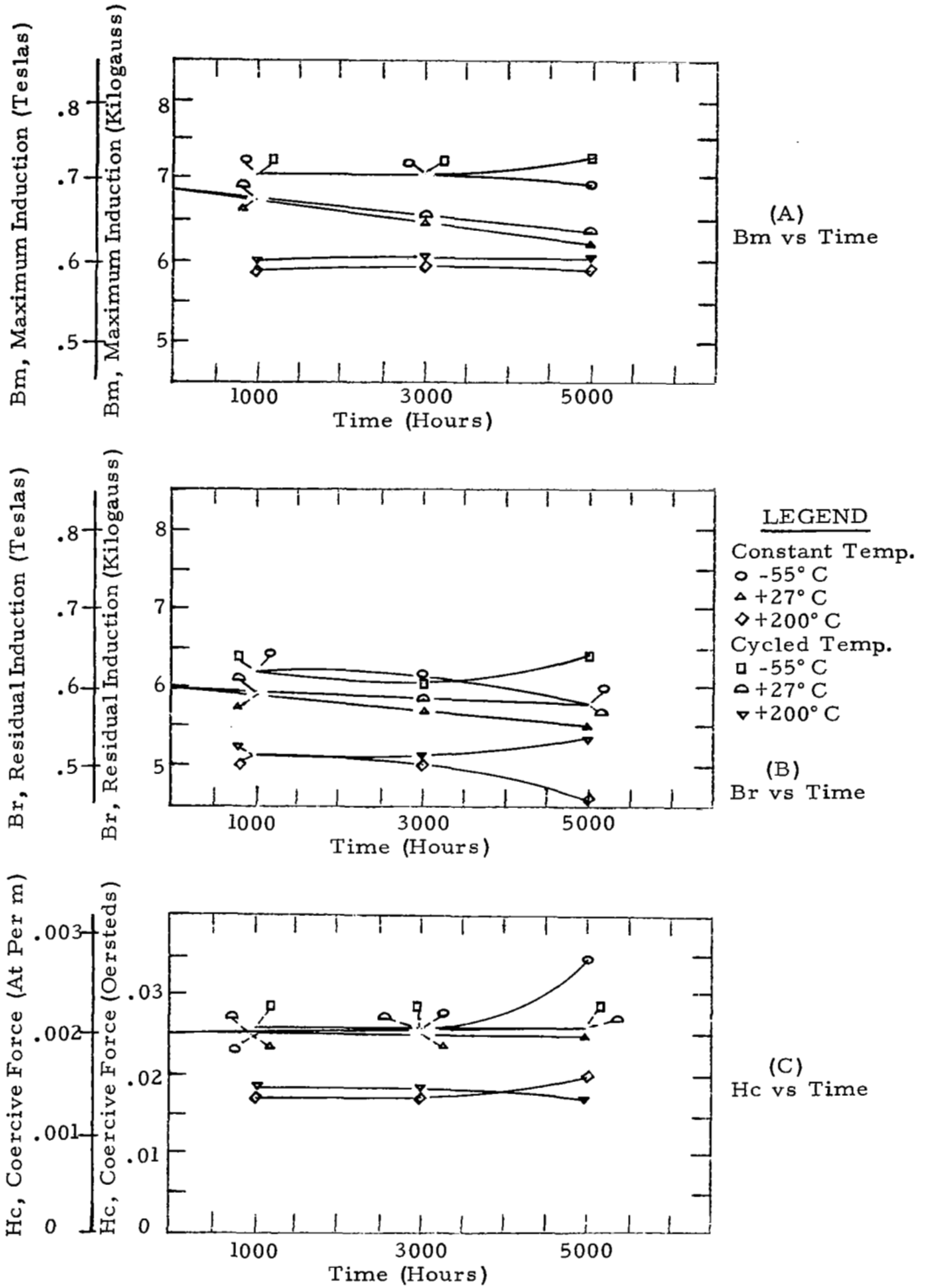
Figure 30 - Maximum and Residual Induction and Coercive Force
obtained from AC Hysteresis Loops, 0.006 Ring Cores,
79% Nickel Alloy
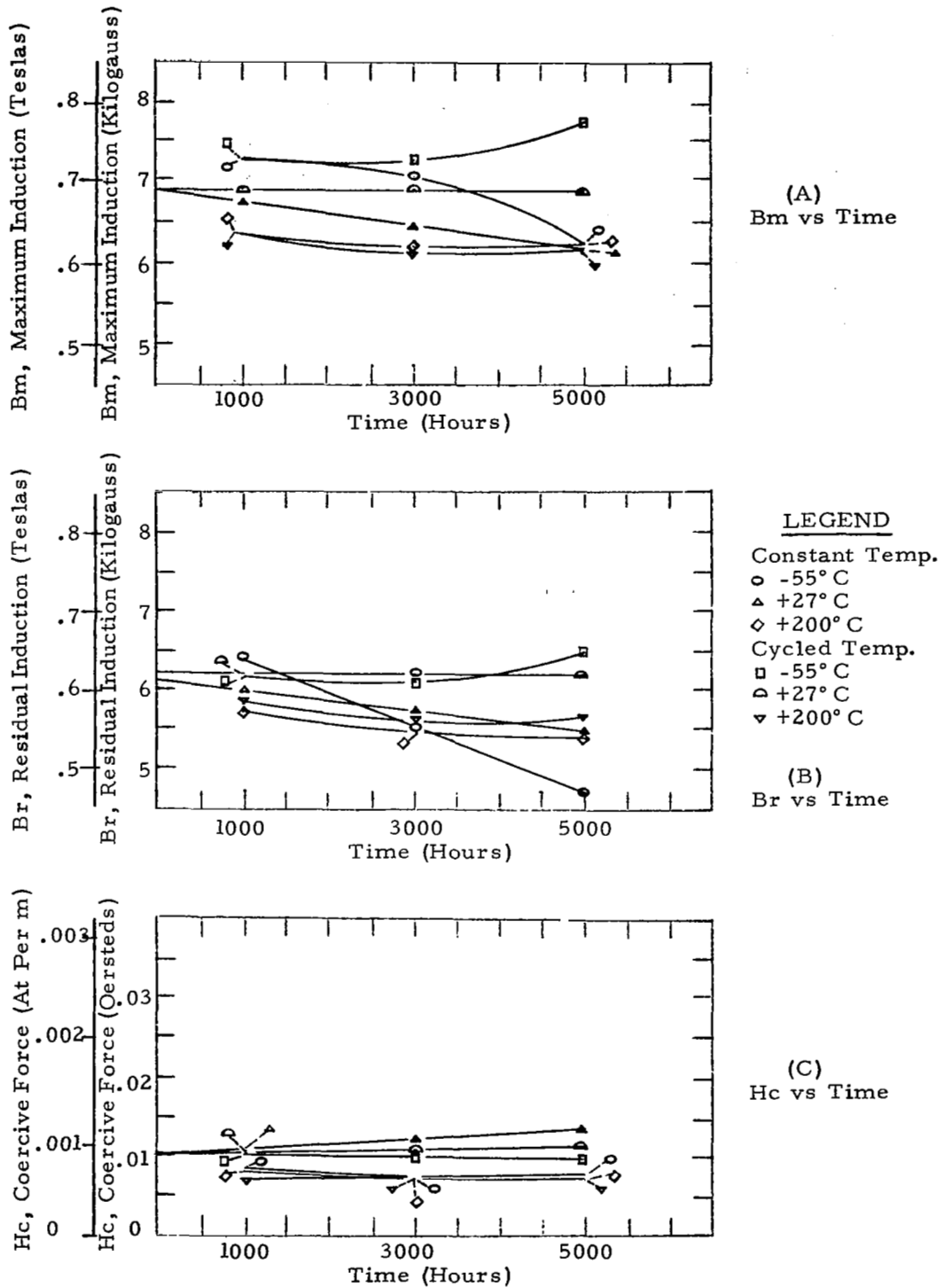
Figure 31 - Maximum and Residual Induction and Coercive Force
obtained from AC Hysteresis Loops, 0.002 inch Tape Cores,
High Purity 80% Nickel Alloy
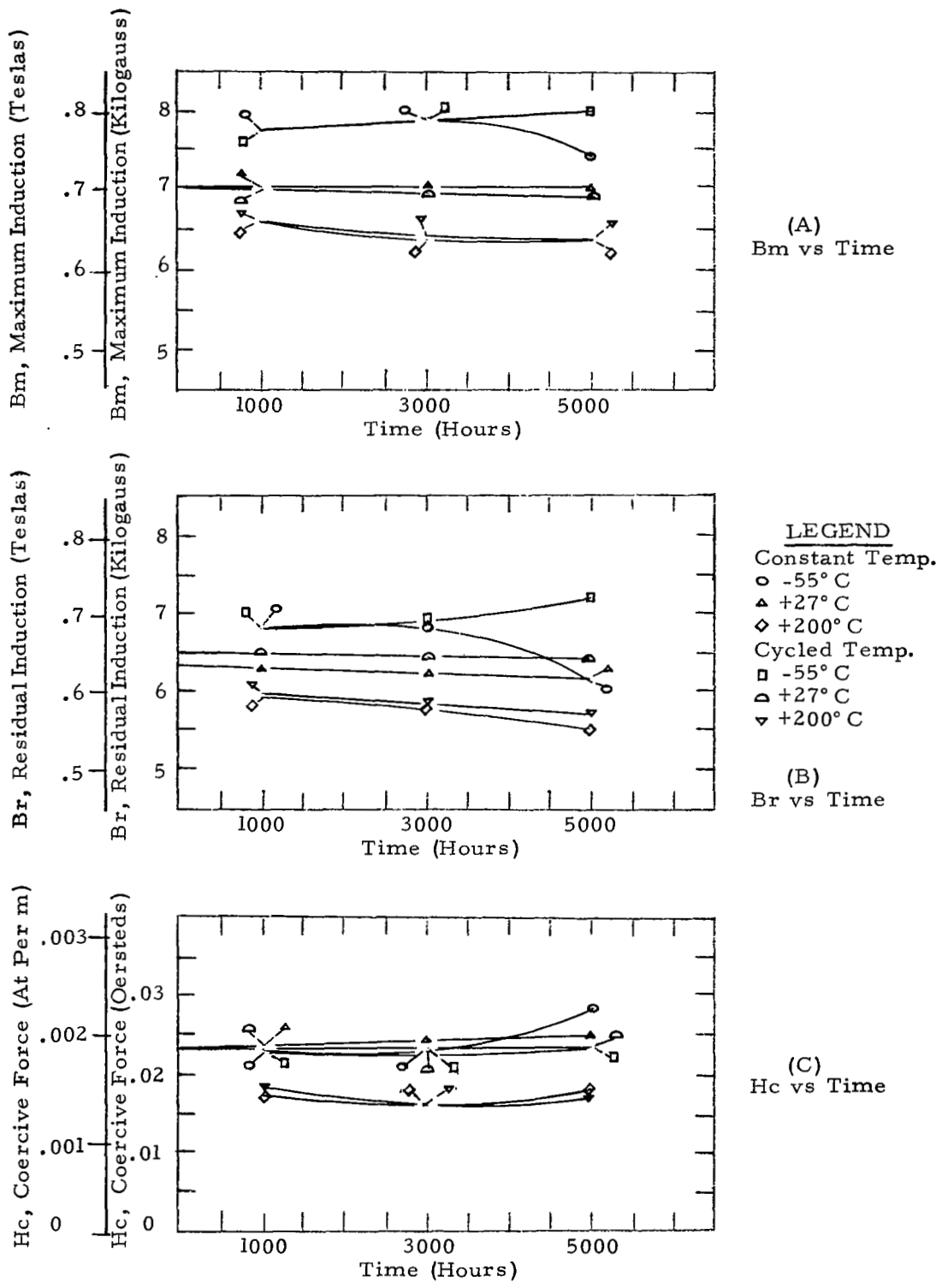
Figure 32 - Maximum and Residual Induction and Coercive Force
obtained from AC Hysteresis Loops, 0. 006 inch Ring Cores,
High Purity 80% Nickel Alloy

46

(A)
Single Grain
Oriented
Silicon Iron

LEGEND

+ 27° C 0 Hrs.
- 55° C 5000 Hrs.
+ 27° C 5000 Hrs.
+ 200° C 5000 Hrs.

(B)
Doubly Grain
Oriented
Silicon Iron.

(C)
49% Cobalt Alloy
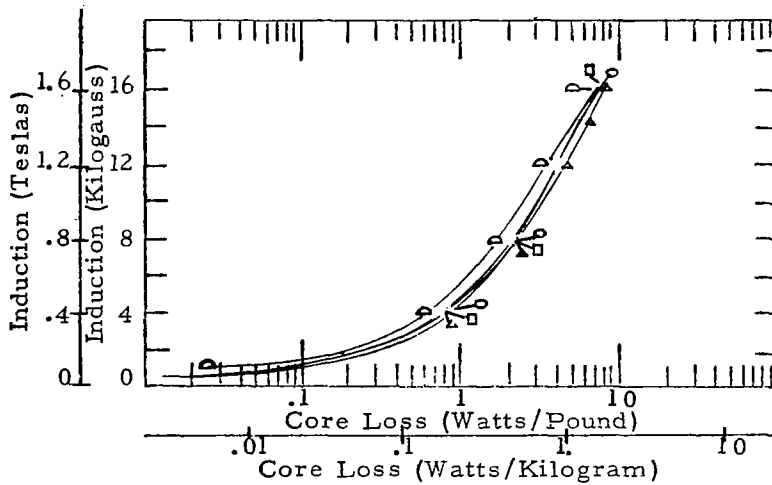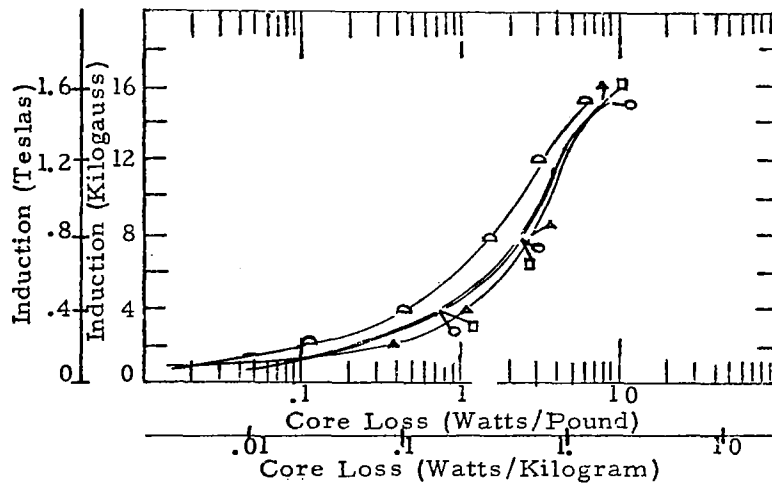
Figure 33 - Core Loss vs. Time and Temperature.
0. 002 inch Tape Cores, Temperature Cycled.
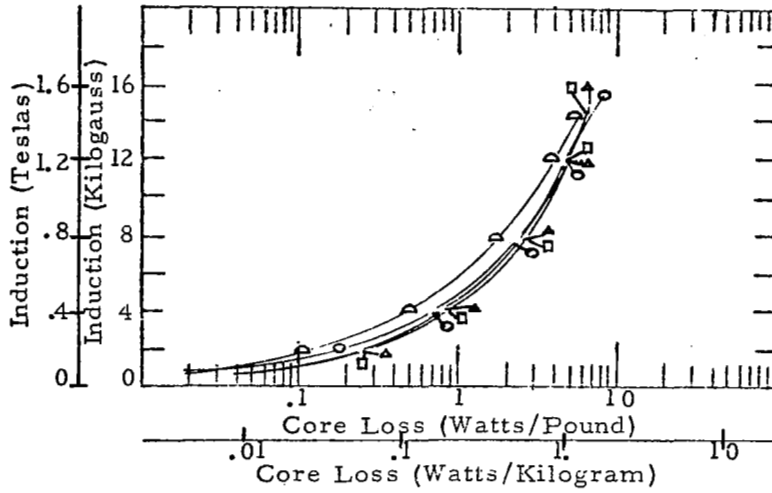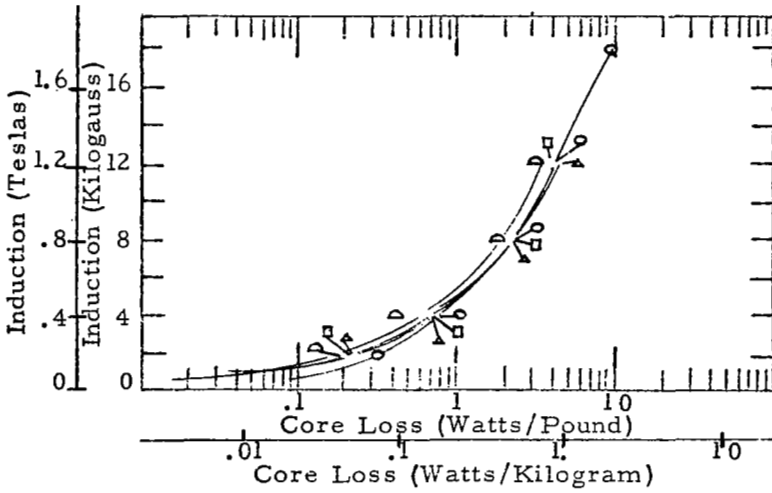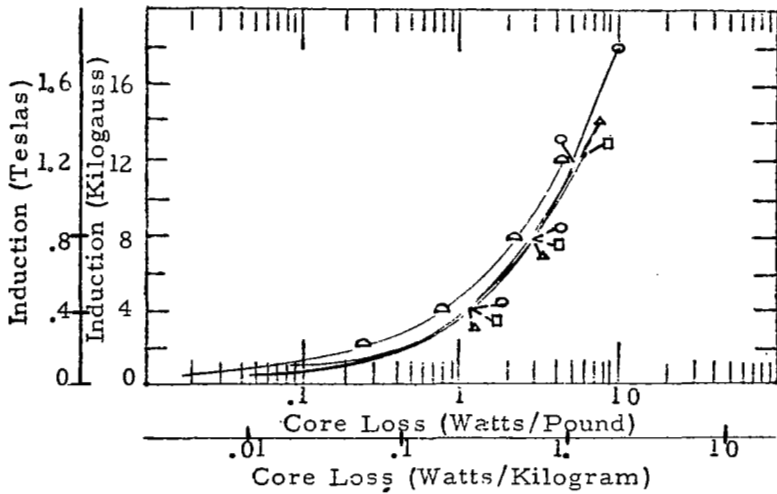
Figure 34 - Core Loss vs. Time and Temperature.
0. 002 inch Tape Cores, Temperature Constant.

48

Figure 35 - Core Loss vs. Time and Temperature.
0. 002 inch Tape Cores, Temperature Cycled.

Figure 36 - Core Loss vs. Time and Temperature.
0. 002 inch Tape Cores, Temperature Constant.
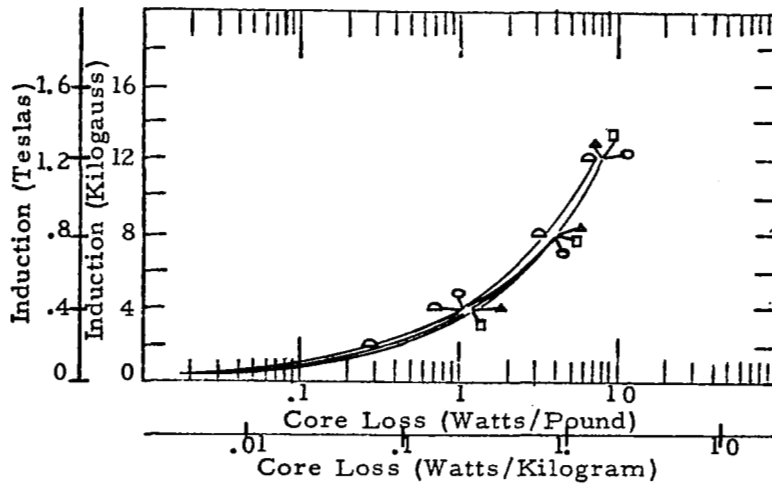
(A)
Single Grain
Oriented
Silicon Iron

LEGEND
+27° C 0 Hrs.
−55° C 5000 Hrs.
+27° C 5000 Hrs.
+200° C 5000 Hrs.

(B)
Doubly Grain
Oriented
Silicon Iron
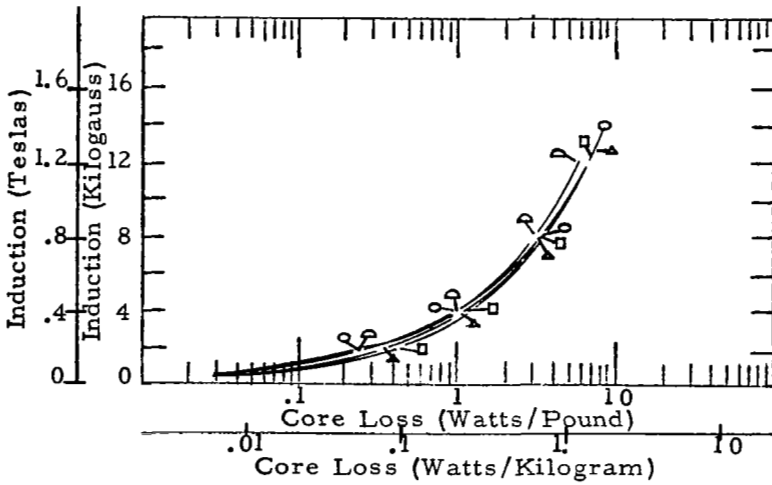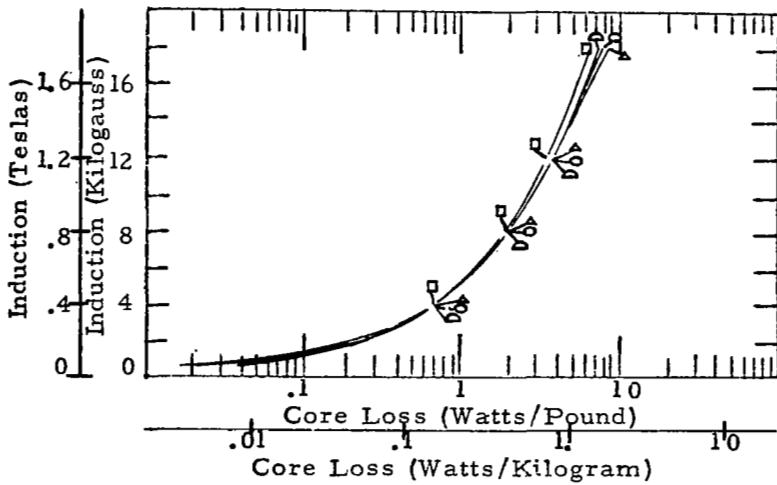
(C)
49% Cobalt Alloy

Figure 37 − Core Loss vs. Time and Temperature.
0. 006 inch Ring Cores, Temperature Cycled.
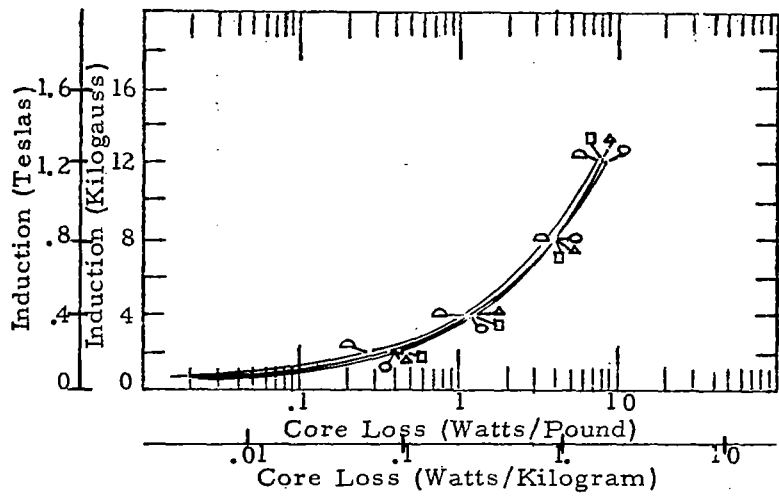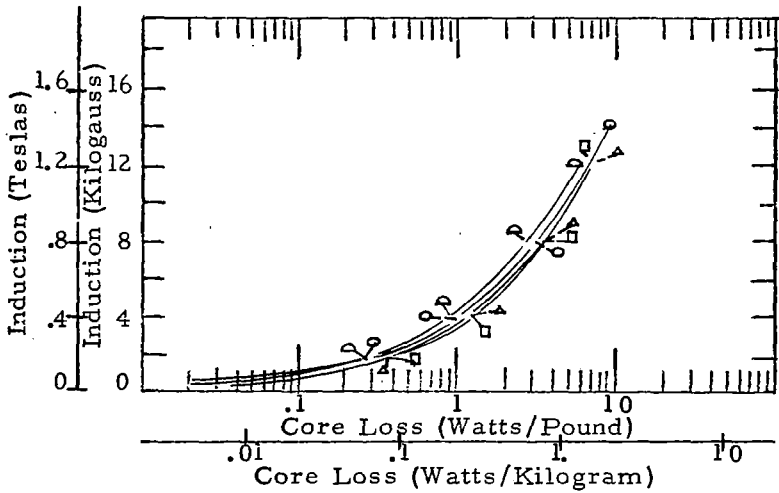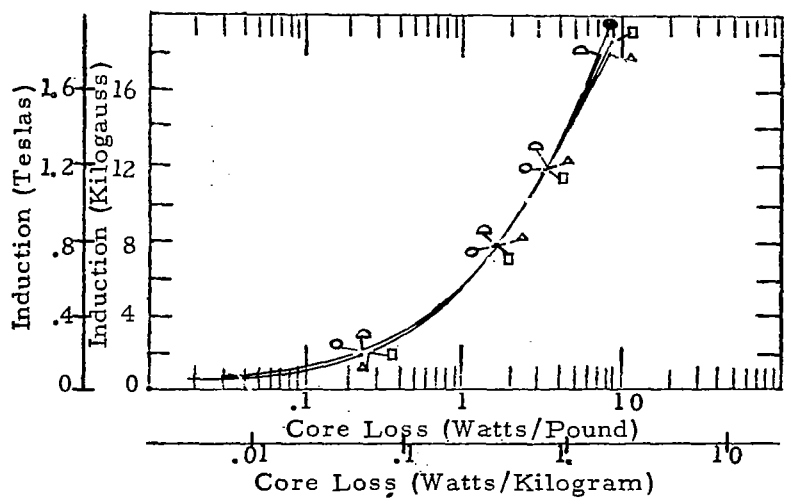
Figure 38 -   Core Loss vs. Time and Temperature.
0. 006 inch Ring Cores, Temperature Constant.

52

(A)
50% Nickel Alloy

LEGEND
+27° C 0 Hrs.
-55° C 5000 Hrs.
+27° C 5000 Hrs.
+200° C 5000 Hrs.
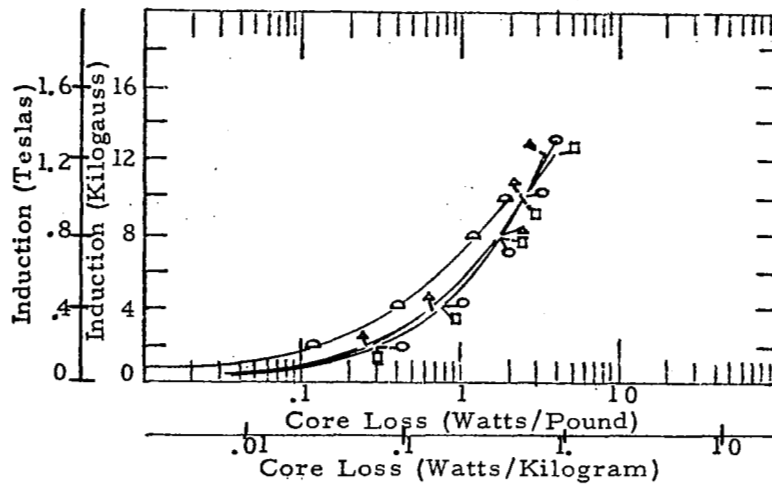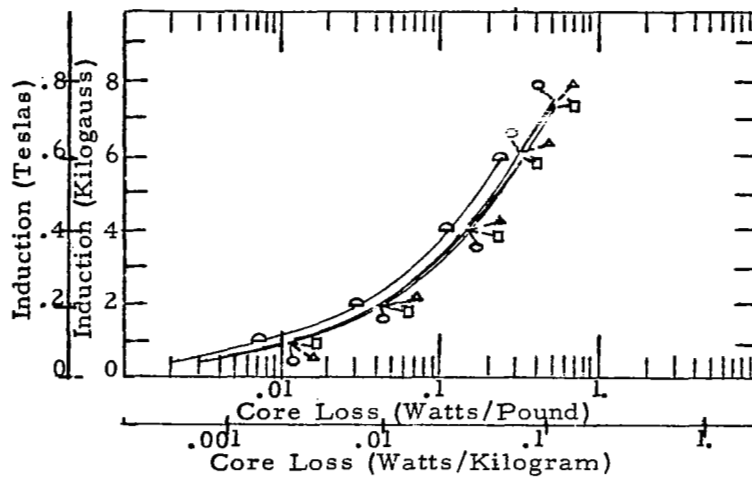
(B)
79% Nickel Alloy
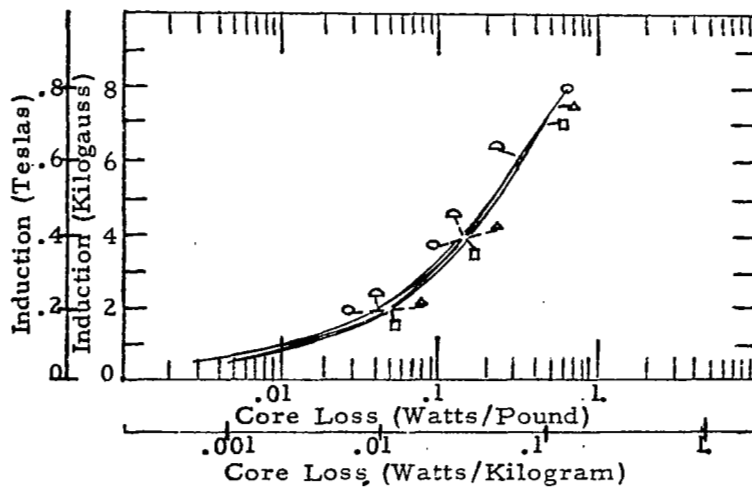
(C)
High Purity
80% Nickel Alloy

Figure 39 - Core Loss vs. Time and Temperature
0. 006 inch Ring Cores, Temperature Cycled.

Figure 40 - Core Loss vs. Time and Temperature
0. 006 inch Ring Cores, Temperature Constant.
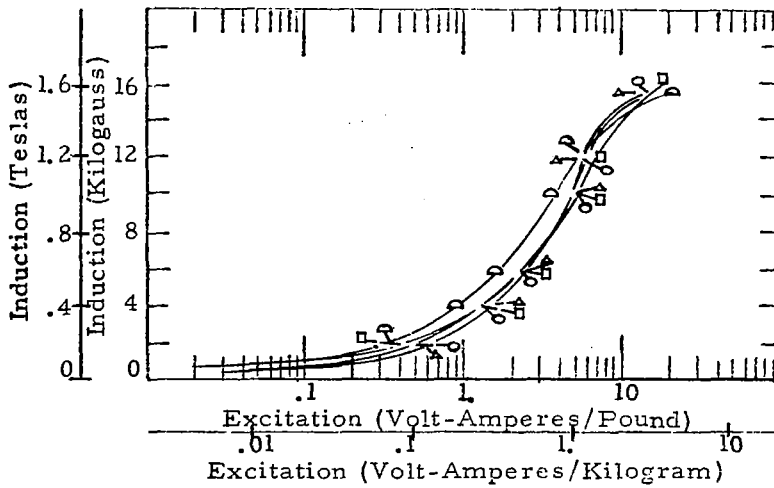
54
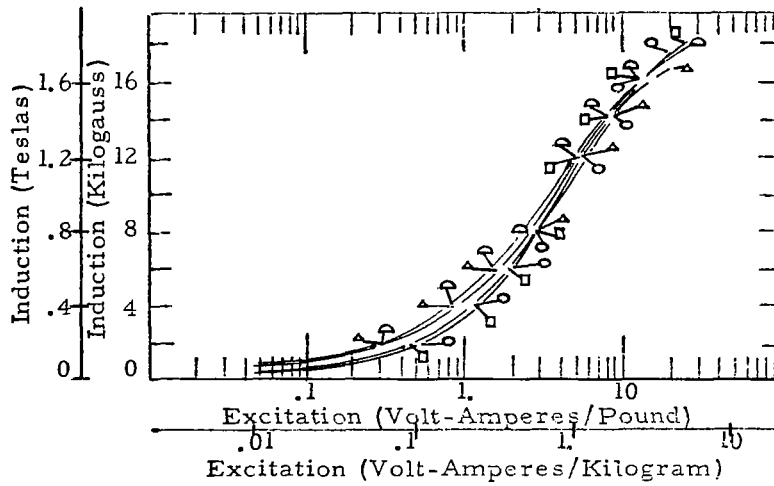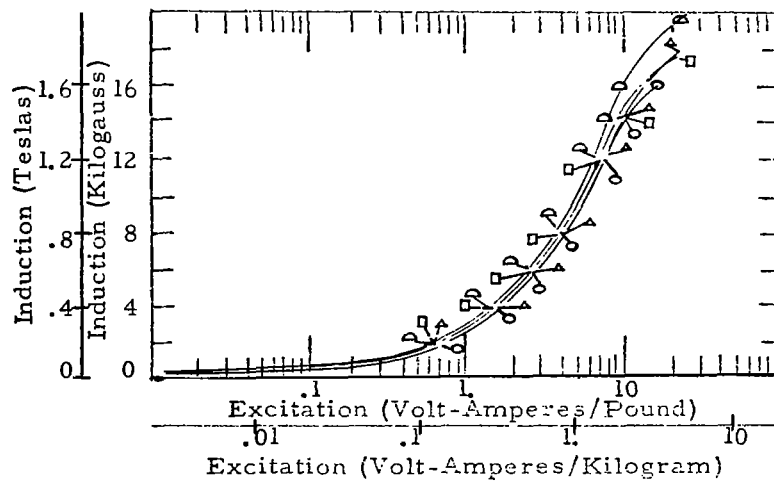
Figure 41 - Excitation vs. Time and Temperature
0.002 inch Tape Cores, Temperature Cycled.
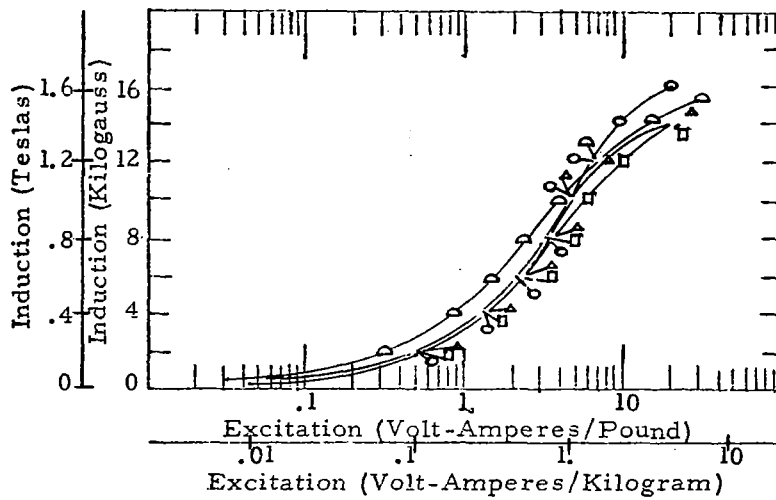
55

(A)
Single Grain
Oriented
Silicon Iron

LEGEND
+27° C 0 Hrs.
-55° C 5000 Hrs.
+27° C 5000 Hrs.
+200° C 5000 Hrs.

(B)
Doubly Grain
Oriented
Silicon Iron
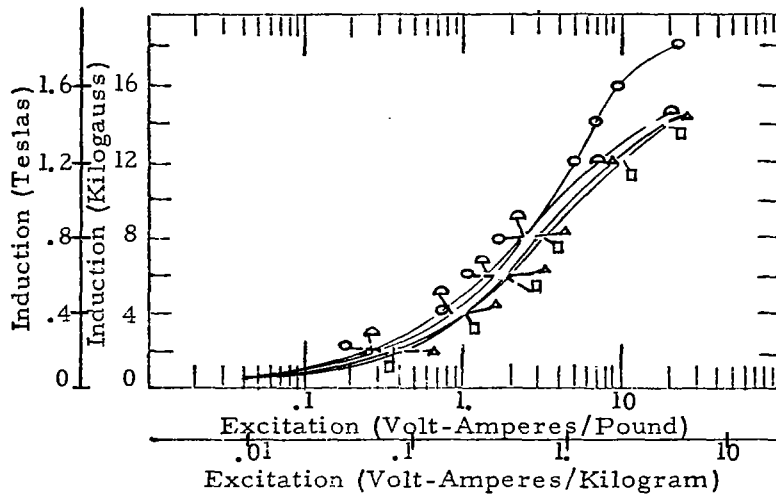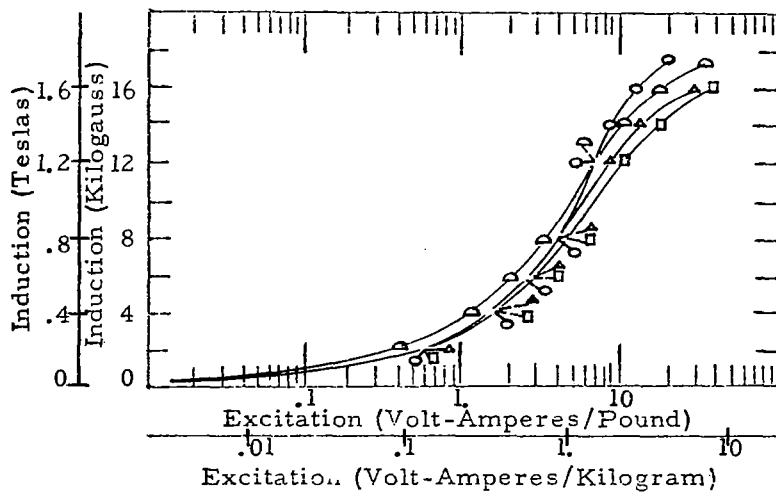
(C)
49% Cobalt Alloy

Figure 42 – Excitation vs. Time and Temperature
0. 002 inch Tape Cores, Temperature Constant.

Figure 43 - Excitation vs. Time and Temperature
0.002 inch Tape Cores, Temperature Cycled.

Figure 44 - Excitation vs. Time and Temperature
0. 002 inch Tape Cores, Temperature Constant.
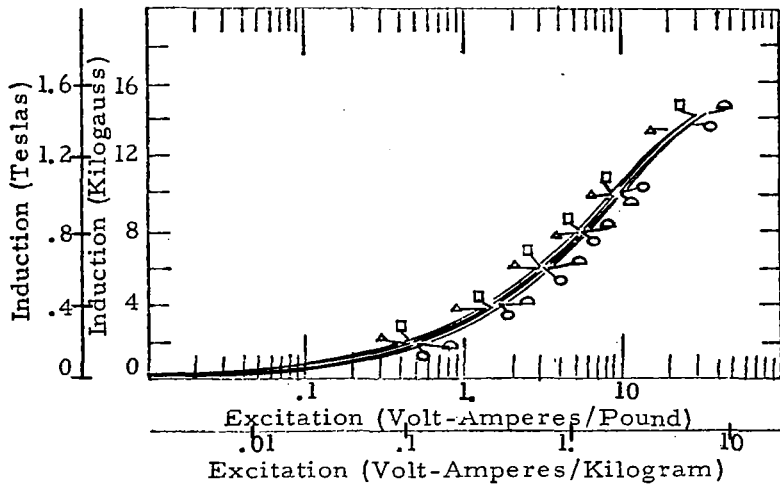
(A)
Single Grain
Oriented
Silicon Iron

LEGEND
+27° C 0 Hrs.
-55° C 5000 Hrs.
+27° C 5000 Hrs.
+200° C 5000 Hrs.

(B)
Doubly Grain
Oriented
Silicon Iron
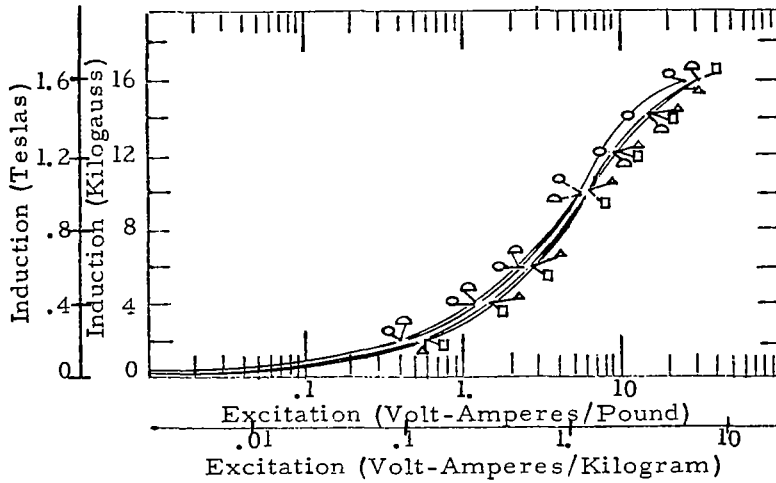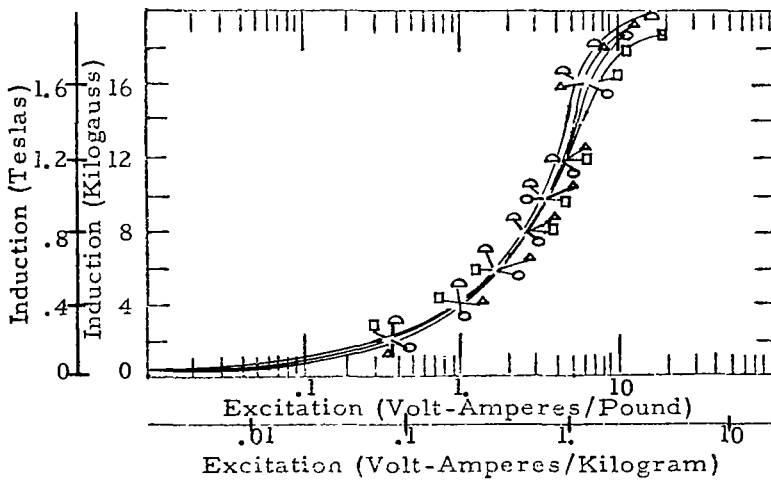
(C)
49% Cobalt Alloy

Figure 45 - Excitation vs. Time and Temperature
0.006 inch Ring Cores, Temperature Cycled.
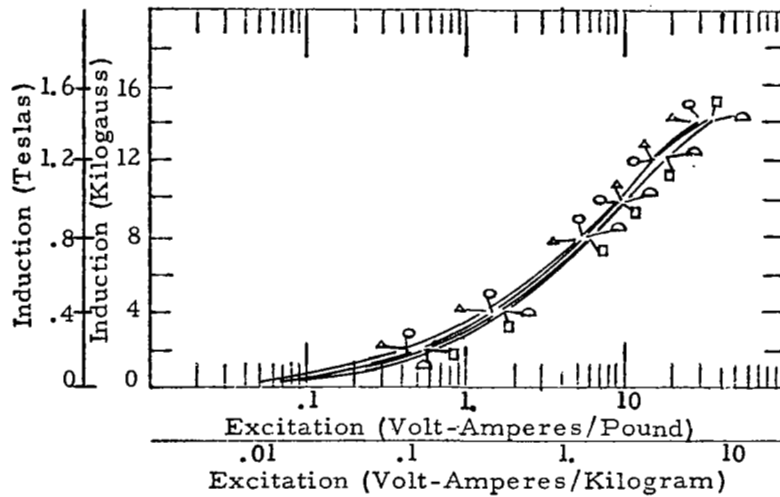
59

(A)
Single Grain
Oriented
Silicon Iron

(B)
Doubly Grain
Oriented
Silicon Iron
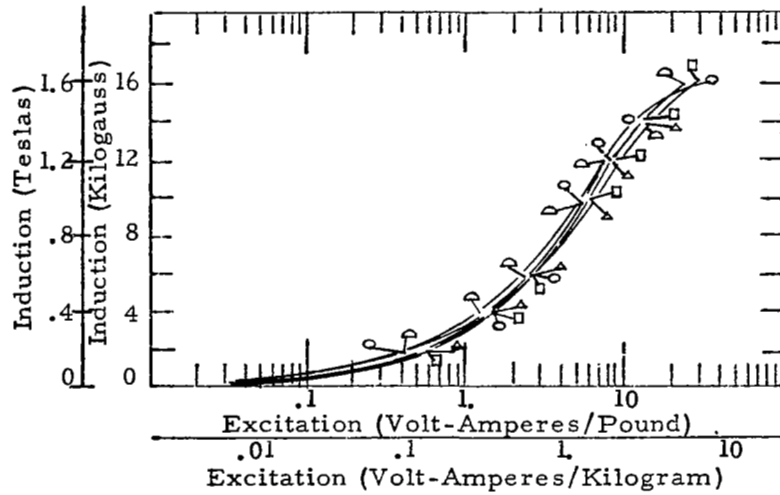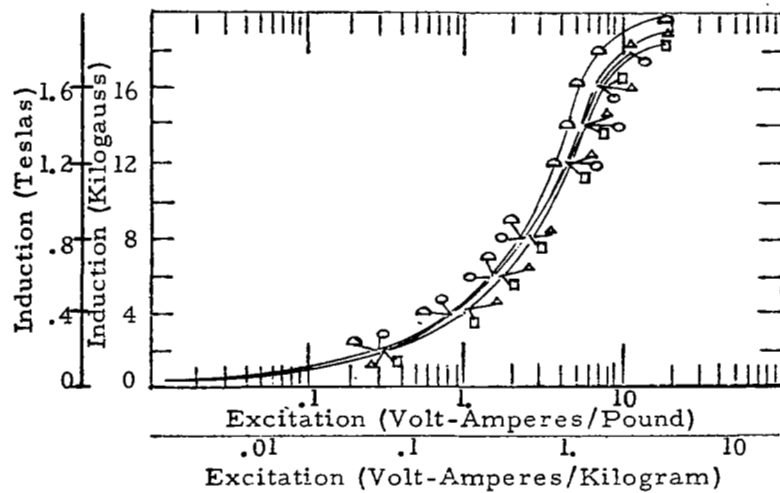
(C)
49% Cobalt Alloy

Figure 46 -   Excitation vs. Time and Temperature
0. 006 inch Ring Cores, Temperature Constant.

Figure 47 – Excitation vs. Time and Temperature
0.006 inch **Ring Cores, Temperature Cycled.**

Figure 48 - Excitation vs. Time and Temperature
0.006 inch Ring Cores, Temperature Constant.
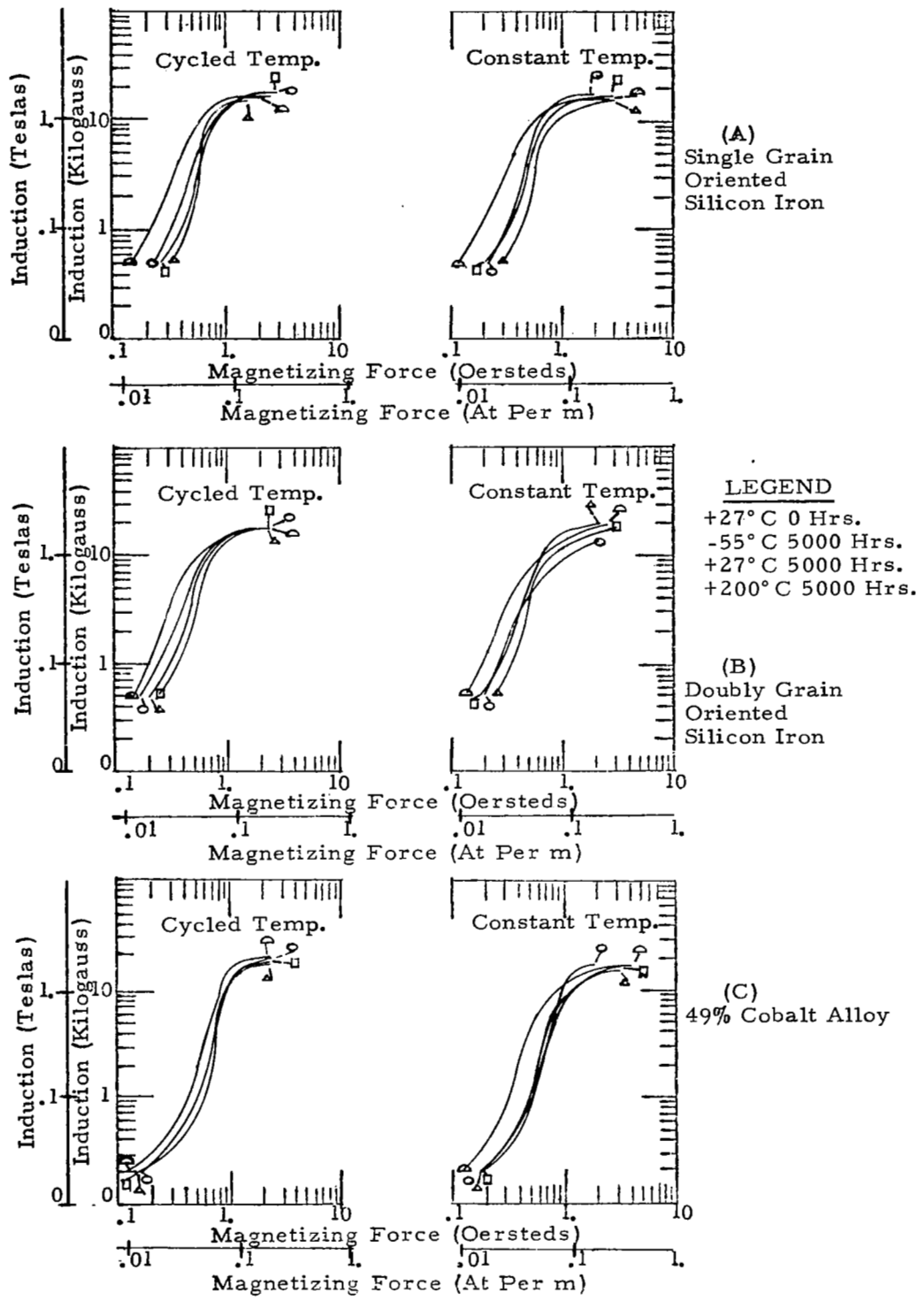
Figure 49 - A. C. Magnetization vs. Temperature at 0 and 5000 hours
0. 002 inch Tape Cores.
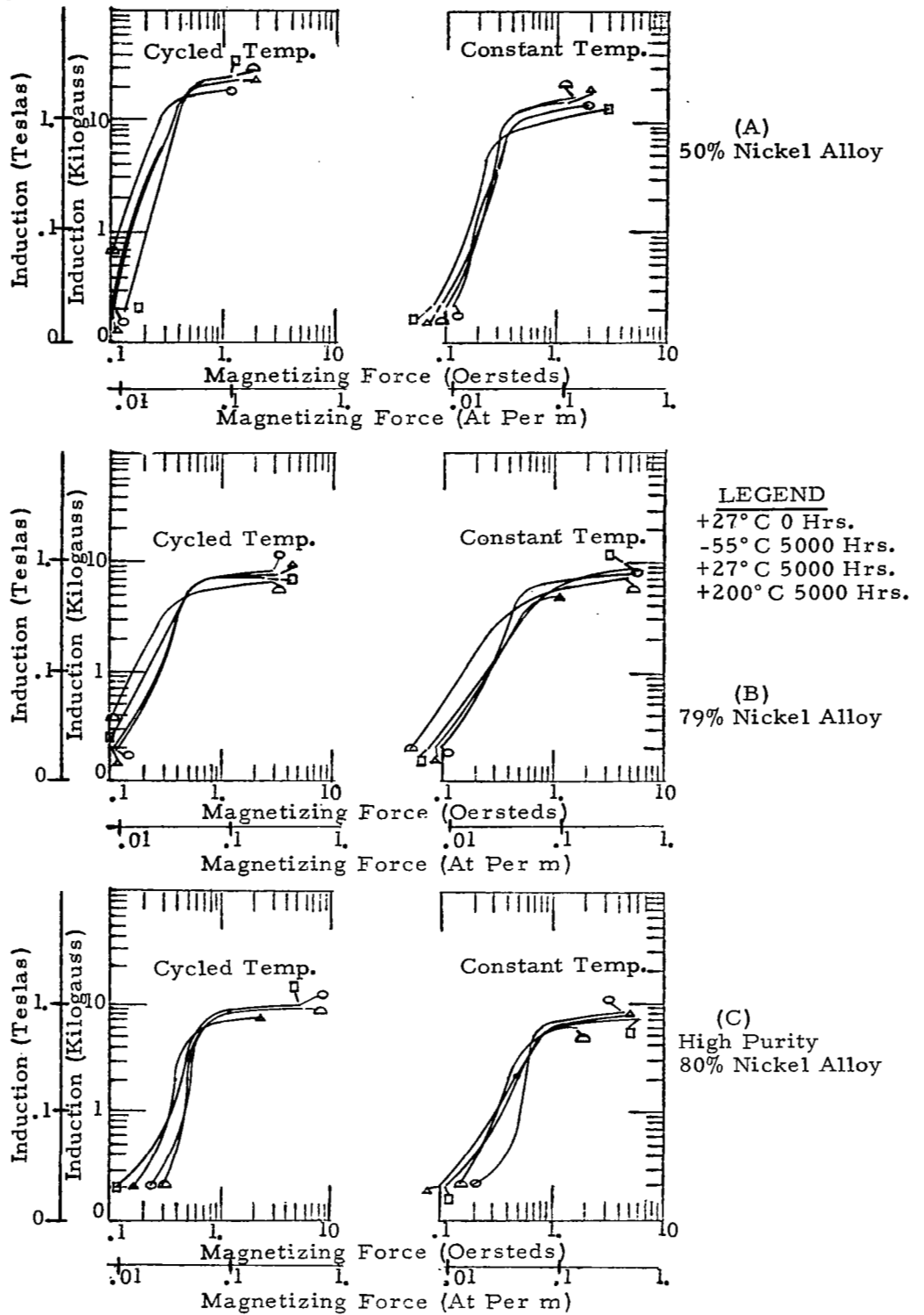
Figure 50 - A. C. Magnetization vs. Temperature at 0 and 5000 hours. 0. 002 inch Tape Cores.

64
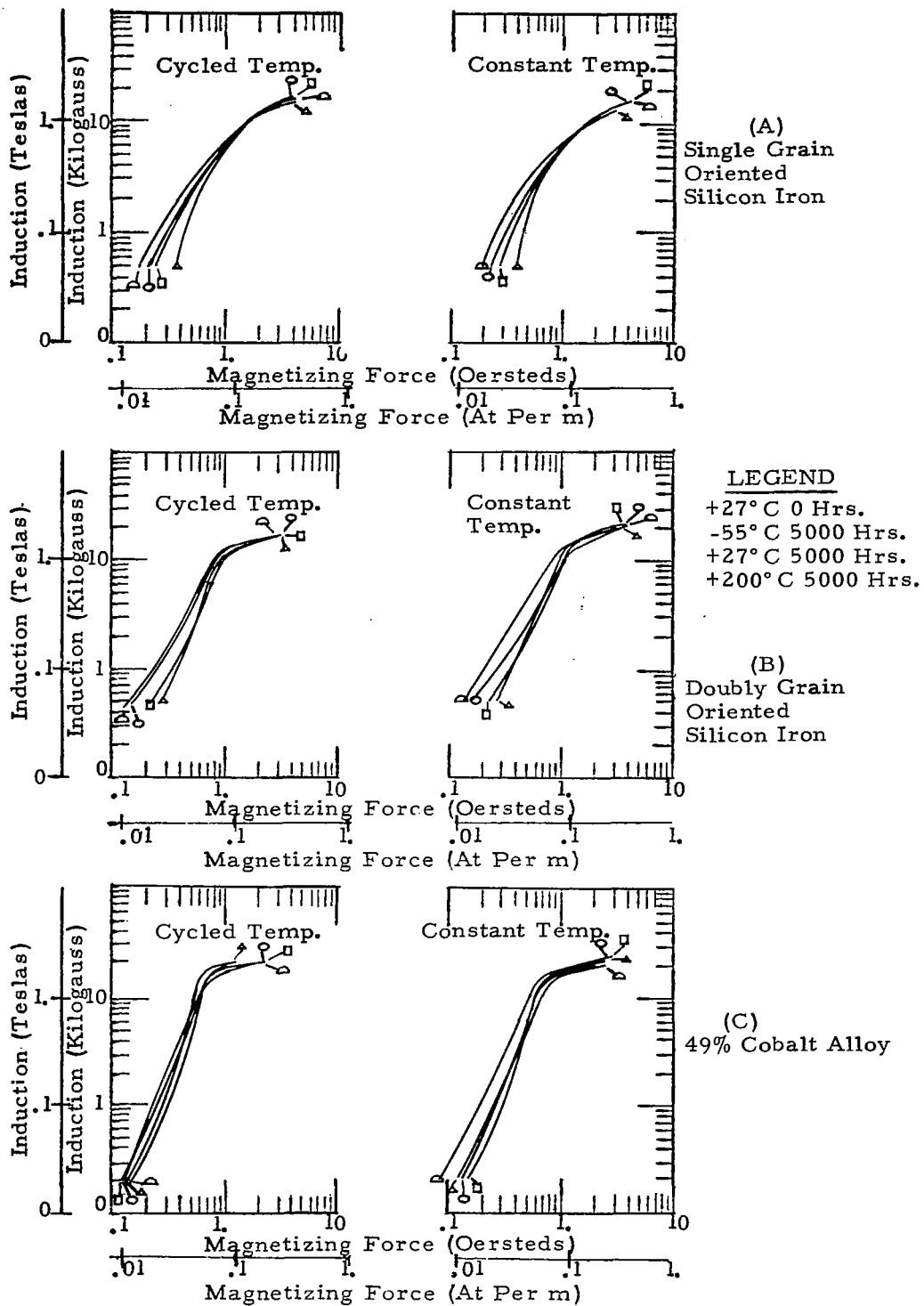
Figure 51 - A. C. Magnetization vs. Temperature at 0 and 5000 hours.
0. 006 inch Ring Cores.

65
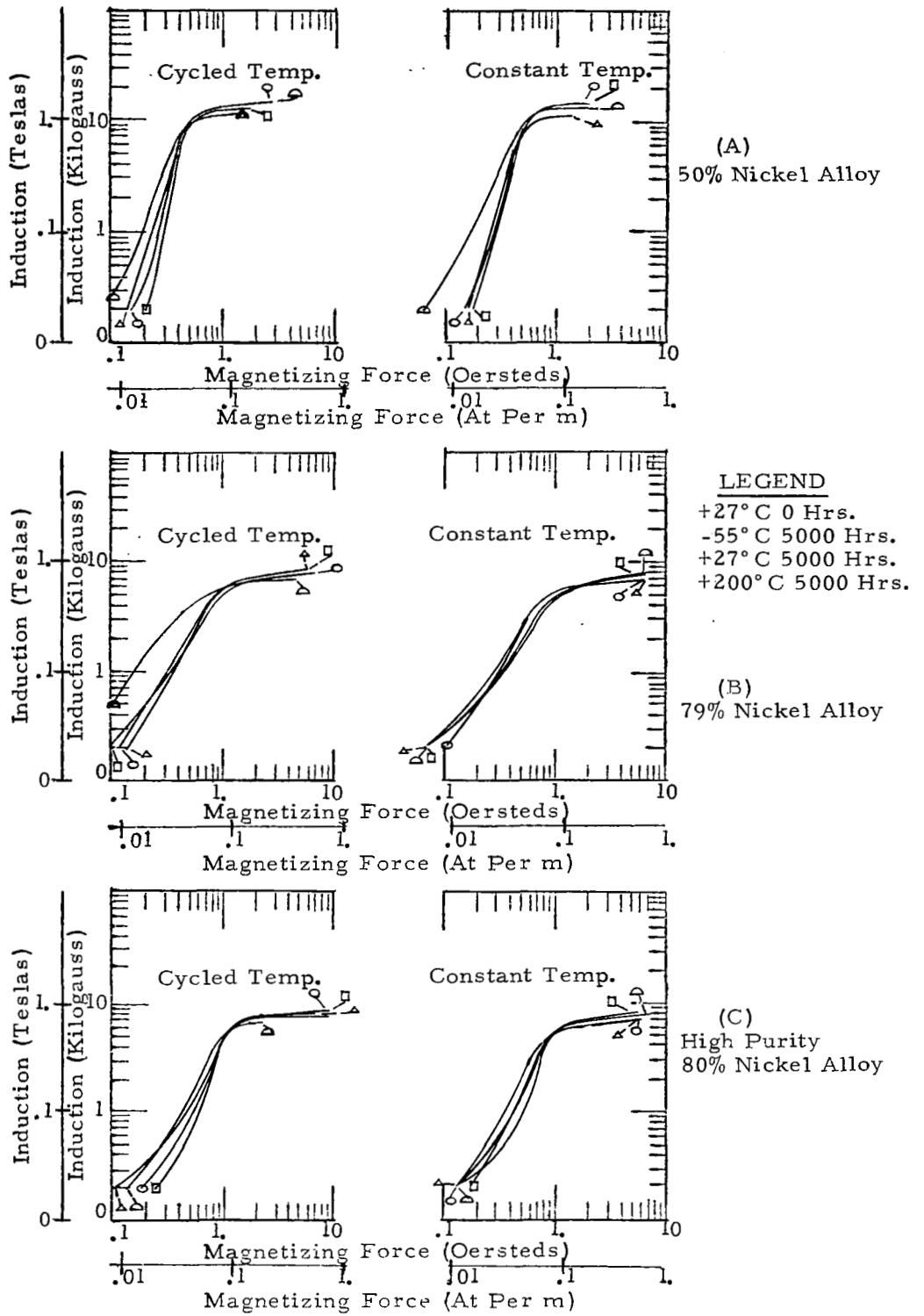
Figure 52 - A. C. Magnetization vs. Temperature at 0 and 5000 hours.
0. 006 inch Ring Cores.
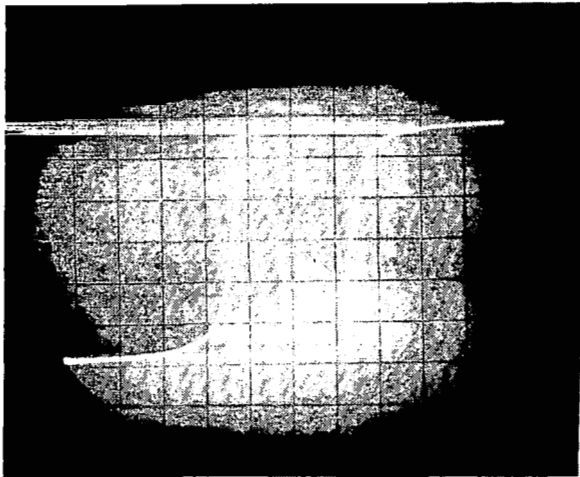
$\mathcal{T}$ = 0 Hours, +27° C
Constant Temperature
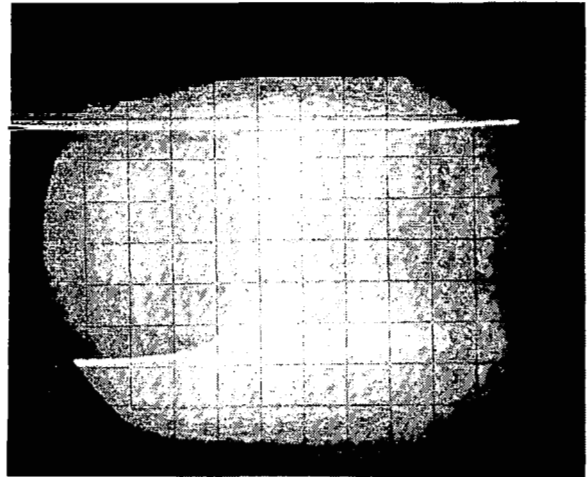
$\mathcal{T}$ = 0 Hours, +27° C
Cycled Temperature
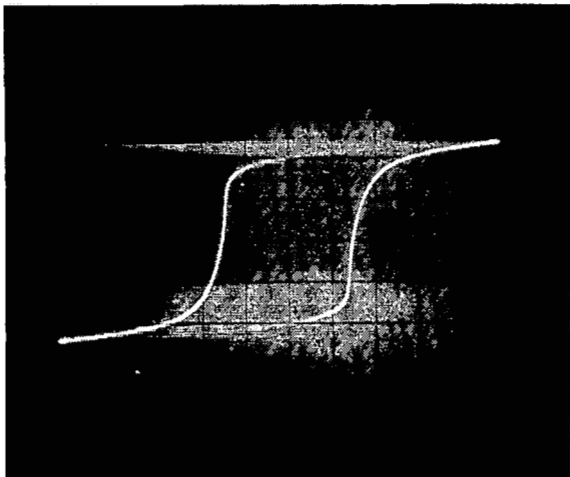
$\mathcal{T}$ = 5000 Hours, +27° C
Constant Temperature
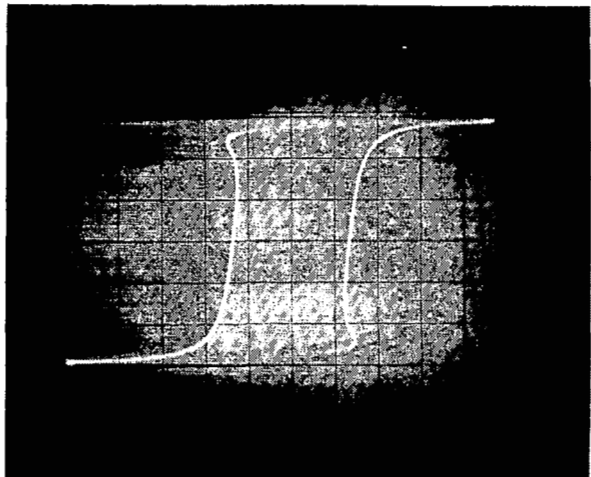
$\mathcal{T}$ = 5000 Hours, +27° C
Cycled Temperature

Figure 53 - Singly Oriented 3% Silicon Steel tape cores A. C. hysteresis
loops at $\mathcal{T}$ = 0 and $\mathcal{T}$ = 5000 hours for cores subjected to cycled
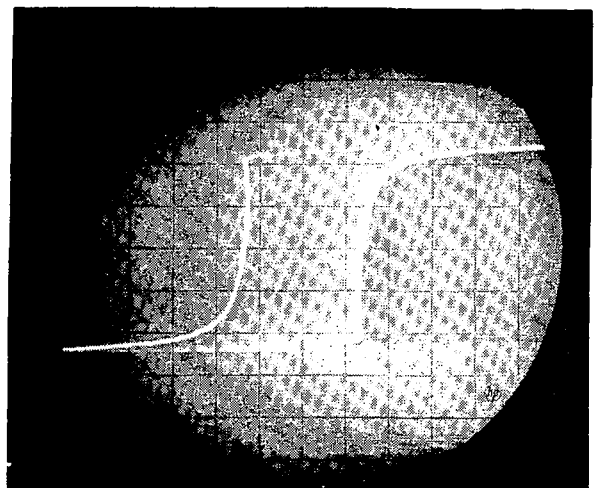temperatures (-55° C to +200° C) and cores subjected to a con-
stant 200° C temperature.

67
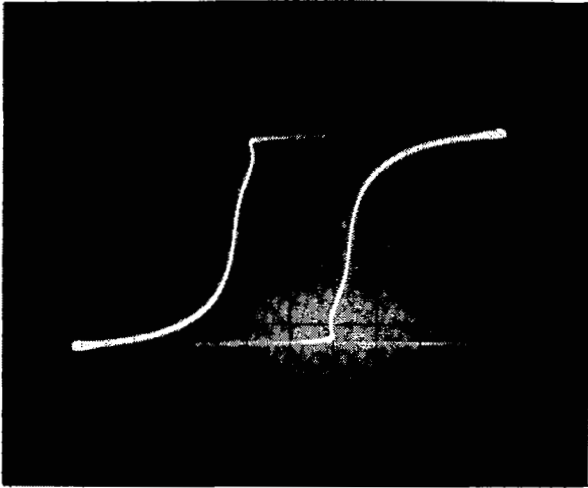
$\mathcal{T}$ = 0 Hours, +27° C
Constant Temperature
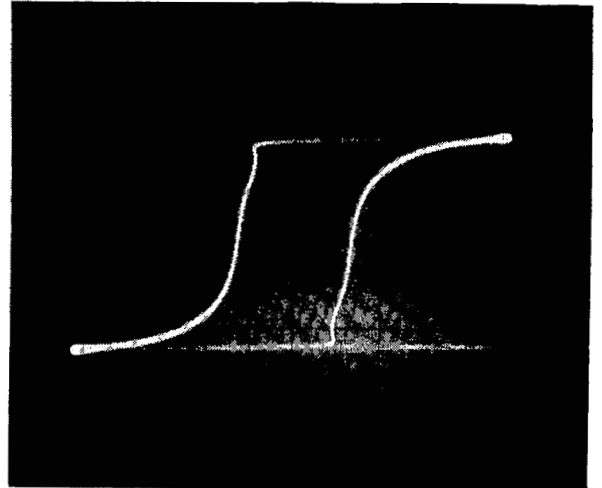
$\mathcal{T}$ = 0 Hours, +27° C
Cycled Temperature
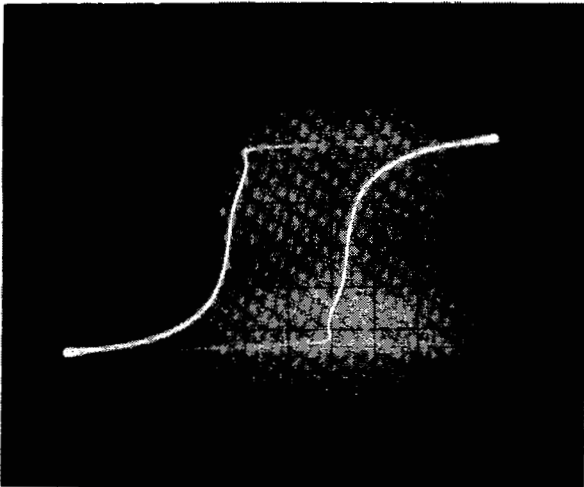
$\mathcal{T}$ = 5000 Hours, +27° C
Constant Temperature
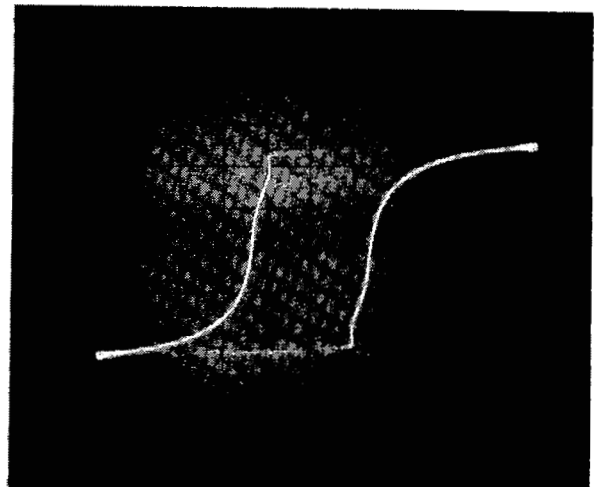
$\mathcal{T}$ = 5000 Hours, +27° C
Cycled Temperature

Figure 54 – Singly Oriented 3% Silicon Steel ring cores A. C. hysteresis
loops at $\mathcal{T}$ = 0 and $\mathcal{T}$ = 5000 hours for cores subjected to cycled
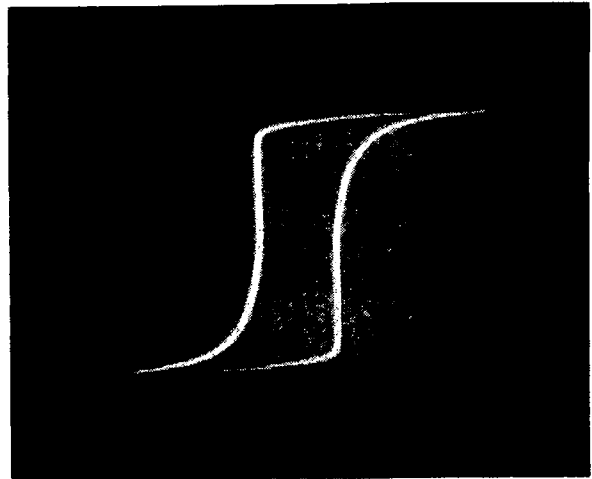temperatures (-55° C to +200° C) and cores subjected to a con-
stant 200° C temperature.
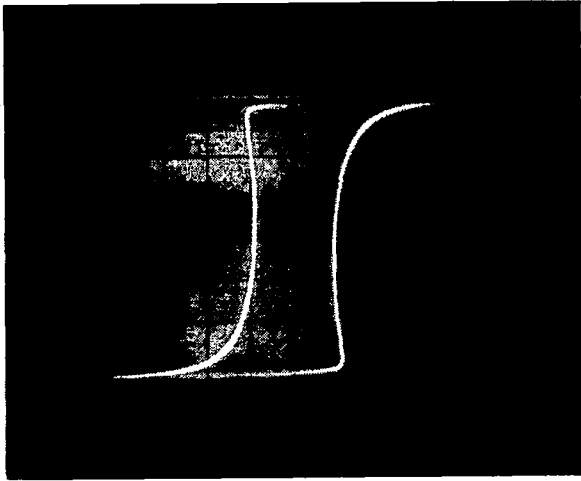
$\mathcal{T}$ = 0 Hours, +27° C
Constant Temperature
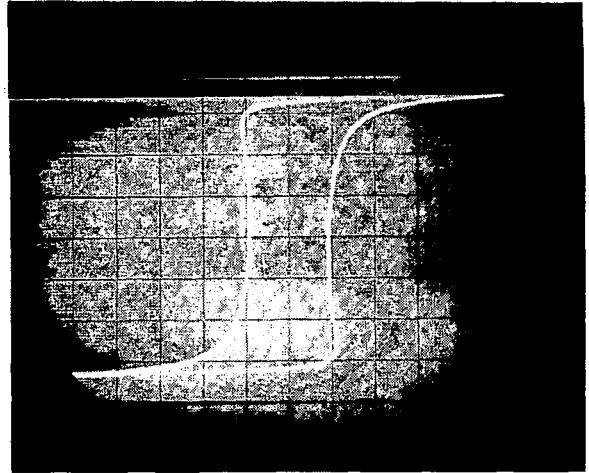
$\mathcal{T}$ = 0 Hours, +27° C
Cycled Temperature
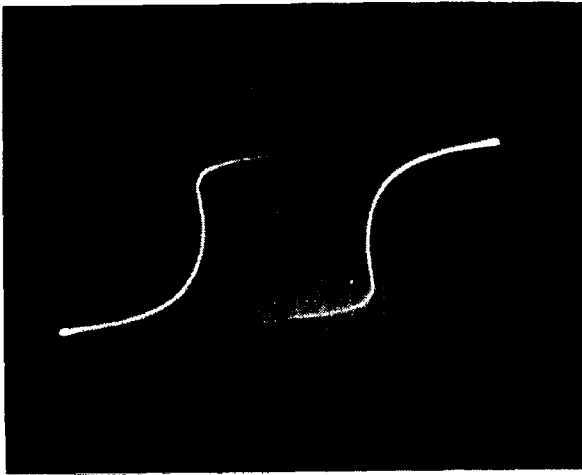
$\mathcal{T}$ = 5000 Hours, +27° C
Constant Temperature
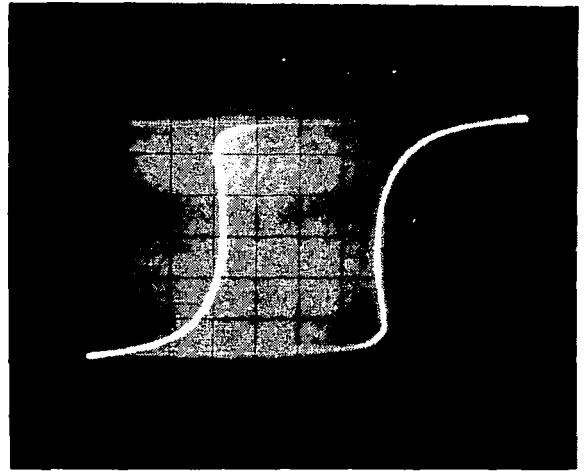
$\mathcal{T}$ = 5000 Hours, +27° C
Cycled Temperature

Figure 55 - Doubly Oriented 3% Silicon Steel tape cores A. C. hysteresis
loops at $\mathcal{T}$ = 0 and $\mathcal{T}$ = 5000 hours for cores subjected to cycled
temperatures (-55° C to +200° C) and cores subjected to a con-
stant 200° C temperature.

69
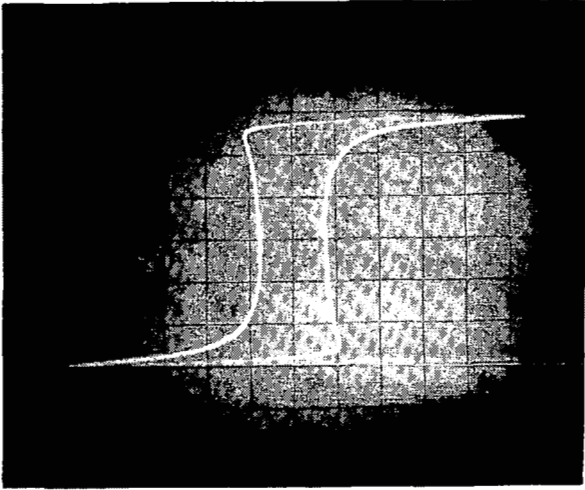
T = 0 Hours, +27° C
Constant Temperature
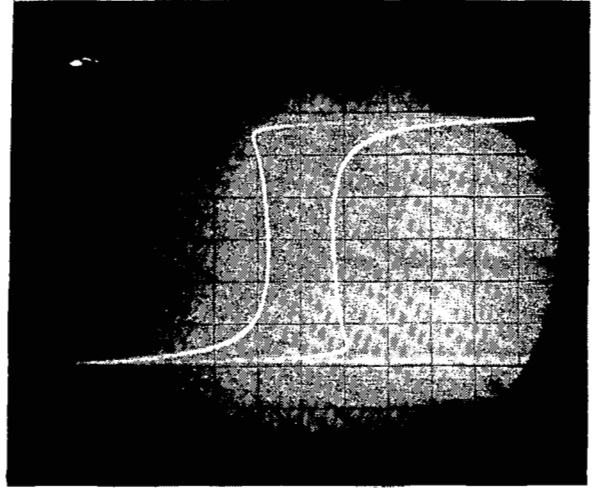
T = 0 Hours, +27° C
Cycled Temperature
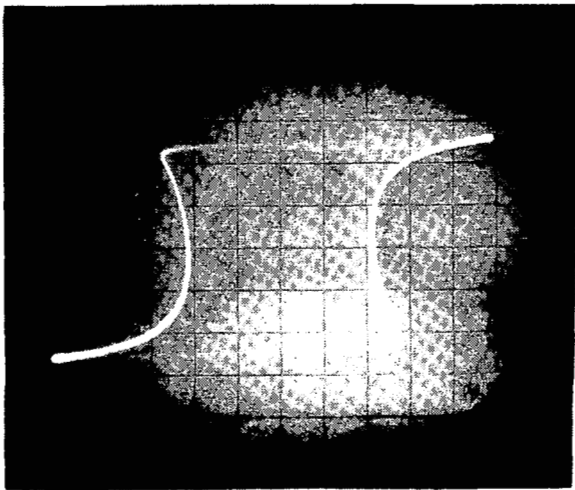
T = 5000 Hours, +27° C
Constant Temperature
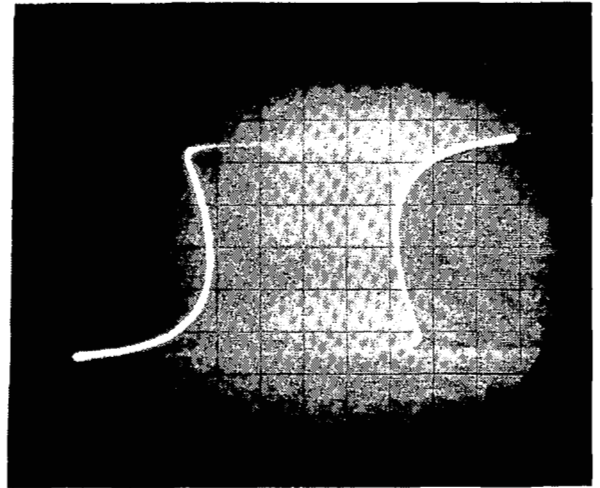
T = 5000 Hours, +27° C
Cycled Temperature
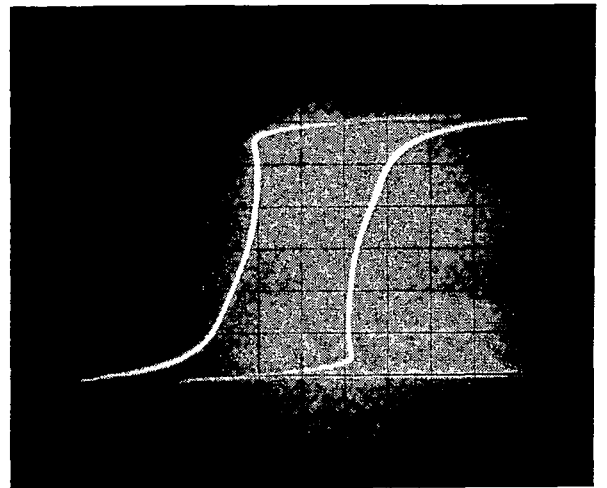
Figure 56 - Doubly Oriented 3% Silicon Steel ring cores A. C. hysteresis loops at T = 0 and T = 5000 hours for cores subjected to cycled temperatures (-55° C to +200° C) and cores subjected to a constant 200° C temperature.

70
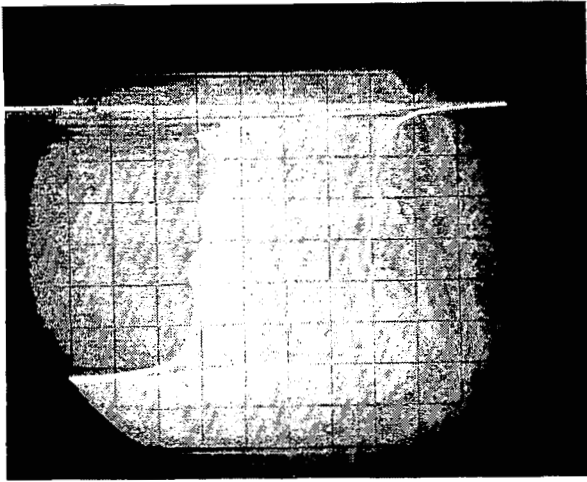
T = 0 Hours, +27° C
Constant Temperature
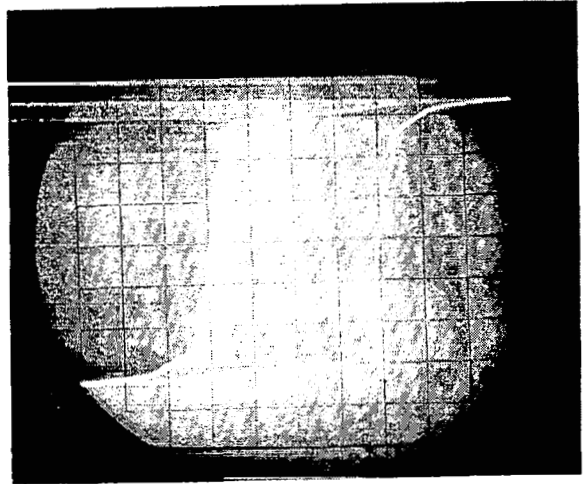
T = 0 Hours, +27° C
Cycled Temperature
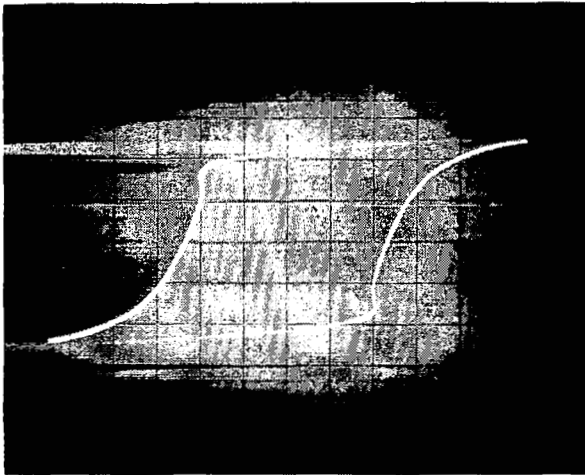
T = 5000 Hours, +27° C
Constant Temperature
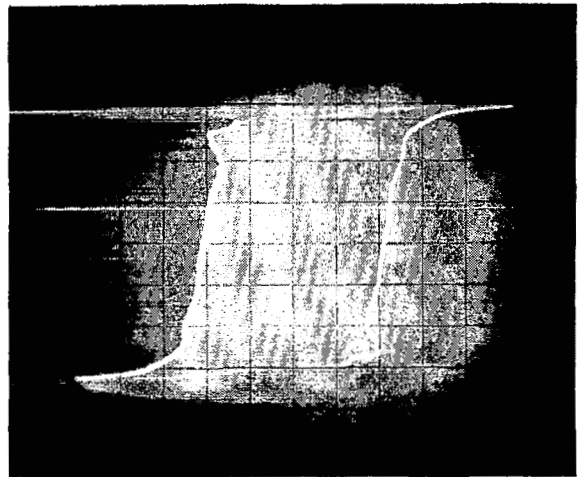
T = 5000 Hours, +27° C
Cycled Temperature

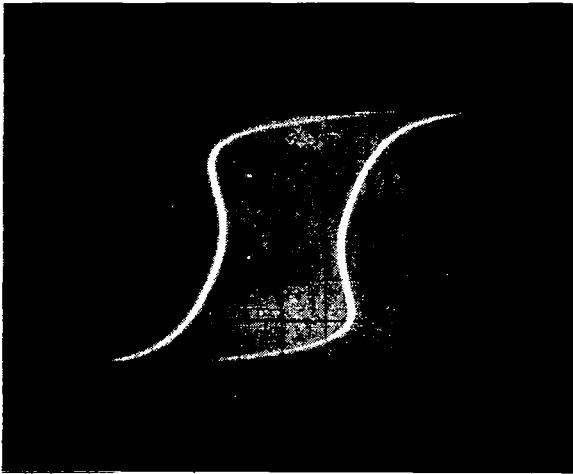Figure 57 - 49% Cobalt - 49% Iron - 2% Vanadium tape cores A. C. hysteresis loops at T = 0 and T = 5000 hours for cores subjected to cycled temperatures (-55° C to +200° C) and cores subjected to a constant 200° C temperature.
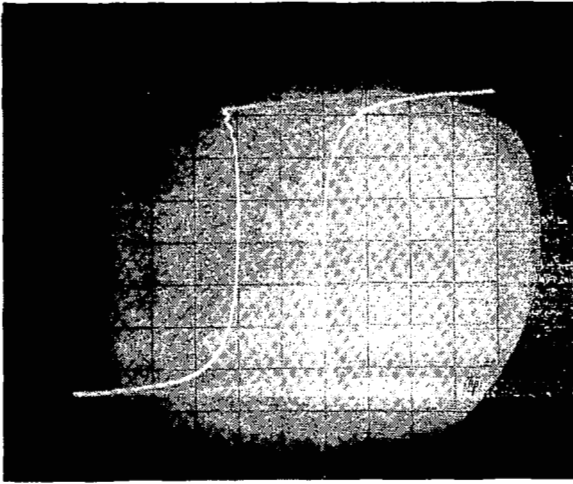
T = 0 Hours, +27° C
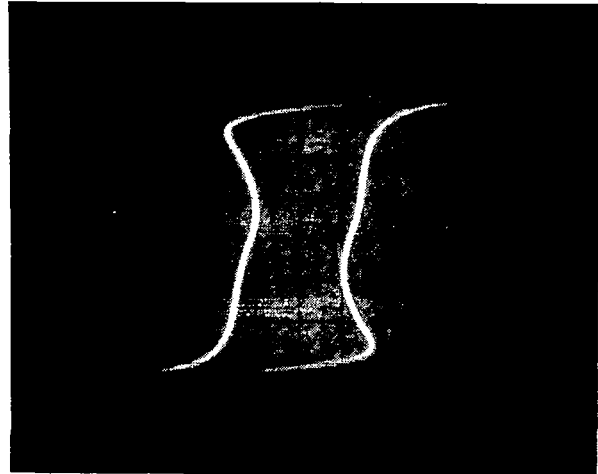Constant Temperature
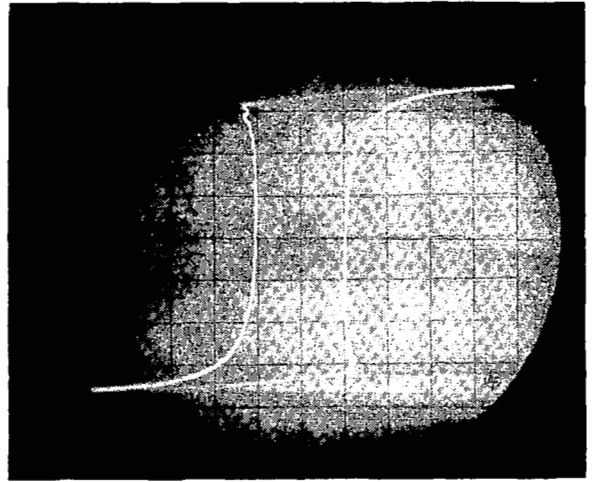
T = 0 Hours, +27° C
Cycled Temperature
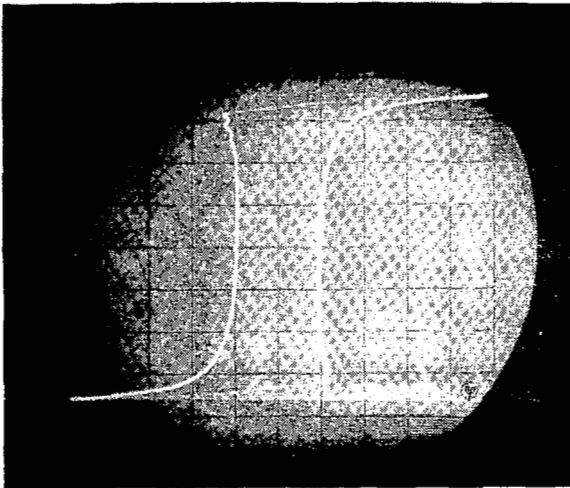
T = 5000 Hours, +27° C
Constant Temperature
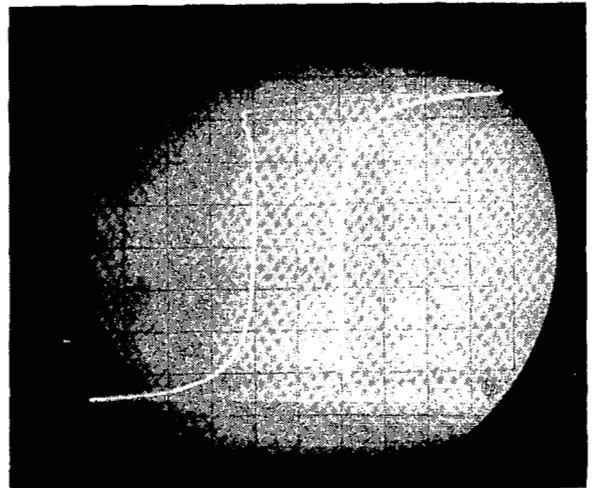
T = 5000 Hours, +27° C
Cycled Temperature

Figure 58 - 49% Cobalt - 49% Iron - 2% Vanadium ring cores A. C. hysteresis
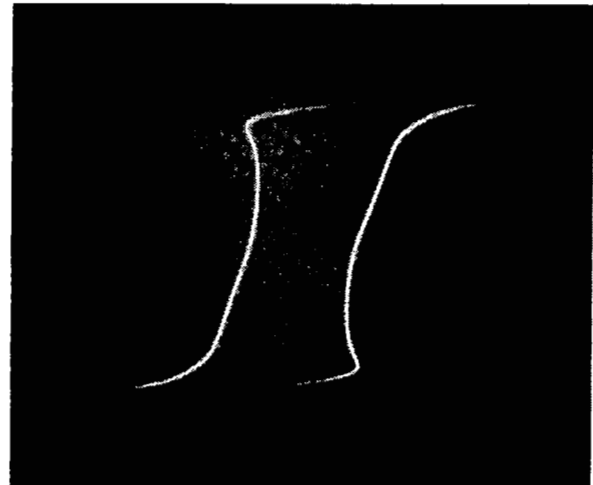loops at T = 0 and T = 5000 hours for cores subjected to cycled
temperatures (-55° C to +200° C) and cores subjected to a constant
200° C temperature.
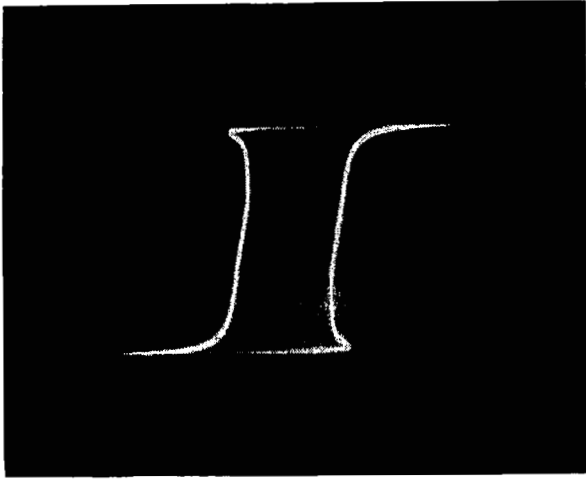
$\mathbf{T}$ = 0 Hours, +27° C
Constant Temperature
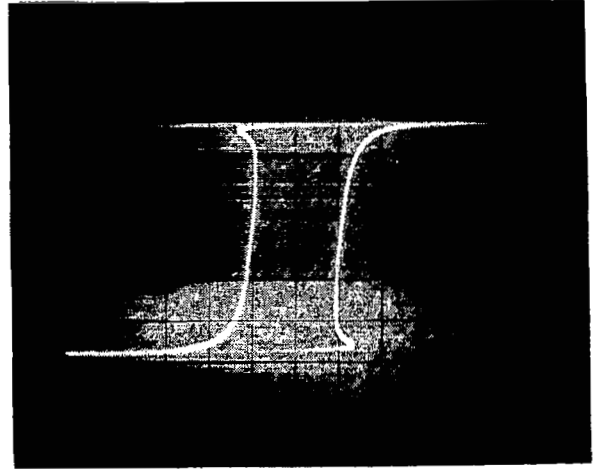
$\mathbf{T}$ = 0 Hours, +27° C
Cycled Temperature
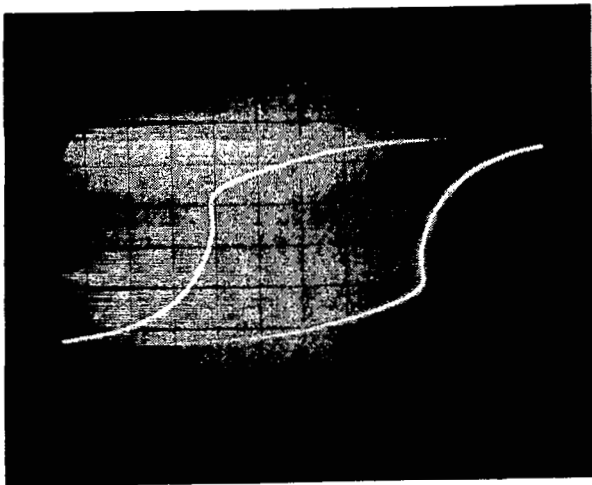
$\mathbf{T}$ = 5000 Hours, +27° C
Constant Temperature
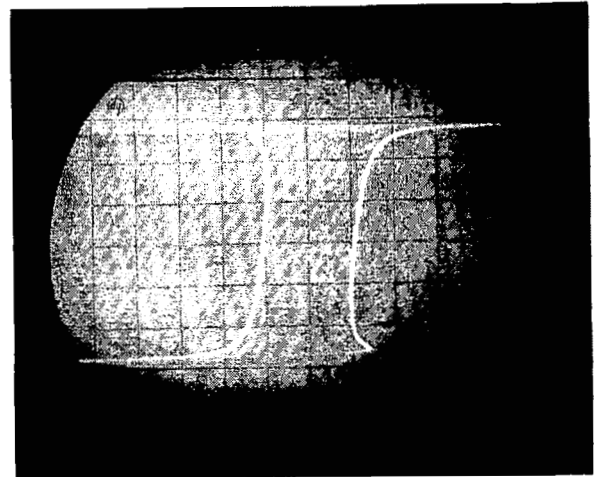
$\mathbf{T}$ = 5000 Hours, +27° C
Cycled Temperature

Figure 59 - 50% Nickel - 50% Iron tape cores A. C. hysteresis loops at
$\mathbf{T}$ = 0 and $\mathbf{T}$ = 5000 hours for cores subjected to cycled tem-
peratures (-55° C to +200° C) and cores subjected to a constant
200° C temperature.
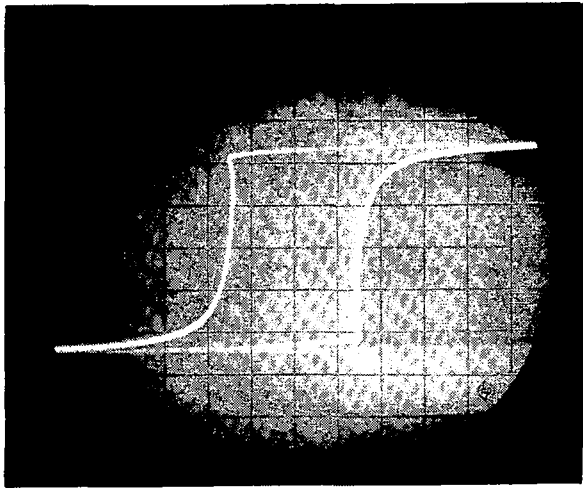
$\mathcal{T}$ = 0 Hours, +27° C
Constant Temperature
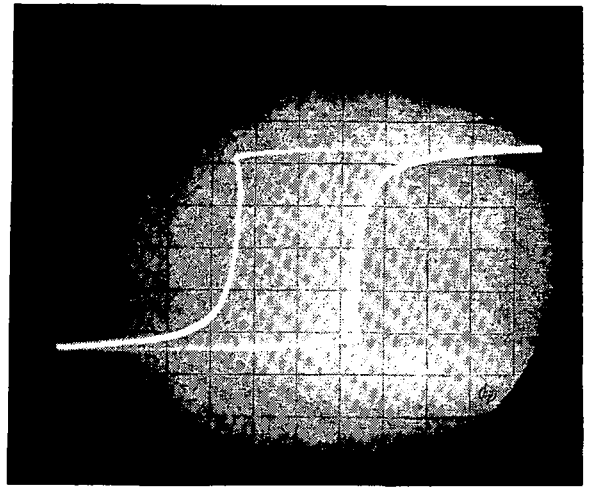
$\mathcal{T}$ = 0 Hours, +27° C
Cycled Temperature
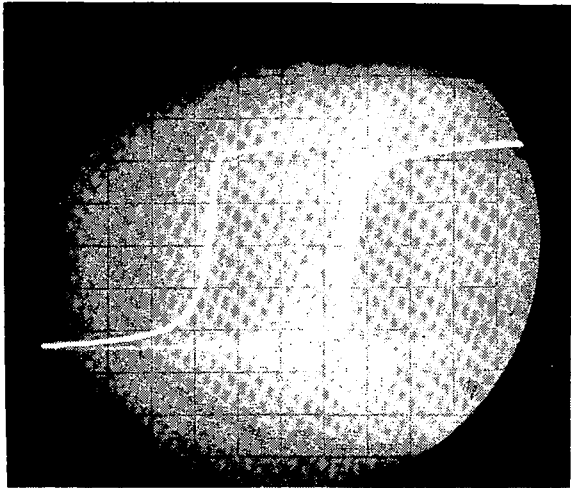
$\mathcal{T}$ = 5000 Hours, +27° C
Constant Temperature

$\mathcal{T}$ = 5000 Hours, +27° C
Cycled Temperature

Figure 60 - 50% Nickel - 50% Iron ring cores A. C. hysteresis loops at
$\mathcal{T}$ = 0 and $\mathcal{T}$ = 5000 hours for cores subjected to cycled tem-
peratures (-55° C to +200° C) and cores subjected to a constant
200° C temperature.
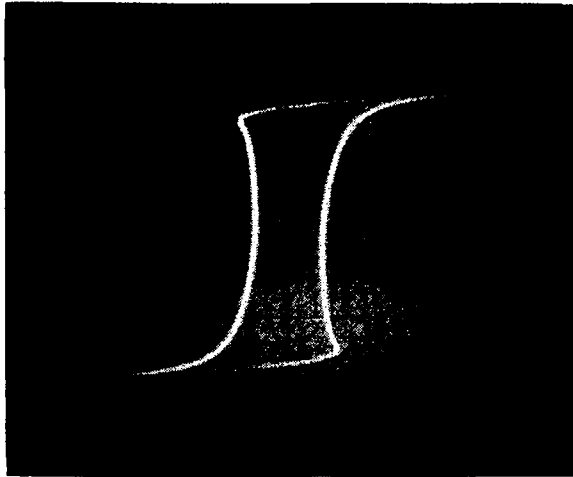
T = 0 Hours, +27° C
Constant Temperature
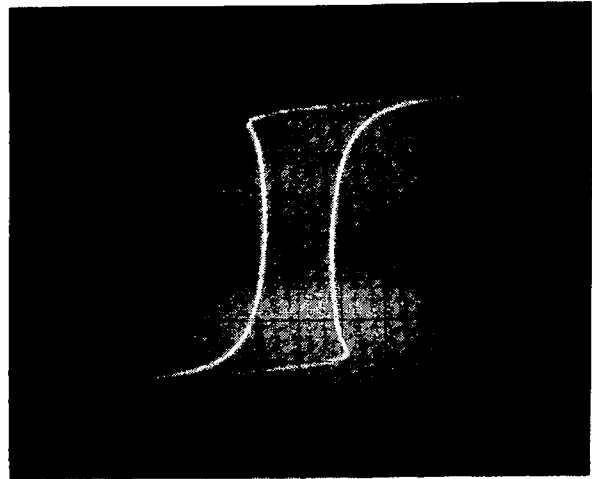
T = 0 Hours, +27° C
Cycled Temperature
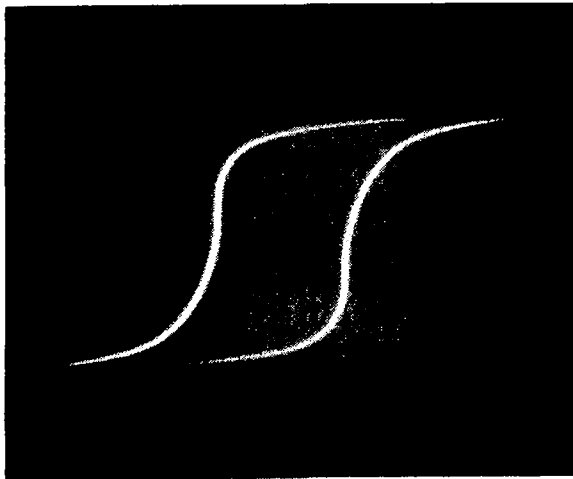
T = 5000 Hours, +27° C
Constant Temperature

T = 5000 Hours, +27° C
Cycled Temperature

Figure 61 - 79% Nickel - 17% Iron - 4% Molybdenum tape cores A. C. hysteresis
loops at T = 0 and T = 5000 hours for cores subjected to cycled tem-
peratures (-55° C to +200° C) and cores subjected to a constant 200° C
temperature.

75
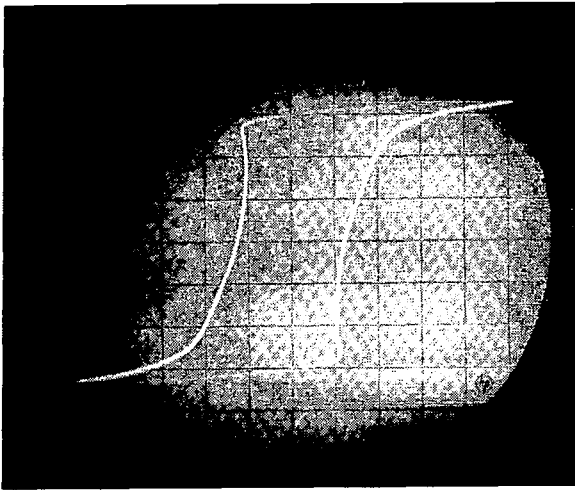
T = 0 Hours, +27° C
Constant Temperature
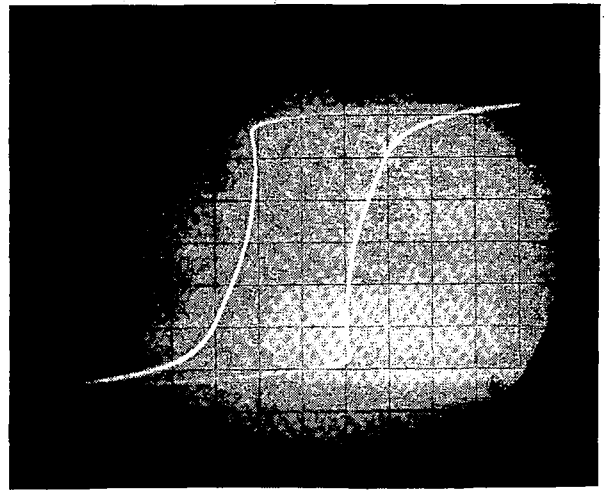
T = 0 Hours, +27° C
Cycled Temperature
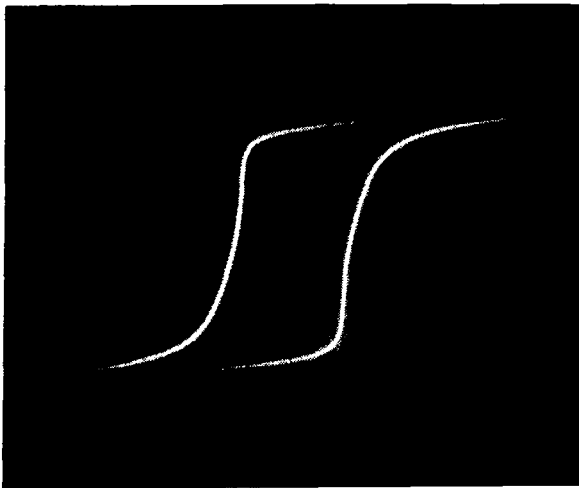
T = 5000 Hours, +27° C
Constant Temperature

T = 5000 Hours, +27° C
Cycled Temperature

Figure 62 - 79% Nickel - 17% Iron - 4% Molybdenum ring cores A. C. hysteresis
loops at T = 0 and T = 5000 hours for cores subjected to cycled tem-
peratures (-55° C to +200° C) and cores subjected to a constant 200° C
temperature.
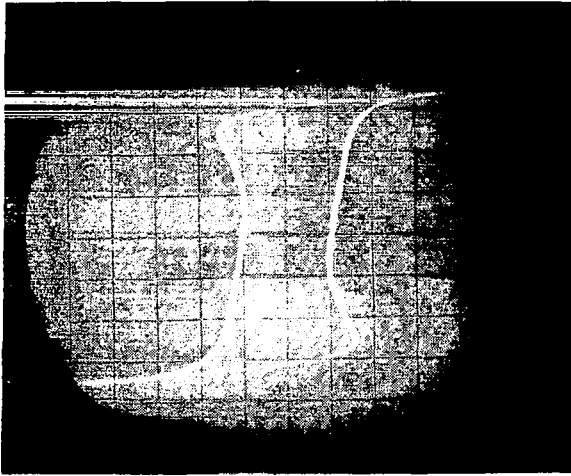
$\mathcal{T}$ = 0 Hours, +27° C
Constant Temperature
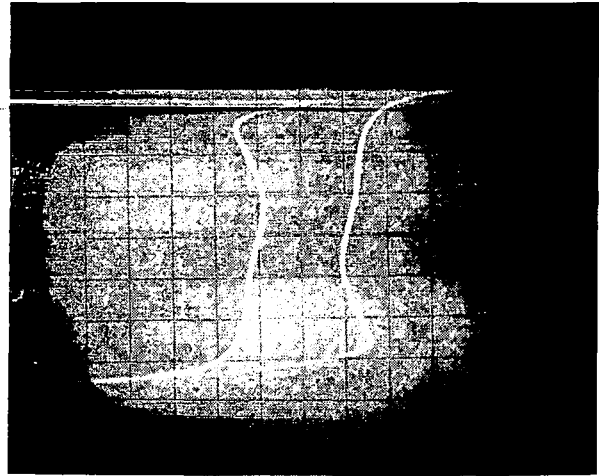
$\mathcal{T}$ = 0 Hours, +27° C
Cycled Temperature

$\mathcal{T}$ = 5000 Hours, +27° C
Constant Temperature

$\mathcal{T}$ = 5000 Hours, +27° C
Cycled Temperature

Figure 63 - High Purity 80% Nickel - 16% Iron - 4% Molybdenum tape cores
A. C. hysteresis loops at $\mathcal{T}$ = 0 and $\mathcal{T}$ = 5000 hours for cores
subjected to cycled temperatures (-55° C to +200° C) and cores
subjected to a constant 200° C temperature.
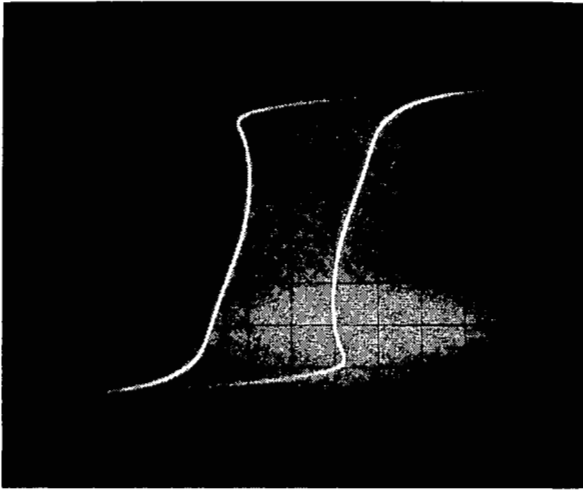
𝒯 = 0 Hours, +27°C
Constant Temperature
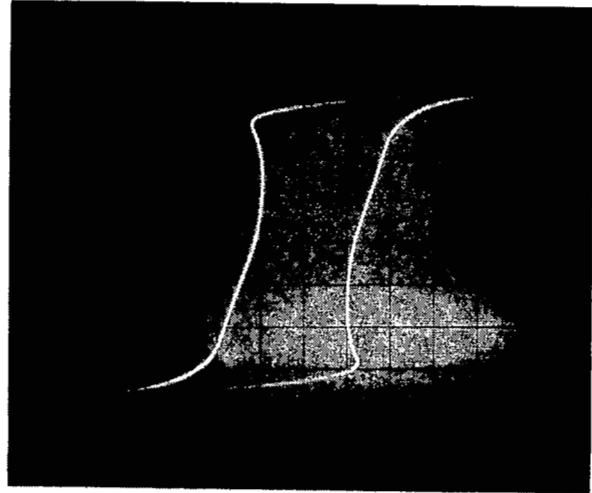
𝒯 = 0 Hours, +27°C
Cycled Temperature
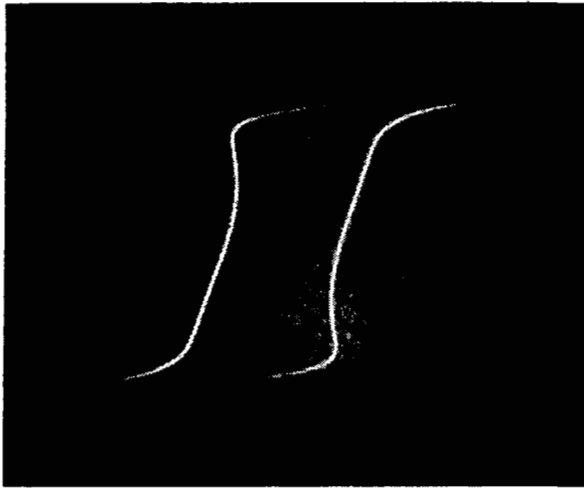
𝒯 = 5000 Hours, +27°C
Constant Temperature

𝒯 = 5000 Hours, +27°C
Cycled Temperature

Figure 64 - High Purity 80% Nickel = 16% Iron - 4% Molybdenum ring cores
A. C. hysteresis loops at 𝒯 = 0 and 𝒯 = 5000 hours for cores
subjected to cycled temperatures (-55°C to +200°C) and cores
subjected to a constant 200°C temperature.
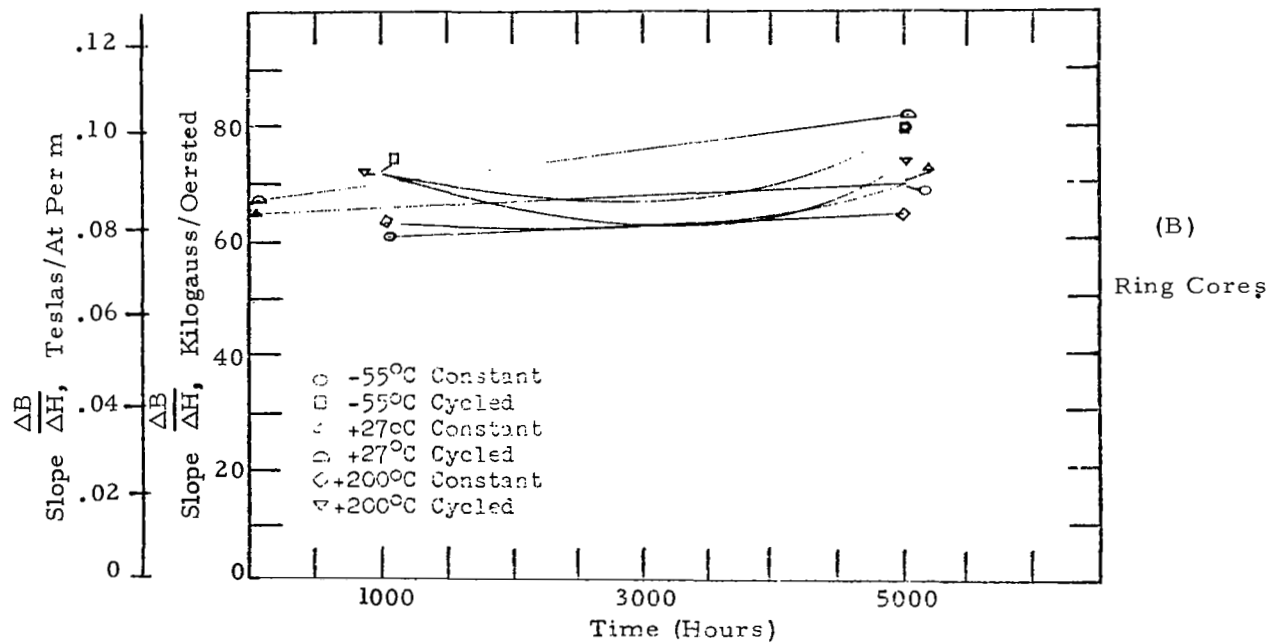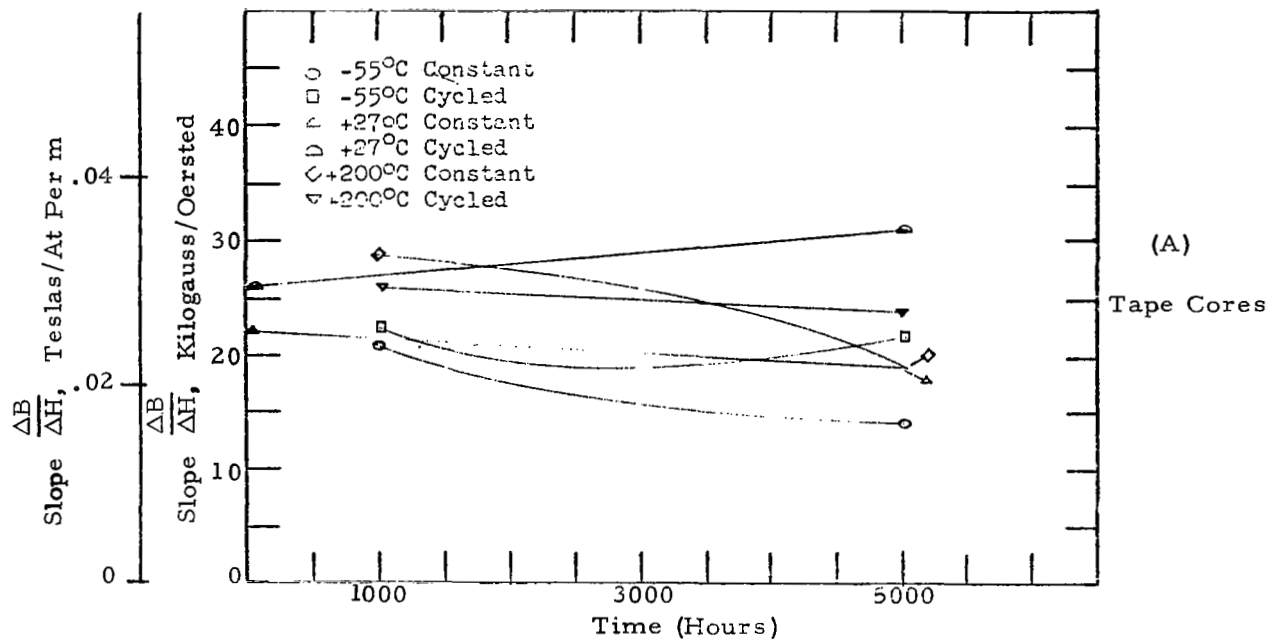
Figure 65 - Slope of A. C. Magnetization Curve from 1/3 to 2/3 of
Maximum Induction. Single Grain Oriented Silicon Iron.
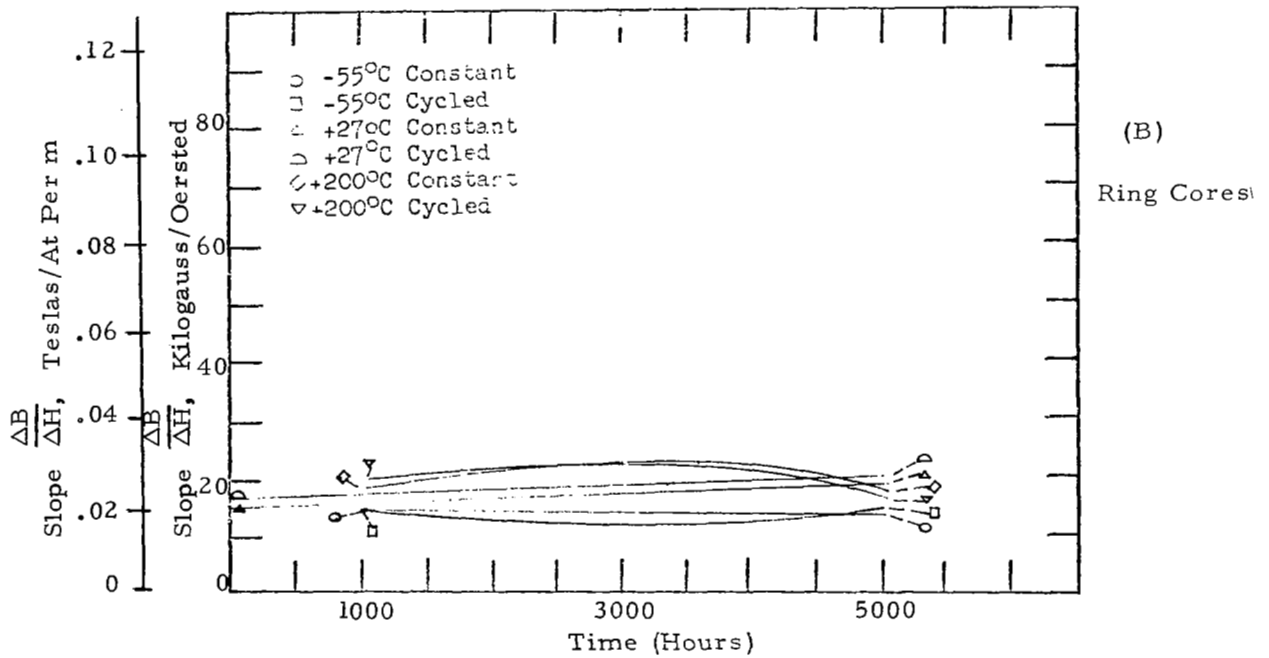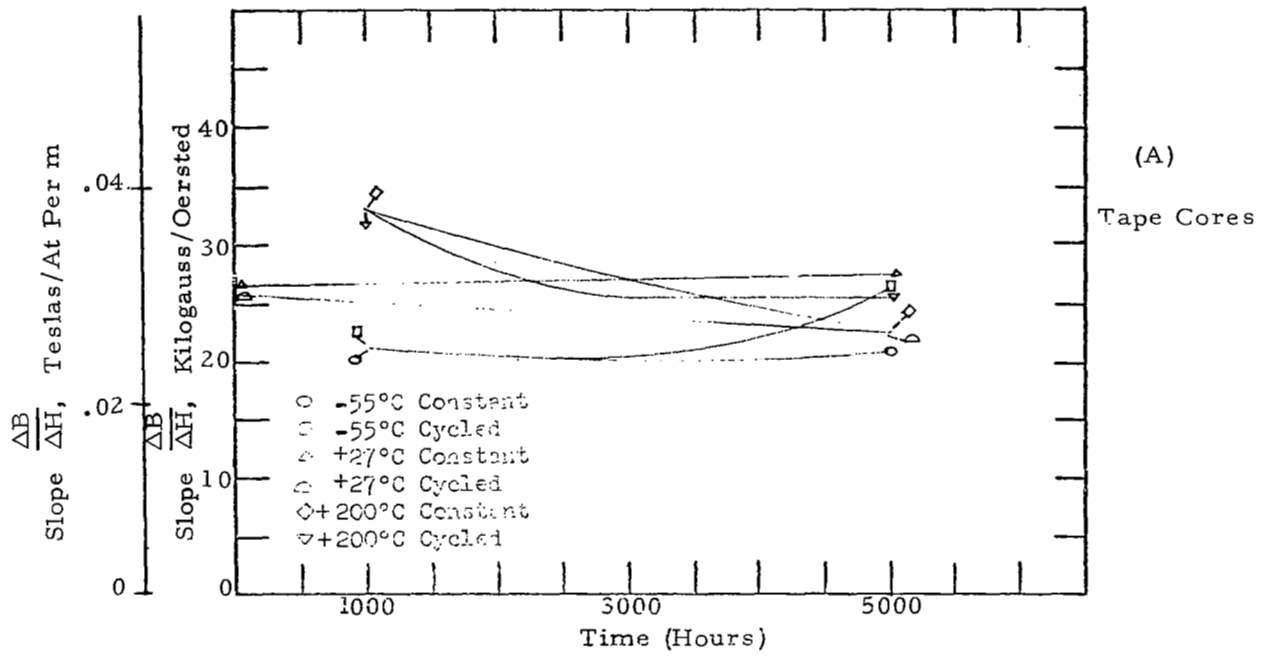
Figure 66 - Slope of A. C. Magnetization Curve from 1/3 to 2/3 of Maximum Induction. Doubly Grain Oriented Silicon Iron.

(A)

Tape Cores

Slope $\frac{\Delta B}{\Delta H}$, Teslas/At Per m

Slope $\frac{\Delta B}{\Delta H}$, Kilogauss/Oersted

.04

.02

0

40

30

20

10

0

⚪ -55°C Constant
⬜ -55°C Cycled
△ +27°C Constant
⌒ +27°C Cycled
◇ +200°C Constant
▽ +200°C Cycled

1000   3000   5000

Time (Hours)

(B)

Ring Cores

Slope $\frac{\Delta B}{\Delta H}$, Teslas/At Per m

Slope $\frac{\Delta B}{\Delta H}$, Kilogauss/Oersted

.12

.10

.08

.06

.04

.02

0

80

60

40

20

0

⚪ -55°C Constant
⬜ -55°C Cycled
△ +27°C Constant
⌒ +27°C Cycled
◇ +200°C Constant
▽ +200°C Cycled

1000   3000   5000

Time (Hours)
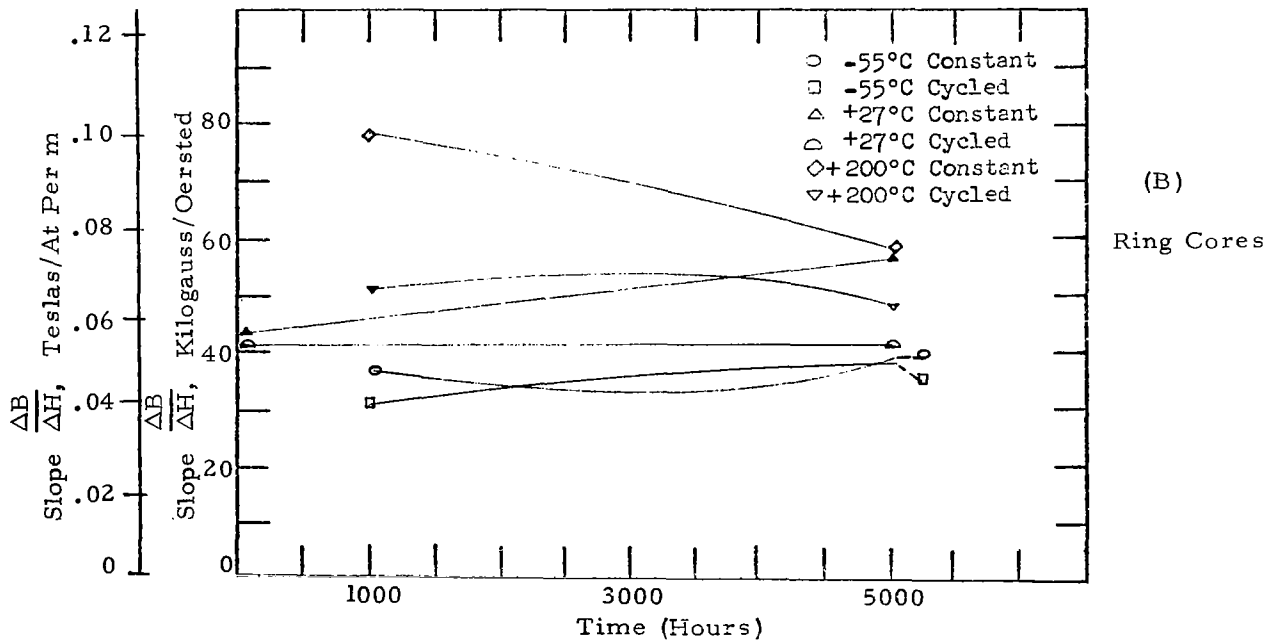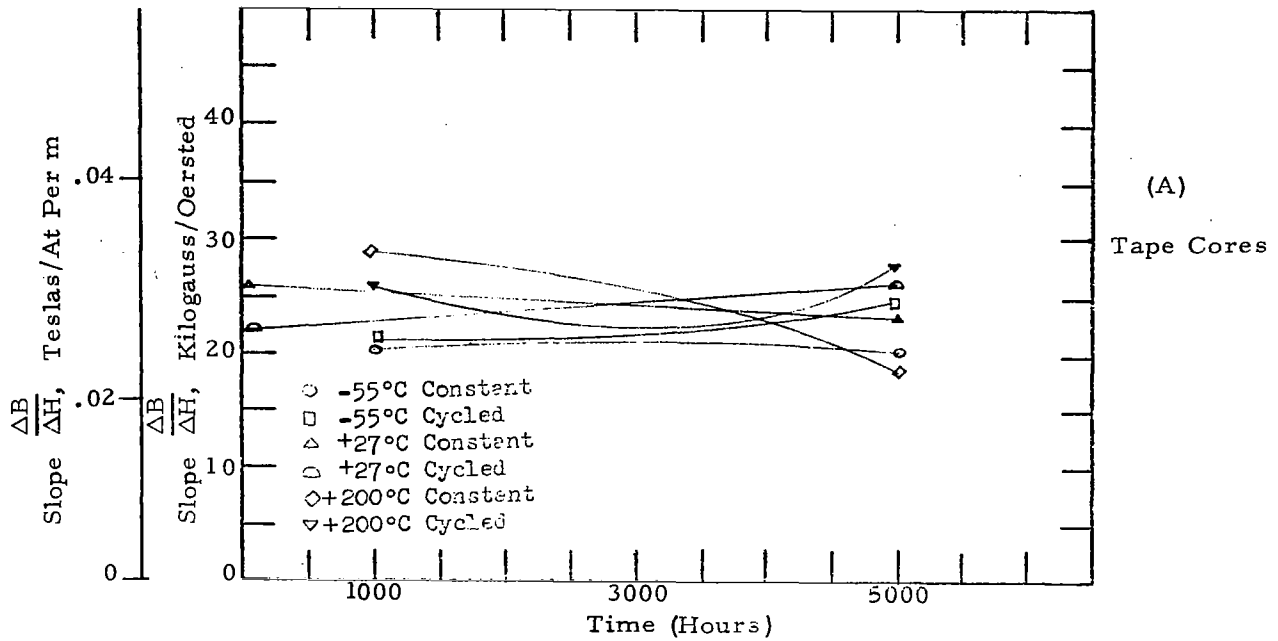
Figure 67 - Slope of A. C. Magnetization Curve from 1/3 to 2/3 of
Maximum Induction.   49% Cobalt Alloy.

81
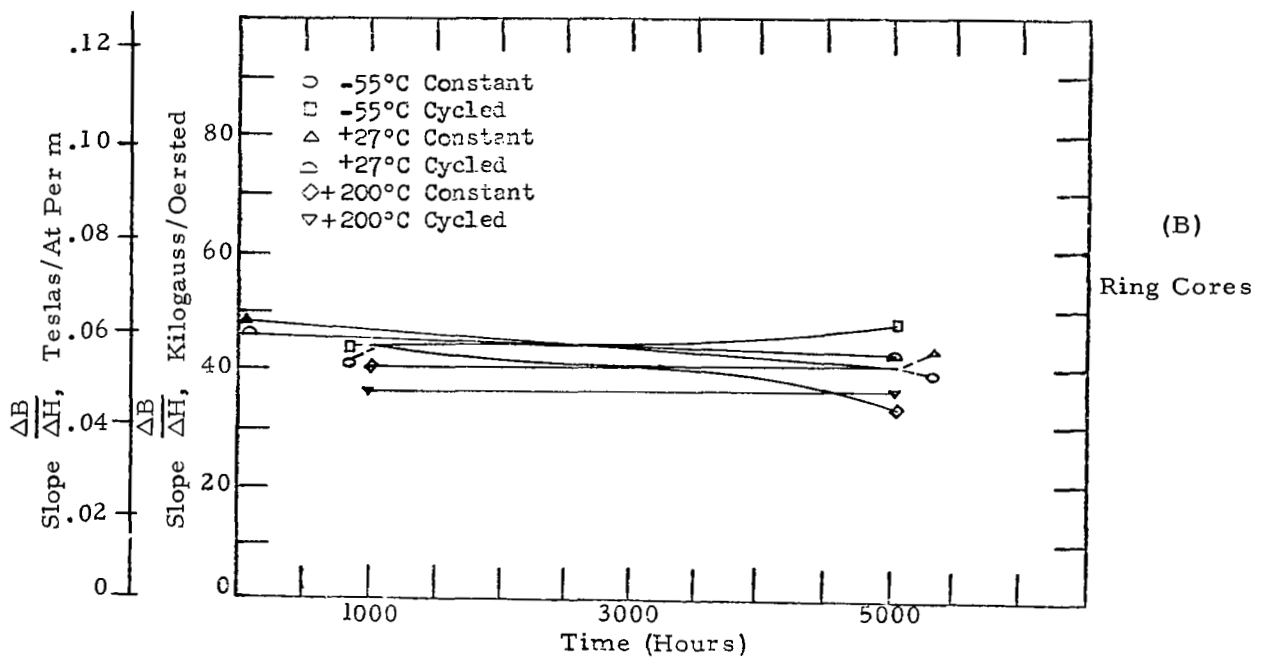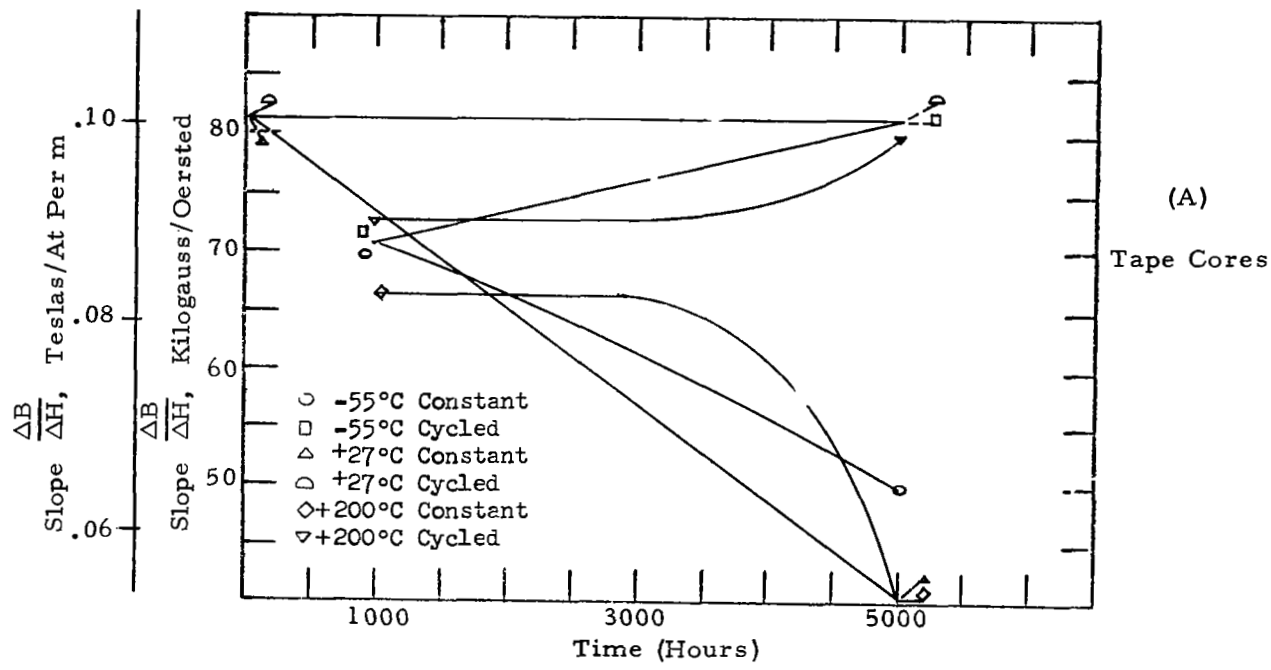
Figure 68 - Slope of A. C. Magnetization Curve from 1/3 to 2/3 of
Maximum Induction - 50% Nickel Alloy
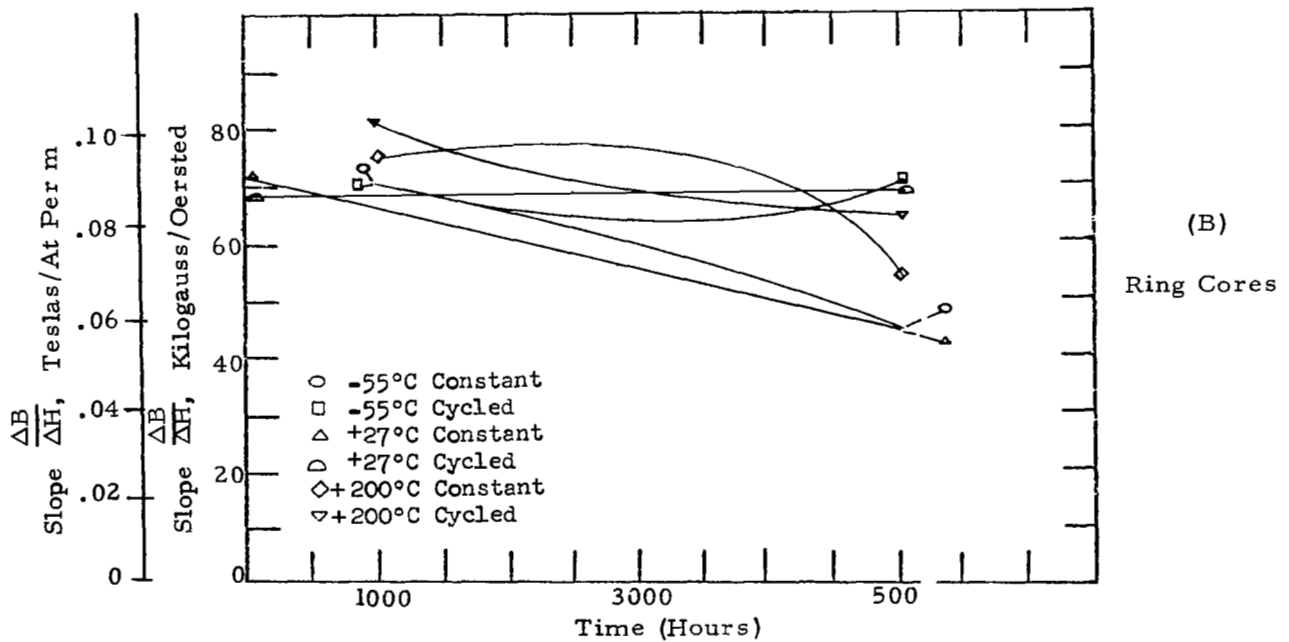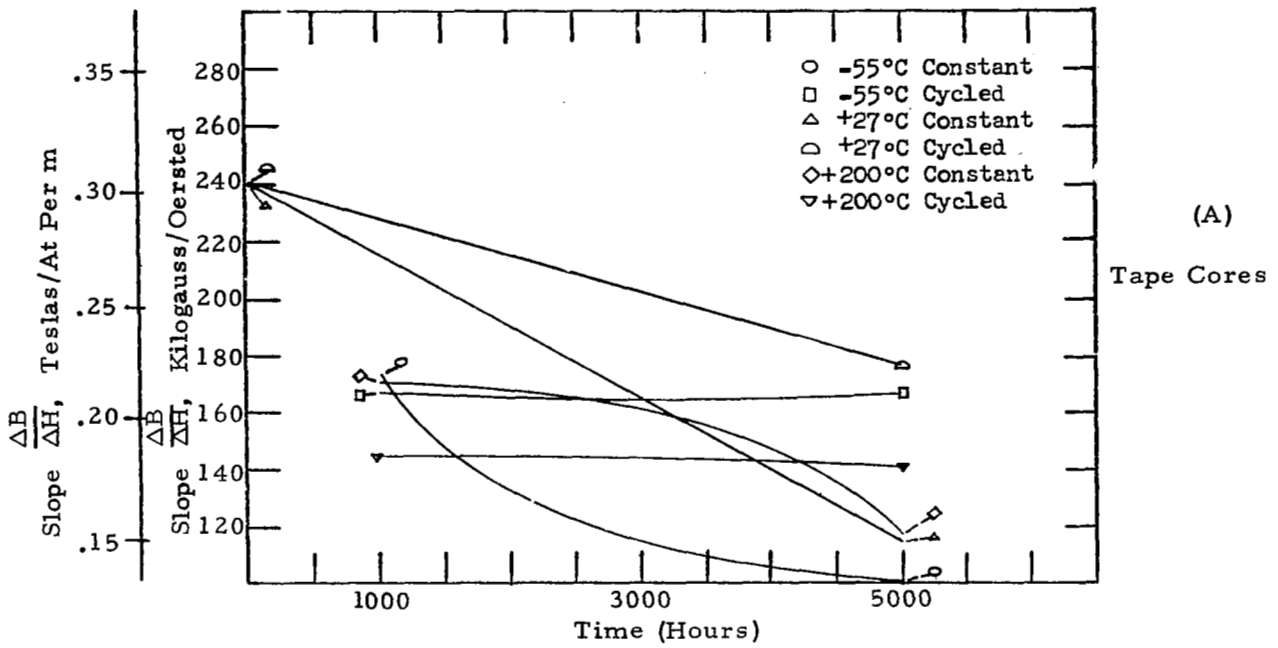
Figure 69 - Slope of A. C. Magnetization Curve from 1/3 to 2/3 of Maximum Induction - 79% Nickel Alloy
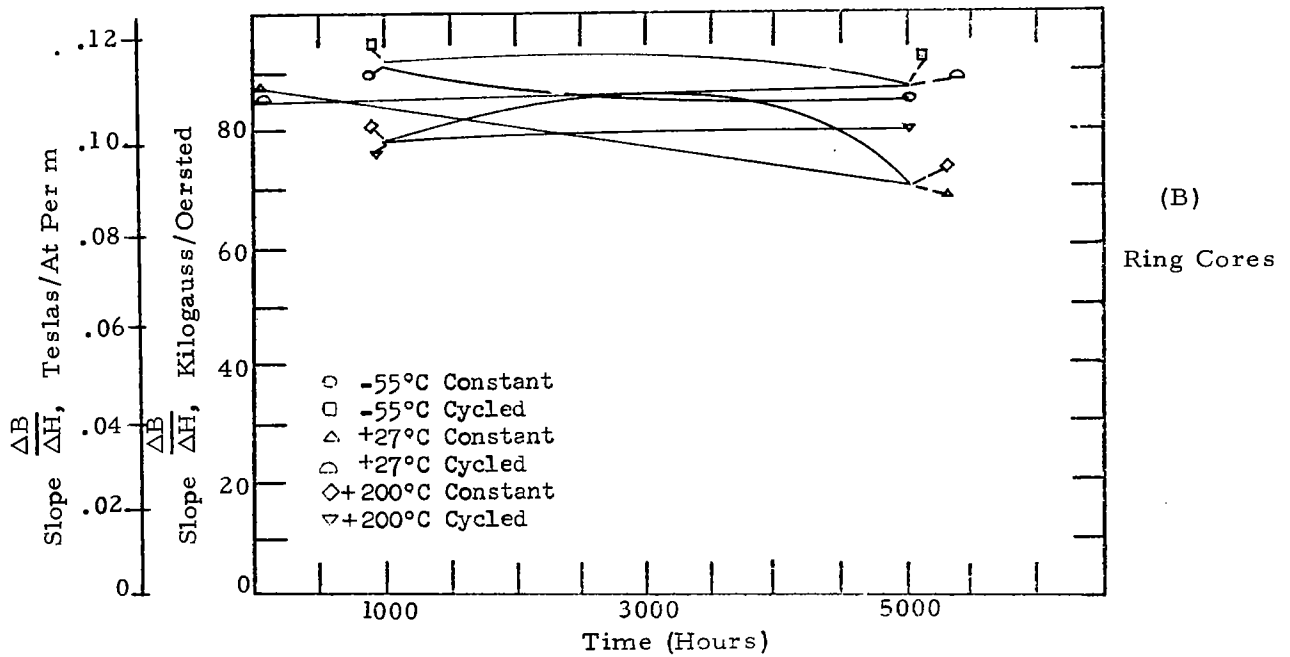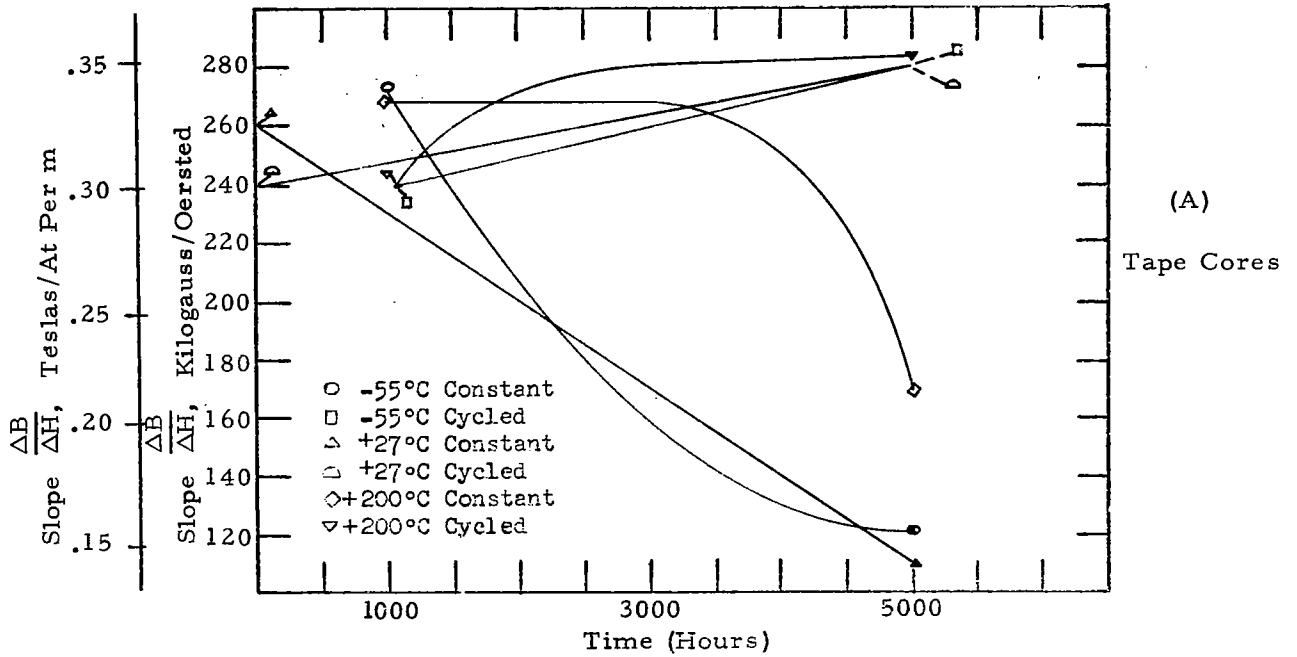
Figure 70 - Slope of A. C. Magnetization Curve from 1/3 to 2/3 of Maximum Induction - High Purity 80% Nickel Alloy.

APPENDIX A

Symbols and Units

Chemical

Al	-	Aluminum
Co	-	Cobalt
Fe	-	Iron
Mo	-	Molybdenum
Ni	-	Nickel
O	-	Oxygen
Si	-	Silicon
V	-	Vanadium

Measurement

Cm	-	Centimeter
$°C$	-	Degrees Centigrade
In	-	Inch
t	-	Thickness
$\mathcal{T}$	-	Time
Te	-	Temperature
α	-	Thermal Expansion Coefficient

Electrical

At per m	-	Ampere-turn per meter
A	-	Amperes
A. C.	-	Alternating current
B	-	Magnetic Induction - Gauss (Tesla)
Bm	-	Maximum Magnetic Induction - Gauss (Tesla)
Br	-	Residual (Remnant) Magnetic Induction - Gauss (Tesla)
Bm-Br	-	Squareness - Gauss (Tesla)
CCFR	-	Constant Current Flux Reset
CGS	-	Electro Magnetic System of Units
D. C.	-	Direct Current
ΔB	-	Incremental Magnetic Induction
ΔB_1	-	Incremental Magnetic Induction at approx. $1/3$ (2Bm) for CCFR
ΔB_2	-	Incremental Magnetic Induction at approx. $1/3$ (2Bm) for CCFR
E	-	Volts
G	-	Gain (Gauss/Oersted)
g	-	Gauss (Tesla)
H	-	Magnetizing Force - Oersteds (At per m)
ΔH	-	Increment of Magnetizing Force from H_1 to H_2
H1	-	Magnetizing Force required to achieve ΔB_1 (CCFR)-Oersted (At per m)
H_2	-	Magnetizing Force required to achieve ΔB_2 (CCFR)-Oersted (At per m)

Electrical (Continued)

Hc	-	Coercive Force - Oersted (At per m)
Hm	-	Maximum (Peak) Magnetizing Force - Oersted (At per m)
Ho	-	Magnetizing Force for 1/2 (2Bm) for CCFR - Oersted (At per m)
Hz	-	Frequency in cycles per second
Oe	-	Oersted (At per m)
T	-	Tesla
W	-	Watts
∿	-	Ohms

APPENDIX B

Period of Temperature Cycle

Temperature stabilization and cycle time was determined by loading the temperature chamber with 24 dummy cores of the same size, weight and materials of those to be tested. The cores were wound with a number of turns to provide a means for monitoring 400 Hz square wave currents. Measurements were made at an induction level of 70% of B_{max} for each material. To establish a starting point the cores were first set at -55°C for 1 hour and B was measured and recorded. The controller was then set for +200°C and kept at this point for 2 hours. B was monitored at 15 minute intervals to determine the point at which the cores reached magnetic stability. There was no change of B after 1 hour and at the end of the 2 hour period the controller was set for -55°C and the same process repeated. Again there was no change of B after 1 hour. The entire cycle was repeated with the results, as shown in Figure 71. On this basis the period for a symmetrical temperature cycle between -55°C and +200°C was established to be 3 hours. The automatic cycling controller was programmed to change every 1 1/2 hours and the chart recorder showed the temperature cycle wave form to be symmetrical with equal time at both temperatures as shown on Figure 72. This cycle program produced 8 complete cycles in each 24 hour period.
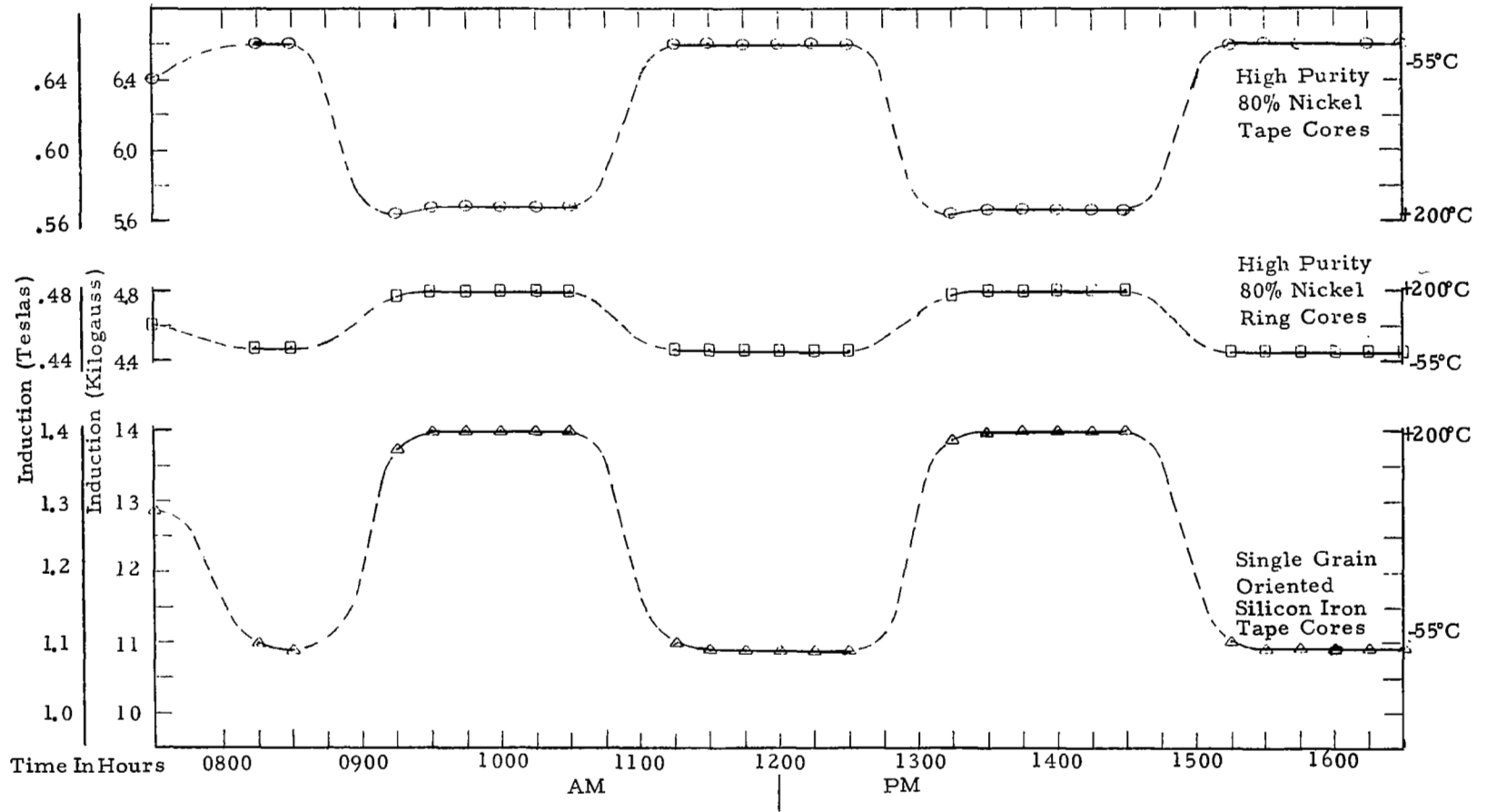
Figure 71 - Stabilization Of Core Temperatures

88
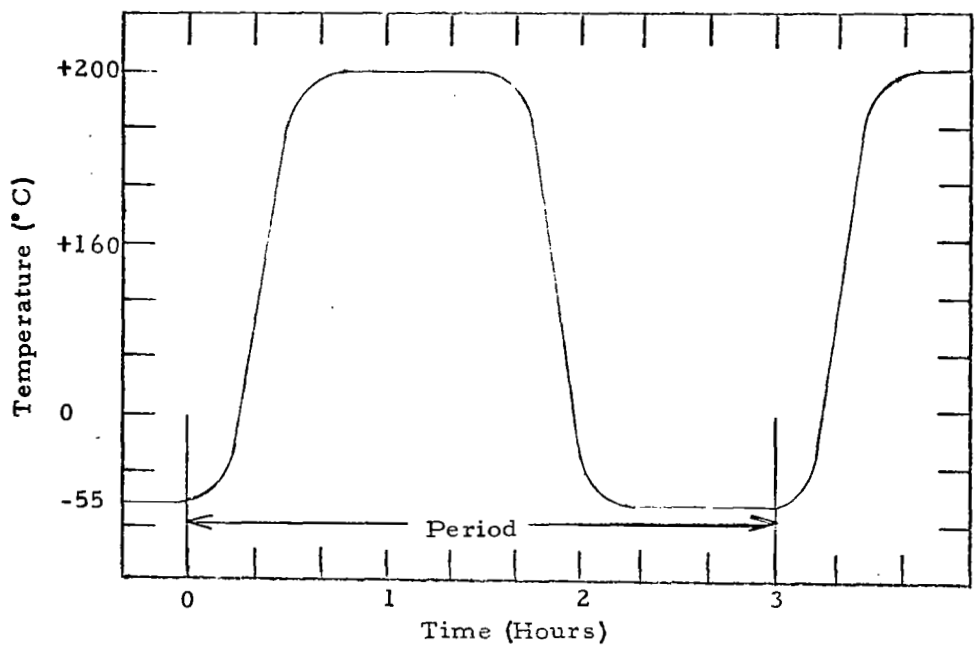
Figure 72 -- Temperature Cycle Period

APPENDIX C

Test and Calibration Equipment

TEMPERATURE CHAMBERS (2)

Statham Model SD-6 -- Closed air circulation system. Electric heater - liquid CO_2 coolant -- one chamber equipped with automatic cycle timer, $\pm 1°C$ control.

GENERATORS

Sine/Square Wave - General Radio type 1210-C oscillator -- square wave of 1 usec max. rise time -- Oscillator drives 6 McIntosh MI-200-AB power amplifiers connected in parallel.

Square Wave/Continuous - C. M. L. Frequency Converter CRS-1000 M with 2 usec max. rise time.

INSTRUMENTATION

D. C. HYSTERESIS LOOP

Lowell D. C. Hysteresograph Model IV plotted by Houston X-Y recorder model HR-97.

CCFR TESTS

Magnetic Metals Company Standard CCFR Tester modified to operate cores over a higher power and wider frequency range than normal low power 60 through 1600 Hz production requirements. Flux readings are read out on Sensitive Research Microammeter model S, excitation is read on a Weston Model 1766 Microammeter calibrated in Oersteds.

V. A. -- A. C. MAGNETIZATION

Volt Amperes and A. C. Magnetization were read with a Hewlett Packard 400H voltmeter for both voltage readings and current readings across a one ohm resistor shunt. This meter has a range of 0.001 volts to 300 volts in 12 ranges with an accuracy of $\pm 1\%$ F. S.

WATTS

Watt readings were obtained with a Fluke VAW meter Model 102, with ranges from .000225 to 18000 watts or V/A. Accuracy is $\pm 3\%$.

RESISTIVITY

Leeds and Northrup Kelvin Bridge Ohmeter No. 4285; range 0. 0001 to 26. 6 ohm; accuracy ±0. 5%.

A. C. HYSTERESIS LOOP

Hewlett Packard Model 130 Oscilloscope with a Hewlett Packard Model HP197A Polaroid camera.

FREQUENCY

Hewlett Packard Model 522B Counter; range 10 Hz to 120 Khz, accuracy ±1 count; stability 10 ppm.

CALIBRATION

VOLTMETERS/AMMETERS - Calibrated with Sensitive Research, Model VAW, 25 - 500 volts, 1/2% accuracy. This a true RMS meter independent of wave shape. This enabled calibration of all ammeters and voltmeters to true RMS values.

KELVIN BRIDGE - Calibrated before each use with Reichanstalt type 0. 1 ohm . 001% resistor, traceable to National Bureau of Standards.

TEMPERATURE CHAMBERS - Calibrated with Arthur H. Thomas precision glass rod thermometers, -5° C to +300° C and -80° C to +20° C, ±1° C accuracy.

FREQUENCY - Referenced to 60 cps power line and calibrated via Lissajous figure.

WAVE SHAPE - General radio type 1900 Wave Analyzer for measuring harmonic content to fifteenth harmonic; range 20-54000 hz; accuracy ±1/2%.

Harmonic Analysis of Output from

Paralleled Amplifiers - Figures 73-80

(A)

Frequency (Kilohertz)
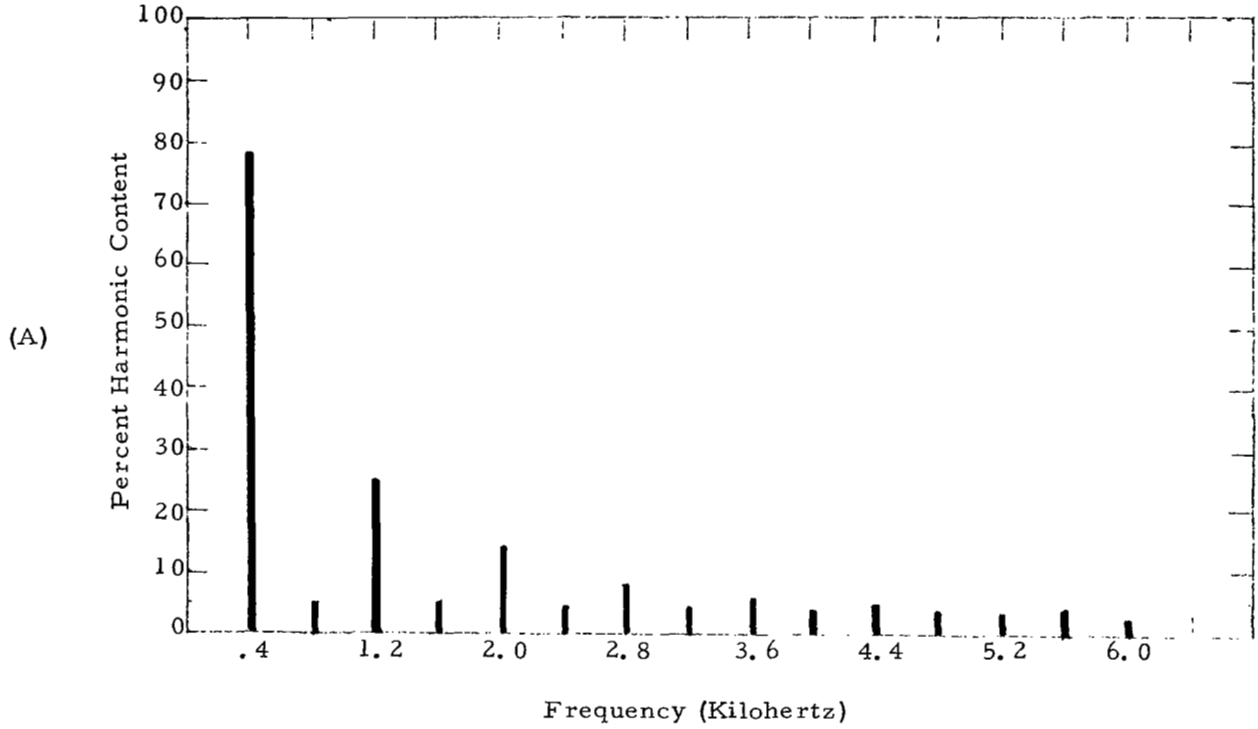
Harmonic Components of 400 Hertz Square Wave

(B)
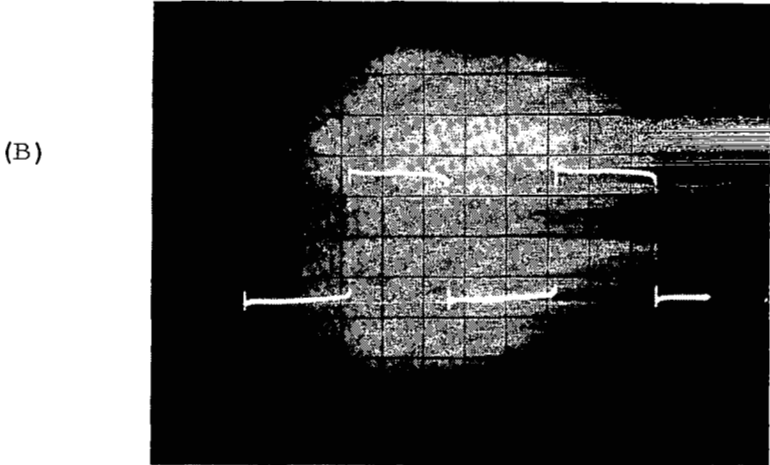
400 Hertz Square Wave

Figure 73 - 400 Hertz Square Wave and Harmonic Analysis
of output from paralleled amplifiers.

(A)

Frequency (Kilohertz)
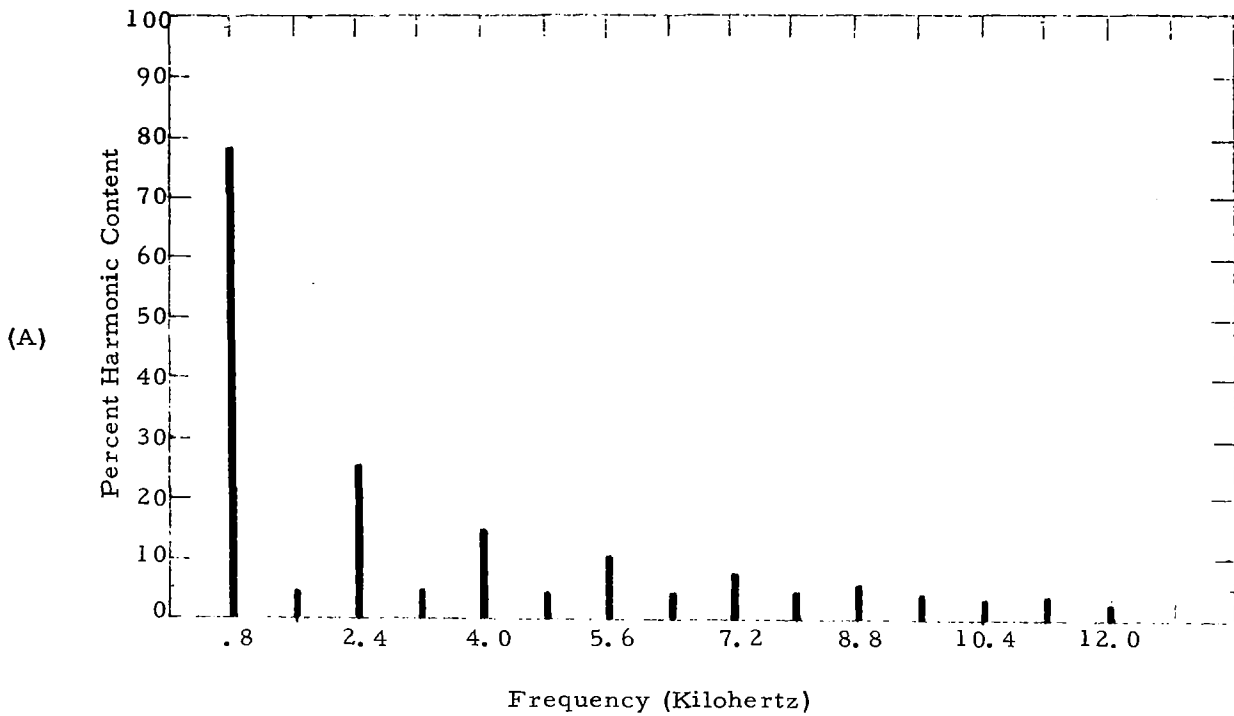
Harmonic Components of 800 Hertz Square Wave

(B)
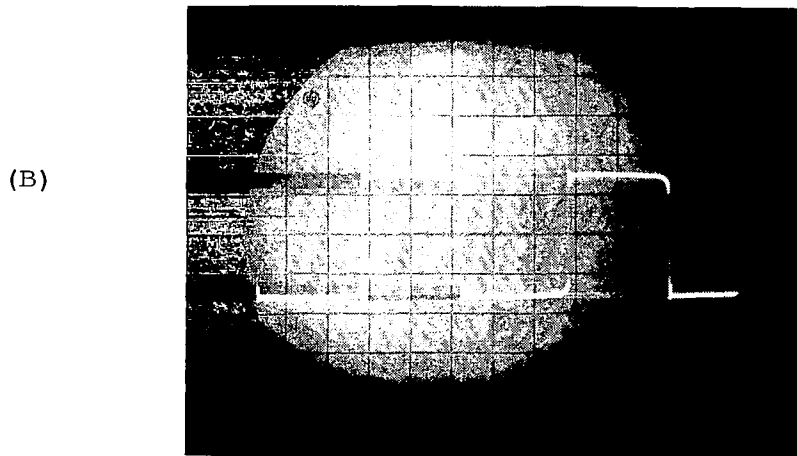
800 Hertz Square Wave

Figure 74 - 800 Hertz Square Wave and Harmonic Analysis
of output from paralled amplifiers.

(A)
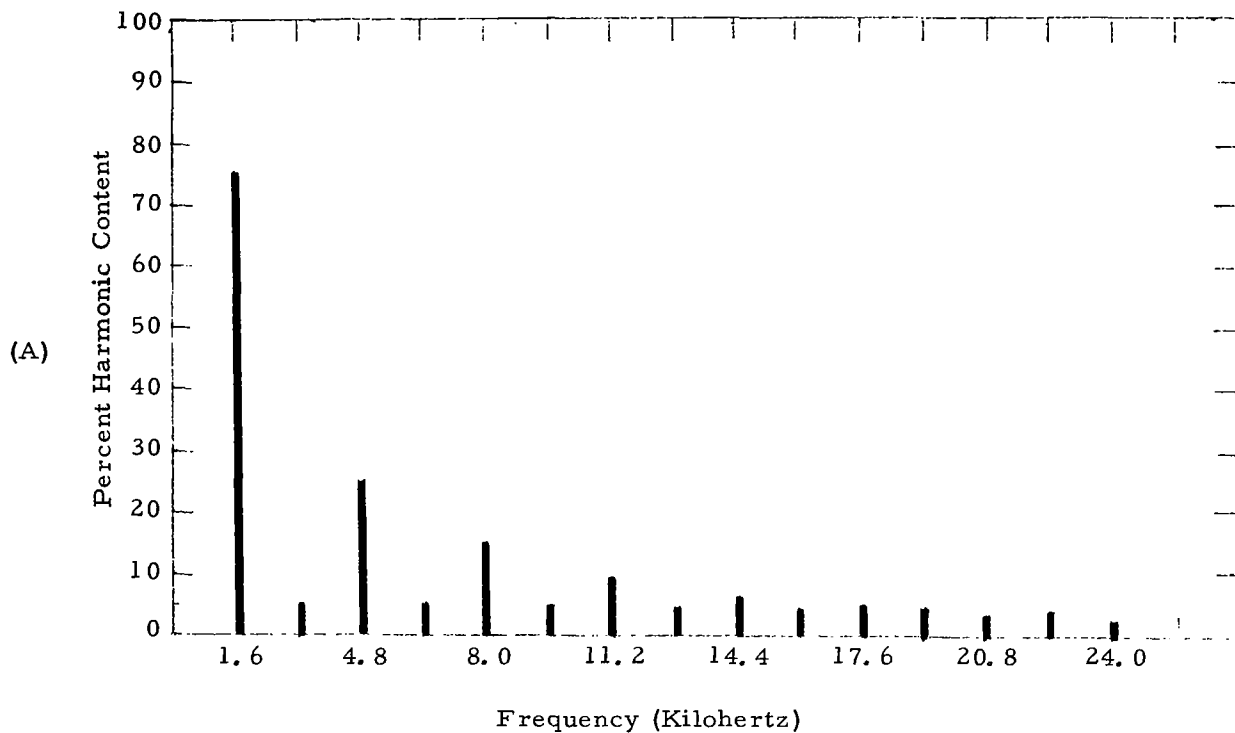
Harmonic Components of 1600 Hertz Square Wave

(B)
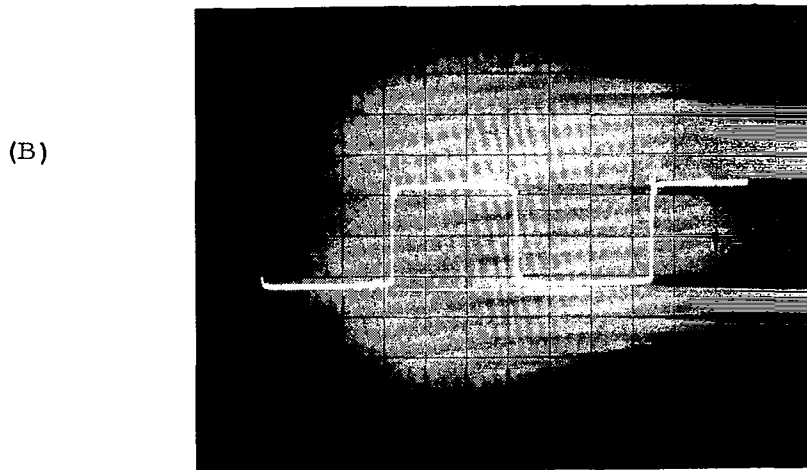
1600 Hertz Square Wave

Figure 75 - 1600 Hertz Square Wave and Harmonic Analysis
of output from paralled amplifiers.

(A)
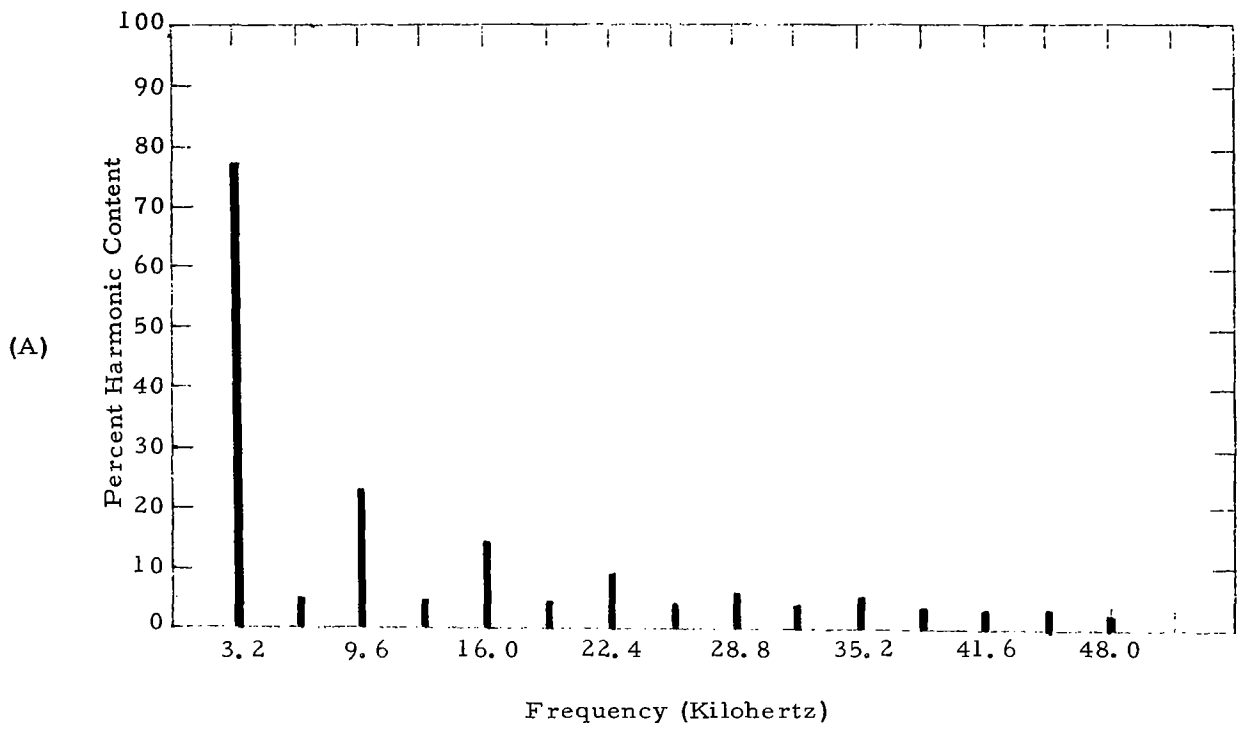
Harmonic Components of 3200 Hertz Square Wave

(B)
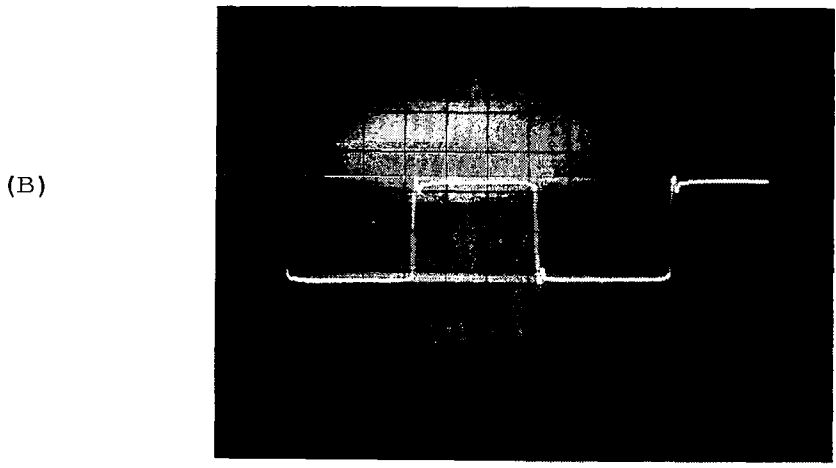
3200 Hertz Square Wave

Figure 76 - 3200 Hertz Square Wave and Harmonic Analysis
of output from paralleled amplifiers.

(A)
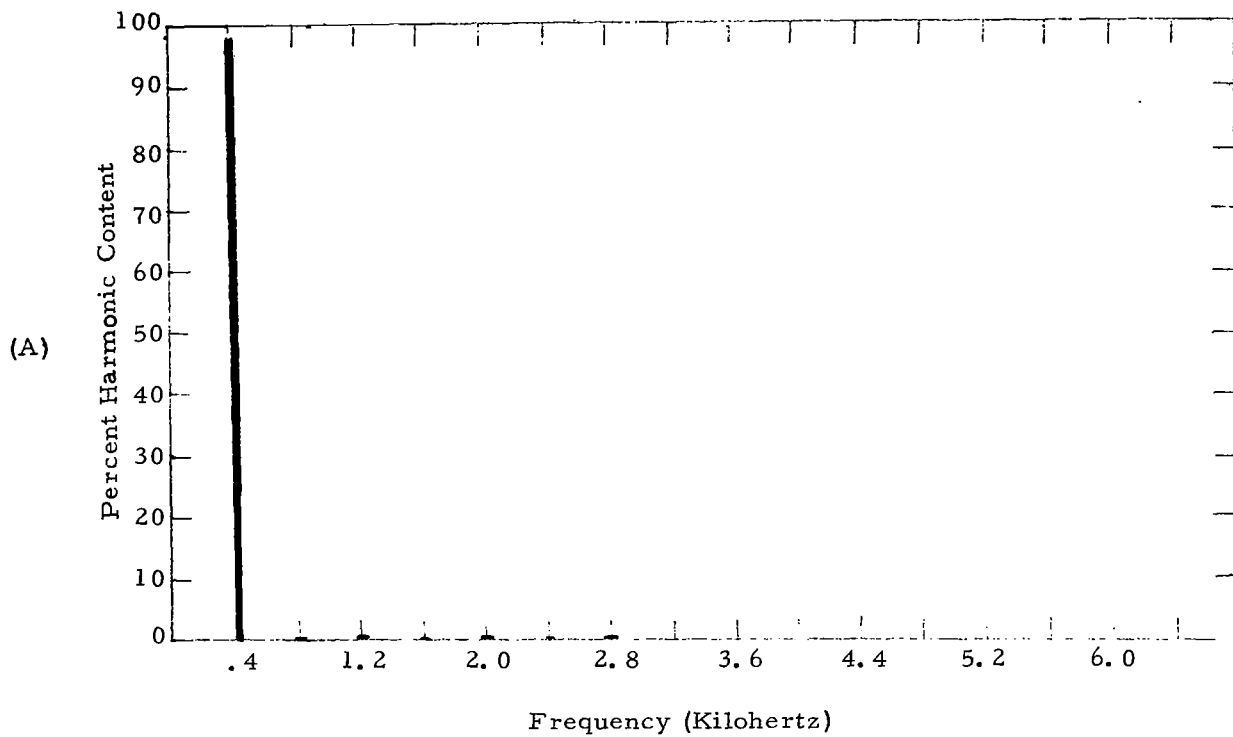
Harmonic Components of 400 Hertz Sine Wave

(B)
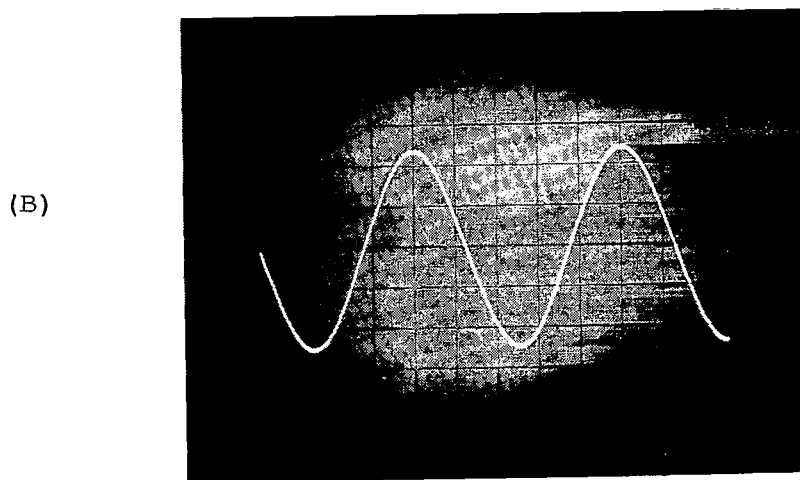
400 Hertz Sine Wave

Figure 77 - 400 Hertz Sine Wave and Harmonic Analysis
of output from paralleled amplifiers.

(A)

Frequency (Kilohertz)
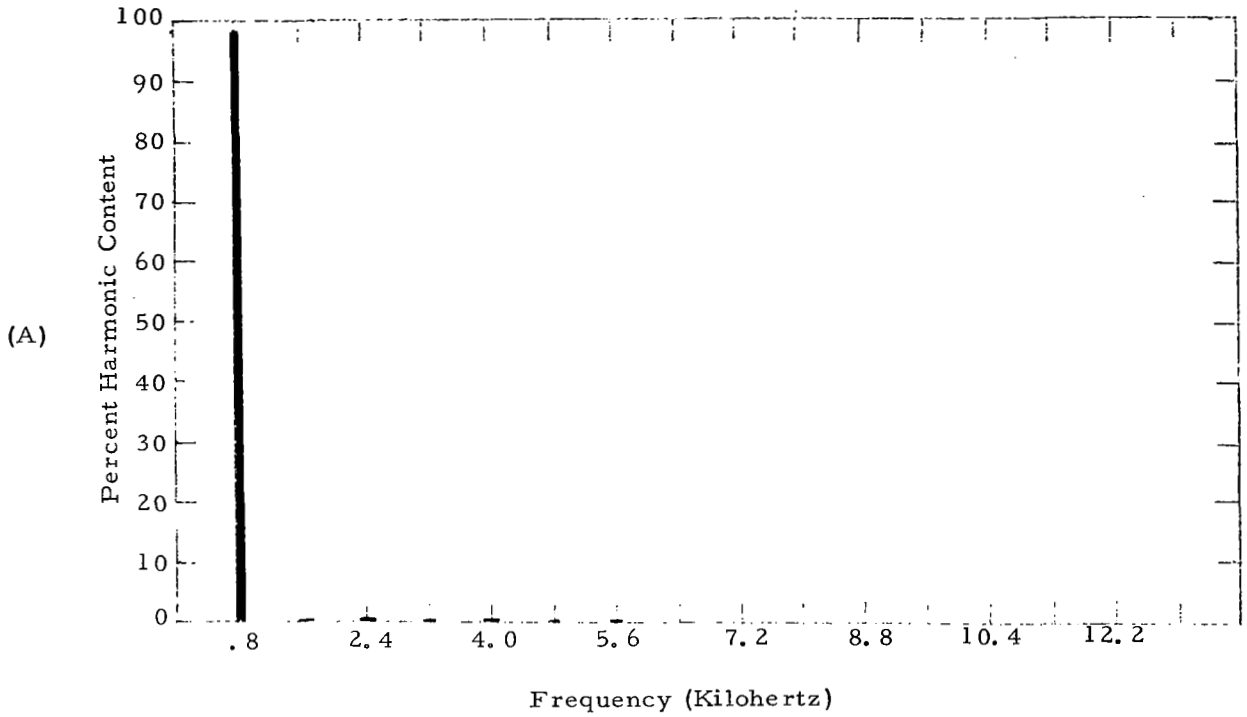
Harmonic Components of 800 Hertz Sine Wave

(B)
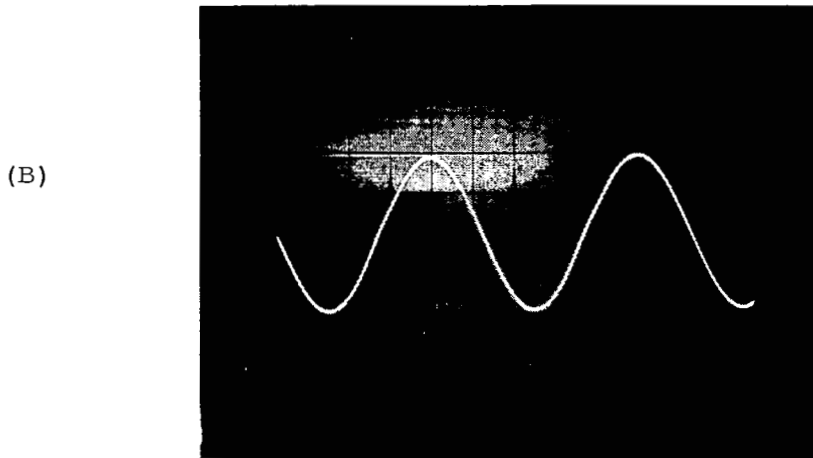
800 Hertz Sine Wave

Figure 78 - 800 Hertz Sine Wave and Harmonic Analysis
of output from paralled amplifiers.

(A)

Frequency (Kilohertz)
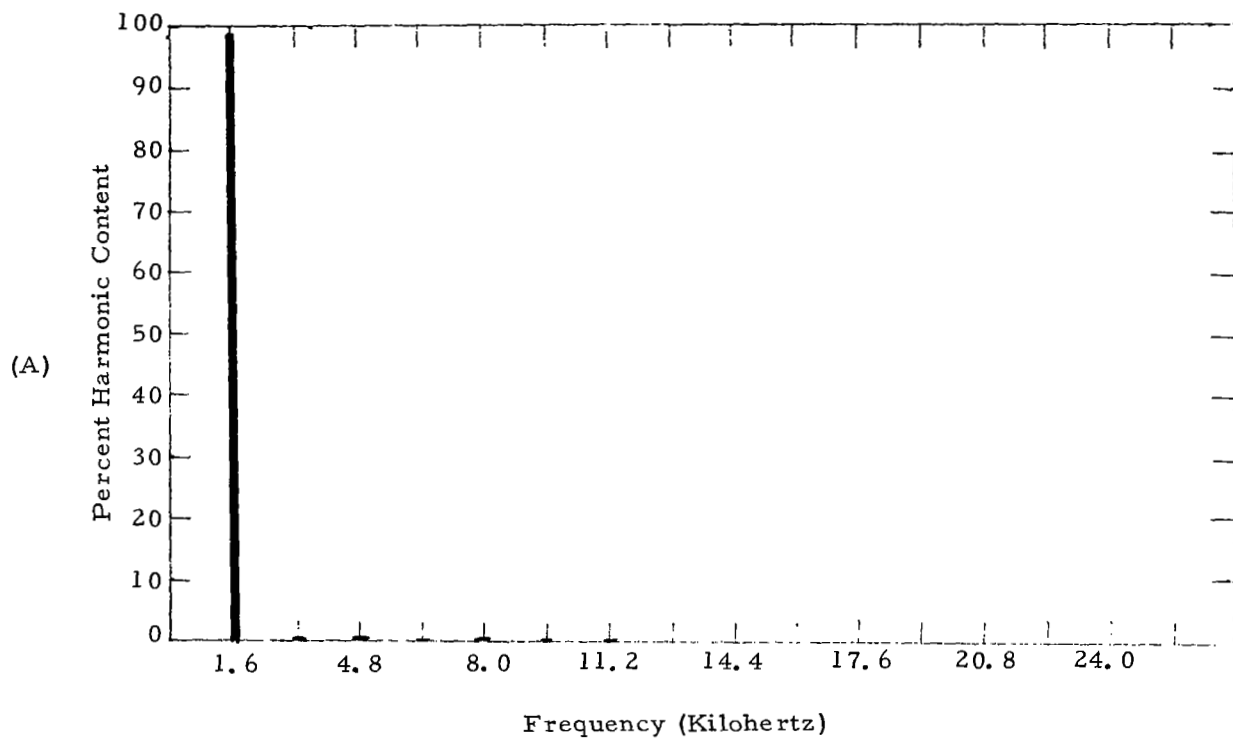
Harmonic Components of 1600 Hertz Sine Wave

(B)
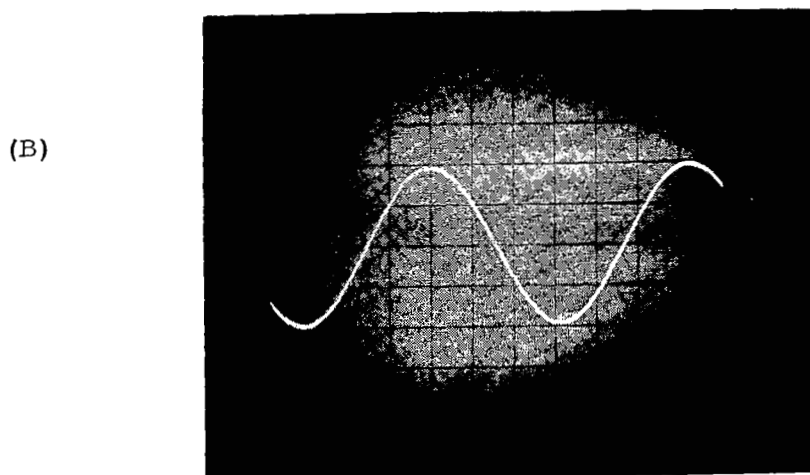
1600 Hertz Sine Wave

Figure 79 - 1600 Hertz Sine Wave and Harmonic Analysis
of output from paralleled amplifiers.

(A)
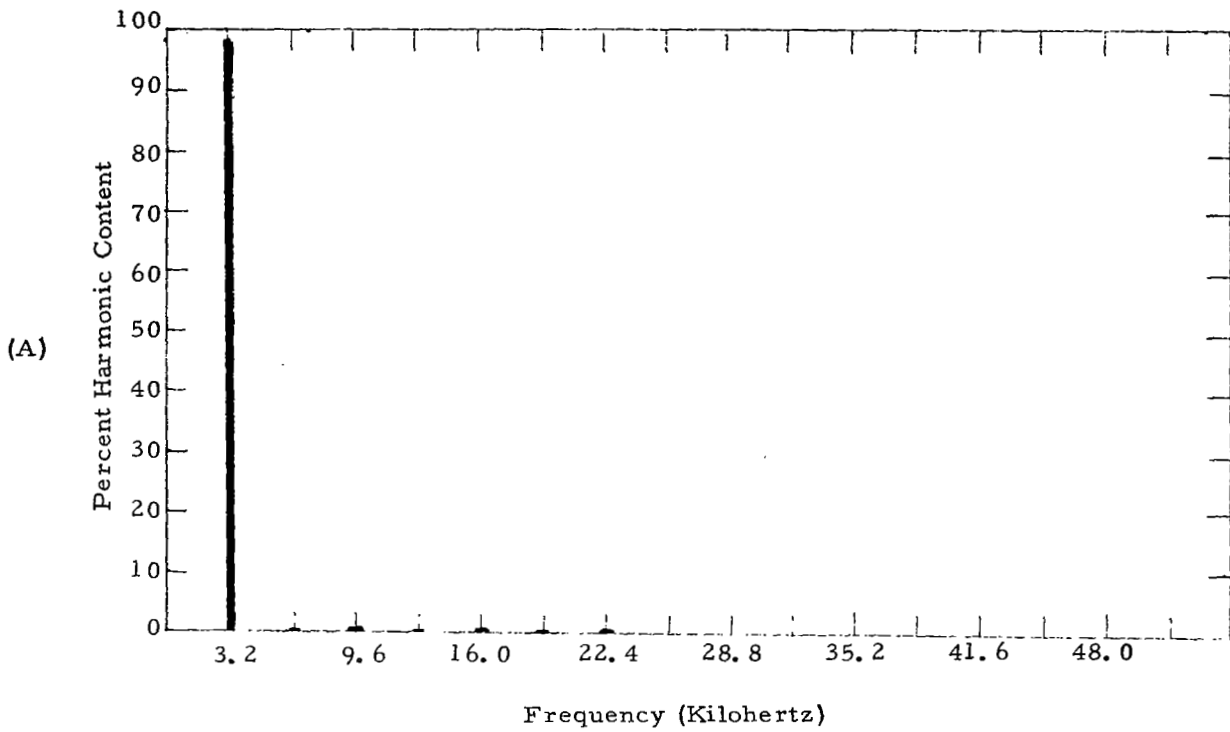
Harmonic Components of 3200 Hertz Sine Wave

(B)
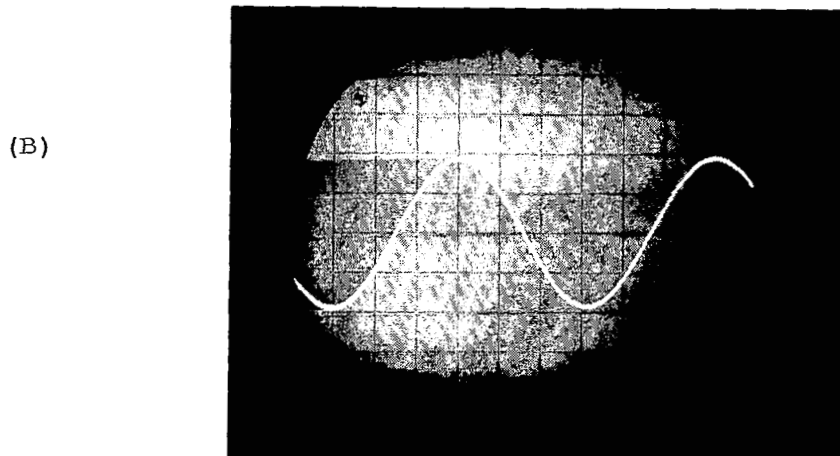
3200 Hertz Sine Wave

Figure 80 - 3200 Hertz Sine Wave and Harmonic Analysis
of output from paralleled amplifiers.
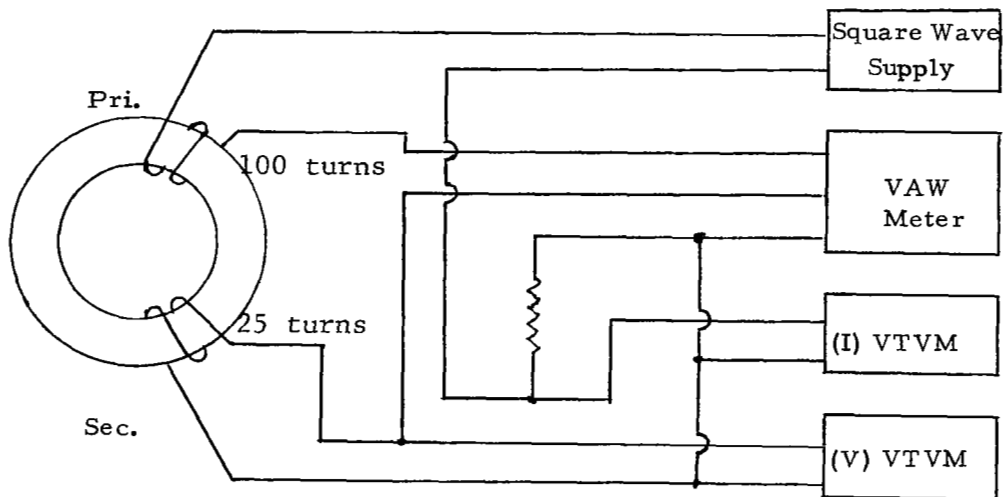
Figure 81 - A. C. Core Loss and Magnetization Circuit

Square wave supply excites 100 turn primary winding. The 25 turn secondary is used to obtain watt readings on the VAW Meter. (I) and (V) VTVM meters are used to measure excitation current and voltage.
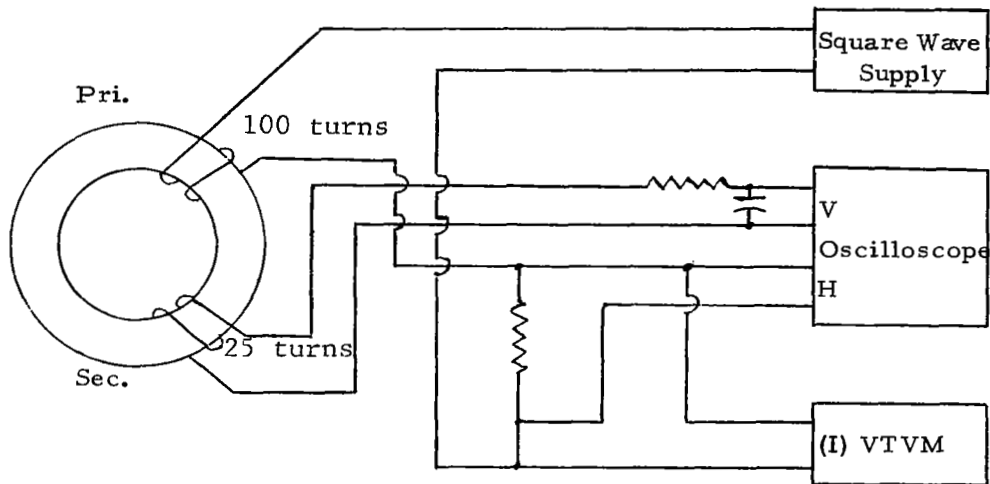
Figure 82 - A. C. Loop Circuit

Square wave supply excites 100 turn primary winding and is applied to oscilloscope horizontal; 25 turn secondary connected through integrator network to oscilloscope vertical. (I) VTVM meter is used to measure excitation current.
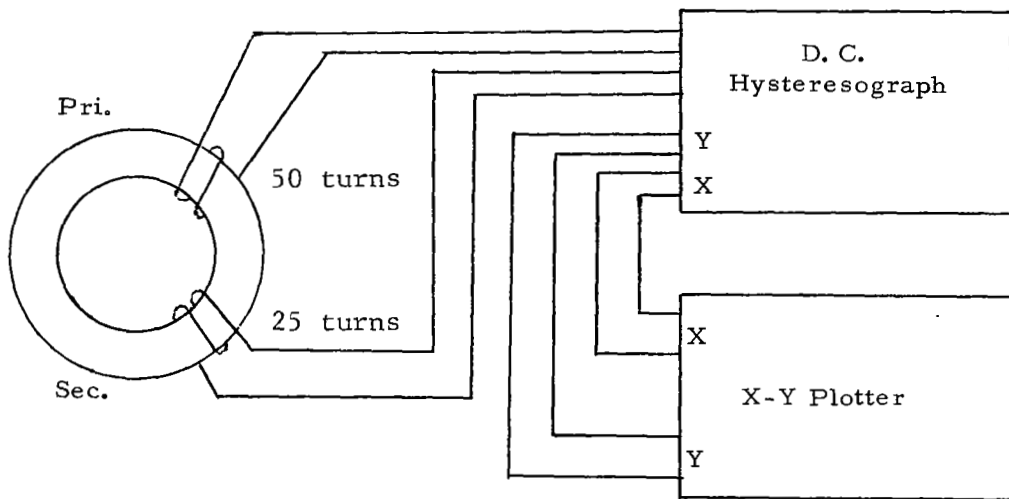
Figure 83 - D. C. Loop Circuit

The D. C. Hysteresograph supplies excitation to 50 turn primary and
measures D. C. flux from 25 turn secondary. The result is fed into
X-Y Plotter which plots on graph paper.
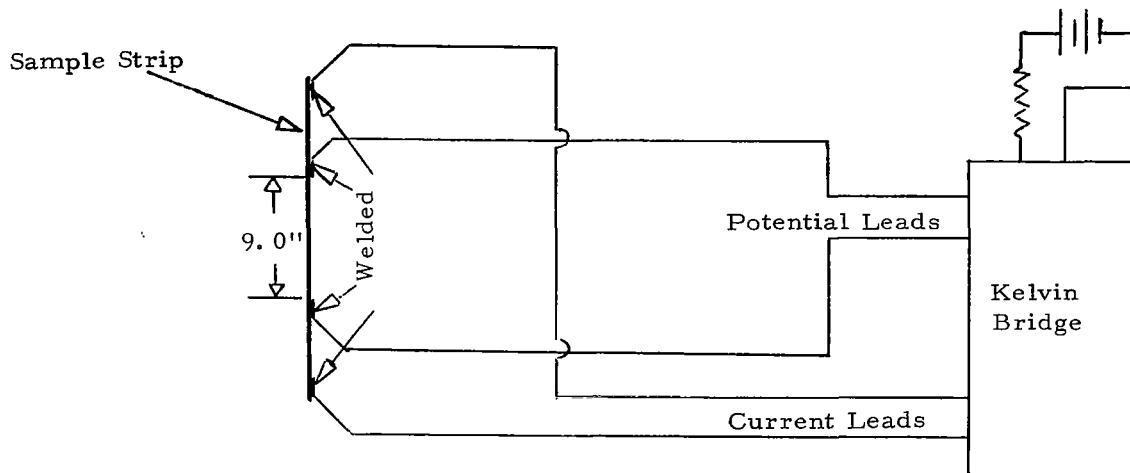
Figure 84 – Resistivity Measurement Circuit

Potential and current leads are welded to a length of 1/4 inch by .006 inch strip High Purity 80% Nickel Alloy with exactly 9 inches between the welded leads. Resistivity is measured with a Kelvin Bridge as per ASTM B70-56.

Modifications to CCFR

1. Replaced standard rectifiers with fast switching, high power types.

2. The values of R in the full wave and half wave circuits were optimized to gain maximum power output to the test cores while meeting the requirements of AIEE 432.

3. Included a 'T' pad for better control of Sine and Square wave oscillator output.

4. Included additional relays and microswitches to control the sequence of all operations.

5. Included additional meters, and fuses to protect D. C. circuits.

6. Included additional meters, and fuses to protect all excitation circuits.

7. Altered calibration circuit to include an external precision Williamson Voltmeter-Ammeter to set proper calibration current for each frequency.

8. Accuracy achieved between 1/2%-1%.
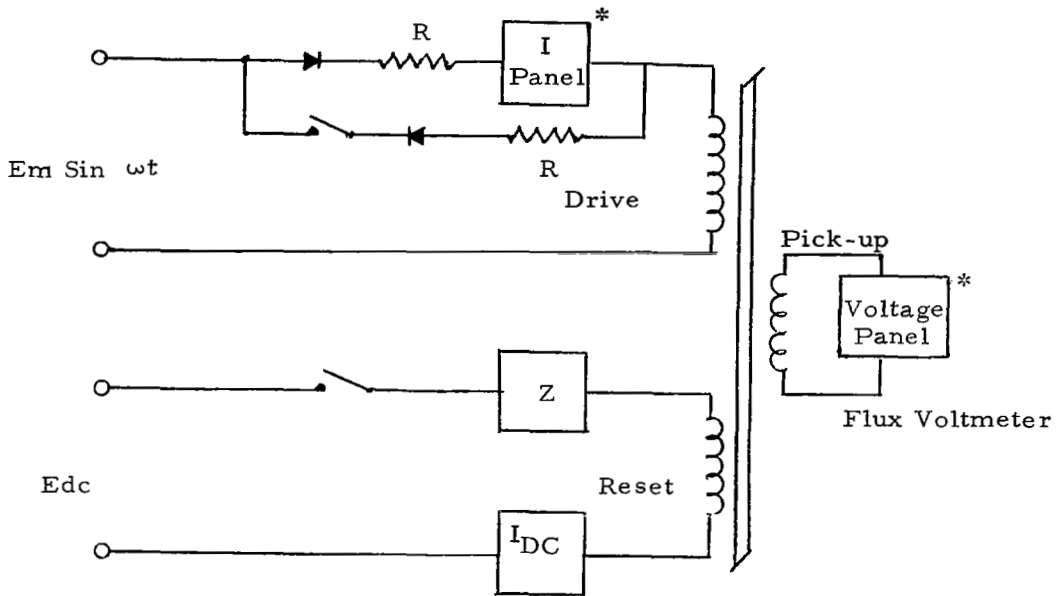
* These sections modified for square wave and high frequency measurements. Tester originally designed for 400 Hz sine wave.

Figure 85 - Simplified Diagram of Constant Current Flux Reset Tester.

Evaluation Test Circuit - Figure 86

The windings of each core in the temperature chamber were connected to a multi-position, multi-deck rotary switch. Sine and Square wave power, monitored by a frequency counter, was used to excite each core when under test. Leads for each of the tests were switched without removing the cores from the chamber.

Cycling Test Circuit - Figure 87

Each winding of each core in the temperature chamber was connected to a multi-position, multi-deck rotary switch. All cores were continuously excited with 400 Hz square wave except when under test. One chamber was periodically cycled -55° C to +200° C with temperature and number of cycles recorded. The other chamber maintained a constant +200° C temperature with temperature recorded.
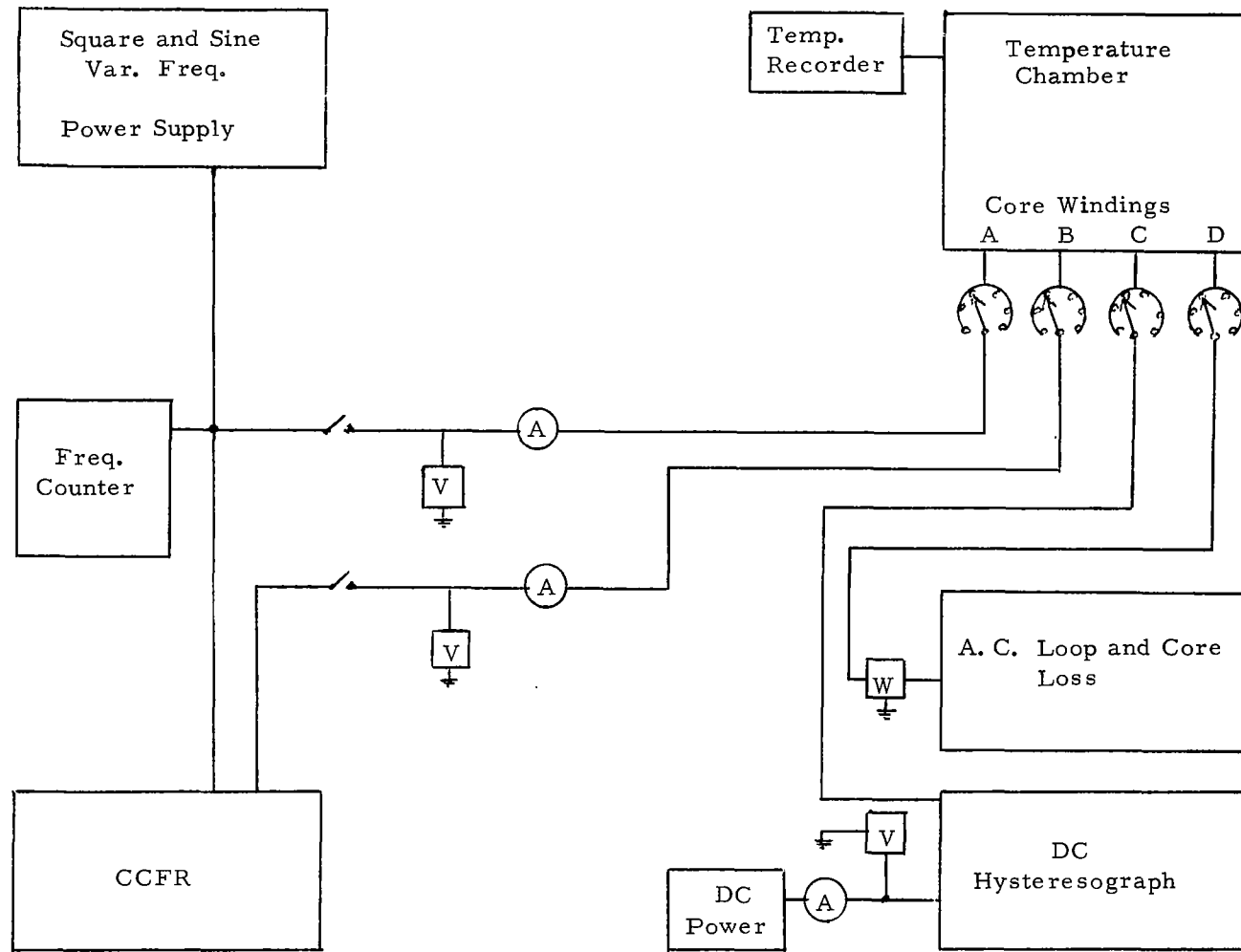
Figure 86 - Schematic Diagram of Evaluation Test Circuits High Purity 80% Nickel Alloy
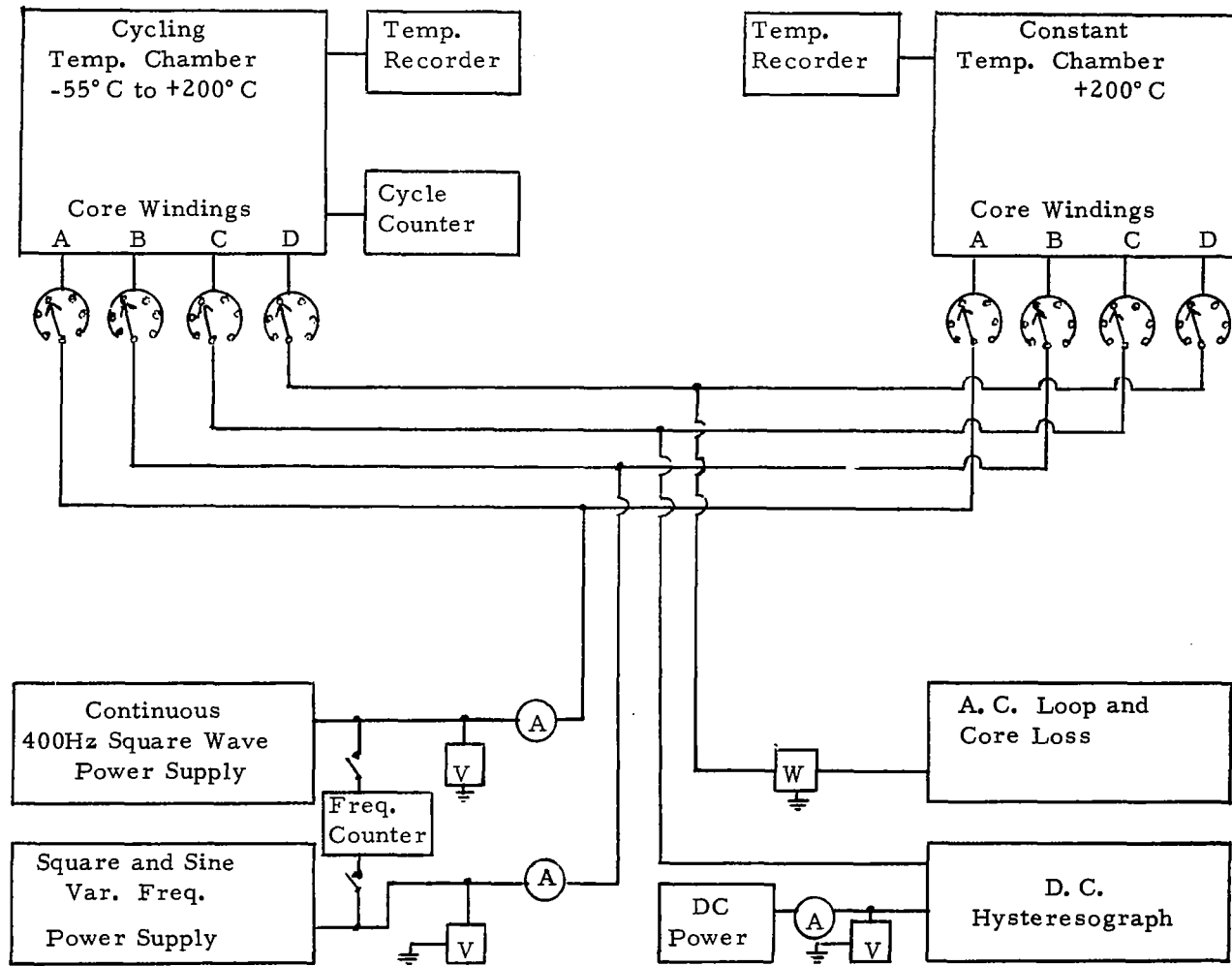
Figure 87 - Schematic Diagram of Cycling Test Circuits

Analysis of Thermal Expansion of Core and Core Box
Assembly for Temperature Range of 25° C to +200° C*

The dimensions of the core and core box at room temperature are as shown below:
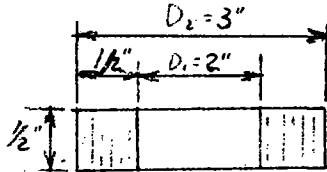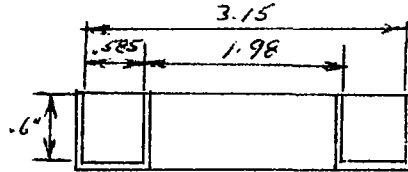
Core at Te = 25° C   Core box at Te = 25° C

Assume the Space Factor is 90%

Then the actual build-up of the metal core is . 9 x . 5 = . 45"

With a tape thickness of . 002", then

the number of turns in the core is $\frac{.45}{.002}$ = 225 Turns,

and the thickness of the insulation coating is $\frac{.05"}{225}$ = . 000222"

Let t = thickness of tape + insulation as shown below:
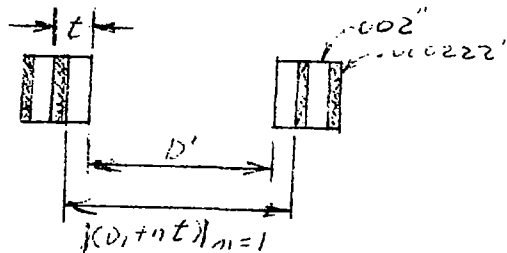
The total length of tape in the core is: $(1) L = \pi \sum_{n=1}^{n=225} (D_1 + nt)$

$$= \pi \left[nD_1 + t \sum_1^{225} n \right]$$

$$\text{or } (2) \; L \cong \left[nD_1 + t \frac{n^2}{2} \right]$$

Evaluating $\frac{tn^2}{2}$ and nD_1

$$t = 002 + 000222 = .002222"$$

$$\frac{n^2}{2} = \frac{(225)^2}{2} = 25312$$

$$\frac{tn^2}{2} = .002222 \times 25312 = 56.24"$$

$$nD_1 = 225 \times 2 = 450"$$

Substituting the values for $\frac{tn^2}{2}$ and nD_1 into equation (2)

$$\left(nD_1 + \frac{tn^2}{2} \right) = 450 + 56.24 = 506.24"$$

$$\text{at } 25°C \; \overset{L}{=} \; \pi \times 506.24 = 1589.6"$$

From reference 1 (p. 15), the thermal expansion coefficient for HyMu 80 is:

$$\alpha = 12.9 \times 10^{-6} \left(\frac{in}{in} \right) \Big/ °C \text{ for } -70 \overset{°}{\underset{C}{\leq}} T_e \leq 200°C$$

The length of the tape at $T_e = 200°C$ is:

$$L^1 = L(1 + \alpha \, T_e)$$
$$L^1 = 1589.6 \left[1 + 12.9 \times 10^{-6} \times (200-25) \right]$$
$$L^1 = 1593.2"$$

and the change in length for the temperature range from 25°C to 200°C is:

$$\Delta L = 1593.2 - 1589.6 = 3.6"$$

$$\% \Delta L = \frac{3.6}{1589.6} \times 100 = +.2265\% \quad \text{This is an in-significant change in length.}$$

The dimensional increase in strip thickness and insulation thickness at 200°C is:

Strip thickness at 200°C $= 002'' (1 + \alpha\ t)$

$$= 002'' (1 + 12.9 \times 10^{-6} \times 175)$$

$$= .0020045''$$

For the insulation coating use the same thermal coefficient as for fused silica i.e., α SiO $= .54 \times 10^{-6}/°C$ (Ref. 3)

Insulation thickness at 200°C $= .000222 (1 + .54 \times 175 \times 10^{-6})$

$$= .000222021''$$

$$t^1 \text{ at } 200°C = \begin{array}{r} 0020045 \\ + \ 0002220 \\ \hline \end{array}$$

$$t^1 = .0022265$$

The width of the tape at 200°C $= .5 (1 + \alpha\ t)$

$$W^1 = .5 \times 1.00226 = .50113$$

From equation (2) D_1 at 200°C is:

$$L^1 = \pi \left[n\ D_1 + t^1 \frac{n^2}{2} \right]$$

$$D_1 = \frac{1}{n} \left[\frac{L^1}{\pi} - t^1 \frac{n^2}{2} \right]$$

$$D_1 = \frac{1}{225} \left[\frac{1593.2}{3.14} - .0022265 \times 25312 \right] = 2.0046''$$

$$D_2 \text{ at } 200°C = 2.0046 + 2 \left[225 \times 0022265 \right]$$

$$D_2 = 3.0065''$$

The core dimensions then at 200° C are:
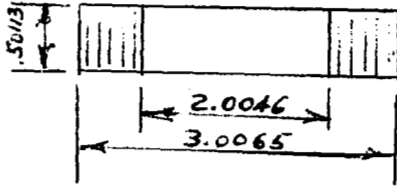
The volume of the core at 200° C is:

$$V^l{}_{core} = \frac{\pi}{4} W^l \left[(D_2)^2 - (D_1)^2 \right]$$

$$= \frac{\pi}{4} \times .50113" \left[3.0065^2 - 2.0046^2 \right]$$

$$V^l{}_{core} = 1.975 \text{ cu"}$$

The volume of the core at 25° C

$$V_{core} = \frac{\pi}{4} \times .5 \left[3^2 - 2^2 \right] = 1.963 \text{ cu"}$$

The thermal coefficient of expansion for aluminum is:

$$\alpha_{Al} = 24 \times 10^{-6}/°C$$

The change in width of the core box at 200° C is:

$$p^l = .585 (1 + 24 \times 10^{-6} \times 175)$$

$$p^l = .58746"$$

The change in height of the core box is:

$$Q^l = .6 \times 1.0042 = .60252"$$

111

The dimensions of the core box at 200°C are:
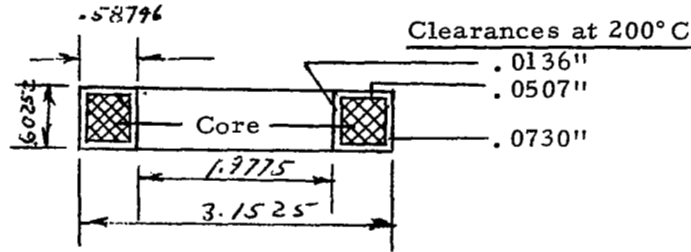
Neglecting the oil in core box at 200°C then the clearances between the core and the inside dimensions of the core box are:

Clearance top and bottom $= \dfrac{1}{2}$ (.60252 - .50113) = .0507"

Clearance on ID $= \dfrac{1}{2}$ (2.0046 - 1.9775) = .0136"

Clearance on OD $= \dfrac{1}{2}$ (3.1525 - 3.0065) = .0730"

Clearance at 25°C

Top and Bottom $=$ 1/2 (.6 - .5) = .05"

ID $=$ 1/2 (2 - 1.98) = .01"

OD $=$ 1/2 (3.15 - 3.0) = .075"

Volume of core box cavity at 25°C

$$V_{CB} = \frac{\pi}{4} \times .6 \left[3.15^2 - 1.98^2 \right] = 2.827 \text{ cu"}$$

Volume of core box cavity at 200°C

$$V^1_{CB} = \frac{\pi}{4} \times .60252 \left[3.1525^2 - 1.9775^2 \right] = 2.851 \text{ cu"}$$

Volume of oil at 25°C = 2.827 - 1.963 = .864 cu"

The coefficient of expansion for Silicone oil is:

$$\propto_{oil} = 9 \times 10^{-4} \ \frac{cm^3}{cm^3} \Big/ °C$$

Volume of oil at 200°C = .864 $(1 + \propto_{oil} Te)$

$$V_{oil}^1 = .864 (1 + 9 \times 10^{-4} \times 175)$$

$$= 1.00008 \ cu"$$

Volume of core + volume of oil at 200°C =

$$V_{core}^1 + V_{oil}^1 = 1.975 + 1.00008 = 2.9751 \ cu"$$

Volume of core box cavity at 200°C = 2.851 cu"

$$V_{core}^1 + V_{oil}^1 \ > V_{core \ box \ cavity} \quad i.e., \ 2.9751 \ > \ 2.851$$

And the expansion of the oil produces stress on the core

$$\% \ \Delta V^1 = \frac{2.9751 - 2.851}{2.851} \ \times 100 = 4.33\%$$

However -- since this stress was anticipated, the cores were heated to +200°C prior to sealing to allow the expanding oil to escape hence also eliminating expanding oil as a factor producing stress.

* This detailed analysis performed by Francis Gourash, Project Manager, NASA Research Center, Cleveland, Ohio.

APPENDIX E

Analysis of Core Loss and Monitoring Data

E-1   Core Loss and Excitation Curves at 5Kg obtained from Evaluation Data of High Purity 80% Nickel Alloy - Figures 88 and 89.

E-2   Core Loss for 1/3, 2/3 and Maximum Induction Curves obtained from Temperature Cycling Data - Figures 90-101.

E-3   Core Loss and Excitation Curves for the Effects of Time and Temperature obtained from Temperature Cycling Data - Figures 102-113.

E-4   Core Loss Curves obtained from Monitoring Data - Figures 114-119.

From additional data that was obtained during this program, the following charts have been prepared to readily show the effects of time, temperature and frequency for each material. The 5Kg flux level in figures 88 and 89 was selected as an average point just below the knee of the magnetization curve. The 1/3, 2/3 and maximum induction levels of figures 90-101 and 114-119 provide a comparison of the response of each material for these levels, while figures 102-113 show the relative effects of time and temperature.

Figure 88 - Total Core Loss at 5 Kg vs. temperature and frequency,
High Purity 80% Nickel Alloy
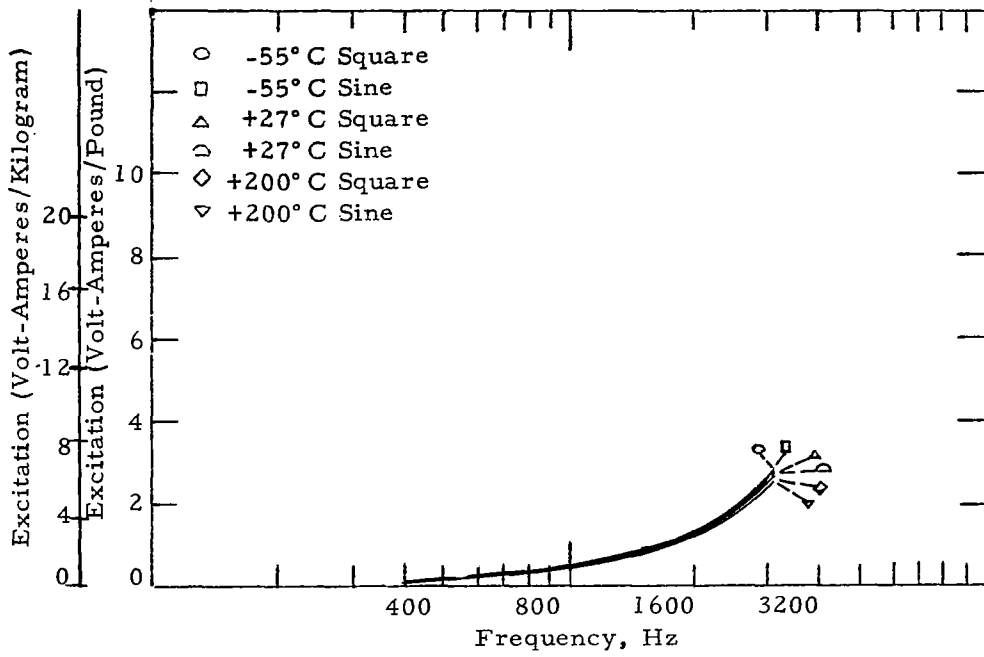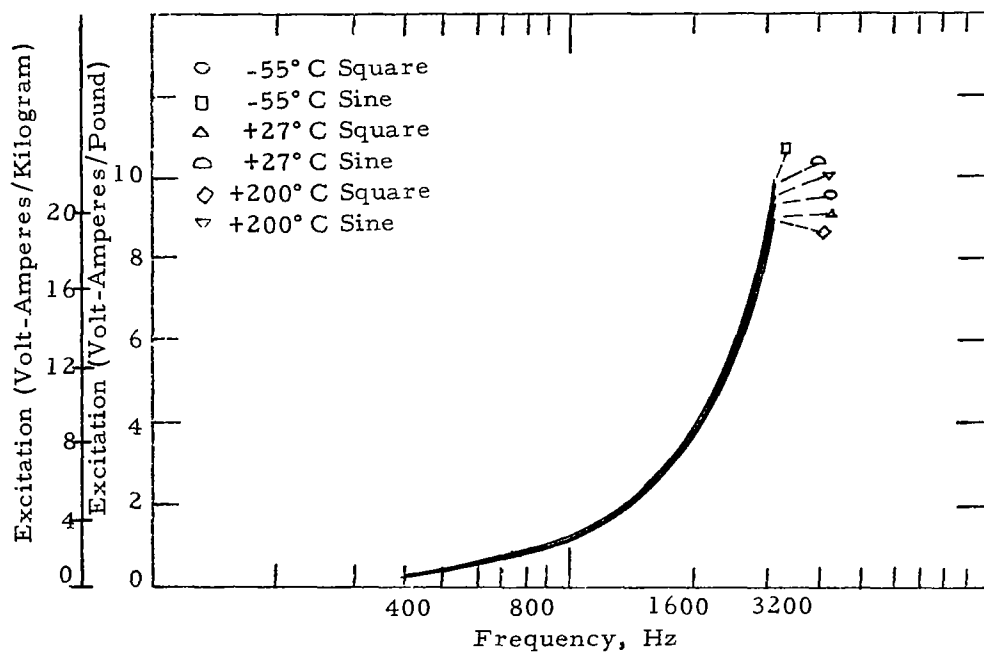
Figure 89 -   Excitation at 5 Kg vs. temperature and frequency,
High Purity 80% Nickel Alloy.

Core Loss for 1/3, 2/3 and Maximum Induction Curves obtained from Temperature Cycling Data - Figures 90-101.
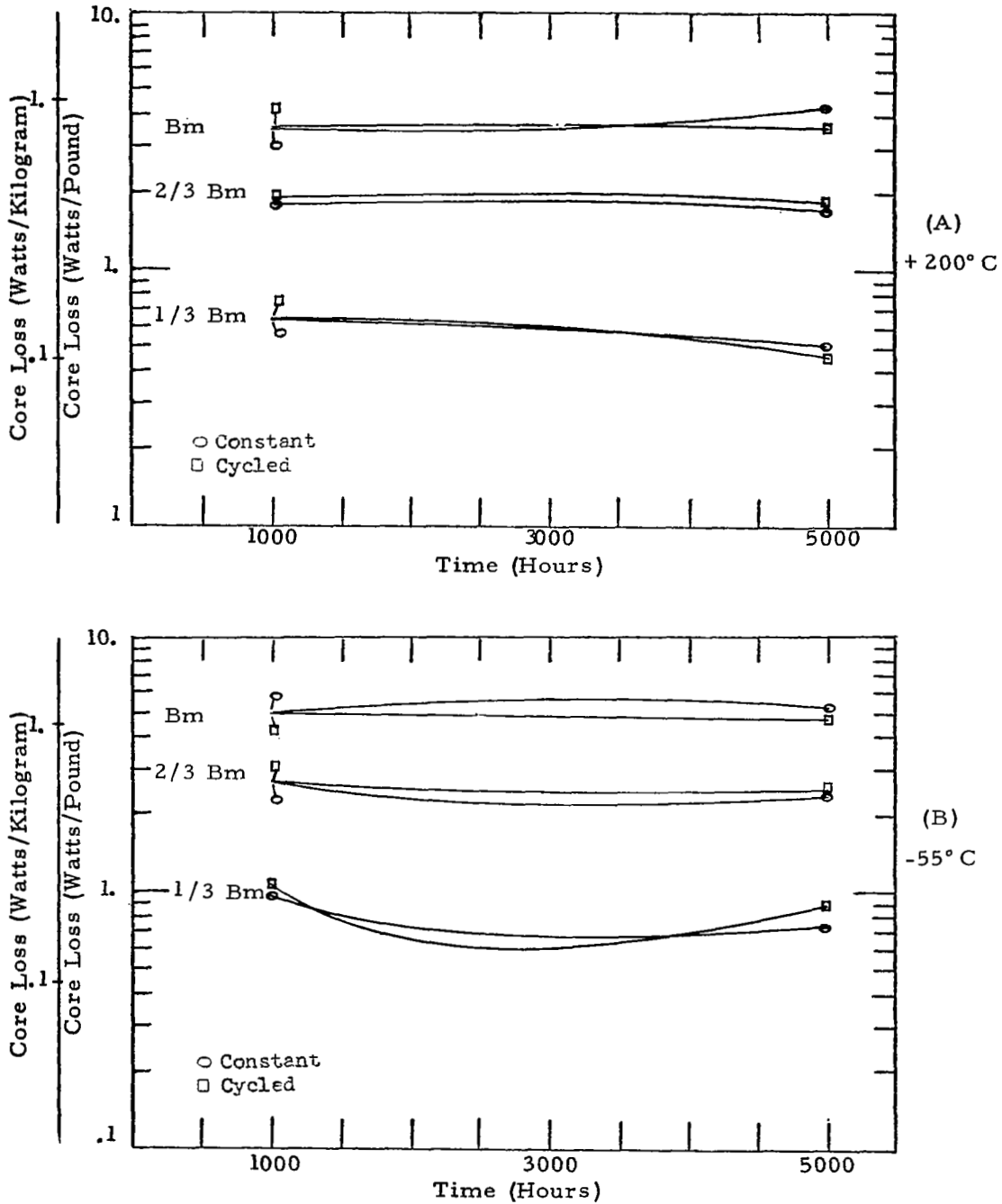
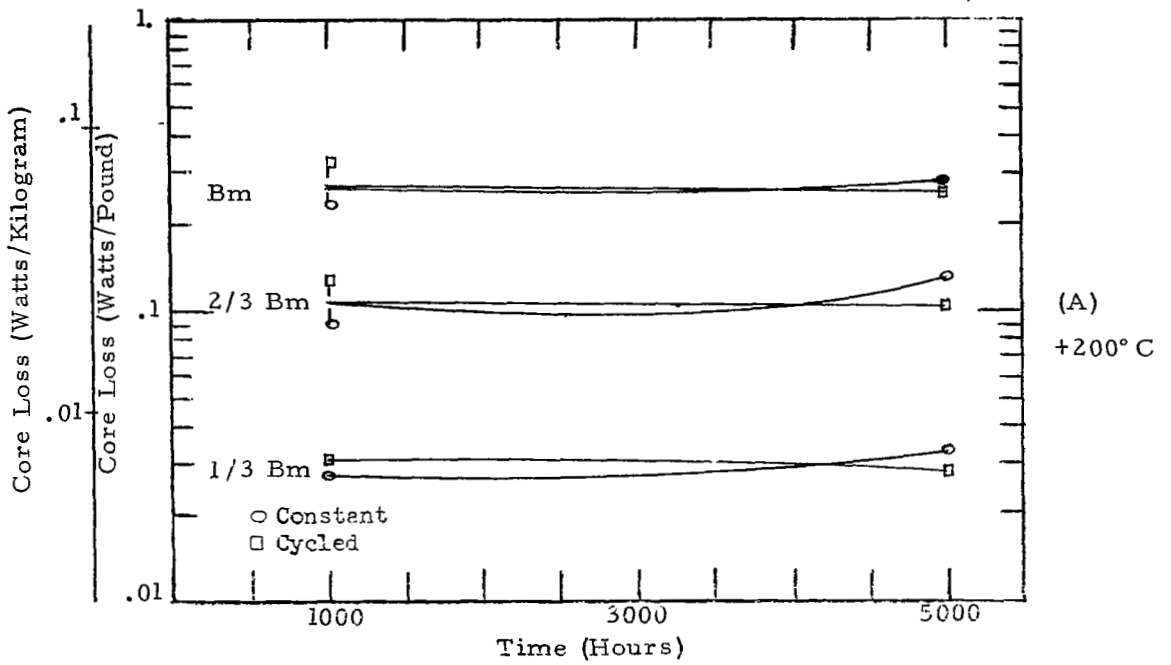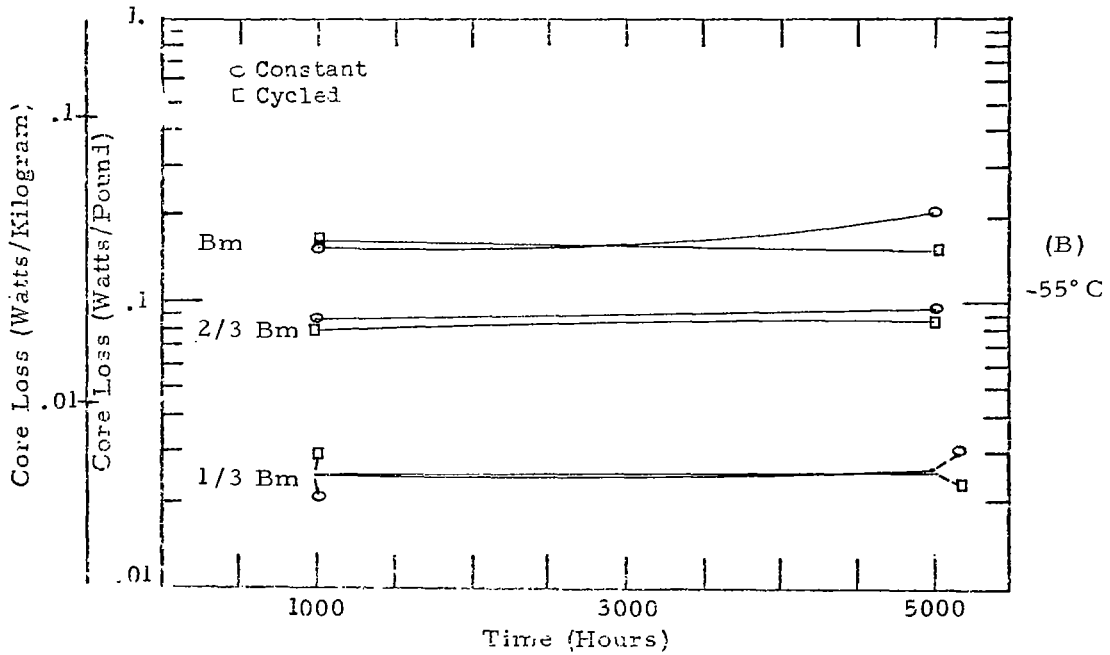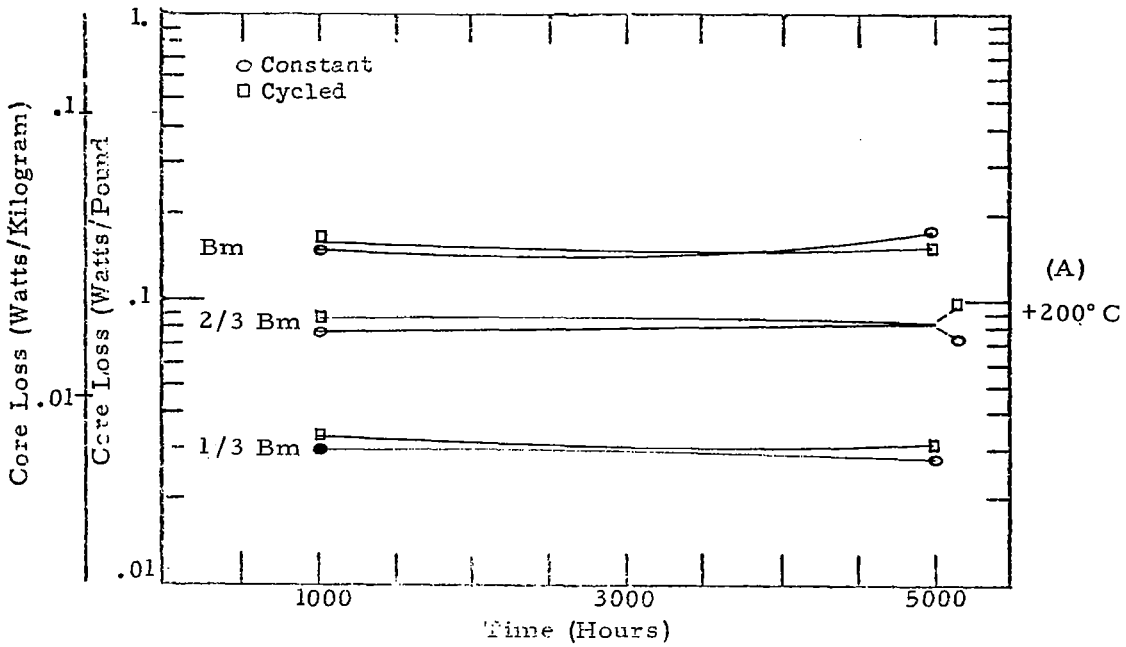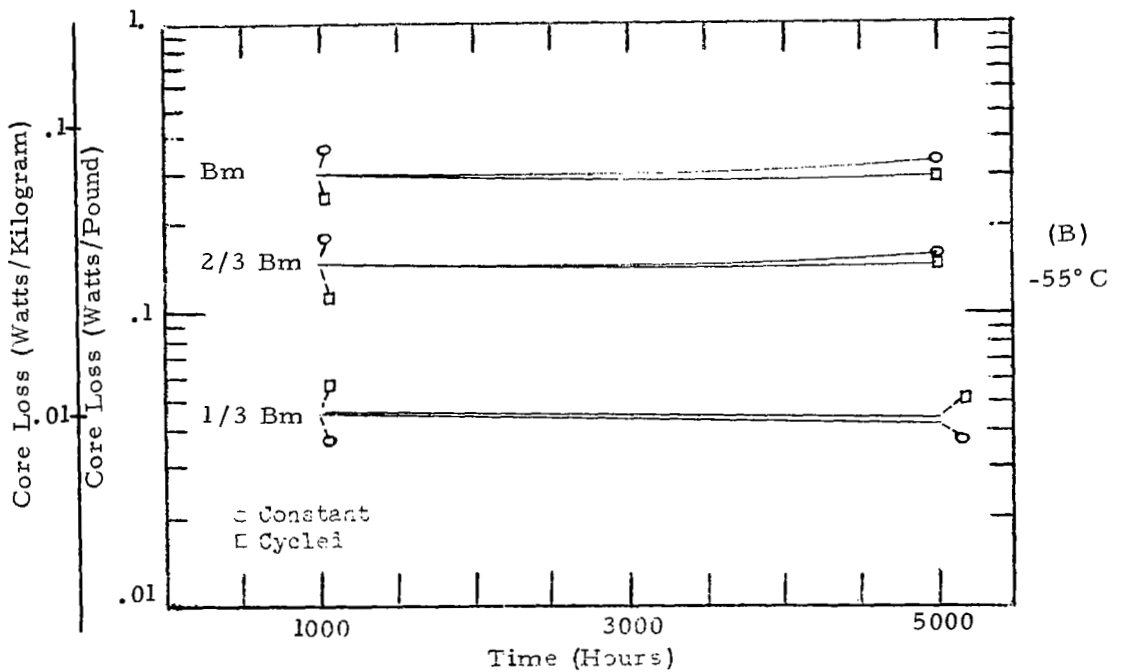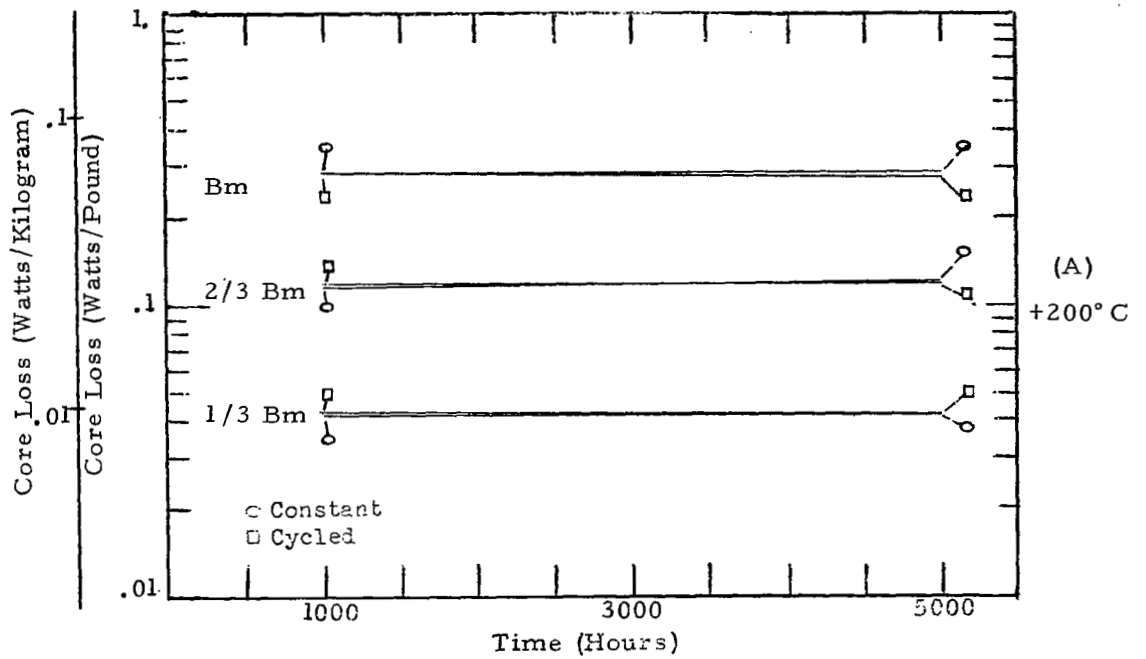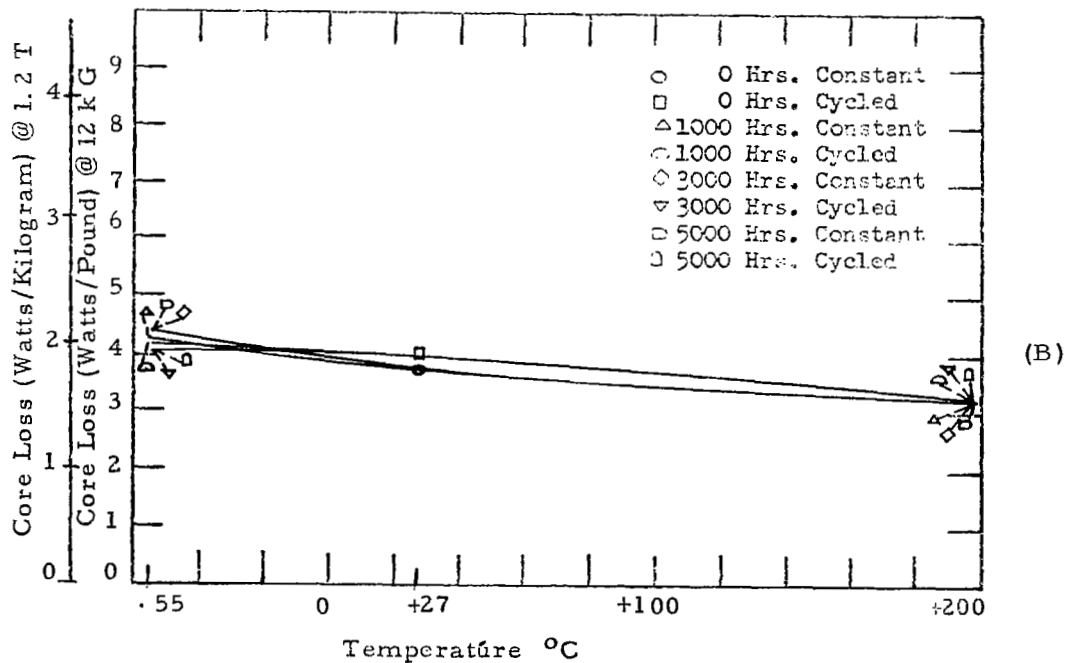Figure 90 - Core Loss for 1/3, 2/3 and Maximum Induction vs. Constant and Cycled Temperatures for -55° C and +200° C. 0.002 inch Tape Cores. Single Grain Oriented Silicon Iron.
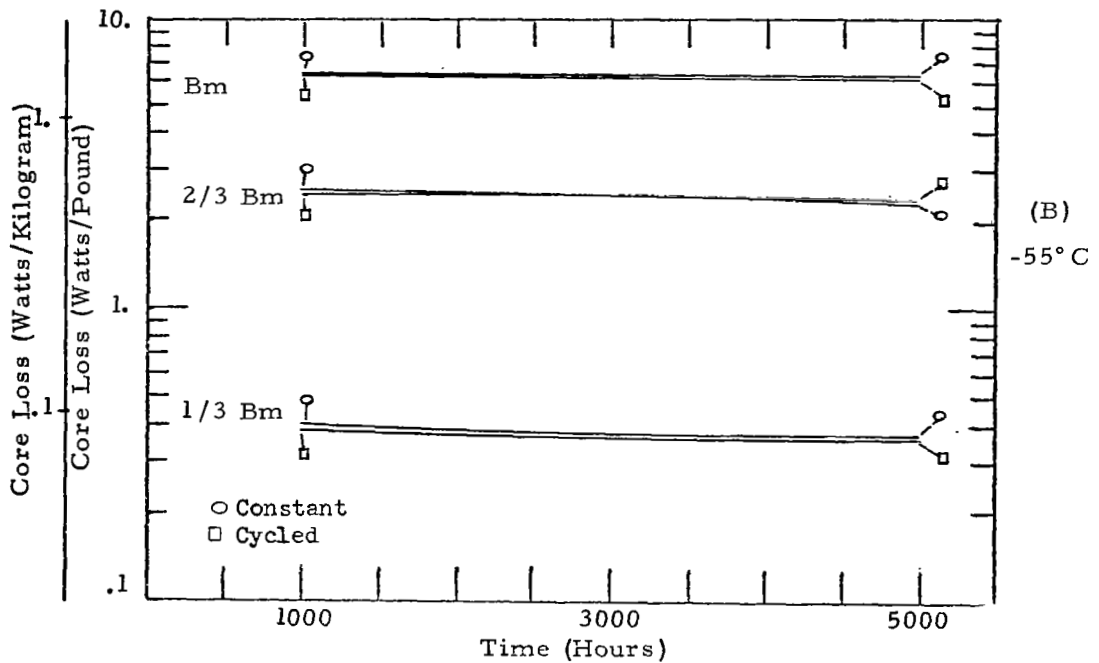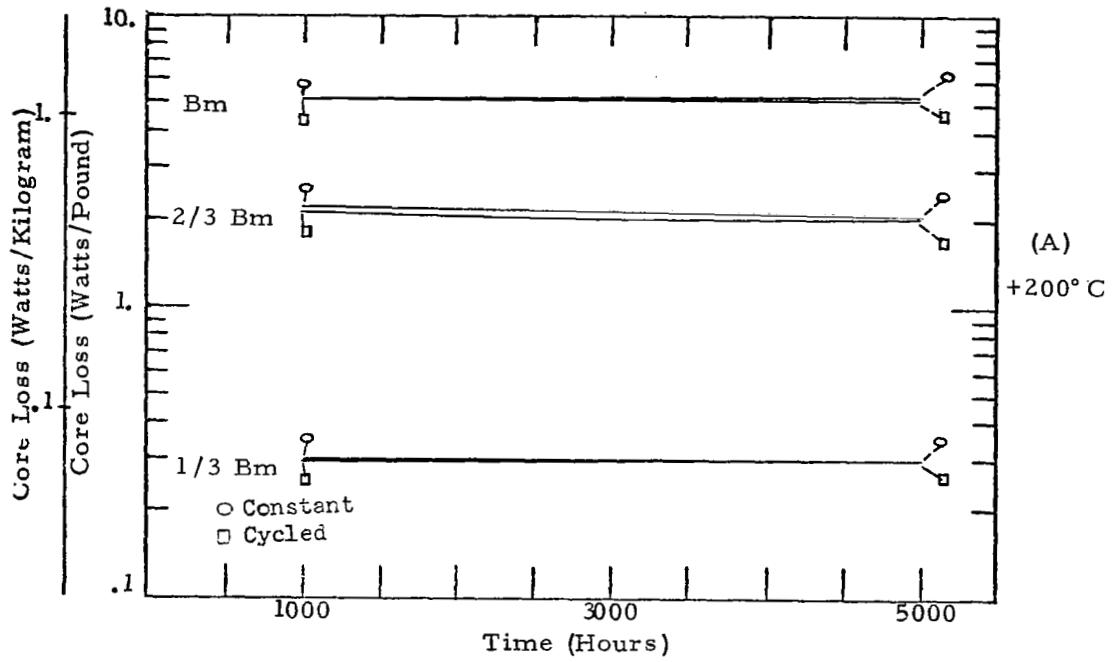
Figure 91 - Core Loss for 1/3, 2/3 and Maximum Induction vs. Constant
and Cycled Temperature for -55°C and +200°C. · 0.006 inch
Ring Core, Single Grain Oriented Silicon Iron.

118
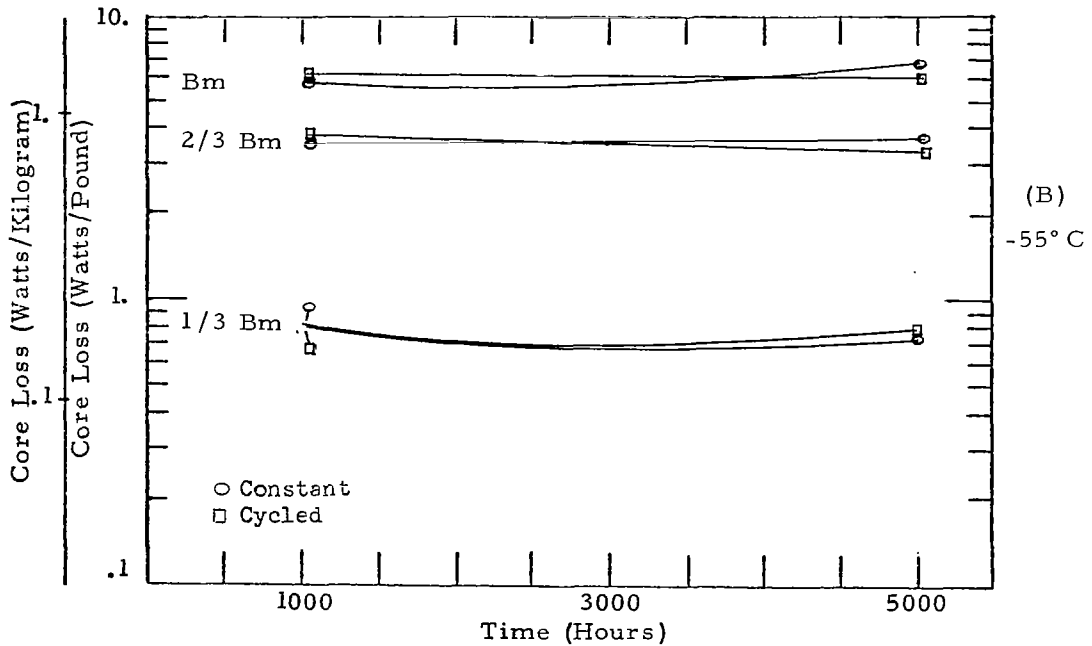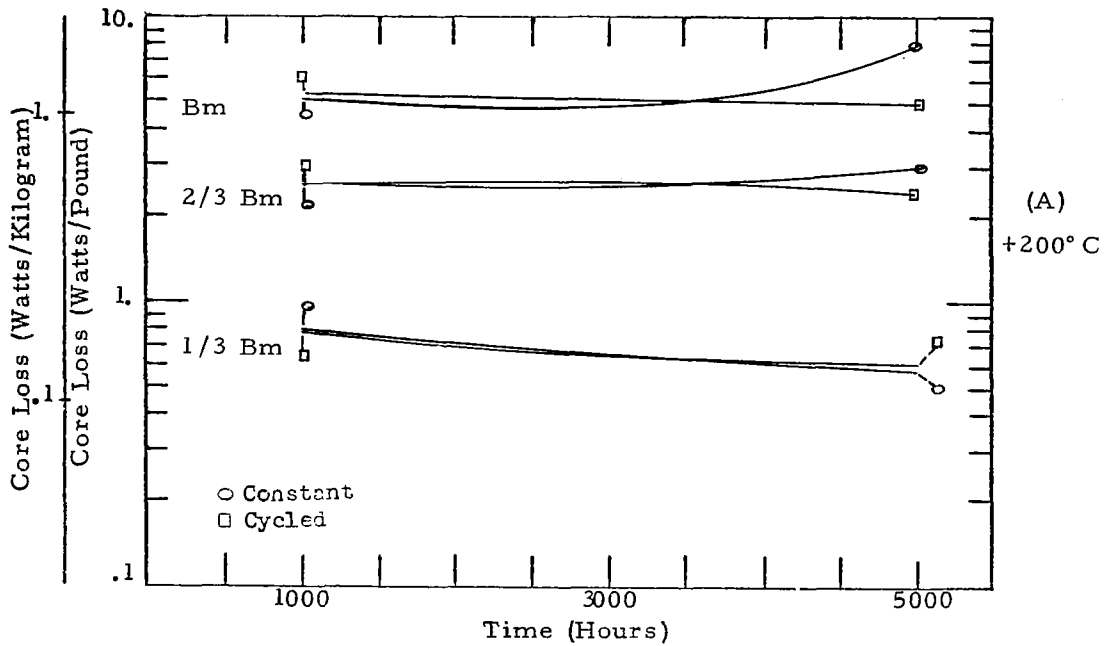
Figure 92 – Core Loss for 1/3, 2/3 and Maximum Induction vs. Constant
and Cycled Temperature for -55° C and +200° C. 0.002 inch
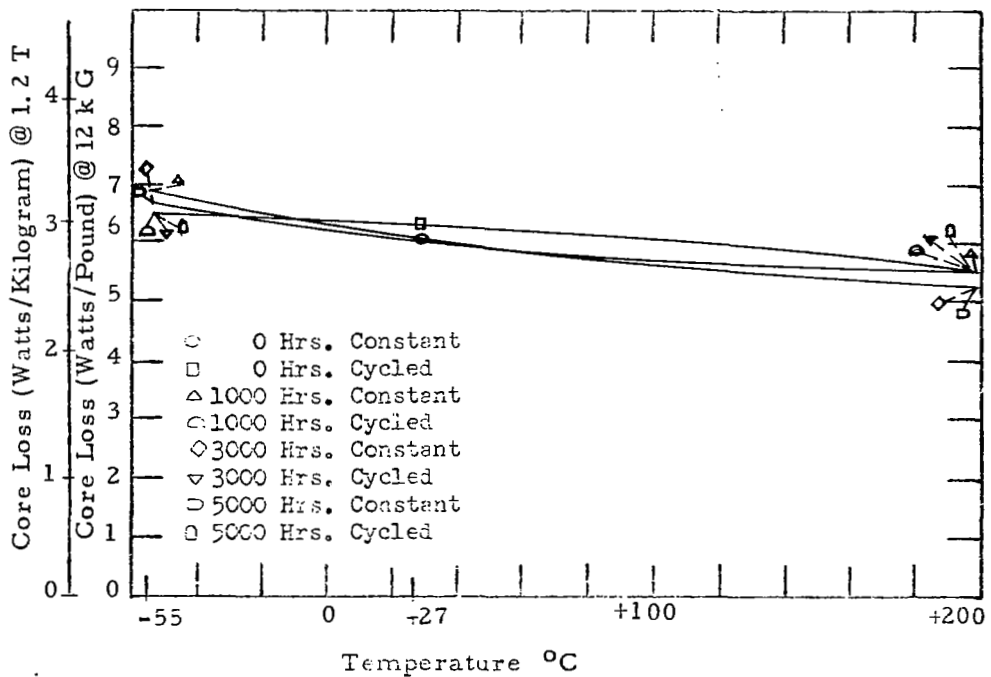Tape Cores, Doubly Grain Oriented Silicon Iron.

119
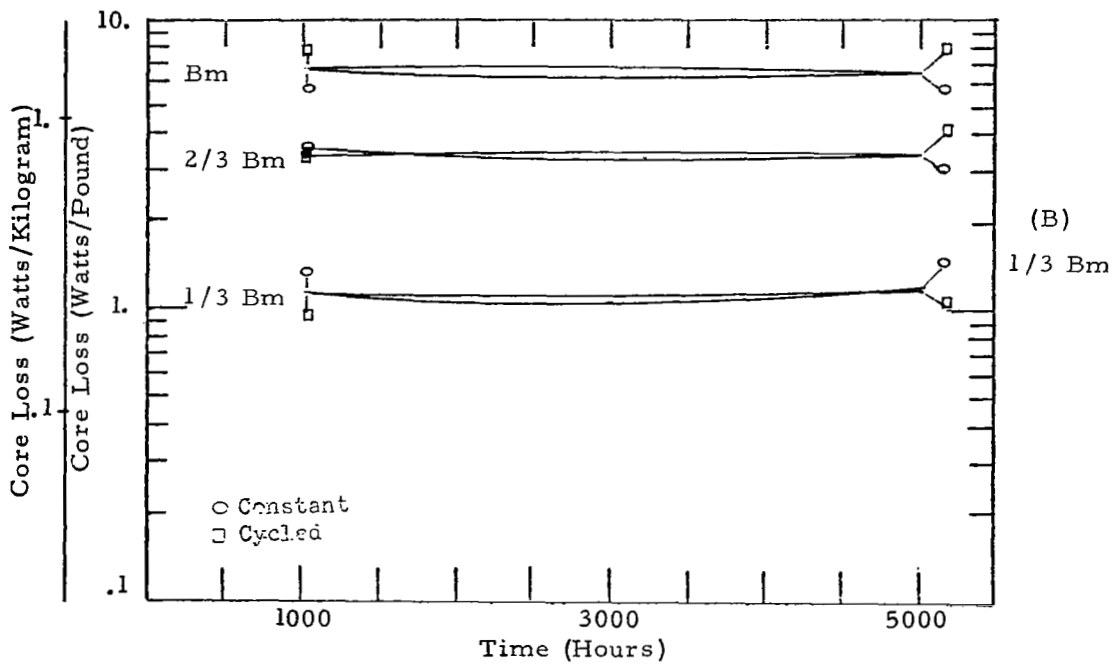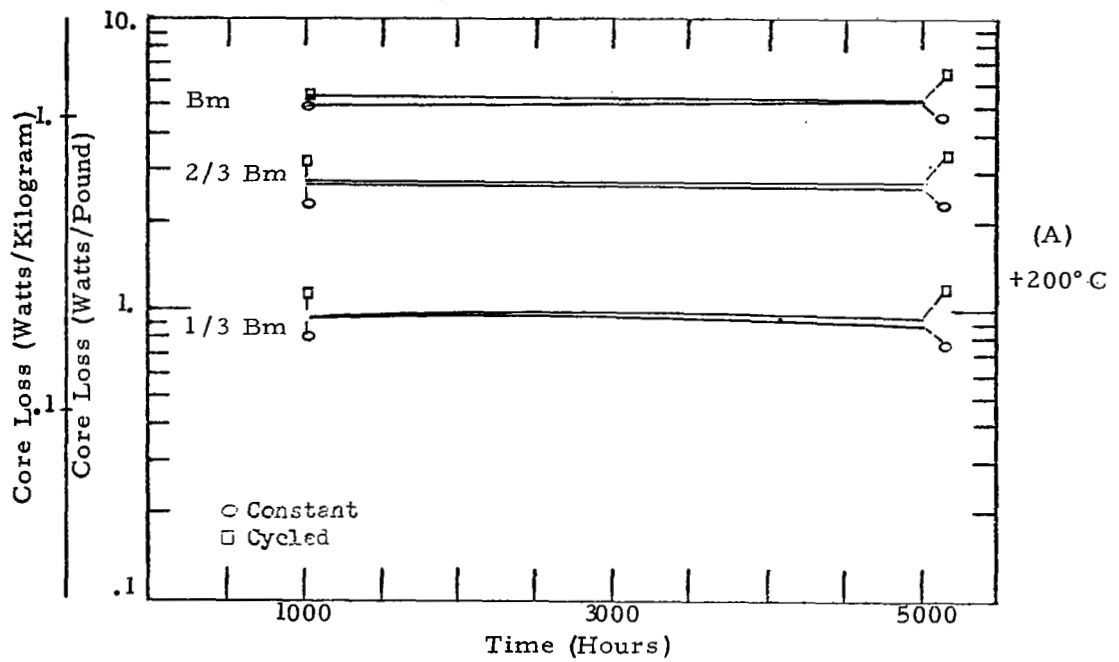
Figure 93 - Core Loss for 1/3, 2/3 and Maximum Induction vs. Constant and Cycled Temperature for -55°C and +200°C. 0.006 inch Ring Cores, Doubly Grain Oriented Silicon Iron.
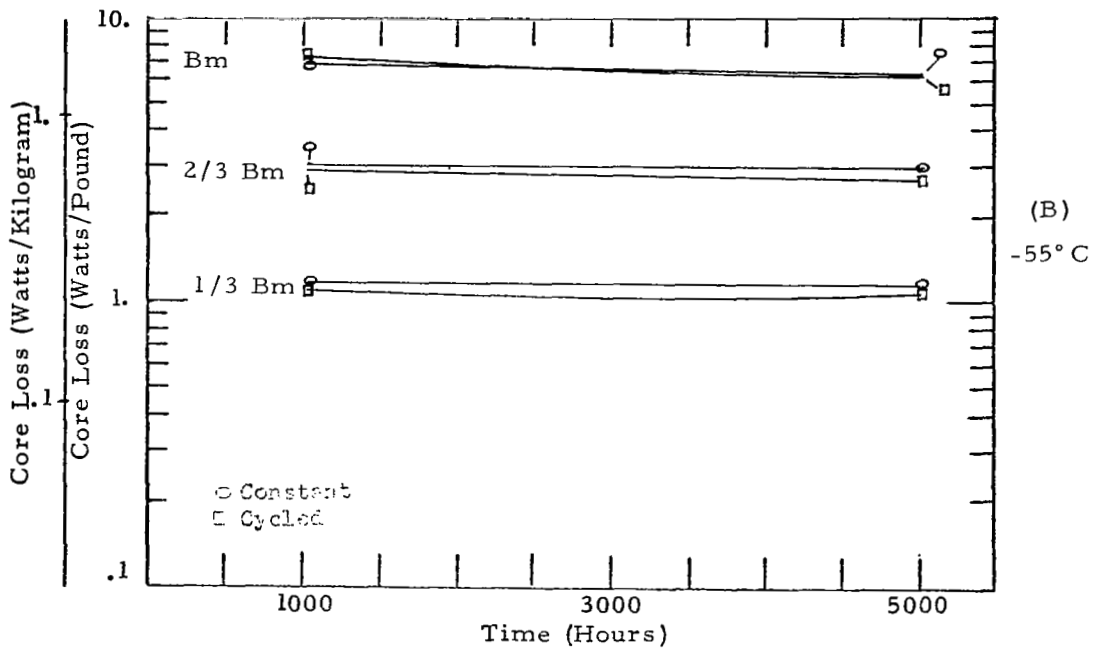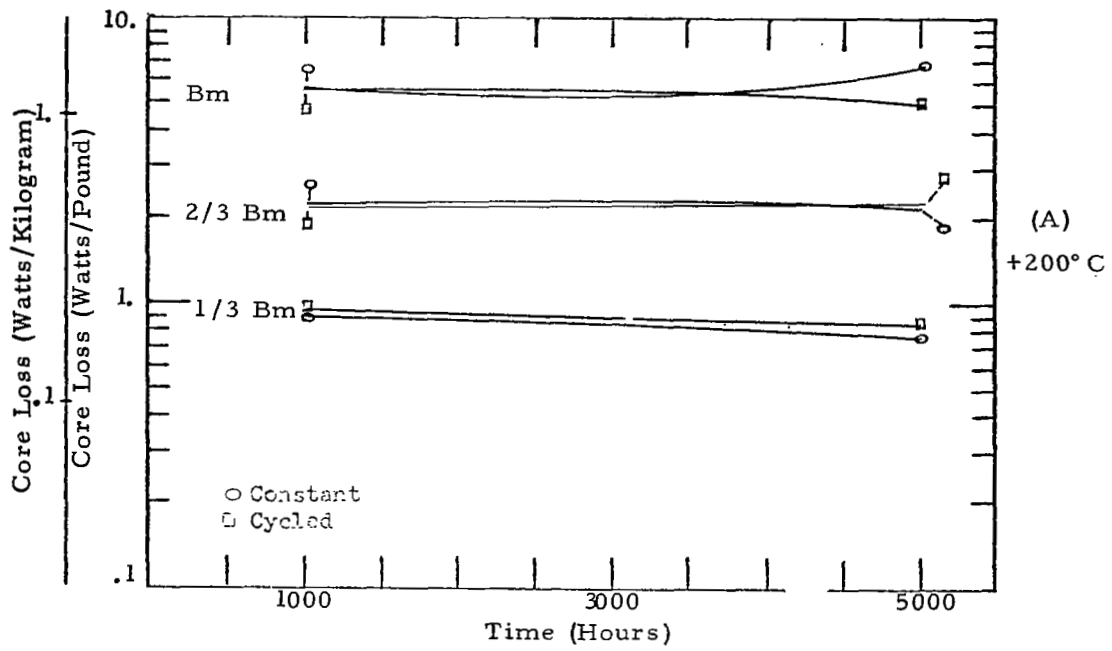
Figure 94 – Core Loss for 1/3, 2/3 and Maximum Induction vs. Constant
and Cycled Temperature for -55° C and +200° C. 0. 002 inch
Tape Cores, 49% Cobalt Alloy.
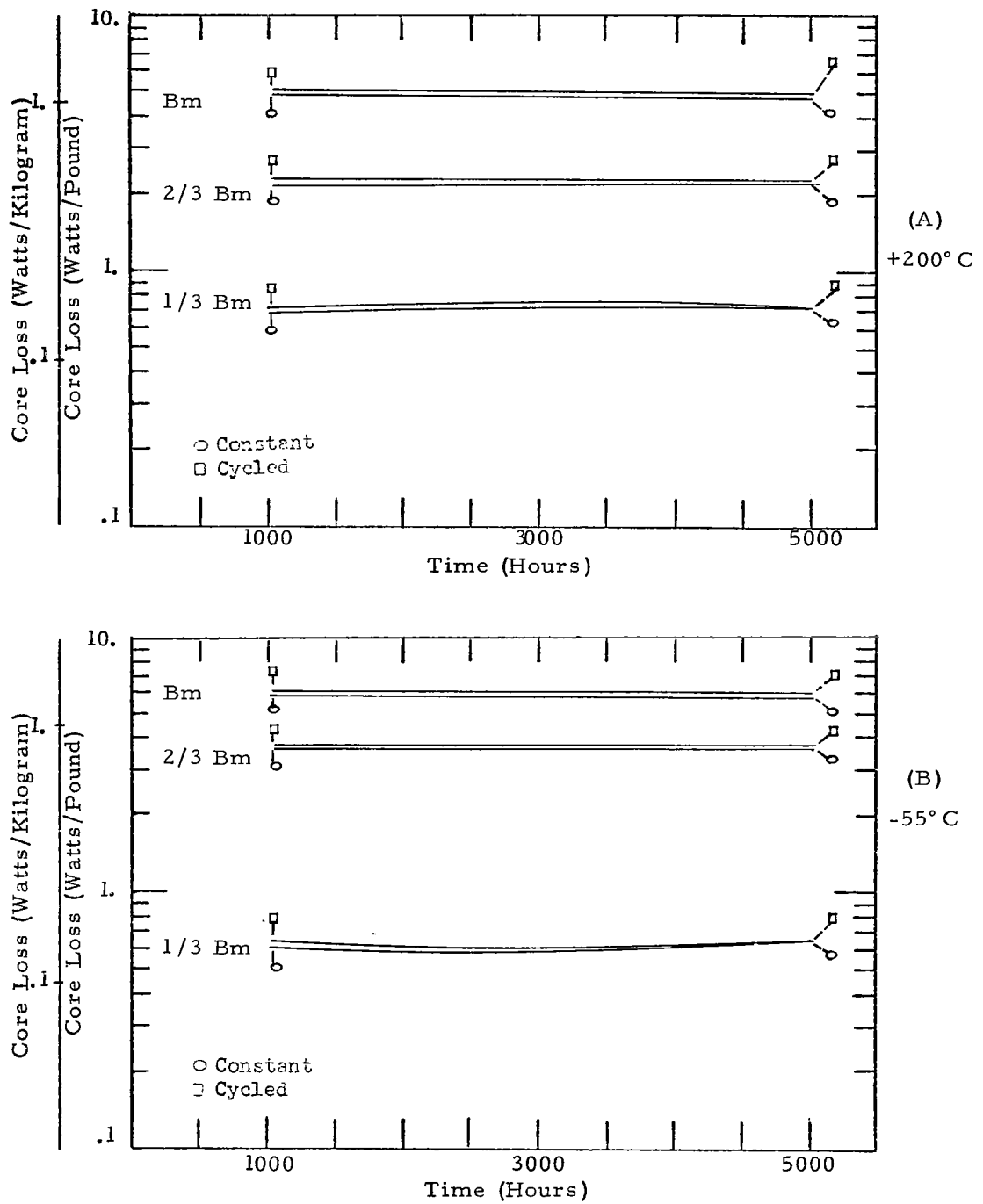
Figure 95 -   Core Loss for 1/3, 2/3 and Maximum Induction vs. Constant
and Cycled Temperature for -55° C and +200° C. 0.006 inch
Ring Cores, 49% Cobalt Alloy.

122
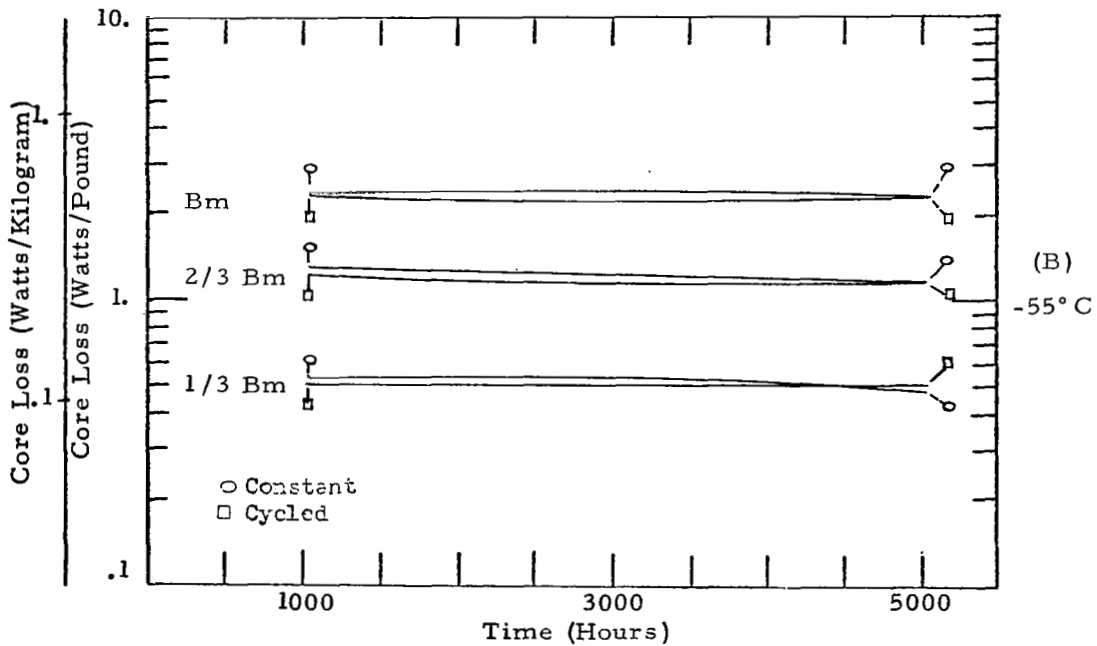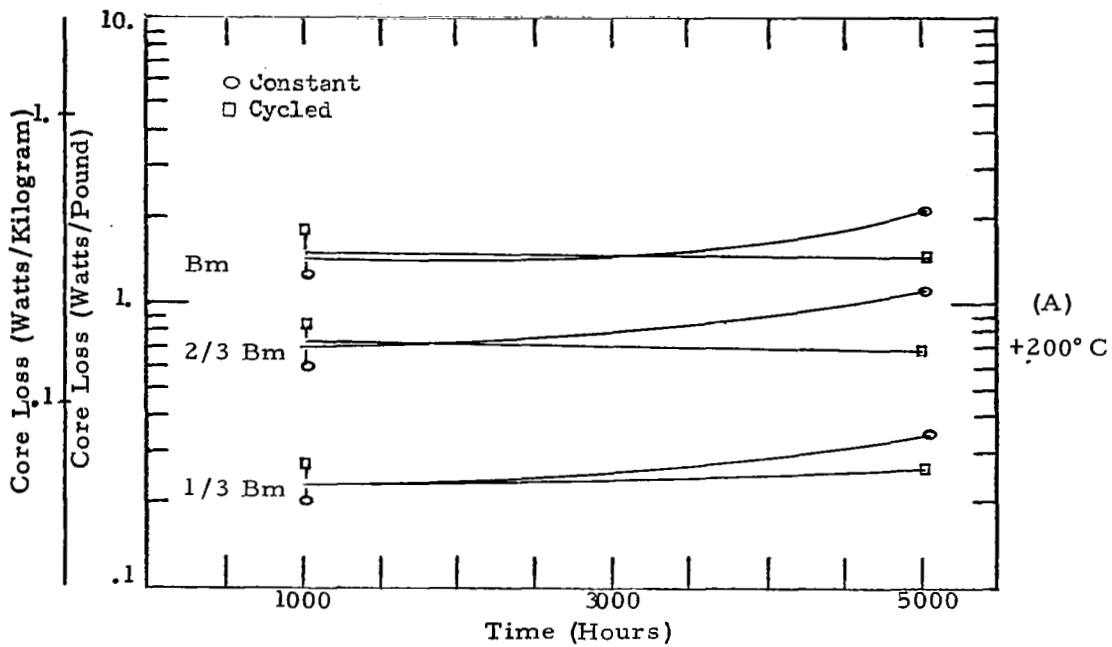
Figure 96 -   Core Loss for 1/3, 2/3 and Maximum Induction vs. Constant
and Cycled Temperature for -55° C and +200° C. ' 0. 002 inch
Tape Cores, 50% Nickel Alloy.

123
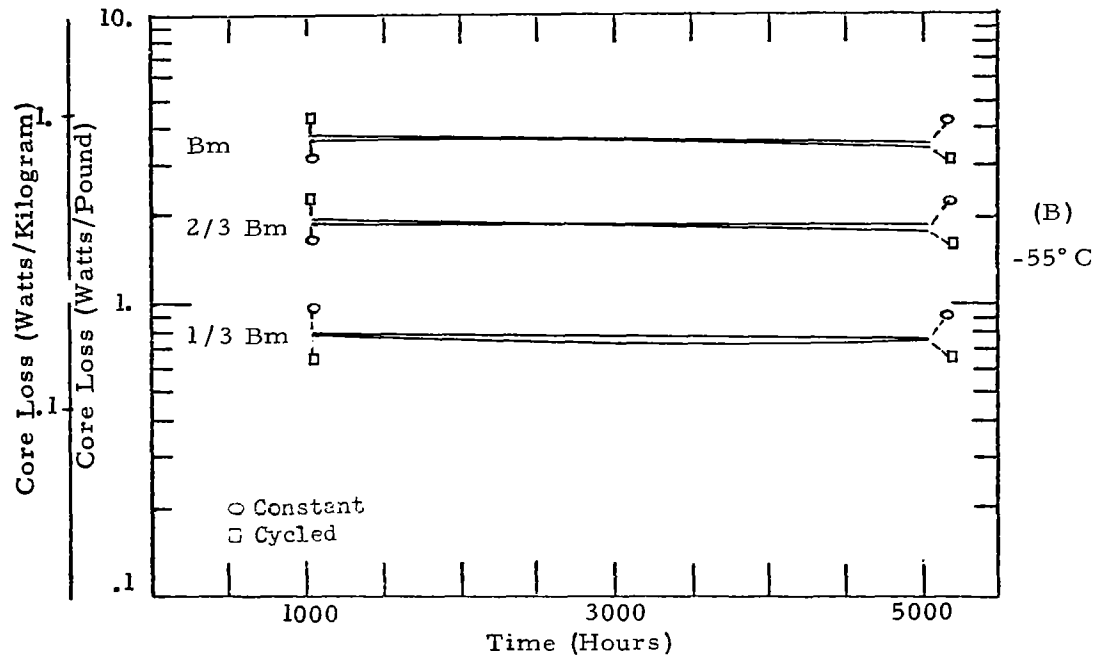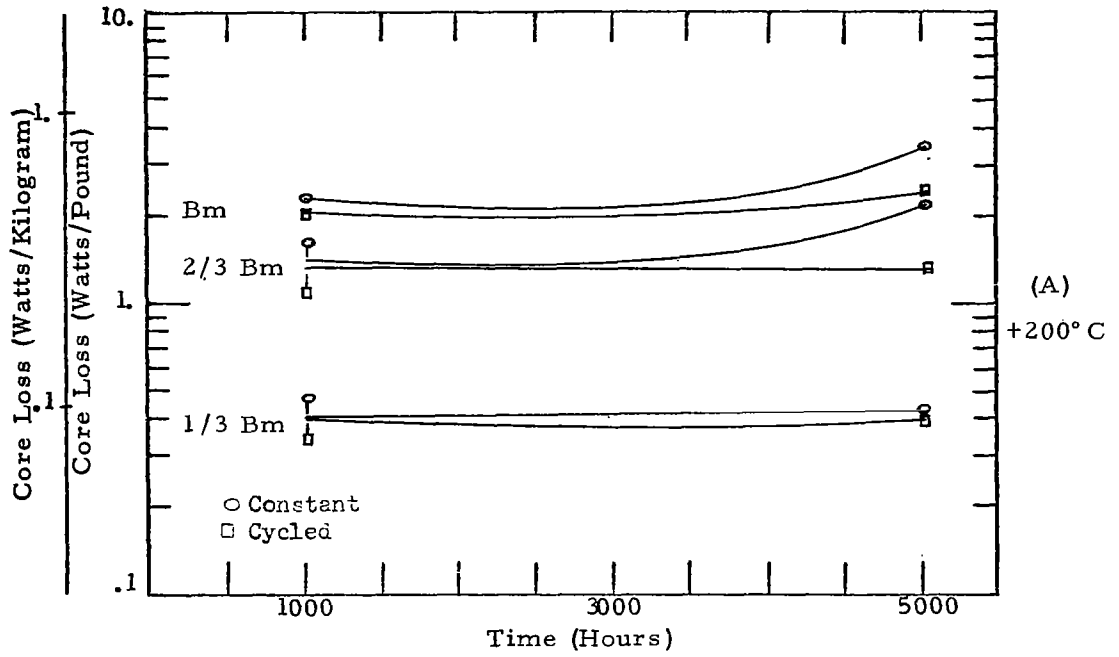
Figure 97 - Core Loss for 1/3, 2/3 and Maximum Induction vs. Constant and Cycled Temperature for -55° C and +200° C. 0.006 inch: Ring Cores, 50% Nickel Alloy.

124
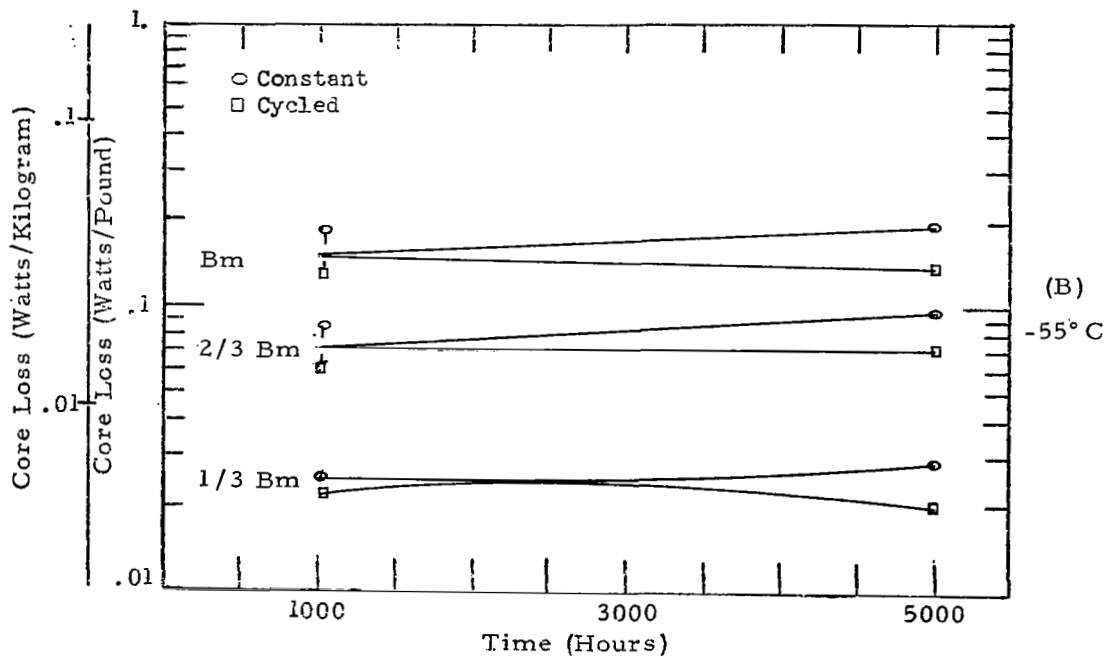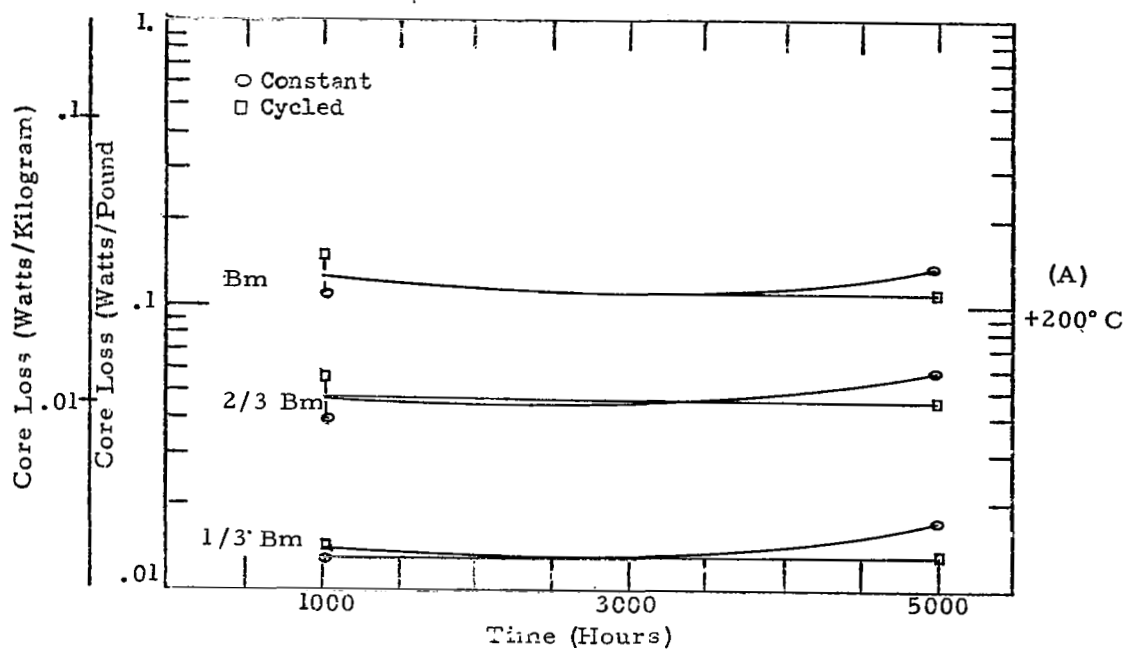
Figure 98 - Core Loss for 1/3, 2/3 and Maximum Induction vs. Constant and Cycled Temperature for -55° C and +200° C. 0. 002 inch Tape Cores, 79% Nickel Alloy.

125

Figure 99 – Core Loss for 1/3, 2/3 and Maximum Induction vs. Constant and Cycled Temperature for -55°C and +200° C. 0. 006 inch Ring Cores, 79% Nickel Alloy.

Figure 100 – Core Loss for 1/3, 2/3 and Maximum Induction vs. Constant andCycled Temperature for -55° C and +200° C.   0. 002 inch Tape Cores, High Purity 80% Nickel Alloy.

127

Figure 101 - Core Loss for 1/3, 2/3 and Maximum Induction vs. Constant and Cycled Temperature for -55°C and +200°C. 0.006 inch Ring Cores, High Purity 80% Nickel Alloy.

Figure 102   -   Core Loss and Excitation vs. Time and Temperature.
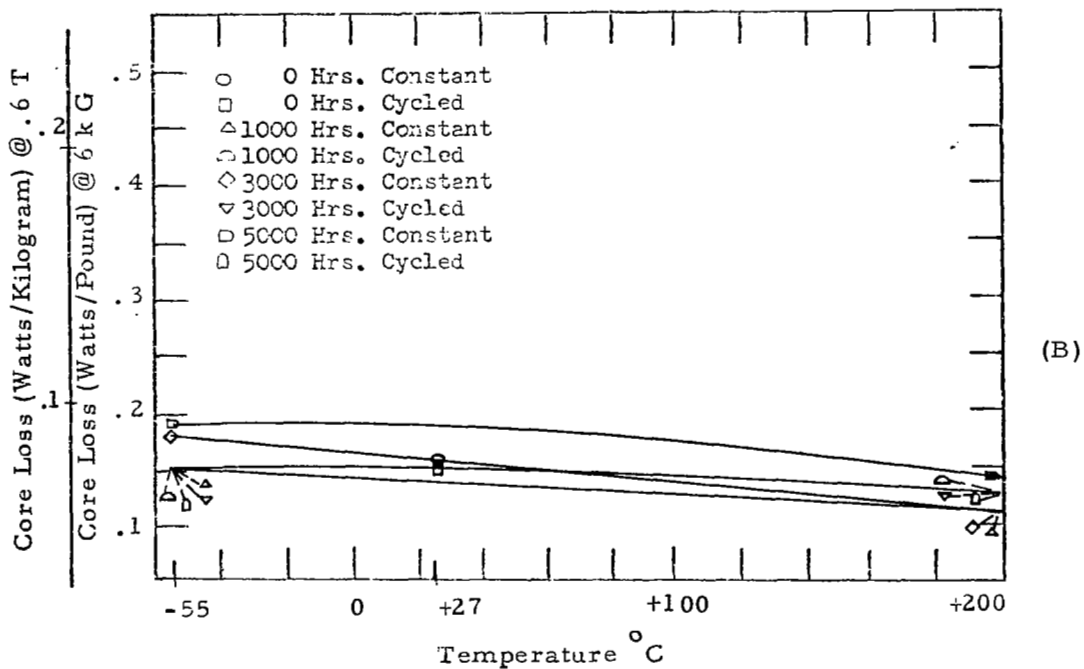0. 002 inch Tape Cores-Single Grain Oriented Silicon Iron.

Figure 103 - Core Loss and Excitation vs. Time and Temperature.
0. 006 inch Ring Cores-Single Grain Oriented Silicon Iron.

130

Figure 104 - Core Loss and Excitation vs. Time and Temperature
0.002 inch Tape Cores-Doubly Grain Oriented Silicon Iron.

Figure 105 - Core Loss and Excitation vs. Time and Temperature.
0.006 inch Ring Cores-Doubly Grain Oriented Silicon Iron.

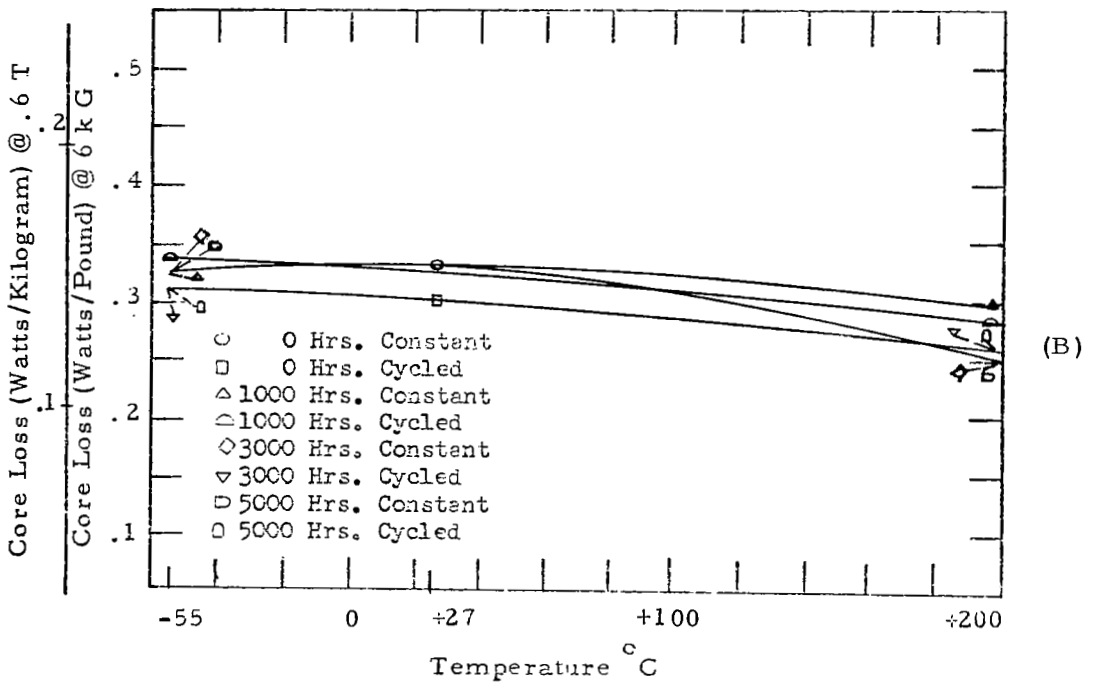Figure 106 – Core Loss and Excitation vs. Time and Temperature. 0.002 inch Tape Cores-49% Cobalt Alloy.
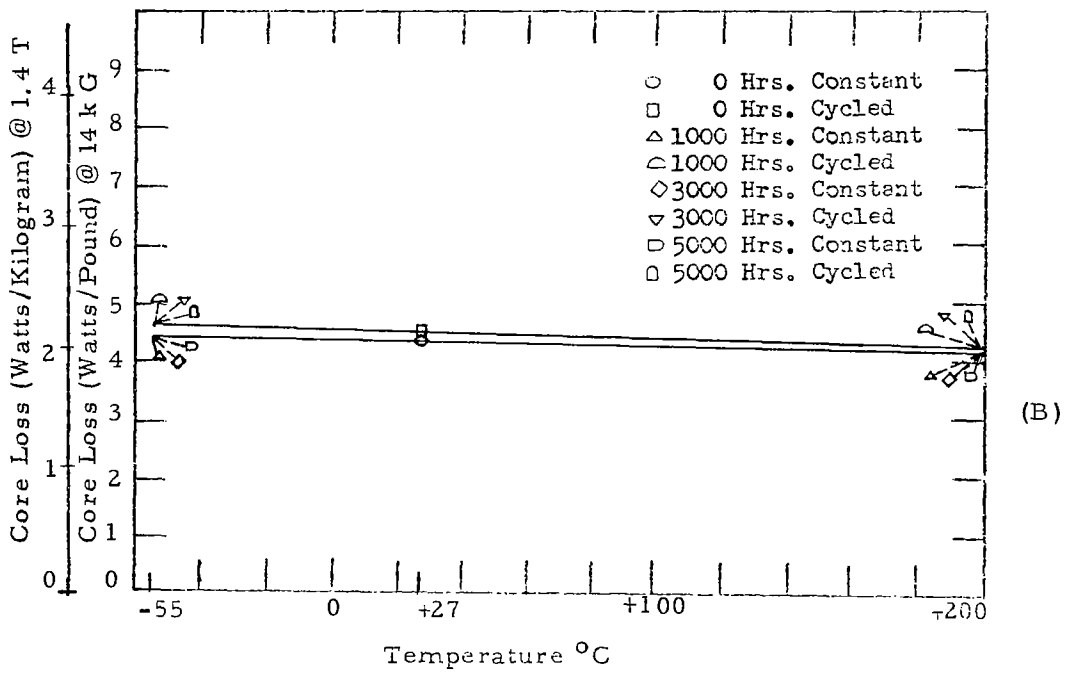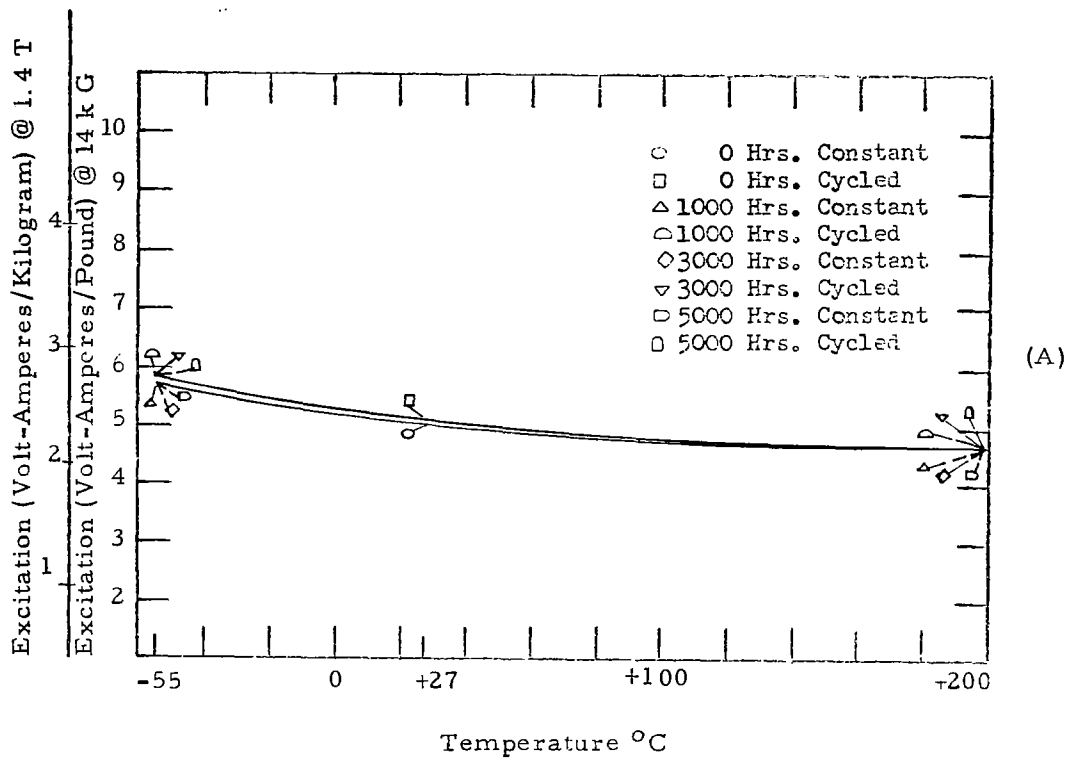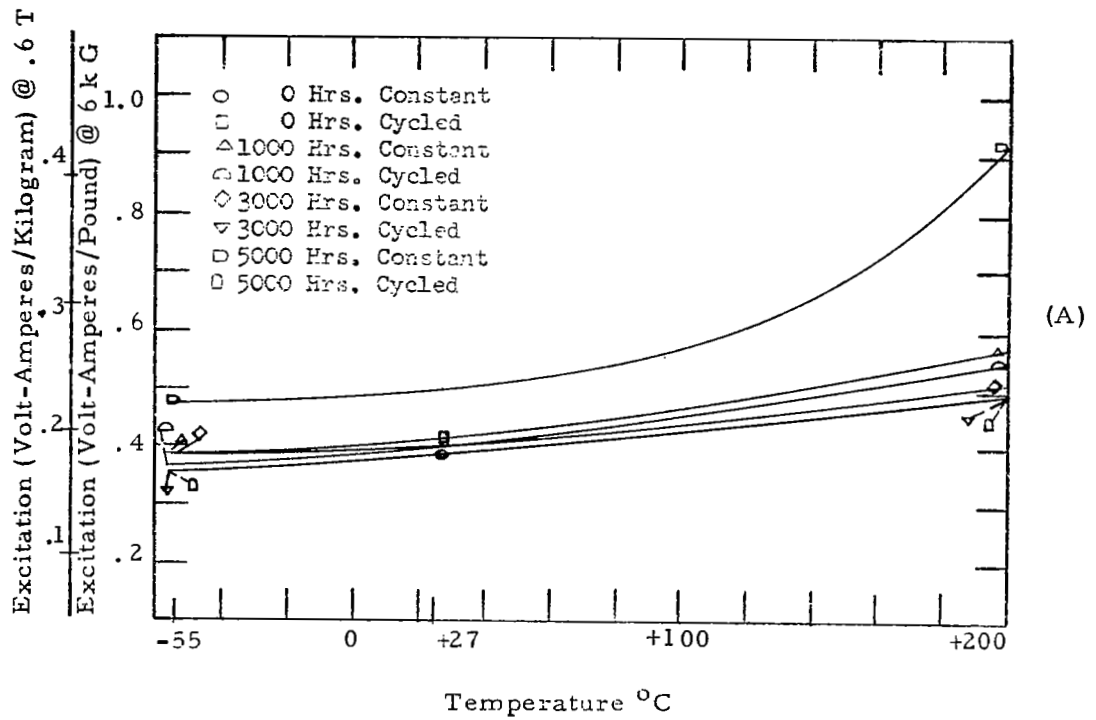
Figure 107 - Core Loss and Excitation vs. Time and Temperature.
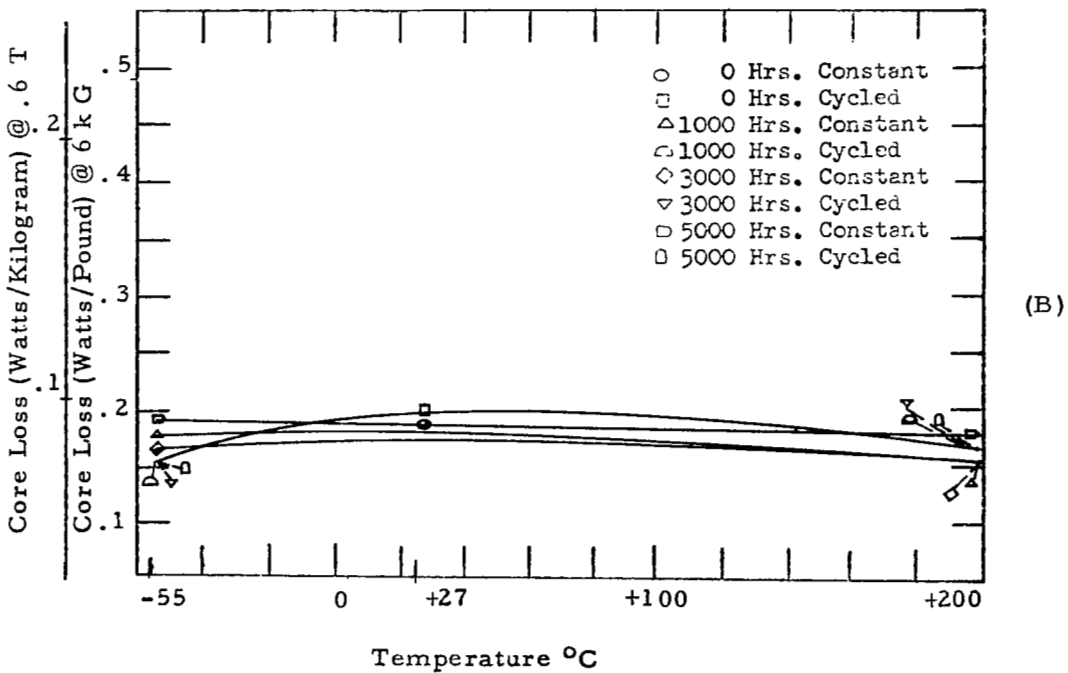0.006 inch Ring Cores-49% Cobalt Alloy.

134
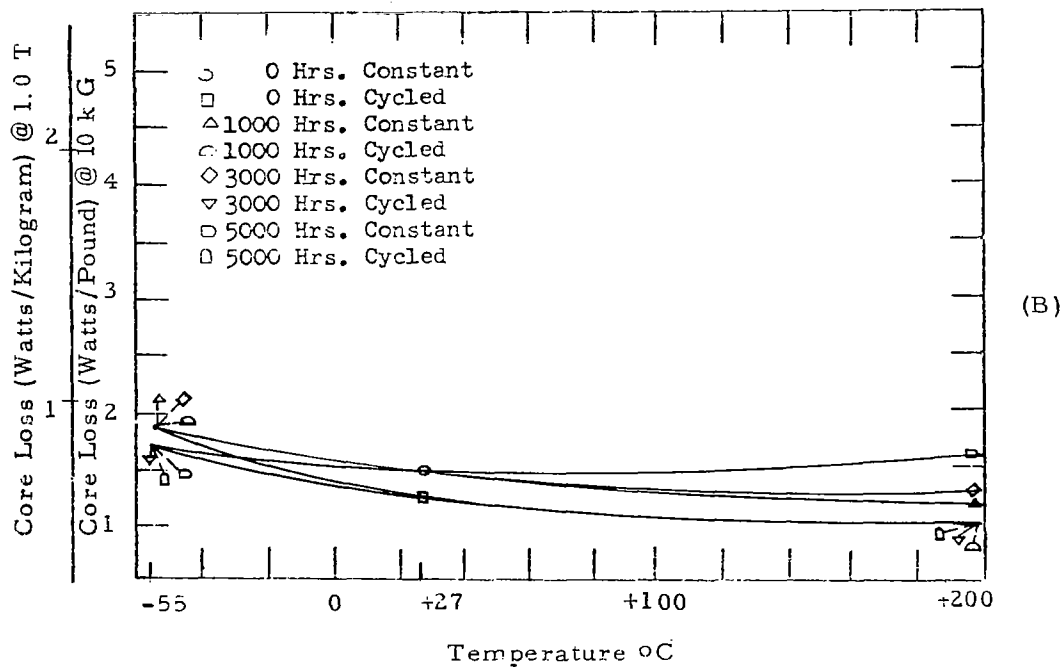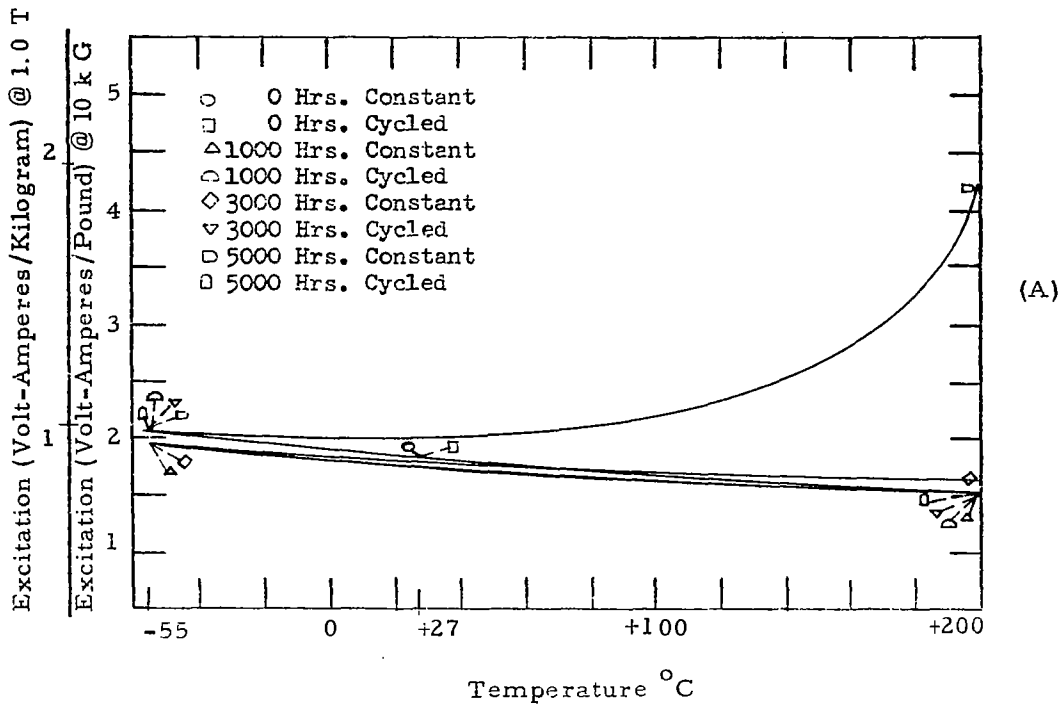
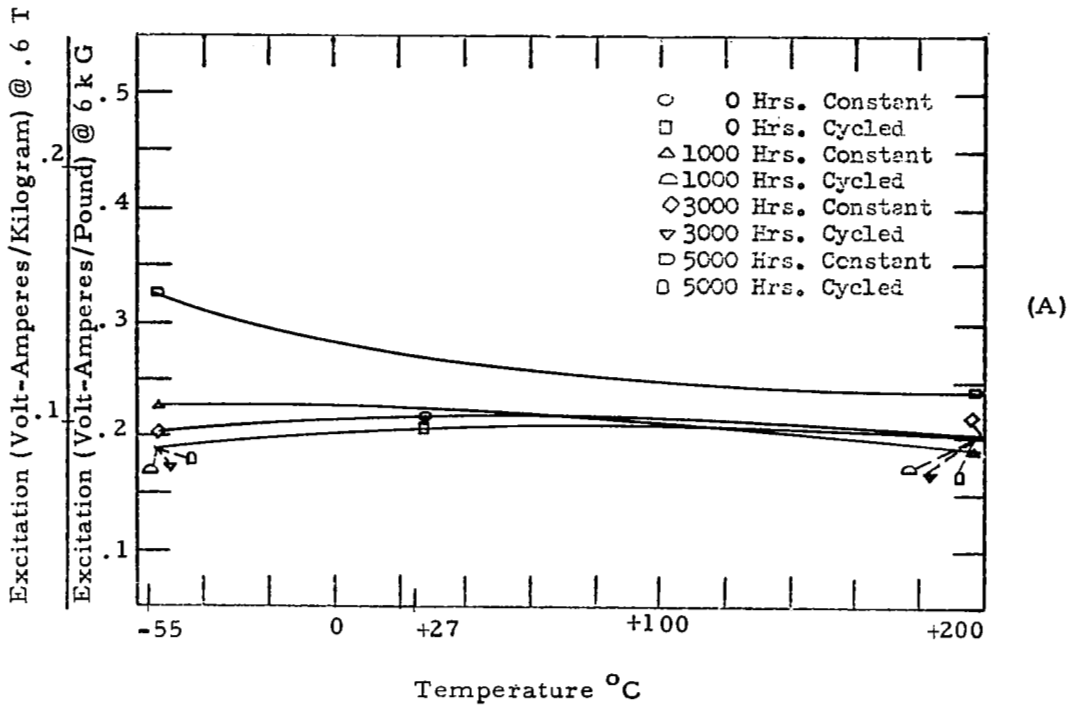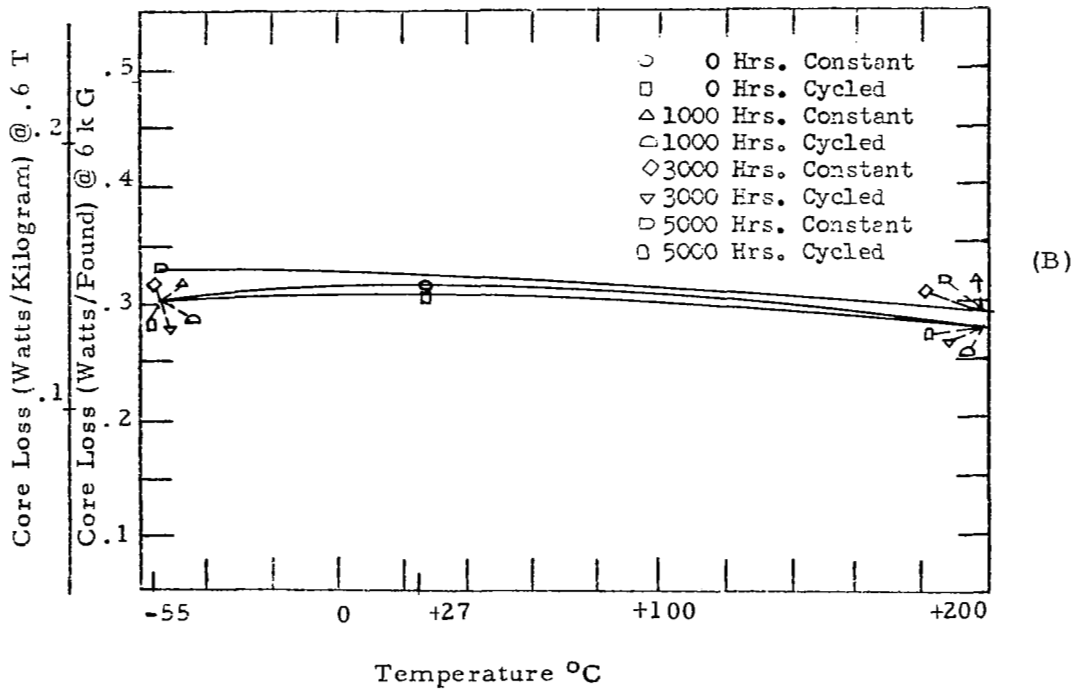Figure 108 - Core Loss and Excitation vs. Time and Temperature. 0.002 inch Tape Cores-50% Nickel Alloy.

135
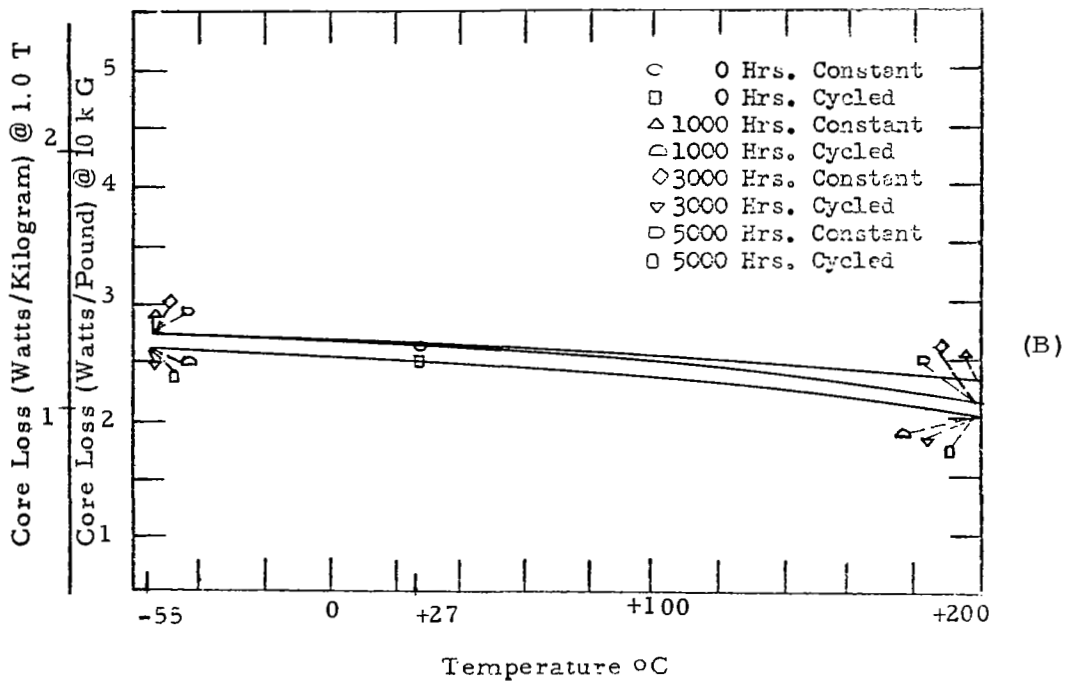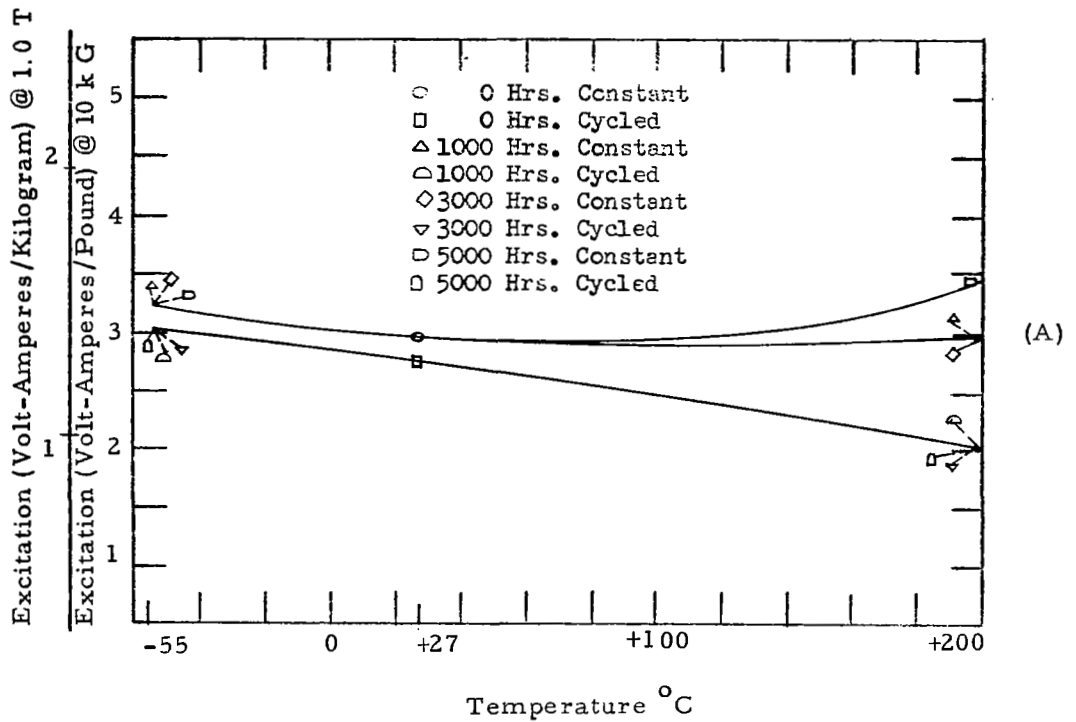
Figure 109 - Core Loss and Excitation vs. Time and Temperature.
0.006 inch Ring Cores-50% Nickel Alloy.

136

Figure (A) — top graph

Y-axis: Excitation (Volt-Amperes/Kilogram) @ .6 T
Secondary Y-axis: Excitation (Volt-Amperes/Pound) @ 6 k G
X-axis: Temperature °C

Legend:
- ○   0 Hrs. Constant
- □   0 Hrs. Cycled
- △ 1000 Hrs. Constant
- ◠ 1000 Hrs. Cycled
- ◇ 3000 Hrs. Constant
- ▽ 3000 Hrs. Cycled
- ◻ 5000 Hrs. Constant
- ◌ 5000 Hrs. Cycled

(A)

Figure (B) — bottom graph

Y-axis: Core Loss (Watts/Kilogram) @ .6 T
Secondary Y-axis: Core Loss (Watts/Pound) @ 6 k G
X-axis: Temperature °C

Legend:
- ○   0 Hrs. Constant
- □   0 Hrs. Cycled
- △ 1000 Hrs. Constant
- ◠ 1000 Hrs. Cycled
- ◇ 3000 Hrs. Constant
- ▽ 3000 Hrs. Cycled
- ◻ 5000 Hrs. Constant
- ◌ 5000 Hrs. Cycled

(B)

Figure 110 - Core Loss and Excitation vs. Time and Temperature.
0.002 inch Tape Cores - 79% Nickel Alloy.

Figure 111 - Core Loss and Excitation vs. Time and Temperature.
0. 006 inch Ring Cores-79% Nickel Alloy.

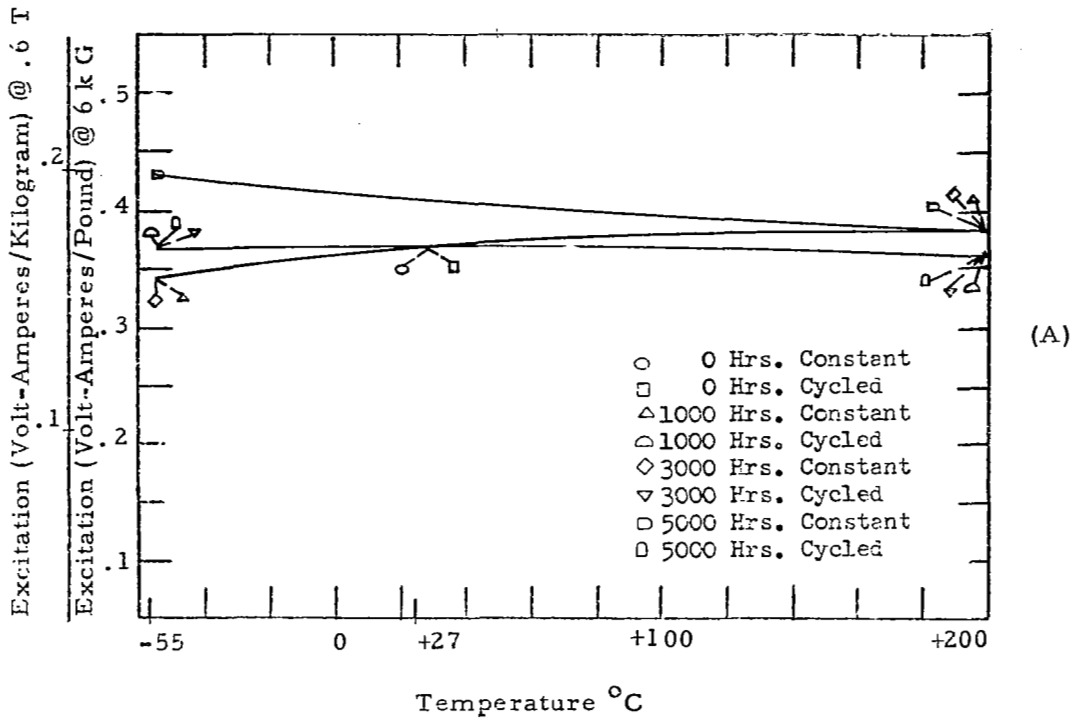Figure 112 - Core Loss and Excitation vs. Time and Temperature.
0.002 inch Tape Cores-High Purity 80% Nickel Alloy.

Figure 113 - Core Loss and Excitation vs. Time and Temperature.
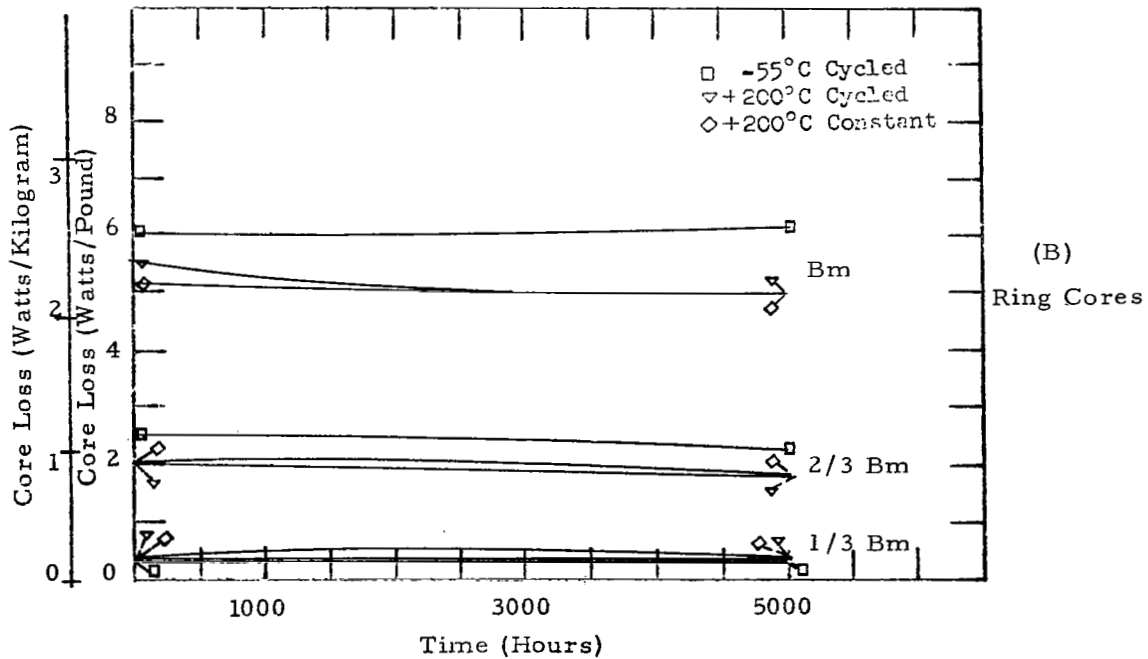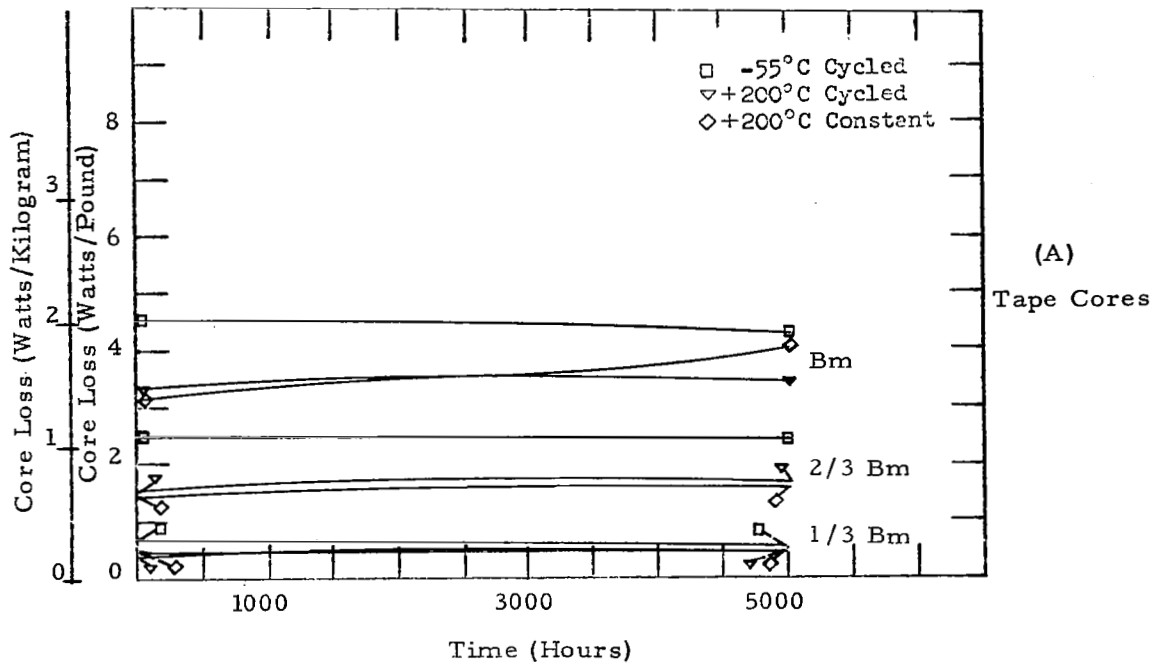0.006 inch Ring Cores-High Purity 80% Nickel Alloy

140

Figure 114 - Monitoring Data - Core Loss at 1/3, 2/3 and Maximum Induction for cycled and constant temperatures. Single Grain Oriented Silicon Iron.
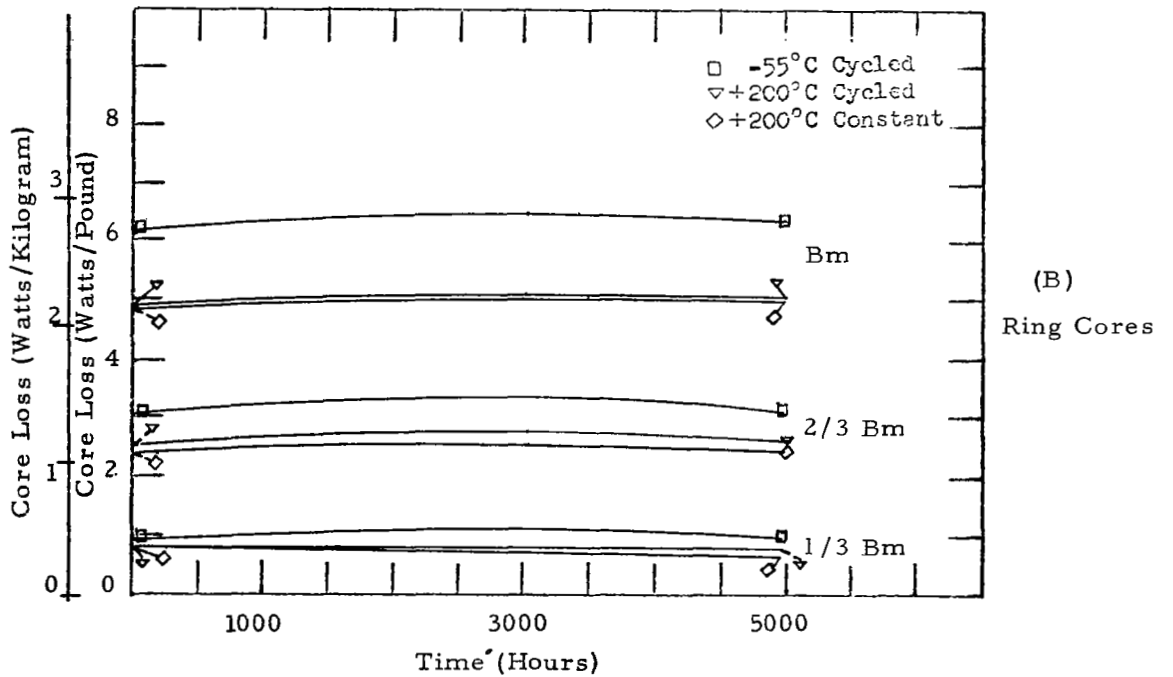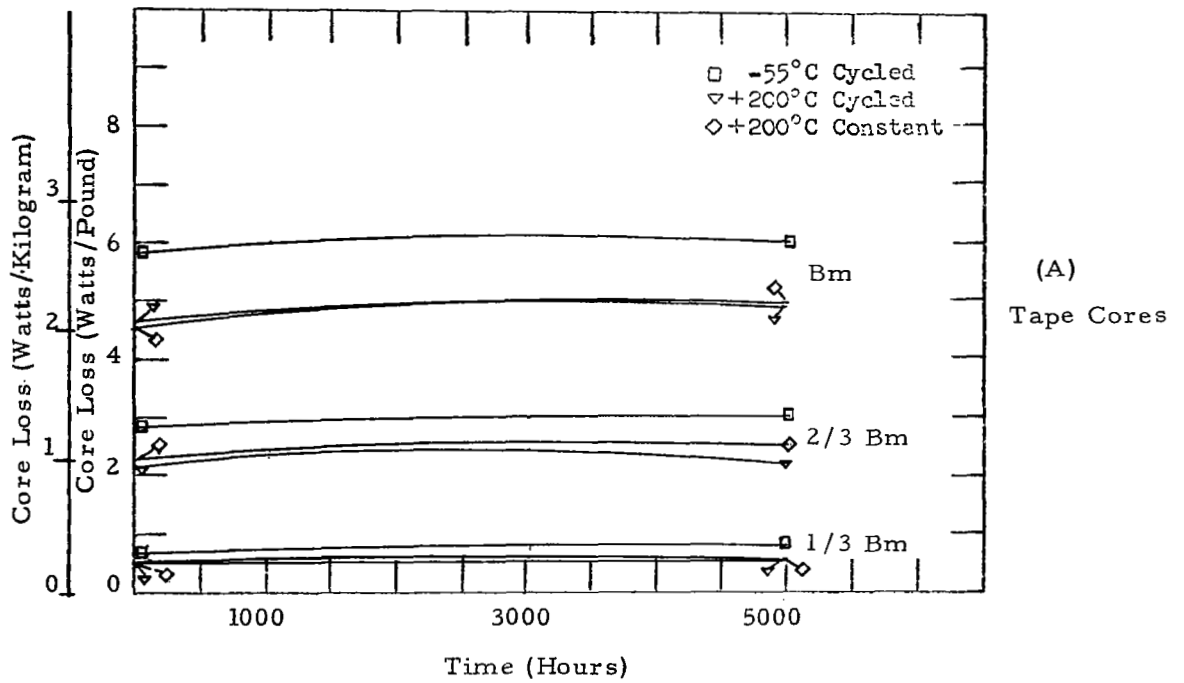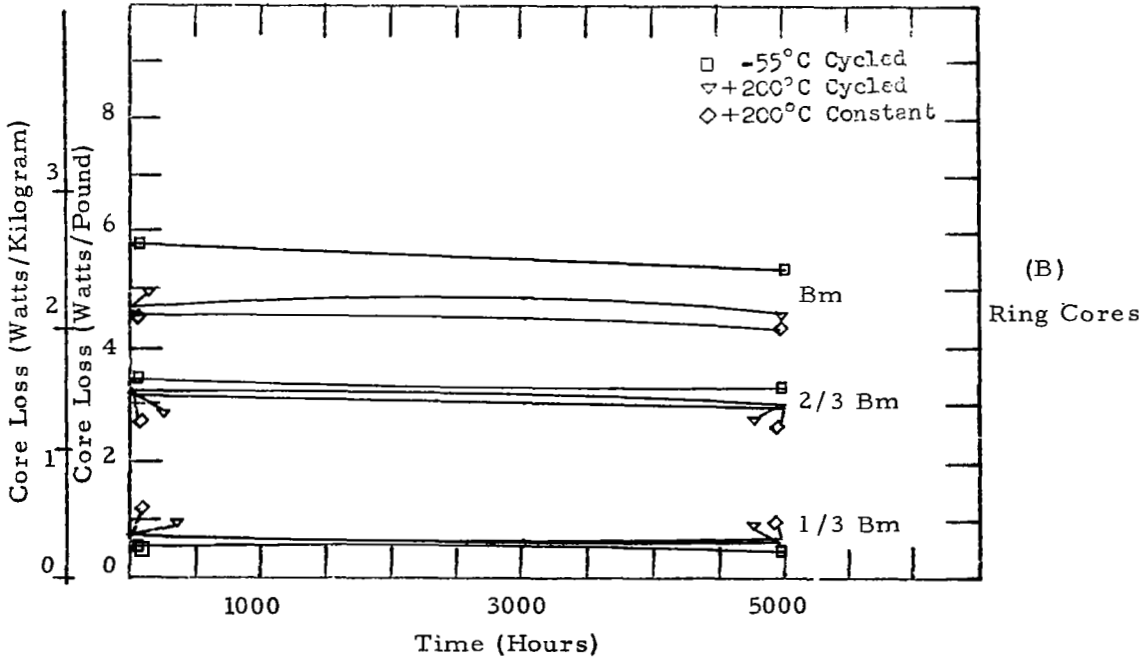
Figure 115 - Monitoring Data - Core Loss at 1/3, 2/3 and Maximum
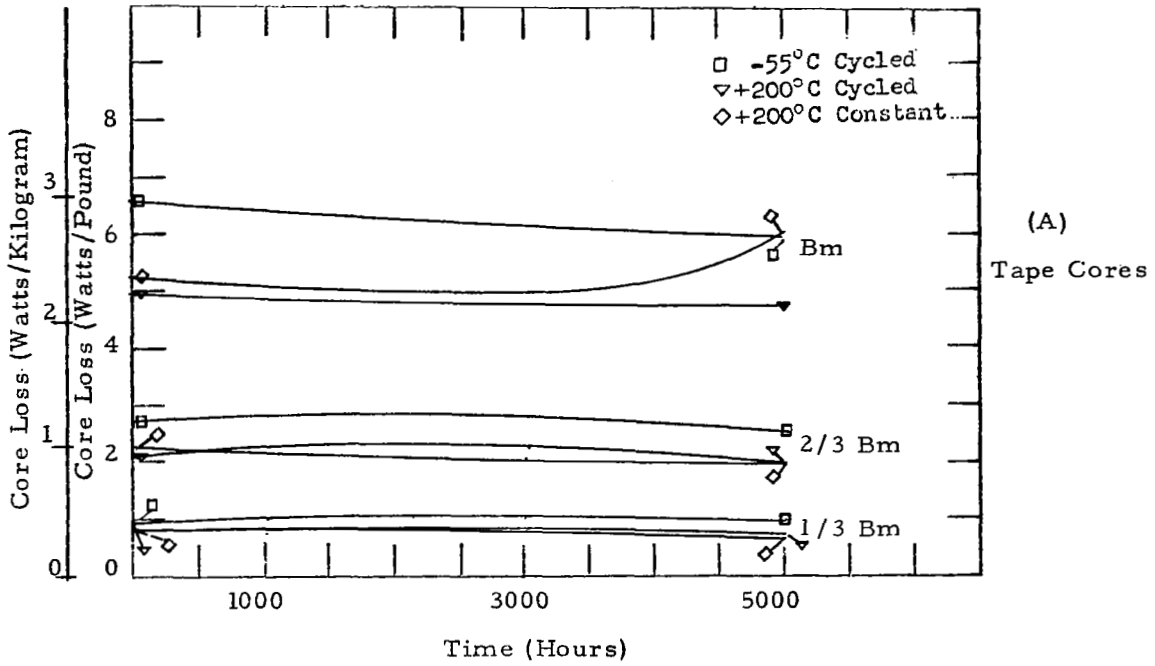Induction for cycled and constant temperatures. Doubly
Grain Oriented Silicon Iron.

142

Figure 116 - Monitoring Data - Core Loss at 1/3, 2/3 and Maximum Induction for cycled and constant temperatures. 49% Cobalt Alloy.
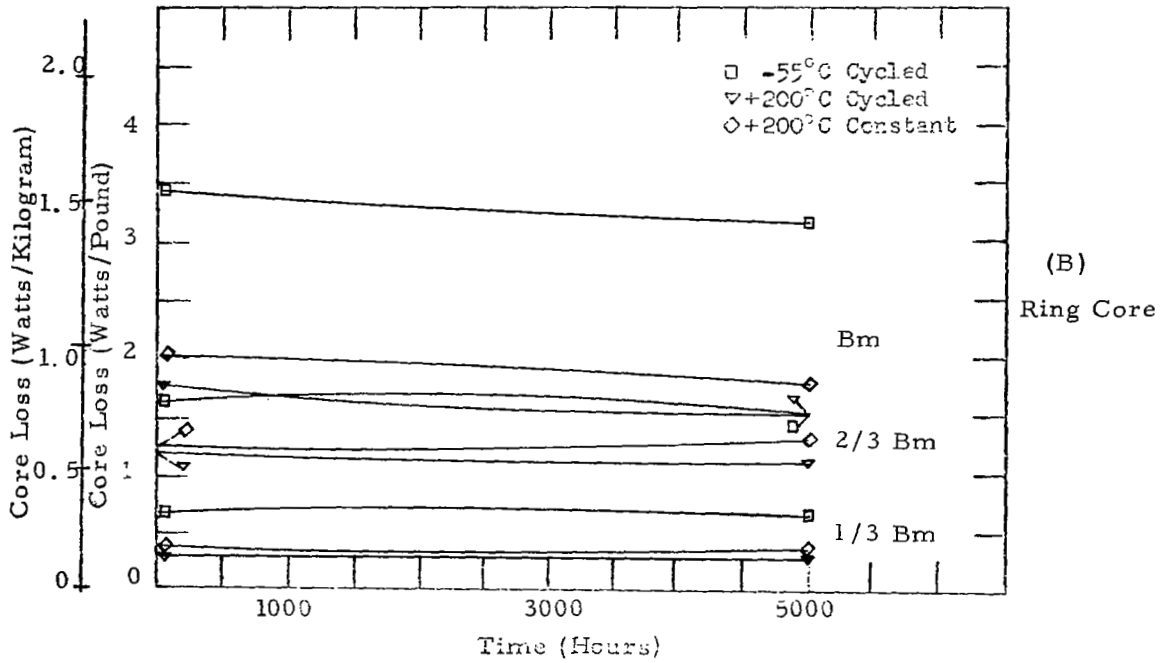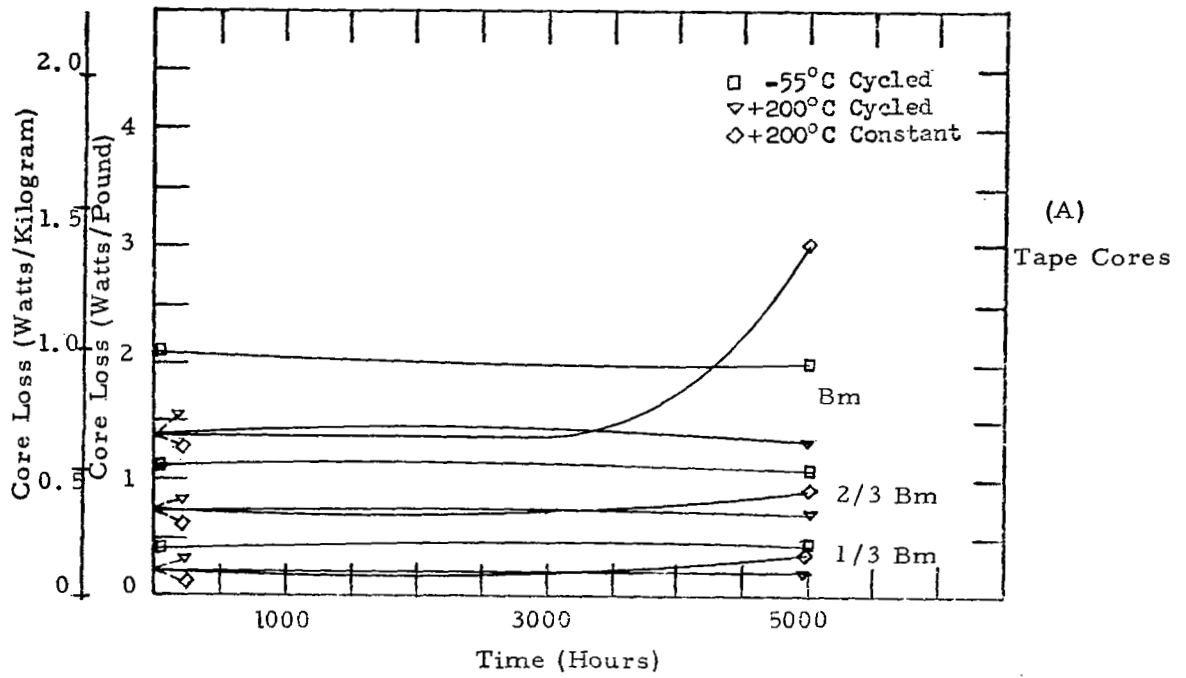
143

Figure 117 -   Monitoring Data - Core Loss at 1/3, 2/3 and Maximum
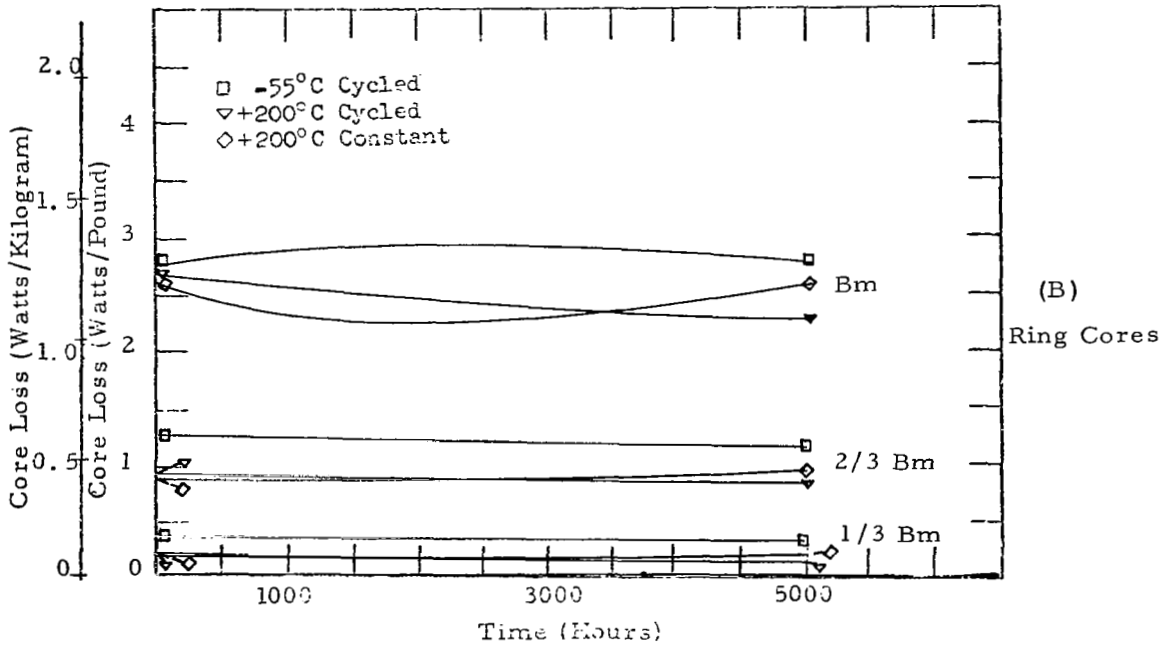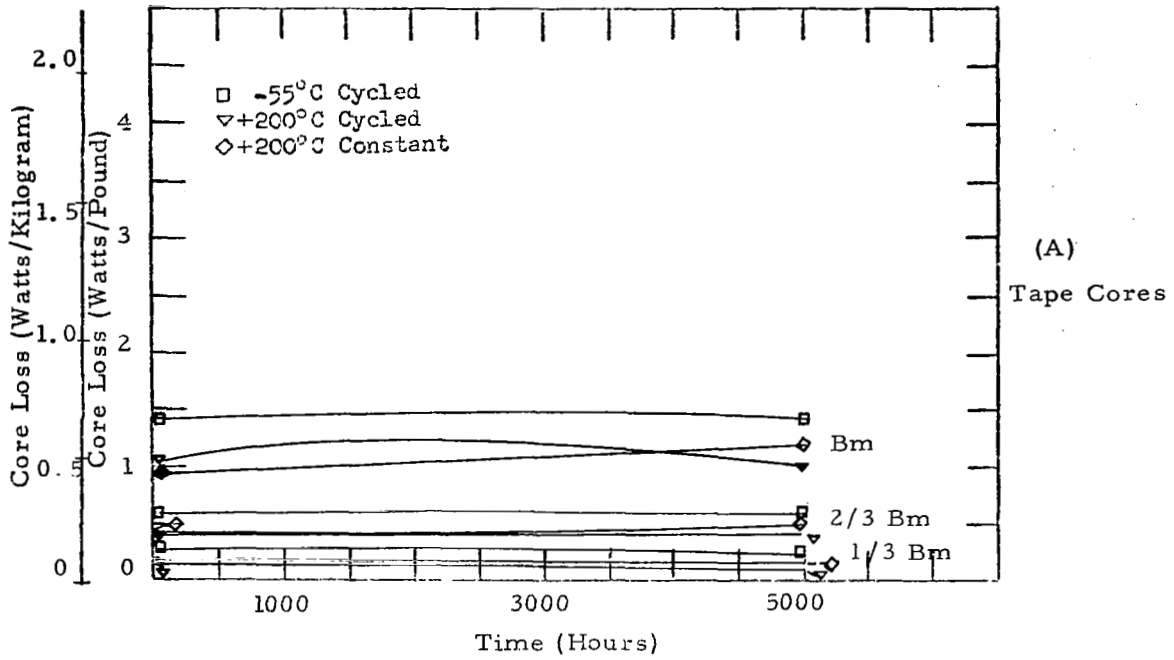Induction for cycled and constant temperatures.   50%
Nickel Alloy.

Figure 118 - Monitoring Data - Core Loss at 1/3, 2/3 and Maximum
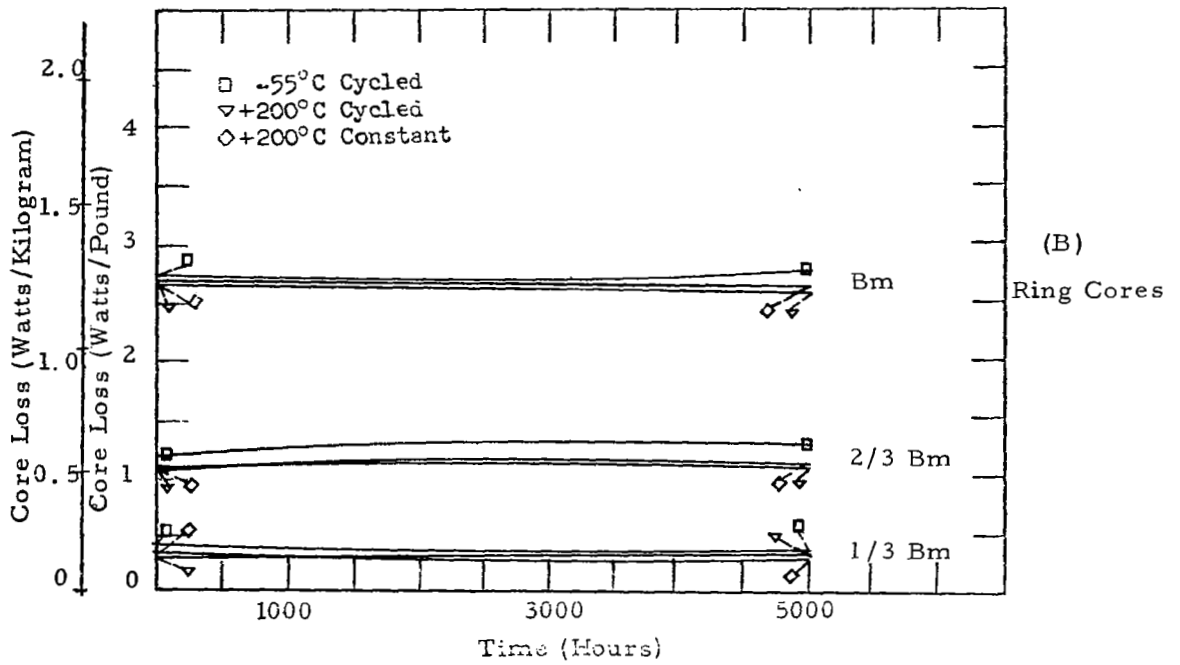Induction for cycled and constant temperatures. 79%
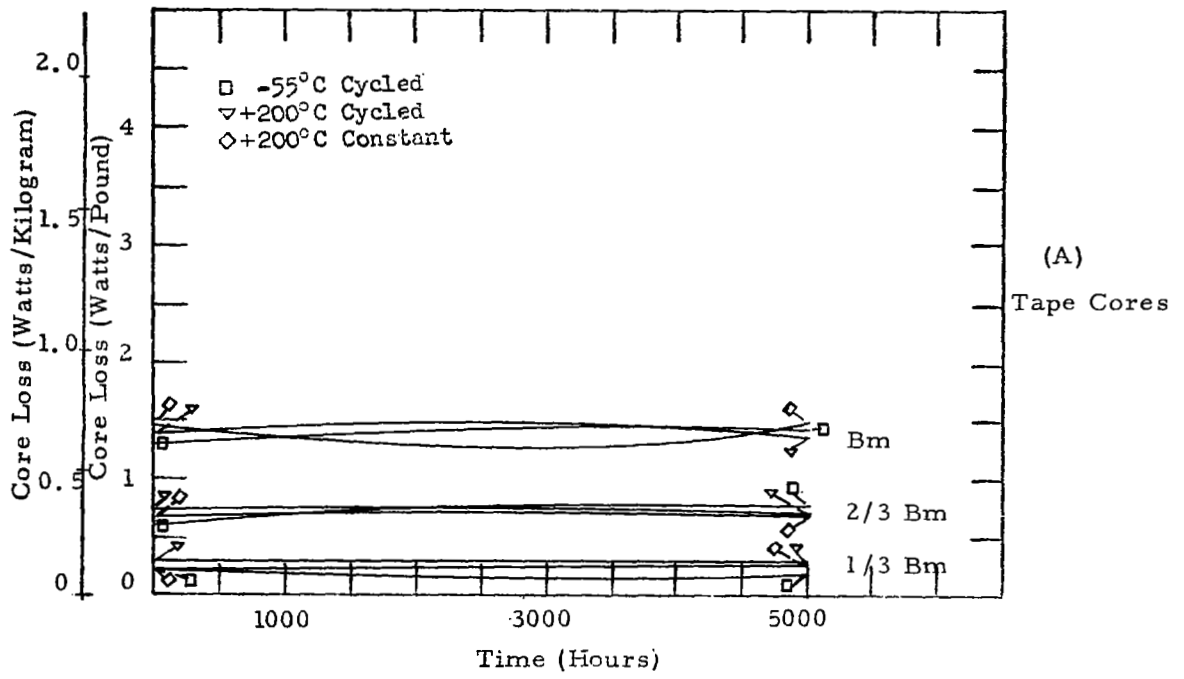Nickel Alloy.

Figure 119 — Monitoring Data — Core Loss at 1/3, 2/3 and Maximum Induction for cycled and constant temperature. High Purity 80% Nickel Alloy.

REFERENCES

(1) Frost, R. M. ; et al; Evaluation of Magnetic Materials for Static Inverters and Converters; NAS CR-1226

(2) Bozorth, R. M. ; Ferromagnetism; D. Van Nostrand Co.

(3) Hausmann, E. ; Slack, E. P. ; Physics, Book, Second Edition, D. Van Nostrand Co. Inc. , New York, p. 235.